

RATIONALE FOR CONTINUING R&D IN DIRECT COAL CONVERSION
TO PRODUCE HIGH QUALITY TRANSPORTATION FUELS

R.D. Srivastava and H.G. McIlvried
Burns and Roe Services Corporation
Pittsburgh Energy Technology Center
P.O. Box 18288
Pittsburgh, PA 15236
D. Gray and G.C. Tomlinson
The Mitre Corporation
McLean, VA 22102
E.B. Klunder
Pittsburgh Energy Technology Center
Pittsburgh, PA 15236

ABSTRACT

For the foreseeable future, liquid hydrocarbon fuels will play a significant role in the transportation sector of both the United States and the world. Factors favoring these fuels include convenience, high energy density, and the vast existing infrastructure for their production and use. At present the U.S. consumes about 26% of the world supply of petroleum, but this situation is expected to change because of declining domestic production and increasing competition for imports from countries with developing economies. A scenario and time frame are developed in which declining world resources will generate a shortfall in petroleum supply that can be alleviated in part by utilizing the abundant domestic coal resource base. One option is direct coal conversion to liquid transportation fuels. Continued R&D in coal conversion technology will result in improved technical readiness that can significantly reduce costs so that synfuels can compete economically in a time frame to address the shortfall.

BACKGROUND

The United States continues to rely heavily on liquid fuels for transportation, and, in spite of the strong interest in using alternative fuels, hydrocarbon liquids will continue to play a significant role in our energy future. This is primarily because of their convenience, high energy density, and the enormous infrastructure in place for their production, distribution, and end-use. Currently, the U.S. consumes about 17.5 million barrels per day (BPD) of oil (about 35 quads/yr - 1 quad/yr equals approximately 500,000 BPD). Of this, 75% is used by the transportation sector.

Current domestic crude production is 6.6 million BPD, having steadily declined from 9 million BPD ten years ago at a decline rate of about 3%/yr. Currently, the U.S. imports over 50% of its petroleum, and the Energy Information Administration (EIA)¹ predicts that this will increase to 68% by the year 2010. The U.S. currently uses 26% of the world's total petroleum production. Even if this percentage were to remain constant, a significant shortfall in the petroleum supply in the U.S. is likely to occur because of declining domestic production. Because of competition from rapid economic development worldwide, the U.S. may not be able to import sufficient oil to meet future demand.

Coal resources in the U.S. are enormous. EIA estimates total reserves at 1.7 trillion short tons. Coal represents an inexpensive, domestic resource that can be used as a feedstock to produce clean, high-quality transportation fuels in an environmentally sound manner.

The Department of Energy (DOE) Fossil Fuel Energy's R&D program has been largely responsible for technological improvements in coal liquefaction in the U.S. The goal of the DOE program is to develop and demonstrate coal liquefaction technology that is competitive with crude oil at \$25-30/bbl in 1993 dollars. The purpose of this program is to reduce vulnerability to energy supply disruptions, to create new high wage jobs, and to do this while respecting the environment.

THE WORLD ENERGY PICTURE

At the last World Energy Congress meeting in 1992², MITRE presented a world energy demand model that was used to estimate total commercial world energy demand to the year 2100. If energy use efficiency does not improve, estimated world demand will reach 2,090 quads by 2100. If energy conversion and end-use efficiencies continue to improve, the world's commercial energy demand will be reduced from 2,090 quads in the no-efficiency-improvement case to about 1,050 quads in 2100. However, even with efficiency improvements, world energy demand will still increase three-fold over the present level of 350 quads per year.

The question is whether this demand can be satisfied with known energy resources. To answer this, the world resources of oil and natural gas must be determined. The United States Geological Survey³ estimates the world's ultimate resource of conventional oil as 1.7 trillion barrels (about 10,000 quads). Estimates for natural gas are less certain; therefore, a range was assumed: 10,000-20,000 trillion cubic feet⁴ (TCF) (10,000-20,000 quads).

Figure 1 shows resource depletion curves. By 2100 oil will be essentially depleted, and natural gas will either be depleted or in rapid decline. Although not shown on the figure, coal availability worldwide is enormous. Estimates range from 45,000 quads⁵ for proved reserves to 240,000 quads⁶ for the total resource, between 500 and 2000 years supply at current usage rates.

The estimated conventional fossil energy resource and the postulated world energy demand scenario can be combined to produce a world energy demand/supply scenario as shown in Figure 2. In this scenario, it is assumed that oil, gas, and present day nuclear use follow the depletion curves shown, coal use remains constant at the present level, and hydroelectric power supply triples between now and the year 2100. The area designated as "21st Century" represents the energy shortfall. In this constant coal use scenario, the shortfall will have to be supplied by advanced nuclear energy technologies and renewable or sustainable energy technologies.

Figure 2 shows that before the year 2030, and perhaps as early as 2010, the demand on world oil is such that supply cannot keep pace, and the world oil supply starts to decline. This scenario is optimistic, since it assumes that world oil use is essentially constant from the present to 2030. However, world oil use is actually increasing, so that the imbalance of oil supply and demand will occur before 2030. If the world energy demand scenario presented above is credible, then the world may have less than 30 years before a significant shortfall in conventional liquid fuel supplies occurs.

THE UNITED STATES ENERGY PERSPECTIVE

Let us now concentrate on the situation in the U.S. The U.S. annually produces about 17 quads of domestic crude oil and natural gas liquids (NGL), and this production is declining. Figure 3 shows a resource depletion scenario from the present to the year 2100 for oil, natural gas, and power from current nuclear plants (nuclear energy from current technologies is assumed to phase out over the time period shown). It is evident from Figure 3 that the declining domestic energy supply, especially liquid fuels, must be made up by expanding petroleum imports or by increasing the use of our domestic coal reserves.

The ability of the U.S. to import oil may be limited. Two import scenarios which may be applied to the U.S. energy situation from now until 2050 are (1) the U.S. will continue to consume 26% of total world petroleum and (2) the U.S. will import a fraction of the world's oil that is proportional to the U.S. GDP compared to the world GDP. In both cases, the supply of oil to the U.S. declines early in the next century.

Two U.S. demand scenarios may be considered. The higher demand scenario is from the EIA, and the essentially constant demand scenario is from the MITRE energy model. Depending on which

scenario is selected, a shortfall in petroleum supply (domestic production plus imports) begins somewhere in the 2005-2015 time period and becomes significant by 2010-2030. The probable shortfall is between 1 and 3.5 million BPD in 2030. This is illustrated in Figure 4.

MEETING THE SUPPLY SHORTFALL

One alternative to meet this supply shortfall is to produce liquid fuels from coal. In direct liquefaction, coal reacts with hydrogen in a hydrogen donor solvent vehicle to produce a distillate product that can be refined into liquid transportation fuels. The product from direct coal liquefaction is easy to refine because it is an all-distillate, low sulfur and nitrogen liquid. Transportation fuels that meet the strict environmental regulations expected to be in force in the next century can be made from domestic coals.

If coal conversion is to play a significant role in alleviating the liquid fuel supply problem before the year 2030, then the liquefaction technologies must be in a state of readiness for commercial deployment about 15 years earlier, because lead times for the introduction of new energy technologies are on the order of 10 to 15 years, even after the technologies are technically ready for commercial deployment. Although direct liquefaction technology has undergone very significant improvements over the past decade and achieved a high level of technical readiness, it is still not cost competitive. Therefore, continuing R&D is needed to reduce costs to meet the target of 2015 for the start of commercial deployment. Further R&D can achieve additional process improvements to permit earlier introduction of coal-derived transportation fuels into the marketplace.

Current liquefaction program activities cover all aspects of technology development from basic and exploratory research through bench-scale operations to proof-of-concept (POC) demonstration. The four integrated elements of the direct liquefaction program are development of the catalytic two-stage direct liquefaction process, coprocessing development, advanced liquefaction concepts development, and POC (3 ton/day) testing of promising technologies.

To help identify the high-cost elements of direct coal liquefaction, DOE contracted with Bechtel⁷ to develop a conceptual commercial design of a direct coal liquefaction facility to produce hydrotreated distillate products from either bituminous or subbituminous coal. The Bechtel design, which represents the current state of the art for direct liquefaction, yielded a cost of about \$34/bbl of crude oil equivalent (COE). Although higher than the present world oil price (WOP) of about \$17/bbl, this cost is significantly lower than earlier estimates of \$40-50/bbl because of process improvements from the R&D undertaken over the last decade. Because direct liquefaction technology is still evolving and additional process improvements are expected, costs will decrease further as improvements are incorporated.

THE IMPACT OF CONTINUING R&D ON DIRECT COAL LIQUEFACTION COSTS

Table 1 shows the elements of cost for the baseline direct liquefaction conceptual commercial plant and the estimated reduction in cost that can be achieved by further R&D. Areas of most importance in reducing costs include decreasing capital investment, improving product yields, and reducing catalyst cost.

Several opportunities are available for reducing capital investment, such as increasing space velocity to reduce the number of liquefaction reactor trains and improving H₂ production. Replacing the current ebullated bed reactors with slurry reactors decreases the COE cost by about \$1-2/bbl. By employing advanced technologies now under development, the capital cost of H₂ production can be decreased by an estimated 12% with a resulting decrease in the COE cost of about \$1/bbl.

Product quality improvement is equally important. One way to do this is to increase the yield of products boiling below 850°F. An increase of 10% in these products will decrease the COE cost by

about \$3/bbl. Catalyst costs are a significant contributor to product costs. If 90% of the catalyst can be recovered and reused, the COE cost will be reduced by about \$2/bbl.

The high probability of achieving the improvements discussed above suggests that a \$6/bbl decrease in the COE price to about \$28/bbl is readily achievable. The R&D strategy is to concentrate efforts over the next few years in the high potential areas listed above. With no further R&D, direct coal liquids will remain at the Bechtel baseline cost of about \$34/bbl of COE, and coal liquids would not be competitive with petroleum until 2030. With continued R&D, the cost of direct liquids will be reduced to about \$28/bbl (\$0.67/gal) and be competitive in 2017, 13 years earlier.

STRATEGY FOR DEVELOPING A COMMERCIAL COAL LIQUEFACTION INDUSTRY
Once cost competitiveness is achieved, the next step is to achieve commercialization. Initial pioneering production of coal-derived transportation fuels will require a capital expenditure of \$3.8 to \$4.6 billion for each plant to produce about 70,000 BPD of liquid fuels; it may require five to seven years to achieve full production. Because of the costs involved, coal-derived liquid fuels will probably not make a major contribution to the nation's transportation fuel needs until a significant imbalance between crude oil supply and demand occurs, expected sometime between 2015 and 2030.

The liquefaction plants to produce coal-derived fuels will be designed to meet the highest standards for environmental compliance. The transportation fuels produced by coal liquefaction technologies will be environmentally superior to their petroleum-derived counterparts and will be capable of meeting all requirements of the 1990 Clean Air Act Amendments. Coal liquefaction technologies can also be utilized to co-convert wastes, such as plastics, to environmentally acceptable fuels.

The key to commercialization will be integration with the existing petroleum refining/distribution infrastructure. In achieving commercialization, two intermediate technologies are important. The first is coprocessing of petroleum-derived wastes (plastics, tires, waste oil) with coal. Development of this technology is being driven by dwindling landfill availability and increases in tipping fees. These additional incentives may permit early implementation of this technology. The second technology is coprocessing of coal with heavy petroleum resids or oils. This technology is seen as being commercially feasible as a mid-term option and is likely to account for the first production of coal-based transportation fuels in existing petroleum refineries.

THE CONTRIBUTION OF DIRECT COAL LIQUEFACTION TO THE U.S. ECONOMY
If construction of coal liquefaction plants can be initiated in the year 2012, one million BPD capacity could be in place by 2030. Although direct coal liquefaction would only provide a portion of the energy mix needed to address the U.S. shortfall, production of high quality transportation fuels from U.S. coal will constitute a new and growing domestic industry that will employ engineering and construction personnel, plant operators, coal miners, and related workers. An estimated 333,000 jobs would be created by a one million BPD industry.

Demonstrating the ability to produce coal-derived transportation fuels at \$28/bbl by the year 2010 could have the effect of moderating the world oil price at \$28/bbl from 2017 onwards with consequent savings to the U.S. economy of up to \$200 billion (1993 dollars) between 2015 and 2030. An R&D program that can reduce dependence on oil imports, help in providing national energy security, provide domestic jobs, and save \$200 billion in balance of payments is a sound investment in the nation's future.

CARBON DIOXIDE EMISSIONS

Concern has been expressed that increased coal use will result in excessive emissions of carbon dioxide into the atmosphere, thereby exacerbating the potential for global warming. Figure 5 shows the

energy mix that will result in no further increase in annual carbon dioxide emissions in the U.S. over the present. This figure shows that, because of the decrease in oil and gas, coal use can be increased substantially after 2015 with no net increase in annual carbon dioxide emissions. Coal use can be increased by about 7 quads over present consumption by 2030 with no further increase in carbon dioxide emissions. If this amount of coal were used for production of liquid fuels, about two million BPD of coal-derived fuels could be produced.

CONCLUSION

Because of the long-term nature of the market opportunity and the consequent long wait for return on investment, without government participation, private industry is unlikely to fund these activities. Therefore, continued government support for laboratory, bench, and POC activities is essential to continue the development of transportation fuels from coal.

The analysis presented in this paper clearly shows that the world will need substantial amounts of "new" energy to continue economic progress in the next century. The U.S. has the opportunity to develop coal liquids technology that will help ensure our continued economic prosperity by creating a new industry with highly skilled jobs and providing opportunity for export of U.S. technology on the world market without compromising environmental quality.

References

1. Energy Information Administration, "Annual Energy Outlook 1995," January 1995.
2. Gouse, S.W., D.Gray, G.C. Tomlinson, D.L. Morrison, "Potential World Development through 2100: The Impacts on Energy Demand, Resources, and the Environment," World Energy Council Journal, December 1992.
3. USGS, 14th World Petroleum Congress, Norway, May 1994.
4. Masters, C.D., "Oil and Gas - Where in the World and Why?" 8th V.E. McKelvey Forum on Mineral and Energy Resources, Houston, TX, February 1992.
5. World Resources Institute, "People and the Environment," Oxford University Press, 1994.
6. Institute of Gas Technology, "World Reserves Survey 1987," 1989.
7. Bechtel and Amoco, "Direct Coal Liquefaction Baseline Design and System Analysis," report prepared for DOE under contract DE-AC22-90PC89857, March 1993.

Table 1. Estimated Cost Impact of Continued R&D on Direct Liquefaction

Cost Elements, \$MM	Baseline 28,776 tpd	Increased Space Velocity	Improvement in Yield	Catalyst Recovery & Recycle	Improvement in Hydrogen Production
Coal Handling	222	222	226	226	226
Liquefaction	941	762	762	822	822
Gas Cleanup/Byprd Rec.	297	297	297	297	297
Product Hydrotreating	107	107	113	113	113
ROSE Unit	46	46	43	43	43
Gasification	334	334	342	342	302
Air Separation	244	244	250	250	220
ISBL Field Cost	2192	2013	2034	2094	2024
OSBL Field Cost	978	978	981	978	968
Total Field Cost	3170	2991	3015	3072	2992
Total Capital	3889	3669	3699	3768	3670
Refined Product Cost, \$/bbl					
Capital*	23.61	22.25	20.37	20.77	20.23
Coal	7.84	7.85	7.51	7.51	7.51
Catalyst	2.57	2.58	2.33	0.23	0.23
Natural Gas	3.59	3.45	2.90	2.74	2.69
Labor	1.66	1.67	1.51	1.51	1.51
Other O&M	0.33	0.33	0.29	0.29	0.30
By-Product Credits	(4.18)	(4.05)	(3.43)	(3.29)	(3.25)
RSP	35.42	34.08	31.48	29.76	29.22
Quality Premium	(1.19)	(1.19)	(1.19)	(1.19)	(1.19)
COE	34.23	32.89	30.29	28.57	28.03
Plant Output, million bbl/yr	24.16	24.16	26.58	26.58	26.58

*Includes maintenance materials, taxes, and insurance.

Depletion Curves for World Resources

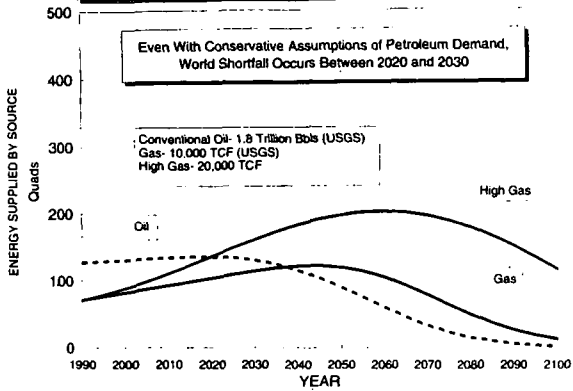


Figure 1

World Energy Mix With Constant Coal Use Nominal Oil and Gas

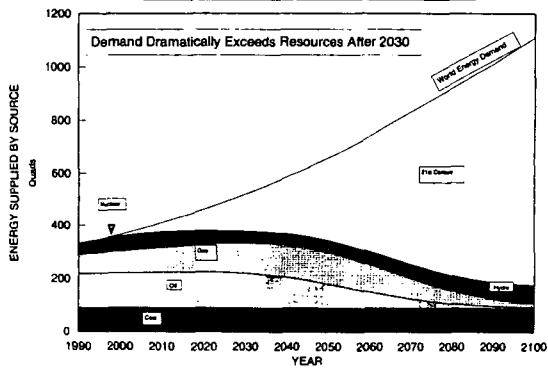
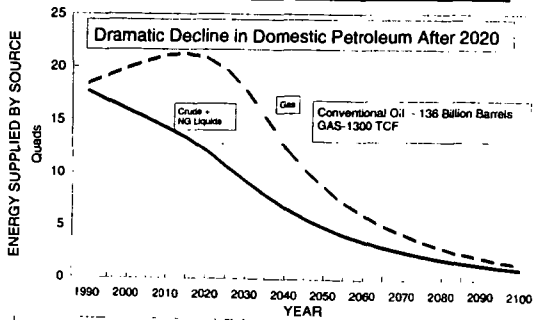


Figure 2

Projected U.S. Energy Production



EIA Projections to 2010 Followed By MITRE Projection Of Resource Depletion

Figure 3

U.S. Oil Supply And Demand Scenarios

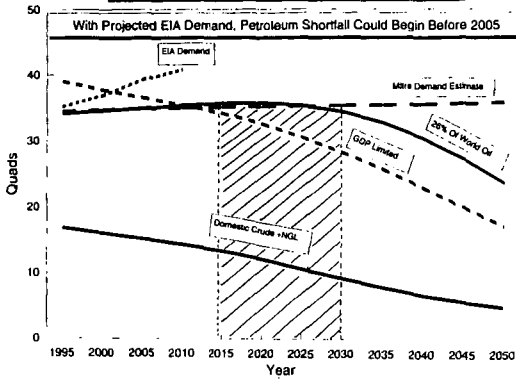


Figure 4

U.S. Energy Mix For Constant Carbon Dioxide Emissions

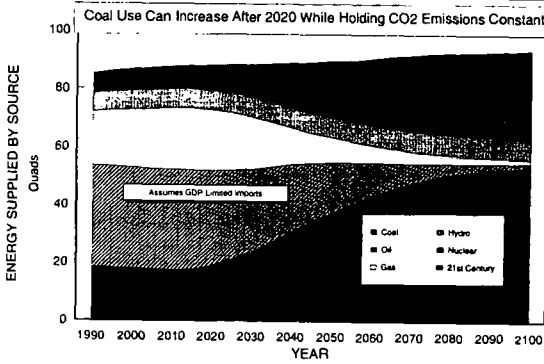


Figure 5

TECHNOECONOMIC ASSESSMENT OF ADVANCED CONCEPTS FOR DIRECT LIQUEFACTION OF SUBBITUMINOUS COALS

Michael Peluso
LDP Associates
32 Albert E. Bonacci Drive
Hamilton Square, N. J. 08690

Keywords: Coal Liquefaction, Advanced Concepts, Economics

INTRODUCTION

For the past three years a group headed by the Center for Applied Energy Research of the University of Kentucky has been investigating, under DOE sponsorship, the use of Advanced Concepts for improving the Integrated Two Stage Liquefaction process practiced at the Wilsonville, Alabama pilot plant(1). Among the concepts tested at the batch scale level were: (1) extraction, dewaxing and hydrotreating of the distillate recycle solvent to improve coal conversion, (2) oil agglomeration of the feed coal to liquefaction to reduce its ash content and improve supported catalyst life, and (3) preparation and use of alternate dispersed and particulate catalysts to improve process performance and/or reduce dispersed catalyst cost.

BASE CASE ASSESSMENT - WILSONVILLE RUN# 263J

Wilsonville pilot plant operation with Black Thunder subbituminous coal was chosen as the basis for defining state-of-the art TSL technology. During Wilsonville Runs #262 & 263, the pilot plant unit was operated in the so-called hybrid mode with dispersed iron and molybdenum catalysts used in the first reaction stage and a supported nickel-moly catalyst used in the second stage ebullated bed reactor. Material balance period #263J was chosen as the basis for developing a baseline conceptual commercial plant case against which the results of this program could be compared(2). An all-distillate product Base Case was formulated in which resid extinction was achieved in the system via a reduction in reactor space velocities as predicted by first order reaction kinetics. All liquefaction distillates are assumed to be upgraded to a common basis (all-gasoline finished product) so that consistent comparisons are assured (3). The Base Case conceptual commercial plant is an all-coal facility located at a mine-mouth Wyoming location. The hydrogen needed for liquefaction is generated by water slurry gasification of ash concentrate from the ROSE unit and coal. Light hydrocarbon gases produced in liquefaction and upgrading are used to close the fuel gas balance. Any excess gas is used to generate hydrogen via the steam reforming process. It is assumed that the electricity needed to help operate the plant is purchased from a nearby utility power plant. A simplified block flow diagram of the conceptual commercial plant is shown in Figure 1. The plant converts 17,929 T/D of Black Thunder coal (MF basis) fed to liquefaction into 68,100 barrels per day(BPSD) of gasoline product. An additional 5,204 T/D of Black Thunder must be gasified in order to meet the plants hydrogen requirements. Overall MAF coal conversion for the Base Case is 92%. A high process solvent to coal ratio of 2.33 is employed since significant quantities of both IOM and ash are recirculated via the ashy recycle technique. Recycled ash is approximately 3.3 times the quantity of ash rejected from the process via the ash concentrate. As a result, the effective concentration of moly on coal to liquefaction is approximately 430 ppm at the Base Case fresh addition level of 100 ppm. Four liquefaction reactor trains in parallel are required to process the 17,929 T/D of coal to liquefaction. Reactor gas rates were determined based on the estimated average reactor partial pressures which existed during Wilsonville Run #263J and the recycle hydrogen gas purity. Actual reactor residence times and space velocities were also based on estimated WR#263J operation with appropriate corrections for the required resid plus IOM conversion level. Organic rejection (i.e. resid, IOM & DAS) from the liquefaction process amounts to 14.5% on an MF coal basis.

ADVANCED CONCEPTS CASE

Three main process variations from the Base Case are incorporated in the ACC. They are:

1. Coal impregnation with moly salt via incipient wetness.
2. Oil agglomeration of the feed coal at low pH, and
3. Distillate solvent quality improvement via solvent extraction, solvent dewaxing and hydrotreating. Used together these three techniques seek to significantly increase product yield per unit of coal feed while reducing solvent recycle rate and liquefaction system additive costs.

• **Coal Impregnation: Moly Salt via Incipient Wetness**

The cost of dispersed iron and moly catalysts in the Base Case accounts for almost \$3/Bbl. of gasoline product selling price. A significant portion of this cost results from the use of an expensive moly source, the oil soluble Molyvan L. A significant reduction in moly cost is achieved when a much cheaper moly salt such as Ammonium Octomolybdate is used. Even when processing costs for preparing the salt solution, impregnating a small portion of the feed coal to liquefaction and driving off the extra water added to the coal are added, the cost of the impregnated moly is still only about 25% of the cost of using Molyvan L. Experimental results indicate that performance with moly impregnated coals is approximately equivalent to the performance with Molyvan L. The cost of using moly for the ACC drops below the cost of using particulate iron oxide at the 1 wt.% on MF coal dosage level of the Base Case. Therefore, the use of iron is questionable and has not been included in the ACC.

• **Oil Agglomeration at Low pH**

Results indicate that the use of oil agglomeration at low pH can remove approximately 50% of the ash in Black thunder coal. Ash reduction at the front end of the liquefaction process reduces organic rejection at the back end of the process, thereby increasing product yield. It also reduces the ash recirculation rate within the process while still maintaining the same catalyst recycle enhancement factor as in the Base Case. At low pH, potential supported catalyst poisons, such as calcium, sodium, magnesium and potassium are also removed. For the ACC it has been assumed that the second stage reactor supported catalyst replacement rate can be reduced by 30%. Tests have indicated that impregnated iron and moly are retained on the coal during agglomeration. The oil agglomeration process is well suited for liquefaction. Distillate recycle solvent can be used as the agglomerating agent. Sour water can be used as makeup water to the system and the slurry reject of solids and dissolved salts can be utilized in the gasification slurry mixing systems. In fact, the dissolved salts may even act as a catalyst in the gasification process. A significant amount of sulfuric acid is consumed in the oil agglomeration unit.

• **Distillate Solvent Quality Improvement**

For the ACC, three process steps are used to treat the waxy distillate recycle solvent used in the Base Case. These processes are Solvent Extraction, Solvent Dewaxing and Hydrotreating. In combination these processes effectively remove and recover the waxy material from the distillate solvent and enhance its donor solvent capabilities (see Figure 3). Both solvent extraction and solvent dewaxing are commercial processes used in the petroleum refining industry.

The benefit of applying these three processes are:

1. Reduction of distillate solvent recycle while improving quality
2. Recovery of a valuable byproduct wax
3. Increased product yield via coal conversion improvement.

It is estimated that the wax yield on MAF coal is 4 wt.%. However, this wax builds up in the distillate recycle solvent until its cracking rate equals production rate. Based on Wilsonville Run#263J data the wax concentration in the distillate recycle solvent is estimated to be approximately 24 wt.%. Removal of a substantial portion of the wax, significantly reduces the distillate solvent recycle rate. The wax that is removed and recovered is a valuable material with an estimated selling price (34¢/lb.) more than double that of gasoline. The solvent extraction process is used upstream of the solvent dewaxing process as a means of significantly reducing the feedrate and the cost of the much more expensive solvent dewaxing process. In the solvent extraction process, a solvent such as N-Methyl-2-Pyrrolidone is used to absorb aromatics from the feed stream. The paraffinic wax is not absorbed and passes thru the unit. For the ACC approximately 70% of the distillate solvent feed to the extraction unit is absorbed, thereby reducing the solvent dewaxing unit feedrate by a factor of 3. In the solvent dewaxing process,

the paraffinic wax is separated from the feed stream by chilling, precipitation and filtration in the presence of a suitable solvent such as methyl ethyl ketone (MEK). When wax production is desired, as in the ACC, a three stage filtration system is used along with a wax finishing step. Conventional fixed bed hydrotreating is used to make the final improvement in distillate solvent quality. For the ACC, a single train system operating at conditions favorable to aromatics hydrogenation (650 to 7500F & 1,800 psig) is used.

The average MAF coal conversion improved 2.4 percentage points when the distillate recycle solvent was fully dewaxed and hydrotreated as compared to using the as-is distillate solvent. Hydrogen uptake in the small scale hydrotreating runs was less than half of what was expected based on Exxon EDS operation. For the ACC it is assumed that the full dewaxing and hydrotreating of the distillate recycle solvent will improve MAF coal conversion by 3 percentage points (95% vs 92% in Base Case). This improvement further increases product yield and reduces the IOM recycle rate.

COMPARATIVE RESULTS

A simplified block flow diagram of the ACC is shown in Figure 2. At the same coal feedrate to liquefaction, gasoline production increases by 4.5% while a significant quantity of the valuable wax byproduct is also recovered. This increase in product yield is directly related to the reduction in Rose unit organic rejection by 6.0% on MF coal. At the same time, recycle solvent rate is reduced by 20% because of wax removal, lower feed ash and higher coal conversion. Moly catalyst recirculation enhancement remains constant. In order to achieve higher product yield, the required per pass resid plus IOM conversion increases in both reaction stages. This increased conversion is achieved by a space velocity reduction (predicted by first order kinetics) of approximately 15% versus the Base Case. Although reactor space velocities are lower, reactor weights are only slightly higher due to the offsetting effect of lower recycle solvent rates. Hydrogen consumption increases in proportion to the increased product rate. With the significant decrease in organic rejection, additional gasification of coal is required to close the hydrogen balance. The total electrical power requirement for the ACC increases by approximately 12% due to increased gasification quantities and the requirements of the added units.

The capital and operating cost estimates for the Base Case were developed using the relevant portions of previous liquefaction plant studies, as well as in-house information (4,5,6). Comparative process units capital costs for the ACC are shown in Table 1. Process units investment increases by \$452 million due to the added units and the increased gasification requirements. Interestingly, liquefaction system capital cost decreases despite the higher distillate production rate. As shown in Table 2, the total capital required increases by \$ 522 million over the Base Case. However, as shown in Table 3 net operating costs drop by approximately \$6.94 per barrel of gasoline product due to the lower liquefaction system additive costs and the significant impact of byproduct wax revenue. At a 15% capital charge factor, the required gasoline product selling price for the ACC is \$4.64/Bbl. lower than that for the Base Case.

REFERENCES

1. Center for Applied Energy Research, Phase 1 Final Report (draft), "Advanced Direct Liquefaction Concepts for PETC Generic Units", DOE/PC/91040-55, March 1995.
2. Southern Electric International, Inc., Technical Progress Report, "Run 263 with Black Thunder Mine Subbituminous Coal from Powder River Basin (with Dispersed Slurry/Supported Catalysts)", DOE Contract No. DE-AC22-90PC90033, October 1992.
3. H. A. Frumkin, "Refining and Upgrading of Synfuels from Coal and Oil Shales by Advanced Catalytic Processes - Tenth Interim Report, Revised Stock Balances and Updated Cost Estimates", DOE# FE-2315-115, March 1985.
4. Ashland Synthetic Fuels Inc. and Airco Energy Company Inc., "The Breckinridge Project Initial Effort, Report VIII, Capital Cost Estimate", DOE/OR/20717-8, 1981.
5. Exxon Research and Engineering Company, "EDS Coal Liquefaction Process Development, Phase V, EDS Wyoming Coal Bottoms Recycle Study Design Addendum - Interim Report", DE 84005843, December 1983.
6. Bechtel Corporation, "Draft Final Report on Design, Capital Cost and Economics for the Low Rank Coal Study", DOE Contract No. DE-AC22-90PC89857, October 1994.

TABLE 1
BLACK THUNDER COAL STUDY
ADVANCED CONCEPTS CASE vs BASE CASE
DIFFERENCES IN PROCESS UNIT INVESTMENT

<u>UNIT</u>	<u>Millions of Mid '94 \$:Wyoming Location</u>
OIL AGGLOMERATION	+ 60
COAL SLURRY PREPARATION & DRYING	- 6
FIRST STAGE REACTION SYSTEM	- 23
SECOND STAGE REACTION SYSTEM	- 4
LETDOWN SYSTEM	- 3
VACUUM FRACTIONATION	- 14
ROSE UNIT	- 7
DISTILLATE SOLVENT EXTRACTION	+ 74
DISTILLATE SOLVENT DEWAXING	+ 207
DISTILLATE SOLVENT HYDROTREATING	+ 95
GAS PLANT HYDROGEN RECOVERY & RECYCLE	Same
ASH CONCENTRATE & COAL GASIFICATION	+ 49
OXYGEN PLANT	+ 17
STEAM REFORMER	- 8
MAKEUP HYDROGEN COMPRESSION	Same
UPGRADING UNITS	+ 15
Difference in Process Unit Investment	= + 452

TABLE 2
BLACK THUNDER COAL STUDY
ADVANCED CONCEPTS CASE vs BASE CASE
DIFFERENCES IN TOTAL CAPITAL REQUIREMENT

	<u>Millions of Mid '94 \$: Wyoming Location</u>
PROCESS UNITS	+ 452
OFFSITE UNITS	+ 54
WORKING CAPITAL	Same
START-UP COSTS	+ 8
INITIAL CATALYSTS & CHEMICALS	+ 8
Difference in Total Capital Required	= + 522

TABLE 3
BLACK THUNDER COAL STUDY
ADVANCED CONCEPTS CASE vs BASE CASE
DIFFERENCES IN ANNUAL OPERATING COST

	<u>\$/Bbl. of Gasoline</u>
TOTAL MF COAL: @ \$7.14/T	+ 0.152
PURCHASED ELECTRICAL POWER, @ 4¢/ Kw-hr.	+ 0.364
LIQUEFACTION SYSTEM ADDITIVES :	
- Iron Oxide @ 12¢/lb. & H2S @ 7.5¢/lb.	- 0.802
- Moly Impregnating/ Dispersed Catalyst	- 1.582
- Supported Ni-Moly @ \$3/lb.	- 0.782
MAKEUP DEASHING UNIT SOLVENT	- 0.222
OTHER LIQ'N CATALYSTS & CHEMICALS	+ 0.577
UPGRADING UNITS CATALYSTS & CHEM.	Same
RAW WATER @ \$ 2.50/1,000 Gallons	+ 0.035
ASH DISPOSAL @ \$5/Ton	- 0.007
OPERATING LABOR	+ 0.075
ADMINISTRATION & OPERATIONS SUPPORT	+ 0.013
MAINTENANCE @ 1.5% of TIC + ICC	+ 0.233
INSURANCE & LOCAL TAXES @ 1% of TPC + ICC	+ 0.156
BYPRODUCT CREDITS:	
• Ammonia, Sulfur & Phenols	- 0.019
• Fully Refined Paraffin Wax	- 5.133

Difference in Annual Operating Cost = - 6.942

Diff. in Annualized Capital Cost (15% Cap'l Charge Factor)= + 2.302

ADVANCED CONCEPTS CASE ADVANTAGE = - 4.640

Continuous Bench-Scale Slurry Catalyst Testing Direct Coal Liquefaction of Rawhide Sub-bituminous Coal

R. F. Bauman, L. A. Coless, S. M. Davis, M. C. Poole, M. Y. Wen
Exxon Research and Development Laboratories, Baton Rouge, LA 70805

KEYWORDS: Coal liquefaction, Slurry reactor, Dispersed catalysts.

Introduction

In 1992, the Department of Energy (DOE) sponsored research to demonstrate a dispersed catalyst system using a combination of molybdenum and iron precursors for direct coal liquefaction. This dispersed catalyst system was successfully demonstrated using Black Thunder sub-bituminous coal at Wilsonville, Alabama by Southern Electric International, Inc. The DOE sponsored research continues at Exxon Research and Development Laboratories (ERDL).

A six month continuous bench-scale program using ERDL's Recycle Coal Liquefaction Unit (RCLU) is planned, three months in 1994 and three months in 1995. The initial conditions in RCLU reflect experience gained from the Wilsonville facility in their Test Run 263. Rawhide sub-bituminous coal which is similar to the Black Thunder coal tested at Wilsonville was used as the feed coal. A slate of five dispersed catalysts for direct coal liquefaction of Rawhide sub-bituminous coal has been tested. Throughout the experiments, the molybdenum addition rate was held constant at 100 wppm while the iron oxide addition rate was varied from 0.25 to 1.0 weight percent (dry coal basis). This report covers the 1994 operations and accomplishments.

Objective

The objective of this DOE sponsored project is to test advanced and novel slurry phase catalysts for direct coal liquefaction. These novel slurry phase catalysts were developed in other DOE sponsored research programs. The properties of the catalysts are presented in Table 1. A number of such catalysts have shown initial promise in laboratory-scale research, typically by experimentation in small batch autoclaves. The efficacy and application of these catalysts is expected to be strongly dependent upon the process steps and overall configuration envisioned for a particular liquefaction process. The most favorable catalysts and relevant approaches must be evaluated in a continuous flow bench-scale facility in order to define and verify the steady-state product yield structures in response to operating parameters and process changes.

In order to help guide the research effort a set of goals was targeted. A summary of the major project goals as listed in DOE's Statement of Work is presented below:

- Demonstrate mechanical operability of continuous bench unit.
- Verify suitability of system design, including use of plug flow reactors.
- Define suitable catalyst screening conditions.
- Test three iron catalysts.
- Test two molybdenum catalysts.
- Conduct limited optimization studies.
- Obtain mass and elemental balances for chosen data periods.
- Define product yield structures for chosen data periods.

Process Overview and Simplified Process Flow Plan

The Recycle Coal Liquefaction Unit (RCLU) is located at the Exxon Research and Development Labs in Baton Rouge, Louisiana. RCLU is a highly automated, highly instrumented pilot plant designed to process 34 kg (75 lbs.) of coal per day. It has redundant computer control and data acquisition systems allowing for efficient trouble shooting, data analysis and material balance calculations. Over the years, RCLU has been re-configured many times to meet specific data requirements for coal and heavy hydrocarbon conversion. Hence, RCLU is versatile and easy to re-configure. RCLU has been a very reliable tool in the past, with many runs over 1000 continuous hours. An overview of the process is described below and a simplified process flow plan is presented in Figure 1.

Slurry Mixing

In this process, coal, make-up catalysts, recycle solvent and recycle bottoms are prepared in 6 to 8 hour batches in the mix tank to form a homogeneous feed slurry. The equipment in the slurry mix area are the mix tank, spared recirculation pumps, the coal/bottoms bin and the solvent tank. The mix tank is totally enclosed to prevent dust and vapors from entering the process streams. The slurry temperature is typically held around 135-143 °C (275-290 °F) to ensure an easily pumpable slurry. The pressure is held at atmospheric or slightly above during non-charging periods. However, a vacuum can be drawn on the solvent tank to aid during feed charging. The tank is equipped with a mixer to mix the coal, bottoms, solvent and catalyst. The feed slurry is further mixed by the recirculation pump.

Slurry Feed

The slurry feed section is used to provide continuous slurry flow to the liquefaction reactors. The major equipment in the area include the feed tank, spared recirculation pumps, and high pressure feed pumps. Periodically, the feed tank is charged with a fresh batch of slurry from the mix tank. The slurry is continuously mixed and recirculated to ensure a homogeneous slurry in the feed tank. The high pressure pumps are used to pump a slip-stream of slurry from the recirculation loop to the liquefaction reactors. Typical holding tank operating conditions are 135 - 143 °C (275 - 290 °F) and atmospheric pressure.

Liquefaction Reactors

The liquefaction reactor system consists of a pretreater and two reactors in series and their associated sandbaths. The pretreater consists of two or three 25 mm (1") ϕ 316 stainless steel pipes and each reactor consists of four or six 25 mm (1") ϕ 316 stainless steel pipes. The reactor pipes are 1.22 m (4 ft) in length and are connected by 9.5 mm (3/8") ϕ 316 stainless steel tubing. The reactors operate in an upflow mode and are capable of having interstage hydrogen addition. The sandbaths are electrically heated and are used to control the reactor temperatures.

The slurry is pumped from the feed tank to the pretreater at a rate of 3.6 to 5.5 kg/hr (8 to 12 lbs/hr). The purpose of the pretreater is to activate the catalyst by sulfiding the iron oxide. The catalyst is activated by treat gas containing 10 volume percent H₂S in H₂. The activated slurry leaving the pretreater is blended with pure H₂ treat gas before it is fed to the first stage reactor. Most of the coal is converted to liquid hydrocarbons and gas via a combination of thermal and catalytic processes in the two liquefaction reactors.

The residence time within the pretreater and each reactor can be varied by varying slurry feed rate or by varying the number of reactor pipes in each sandbath. The nominal residence time of the pretreater ranges from 20 to 30 minutes while the nominal residence time of each reactor ranges from 40 to 55 minutes. The pretreater and liquefaction reactors operate at 17.2 Mpa (2500 psig). The pretreater operates between 296 - 302 °C (565 - 575 °F) while the liquefaction reactors operate between 427 - 454 °C (800 - 850 °F). A slight exotherm exists in the first two tubes of the first stage reactor. Otherwise, the reactors operate close to isothermal operation and have minimal pressure drop.

High Pressure Separations

RCLU uses high pressure separation vessels to separate the heaviest fraction of the reactor product from the lighter fraction. The high pressure separations consist of both hot and cold separators operating at slightly below reactor pressure. The hot separator is used to split the reactor effluent into two streams; an overhead stream consisting of gases, water and light oil and an underflow stream consisting of heavy oil and mineral matter. The overhead stream from the hot separator passes through two heat exchangers before entering the cold separator. The exchangers cool the stream, thus condensing some of the light oils which are captured in the cold separator. The hot separator underflow stream proceeds to the bottoms stripper where it is stripped with the offgas from the cold separator. The cold separator underflow stream proceeds to fractionation.

Bottoms Stripping

The bottoms stripper separates nominally 1000 °F- hydrocarbons from heavier hydrocarbons and mineral matter (bottoms). Bottoms are periodically withdrawn into a bucket and allowed to cool and solidify. The bottoms is then crushed and a fraction is recycled to the mix tank. The overhead gas and the stripped hydrocarbons are cooled before going to fractionation.

Fractionation

The cold separator underflow stream and the bottoms stripper overhead stream are combined in the fractionator feed surge tank. The product gas passes through several

flowmeters before the stream is released to the flare vent. A slipstream of the gas is sent to an online process gas chromatograph (GC) system after the flowmeters. The GC system samples the product gas continuously and analyzes the stream for H₂, H₂O, CO, CO₂, N₂, H₂S, O₂, C₁, C₂, C₃, C₄ and C₅+. The information from the product gas flowmeters and GC system are used to develop daily online material balance closures and later for the complete data workup.

The liquid is pumped from the fractionator feed surge tank to a preheater before it is fed to the fractionator. The fractionator is designed to split the nominally 1000 °F- stream into two components, solvent (also called VGO) and light oil. The heavier component has an initial boiling point (IBP) between 550 °F and 650 °F depending upon tower temperatures. The lighter component has a C₅ IBP. The tower underflow stream is periodically removed and partially recycled to the mix tank. The overhead stream is condensed, refluxed and periodically removed.

Material Balancing and Analyses Procedures

Material balances are based on a 24 hour operating period at constant conditions. Ideally, the conditions are at or near steady state before a yield period (material balance period) is initiated. There is a compromise between the number of conditions and the approach to steady state for a given amount of operating time. For these experiments, some approach to steady state was sacrificed for maximizing the number of operating conditions. The yield periods were initiated when the bottoms conversion started to level off.

From past experience at Exxon, the ash content of recycle bottoms provides a good indication of coal conversion level with known feed coal ash content. In typical bottoms recycle pilot plant operations, the ash content of the recycle bottoms are monitored daily in a screening test. The final ash content in the recycle bottoms is conducted by the analytical labs several weeks later. The procedure for both tests are essentially the same. The main differences are that the analytical tests are automated and use a different purge gas. The ash content of bottoms are measured in duplicate by combustion of small samples of bottoms at 950°C for at least three hours. The average ash content of bottoms and known feed coal ash content are input to a computer model with an equation built in assuming 100% ash balance. The model calculates DAF coal conversions and data are plotted daily to monitor the trend of new conditions vs. the previous conditions. In a typical case, a significant change in the coal conversion is observed in the first few days after starting a new condition. The coal conversion gradually levels off in about 3-5 days after the change to the new condition. The yield periods are initiated when the bottoms ash content begins to level off. The screening tests compare well with the analytical lab tests.

Material balances are conducted after a yield period is complete. RCLU utilizes two levels of material balancing. The first level is on-line material balancing and the second level is material balancing that utilizes data reconciliation techniques. The on-line material balances are often completed within 24 hours after the end of the yield period. They are used to guide unit operations, identify data acquisition problems, and provide preliminary product yields leading to the determination of subsequent run conditions.

The raw data and process variables of each yield period are stored in the RCLU computer system. The on-line material balancing program retrieves these raw data from the RCLU computer system along with input data from unit engineers to calculate the overall material balance, DAF coal conversion, hydrogen consumption, and gaseous and distillate yields for each yield period. The input data from unit engineers include moisture and ash contents of feed coal, and percents of 1000°F+ material in the recycle solvent and 1000°F- material in the recycle bottoms. In order to cross-check the data, balances and yields are calculated using three different slurry feed bases. If balances are poor or yields deviate substantially from the expected then the weights and analyses are re-checked for errors. If no errors are found, an investigation is initiated to determine possible unit material losses and/or errors in data acquisition.

The second level of material balancing utilizes the results of the on-line material balances as well as elemental analyses of each feed and product stream, and simulated distillation by gas chromatography (GCD) analyses of hydrocarbon streams. The reconciled balances are usually not finalized until at least three weeks after the end of a given yield period. Reconciled balances are considered the finalized results and are the results most often reported. Once finalized, reconciled results are used to compare the effects of process variables and/or catalysts on product yields and product distribution.

In order to reconcile the data, a mainframe computer program which utilizes geometric programming techniques is used to adjust the data to comply with a set of constraint equations. The objective of data reconciliation is to legitimately adjust data values to balance elemental weights of feed and product streams. Data is therefore adjusted by taking into account the

reliability of each data measurement. Those variables which have poor reliability are preferentially changed in order to achieve data consistency. Neither the constraint equations nor variable reliabilities are changed from yield period to yield period.

Data reconciliation is an iterative procedure that is designed to be used only when "as-measured" balances are good. Typically, data reconciliation requires that the total material balances are between 98 and 102%. However, material balances between 95 and 102% are tolerable. If the balances do not meet the above criterion, the data is re-analyzed for obvious errors and suspect samples are resubmitted for analyses.

Data from any single reconciled yield period should not be used in data comparisons due to operational variations. Rather, the results from several yield periods (≥ 3) at one condition should be used for comparison purposes.

Results and Discussion

Eight conditions were tested during the 1994 operations, covering the impact of solvent to coal ratio, time-temperature trade off, and type and make-up rate of iron oxide catalyst as shown in Table 2. The molybdenum make-up rate remained constant throughout the experiments. However, the source of molybdenum was varied. A summary of the operating conditions are presented in Table 3. Three 24 hour balances (yield periods) were performed at each condition. A summary of the reconciled yields and overall conversion are presented in Table 4. The values shown in Tables 3 & 4 are the average values at each condition.

General Observations

In general, catalyst changes had very small impact on performance. Of all of the changes tested, one process change, reducing the recycle ratio had the most striking impact. Apparently, recycle ratio has more impact on performance than catalyst over the range of the tests. It may be that the constant addition of 100 wppm molybdenum is masking other changes, such as type and amount of iron catalyst addition rate. Discussions with PETC have indicated to us that the constant molybdenum addition rate was specified based on results at Wilsonville.

Reduced Recycle

The impact of reduced recycle is shown by comparing condition 1 with 2A. The total recycle was reduced from 1.92 to 1.65 on dry ash free (DAF) coal. The result was a significant shift towards a heavier product slate, and higher conversion.

Reduced Sulfur Addition Rate

The impact of reduced sulfur addition rate is shown by comparing condition 2A and 2B. The result was a small reduction in gas yields and hydrogen consumption. No other statistically significant changes were observed. While statistically significant, a small systematic error in the feed gas or product gas sulfur content may have clouded the data. Thus our interpretation of the test result is that the reduction in sulfur had no significant impact on yields or conversion.

Increased Stage 1 Temperature and Mass Velocity

The impact of increasing the first stage reactor temperature and the mass velocity can be seen by comparing condition 3 with 2B. Conversion and liquid yields dropped. Conversion went from 88.60 to 86.88 wt % on DAF coal. C₅-1000°F dropped from 59.1 to 56.5 wt% DAF coal. The temperature and mass velocity were increased to make the impact of a better catalyst easier to detect.

Changed Iron Oxide Catalyst

The impact of iron catalyst type, Bailey vs. Bayferrox is shown by comparing conditions 3 and 4. There was an unintended drop in the first stage reactor temperature of about 2 °C during condition 4, otherwise, conditions were held nominally constant. Conversion, gas yield, and hydrogen consumption all dropped significantly. As with all of these tests, the molybdenum addition rate was held steady at 100 wppm on dry coal. Liquid yields held their own and gas selectivity (100 x C₁ to C₄ yield/total conversion) decreased. Directionally this seems to indicate that an improved iron catalyst could lead to a more selective liquefaction process.

Reduced Iron Oxide Addition Rate

The impact of reducing the iron oxide addition rate from 1.0 to 0.25 wt% DAF coal is shown by comparing condition 4 and 5. The temperature control was improved during condition

Table 1
Properties of Slurry Catalysts

Catalyst	Particle Size, Microns	Surface Area, m ² /g	Bulk Density, g/cm ³	Physical Form	Composition wt %
NANOCAT [®] Superfine Iron Oxide (SFIO)	0.003	250	0.05	Reddish-brown powder	100 % Fe ₂ O ₃
Bayferrox PK 5210 Technical Iron Oxide	0.020	123	n/a	Reddish-brown powder	100 % Fe ₂ O ₃
Bailey Iron Oxide	96 wt% <44 μm	n/a	n/a	Reddish-brown powder	100 % Fe ₂ O ₃
MOLYVAN L, Molybdenum containing lubricant	n/a	n/a	1.08	Dark green liquid	8.1 % Mo
MOLYVAN A, Molybdenum containing powder	5 to 10	n/a	1.58	Yellow-orange powder	30.0 % Mo
Ammonium heptamolybdate	n/a	n/a	2.50	White powder	54.3 % Mo

Table 2
Summary of Experimental Design

Condition	Comment	Yield Periods of Interest
1	Initial conditions.	409-411
2A	Reduced solvent to coal ratio compared with initial conditions.	412-414
2B	Reduced H ₂ S treat rate compared with conditions 1 and 2A	415, 416, 418
3	Increased first stage reactor temperature and increased mass flow rate compared with previous conditions.	419-421
4	Switched from Bailey iron oxide to Bayferrox PK5210 iron oxide catalyst.	422-424
5	Reduced iron oxide addition rate from 1.0 to 0.25 wt% on dry coal.	425-427
6	Switched from Bayferrox PK5210 to Mach 1-Nanocat SFIO catalyst.	428-430
7	Switched from organic to inorganic source for molybdenum catalyst and switched back to Bayferrox PK5210 iron oxide.	431-433

Table 3
Summary of Test Conditions

Condition	Fe ₂ O ₃ Type	Fe ₂ O ₃ wt %	Mo Type	S/C: B/C	H ₂ S as S wt %	NRT, min.	Reactor 1 st °C (°F)	Temperature 2 nd °C (°F)
1	Bailey	1.03	Org.	1.07:0.85	5.8	49	430.6 (807.0)	450.6 (843.0)
2A	Bailey	0.99	Org.	0.94:0.71	6.0	53	431.1 (808.0)	451.1 (844.0)
2B	Bailey	1.00	Org.	0.90:0.75	2.7	50	431.3 (808.3)	449.3 (840.7)
3	Bailey	1.02	Org.	0.95:0.79	3.4	41	441.3 (826.3)	450.0 (842.0)
4	Bayferrox	1.00	Org.	0.94:0.76	3.3	41	439.3 (822.7)	449.6 (841.3)
5	Bayferrox	0.25	Org.	0.91:0.80	3.0	41	441.5 (826.7)	450.6 (843.0)
6	Mach 1	0.26	Org.	0.91:0.83	3.1	42	440.9 (825.7)	450.4 (842.7)
7	Bayferrox	0.26	Inor.	0.98:0.85	3.1	41	440.9 (825.7)	450.0 (842.0)

Table 4
 Summary of Reconciled Yields and Conversion,
 (wt% Based on Dry Ash-Free Coal)

Condition	Yield Period	H ₂	C ₁ -C ₄	C ₅ -350	350-650	650-1000	Conversion
1	409-411	-6.12	15.34	14.48	33.93	9.06	88.56
2A	412-414	-6.11	14.51	13.54	32.55	13.57	89.26
2B	415-418	-5.77	13.69	12.86	31.35	14.87	88.60
3	419-421	-5.76	13.31	12.30	29.61	14.59	86.88
4	422-424	-5.43	12.48	12.71	31.33	13.70	85.62
5	425-427	-5.76	14.08	12.24	31.22	13.54	87.01
6	428-430	-5.46	12.82	11.66	30.69	14.67	85.19
7	431-433	-5.65	12.61	12.27	32.14	12.57	85.74

DOE PROOF-OF-CONCEPT DIRECT COAL LIQUEFACTION PROGRAM
Activity of Recovered Catalysts from POC Run No.1

L.K. Lee, A.G. Comolli and E.S. Johanson
Hydrocarbon Technologies, Inc. P.O.Box 6047, Lawrenceville, NJ 08648

Keywords: Coal Liquefaction, Catalyst Activity

INTRODUCTION

In POC Run No. 1 HRI's Catalytic Two-Stage Liquefaction (CTSL) process was evaluated using Illinois No. 6 coal from Crown II Mine in a 3 ton/day process development unit. Solid Separation was accomplished using a vacuum still and subsequently switched to a Kerr McGee residual oil solvent extraction unit (ROSE-SRSM). Akzo AO-60 1/16" extrudate catalyst, a Ni/Mo supported catalyst, was used in both stages. The temperature of the first stage reactor was in the range of 407° to 414°C and about 16° to 27°C lower than that of the second stage. Throughout most of the 57 days operations, catalysts were added and withdrawn from each reactor to maintain consistent process performance. In this paper the activity of the withdrawn catalysts from both reaction stages at selected operation periods is discussed in respect to the degree of carbon lay down and total contaminations.

EXPERIMENTAL

The catalytic activity of fresh and withdrawn catalysts was characterized by its ability to convert a resid containing coal derived liquid to lighter products using a 20 cc shaking microautoclave reactor. As a common test oil the filtered liquid (227-55-23A PFL) that had been obtained during the CTSL Bench Unit operations with Black Thunder Mine coal of Period 23A of Run 227-55, was used. The experiments were all carried out with 13.8 MPa hydrogen pressure, and 30 minutes time after insertion of the autoclave into a fluidized sand bath heater maintained at 440°C. At the end of this time the temperature of autoclave was dropped rapidly by plunging the autoclave into a water bath. The catalyst tested was held in a wire basket in the autoclave and catalyst-oil contact was promoted by the vertical agitation of the autoclave during the experiment. Each experiment used 2 grams of the test oil, and, usually, an amount of oil-free catalyst (toluene extracted) that corresponded to 2 grams of uncontaminated fresh catalyst after correction for the estimated contaminant content, so that the experiments had an approximately common severity of around 30 minutes x grams uncontaminated catalyst/gram test oil.

The product oil was washed from the autoclave and the catalyst using THF as a wash solvent. The THF was removed from the washings by vacuum evaporation using a roto-evaporator in a hot oil bath at 46°C. The residual oil (524°C+) content in the reference oil and product oils were determined by using a TGA procedure. Typically, the 227-55-23A PFL reference oil containing 29.6 W% 524°C+ residual oil, as determined by ASTM D-1160 procedure, was reported as having 29.6-30.6 W% residual oil content by TGA analysis. Several analyses were performed to determine the amount of contaminants on the oil-free catalysts withdrawn during the POC program. These analyses were bulk and particle densities, elemental (CHNS), ignition loss and major metals (Mo, Ni, Fe, Na, Ca).

CARBONACEOUS AND OTHER CONTAMINANTS

Considering four possible methods of using different analyses (particle density, sum of individual contaminants, nickel and molybdenum content) for estimation of the actual contaminant content in the catalysts, these methods do not agree very closely, as follows comparing the average results for the 13 cases where all of the four methods could be used.

Nickel	47.3%	Molybdenum	46.8%
Particle Density	32.6%	Total Measured Contaminants	25.9%

The Ni and Mo analyses appear to be erratic, with a possibility the Mo and Ni contents of the fresh catalyst are not as high as the cited analyses. The difference in apparent contaminant content based on particle density and contaminants analyses, by an average of 6.7% more contamination indicated by the particle density values, could have been caused by failure to determined all of the metallic contaminants. Titanium content of one of the sample (Period 26), which proved to be higher than the Fe, Na, and Ca contents of the first stage catalyst and also higher than the average of those others elements in the second stage catalyst, have been determined. However, the amounts of Ti (as TiO₂) were only 1.6 and 0.7 W%, which were considerably less than the above difference in indicated total contaminants content. Figure 1 compares the amounts of catalyst contamination, Period by Period, based on the latter methods. The actual contaminants analyses persistently indicated more

contamination of the second stage catalyst, but the catalyst density values indicate more contamination of the first stage catalyst. Because it was uncertain that all of the contaminating constituents had been determined by chemical analyses, and uncertainty concerning the reliability of such analyses, the estimated fresh catalyst contents that were used were those indicated by the particle density measurements.

CATALYST ACTIVITIES

The activity of the tested catalysts are expressed as percentage of that of a reference catalyst. The reference catalyst was Criterion C-317 catalyst that had been presulfided with a TNPS/gas oil mixture using a fixed bed. The nominal accuracy of the tests was estimated on the basis of the four pairs of replicate tests, as follows:

Test No.	Catalyst	Relatives Activities (%)	Oil Recovery (%)
72 & 73	Fresh AO-60	70, 70	94, 92
90 & 91	Presulfided AO-60	167, 164	89, 90
99 & 104	Period 33 1st Stage	98, 98	92, 100
97 & 103	Period 33 2nd Stage	62, 62	88, 98

The charge catalyst to Run POC-01, Akzo AO-60 catalyst, when not presulfided was of lower activity (70%) than the reference catalyst. Upon presulfidation with dimethyl disulfide or thionyl polysulfide in tetralin increase the catalyst to 164-167% of the reference catalyst. Similar observation was obtained when Shell S-317 catalyst was presulfided. It's activity increased to 182% of the reference catalyst.

Figure 2 compares the activities of withdrawn catalysts from various periods of Run POC-01. The first samples, Period 1, were less active, 50-62% of the reference activity, than the fresh (unpresulfided) AO-60 catalyst. This pattern was caused by incomplete presulfiding and accumulating of contaminants on the catalysts. These catalysts contained only 35-53% of theoretical sulfur content as compared to values averaging 97% of theoretical sulfur content for catalyst samples later in the run. The activities of the catalysts can be grouped into two regions corresponding to the changes in the operating conditions. In the initial period, Periods 4 to 20, the first and second stage catalysts ranged from 88 to 104 % of the activity of the reference catalyst. There were no on-line catalyst addition/withdrawal in the first 9 operating periods, during which the aging of the catalysts were accelerated to the equilibrium values. Catalyst addition/withdrawals were initiated in Period 10 but on reduced rates on alternate days basis (0.5 lb/ton coal tot he first stage and 1.0 lb/ton coal tot he second stage). The first and second stage temperatures ranged from 399° to 407°C and 427° to 432°C, respectively. Also, the unit was in an ashy recycle mode in the initial periods and was phased out gradually when the ROSE-SRSM solid separation unit was introduced since Period 13. Solid-free recycle mode was implemented from Period 21 onward.

Catalyst samples from the later periods, Periods 26 to 57, were of relatively low activity at 59-72% of the reference catalyst activity. In these later periods, coal feed rate was increased 50% with higher reactor temperatures. The first and second stage temperature were raised by approximately 3° and 5° to 8°C, respectively to cope with the higher coal feedrate. These higher temperatures resulted in higher coke lay down on the catalyst, especially that of the second stage catalyst, as shown in Figure 3. Also, starting from Period 20, catalyst addition rates were increased to target equilibrium values of daily additions of 1.5 and 3.0 lb/ton to first and second stages, respectively.

With the exception of Period 1 catalyst, the activities of the other catalyst samples were largely related to the degree of contamination, as shown in Figure 4. A correlation considering contents of both carbon and other contaminants gave the following equations:

$$\text{Relative Activity} = A + B * W_{\text{carbon}} + C * W_{\text{others}}$$

	A	B	C	Confident Limited (%)
All Catalysts	187.4	-5.11	2.72	>99.99
Without Presulfided Catalysts	179.7	-4.82	2.44	99.91

where, W_{carbon} and W_{others} are the weight percent of carbon and other contaminants on the catalysts, respectively. Despite the lower catalyst replacement rate to the first stage (by a factor 1/2), first stage

catalysts were generally more active than the second stage catalysts by an average of 7%. The relative activity of the first and second stage catalysts appears to be related principally to the lower content of carbon on the first stage catalyst and not to the total amount of contaminants. Excepting the Period 1 catalysts, where the first stage and second carbon contents were virtually the same, in the other six pairs of first and second catalysts (as given in *Figure 3*) the second stage catalyst contained more carbon, by 0.8 to 7.8 W%. The following tabulation gives average values of these factors for the first and second stage catalysts that have been tested:

Stage	Catalyst Activity	Carbon Content (%)	Catalyst Content (%)
First	80	14.56	73.0
Second	72	17.93	75.0

The multiple correlations summarized above indicated that the average activity of the first stage catalysts would be 4% higher than that of the second stage catalysts.

COMPARISON OF EVALUATIONS WITH PROJECTED ACTIVITIES

The residual oil yields in CTSL Bench Unit coal liquefaction operations have been correlated as being dependent on catalyst age by a functionality that assumed catalyst activity declined by a constant proportion for each day of operations at the liquefaction conditions. Projections were calculated for the first and second stage catalyst activities during the course of Run POC-01, using the actual pattern of catalyst addition/withdrawal that occurred during the run. In these calculations, the catalyst deactivation factors for the two stages were based on those given in the Final CTSL topical report. For the interval of Run POC-01, Period 26 through 43, during which equilibrium catalyst addition rates were maintained the average of the microautoclave catalyst evaluation results were lower for the first stage catalyst, and higher for the second stage catalyst, than the projected values. The trends in the evaluated catalyst activities for this interval of the run were directionally in agreement with those of the projections, showing a possible small decline in the first stage catalyst activity and essentially no change in second stage catalyst activity.

However, the evaluation results differ even more markedly from the projected values for the first interval of the run before Period 20 where there were low rates of catalyst addition to "aged" the initial charge of catalysts, and for the final interval of the run after Period 45 where there was no catalyst addition to the second stage with reduced catalyst input to the first stage.

Figure 5 summarizes the results of calculations for projection activities using the first and second stage deactivation factors adjusted to give a close fit to the evaluations for Periods 26, 32, and 43. This figure also includes the experimental evaluations throughout the run. The adjustments of the deactivation factors were approximately 42% higher for the first stage and 51% lower for the second stage, as compared with the CTSL Bench unit factors.

SUMMARY AND CONCLUSION

The un-presulfided form, "fresh", of Akzo AO-60 catalyst was 2.5 times less active in term of converting to lighter products. Due to the addition of "fresh" catalyst directly into the reactor, the equilibrated catalyst activity was only half of the fully presulfided fresh catalyst, while the second stage equilibrated catalyst was even lower and was similar to that of the un-presulfided fresh catalyst. These microautoclave evaluation results correlated with carbon content of the catalyst, and more strongly with total contamination, including metal contamination. A multiple regression correlation indicated significant effects of both carbon content and other contaminants with the greater impact of the carbon content.

ACKNOWLEDGMENT

The authors would like to acknowledge the support of the Pittsburgh Energy Technology Center for providing funding under the contract DE-AC22-92PC92148.

FIGURE 1
CONTAMINATION OF CATALYST DURING RUN POC-01

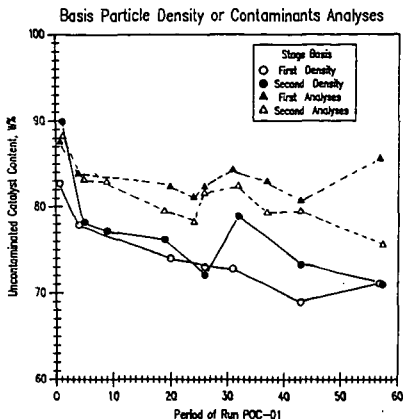


FIGURE 2
RELATIVE ACTIVITY OF RUN POC-01 CATALYSTS

MA Eval. - Analyses THF, Ash-Free Adj. for Excess Oil
Tests With Very High Recoveries Discarded

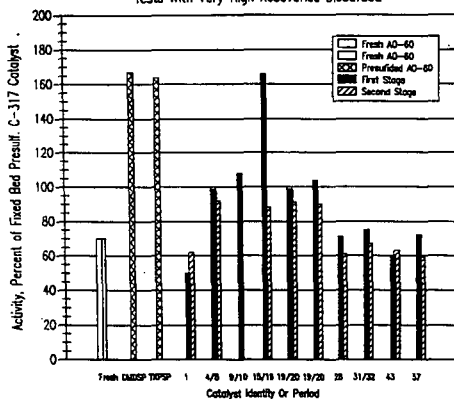


FIGURE 3
CARBON CONTENT OF CATALYSTS DURING RUN POC-01

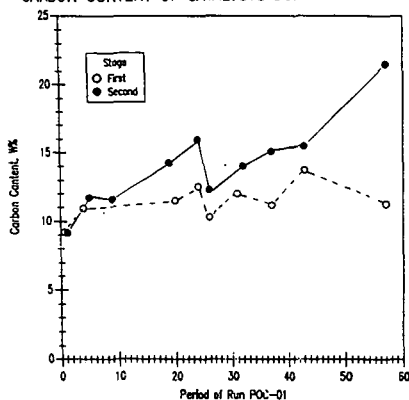


FIGURE 4
 ACTIVITY OF POC-01 CATALYSTS IN MICROAUTOCLAVE TESTS
 Versus Contamination (Basis Particle Density)

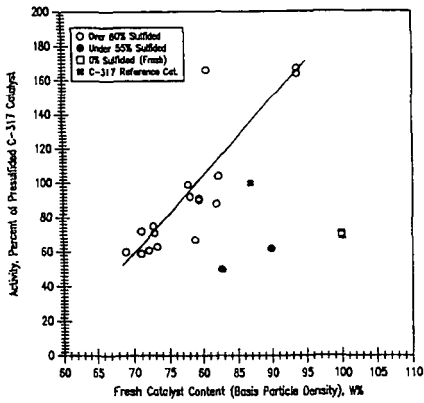
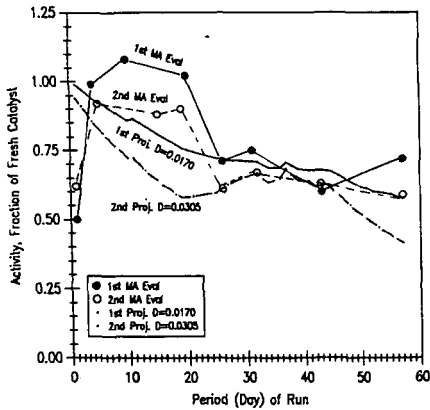


FIGURE 5
 POC-01 CATALYST ACTIVITY - EVALUATIONS AND PROJECTIONS
 Deactivation Factors to Fit Period 26 to 43 Results



PROMOTING COAL HYDROLIQUEFACTION THROUGH CO-USE OF WATER AND DISPERSED MOLYBDENUM SULFIDE CATALYST

Russell Byrne* and Chunshan Song
Fuel Science Program, 209 Academic Projects Building,
The Pennsylvania State University, University Park, PA 16802, USA

Keywords: Coal liquefaction, water, dispersed catalyst, synergism

INTRODUCTION

Work in our laboratory has demonstrated a remarkable synergism between water and a dispersed molybdenum sulfide catalyst for promoting liquefaction of Wyodak subbituminous coal at relatively low temperature (350-375°C). These results appear to be contrary to conventional wisdom regarding the detrimental effects of water during the catalytic hydroliquefaction of coal [1-4]. Our findings, to date, indicate that both reaction temperature range and water/coal ratio are key factors in determining the net influence of water upon the catalytic liquefaction of this particular coal [5-9]. Significantly, we have observed the same promotional trends arising from the co-use of water and dispersed molybdenum sulfide catalyst both in solvent-free experiments, and in liquefaction experiments performed in the presence of either a non-donor (1-methylnaphthalene), or a H-donor (tetralin) [6,9]. In contrast, however, for catalytic runs at higher temperature (400-450°C), using ATTM without added water always gives the highest conversion, either with or without an organic solvent [6,9]. These interesting results have demonstrated unequivocally that within a specific temperature window, and in the correct proportion, water can have a dramatic promoting effect on the catalytic liquefaction of Wyodak subbituminous coal.

Our findings with Wyodak coal have provided the impetus behind an ongoing fundamental and exploratory study on the promotional effects of water on catalytic coal liquefaction. Although the synergistic enhancement in conversion through co-use of water and dispersed Mo sulfide catalyst has been amply demonstrated for Wyodak subbituminous coal, one of our present primary interests is to determine whether this potentially significant phenomenon is observable with other coals, particularly coals of different rank. In this paper preliminary results from recent work using Pittsburgh #8 high-volatile bituminous coal are presented which indicate a similar marked improvement in coal conversion upon addition of a small amount of water in the presence of dispersed molybdenum sulfide catalyst. The overall improvement in conversion observed for the higher-rank coal, however, is somewhat less dramatic than that for Wyodak coal. Reactions performed at two different temperatures (350 and 400°C) are discussed and compared to those for Wyodak coal. Effects of catalyst loading levels are also described.

EXPERIMENTAL

The coals used were Wyodak subbituminous coal and Pittsburgh #8 high-volatile bituminous coal. These are Department of Energy Coal Samples (DECS-8 and DECS-12, respectively) maintained in the DOE/Penn State Coal Sample Bank, ground to ≤ 60 mesh, and stored under argon atmosphere in heat sealed, argon-filled laminated foil bags consisting of three layers. Wyodak subbituminous coal contains 28.4% moisture, 32.4% volatile matter, 29.3% fixed carbon and 9.9% ash, on as-received basis; 75.8% C, 5.2% H, 1.0% N, 0.5% S, and 17.5% O, on dmmf basis. Pittsburgh #8 high-volatile bituminous coal contains 2.4% moisture, 35.2% volatile matter, 52.4% fixed carbon and 10.0% ash, on as-received basis; 84.8% C, 5.7% H, 1.4% N, 0.8% S, and 7.4% O, on dmmf basis. Both fresh raw coals, and coals pre-dried in a vacuum oven (vd) at 100°C for 2h were used. Reagent grade ammonium tetrathiomolybdate (ATTM), obtained from Aldrich with 99.97% purity) was employed as the dispersed catalyst precursor. The water-soluble inorganic salt ATTM is expected to generate molybdenum sulfide particles on the coal surface upon thermal decomposition at $\geq 325^\circ\text{C}$. ATTM was dispersed onto either the raw coal or vacuum-dried coal samples by incipient wetness impregnation from its aqueous solution. The metal loading was kept constant at 1 wt% Mo on dmmf coal basis, unless otherwise specified. Following impregnation, the coal samples were dried in a vacuum oven at 100°C for 2h prior to use.

Liquefaction experiments were carried out in 25 ml tubing bomb reactors with around 4g of coal at 350 or 400°C for 30 min (plus an additional 3 min for reactor heat-up time). For both thermal and catalytic experiments with added water, the weight ratio of water to dmmf coal was kept at around 0.46. All reactions described in this paper were performed in the absence of any organic solvent. The reactors were purged several times with H₂ and finally pressurized with 6.9 MPa H₂ (cold). A fluidized sandbath maintained at the desired temperature was used as the heater. After the desired reaction time, the reactors were removed from the sandbath and quenched in a cold water bath to rapidly bring down the temperature $< 150^\circ\text{C}$, then were allowed to cool down to ambient temperature in air. The reactors were vented and the mass of product gases (including residual H₂) determined. Gaseous products were analyzed by GC, with the aid of gas standards for quantitative calibration of GC responses of CO₂, CO, H₂ and C₁-C₄ hydrocarbon gases. H₂ consumption was determined by subtracting the mass of residual H₂ found in the product gases (determined by GC) from the mass of H₂ initially charged. The liquid and solid products were carefully recovered from the reactor and transferred to an extraction thimble. The products were subsequently separated by sequential Soxhlet extraction into oil (hexane soluble), asphaltene (toluene soluble but hexane insoluble), preasphaltene (THF soluble but toluene insoluble), and residue (THF insoluble). Further experimental details may be found elsewhere [6-8].

RESULTS AND DISCUSSION

Experimental results for the catalytic and non-catalytic solvent-free reactions of Pittsburgh #8 coal, performed in both the presence and absence of added water, are illustrated in Figure 1 (350°C) and Figure 2 (400°C). Equivalent data for Wyodak coal is also given in Figure 3 (350°C) and Figure 4 (400°C), respectively. The catalyst loading level employed in these experiments was 1 wt% Mo on dmmf coal basis. The effects of reducing catalyst loading to 0.1 wt% Mo for reactions of Wyodak coal at 350°C are summarized in Figure 5.

Positive Effect of Added Water in Catalytic Liquefaction at 350°C. Our earlier findings concerning the strong promotional effects of added water on the catalytic liquefaction of Wyodak subbituminous coal at 350°C are exemplified in Figure 3. These results have been previously discussed in detail elsewhere [7]. In brief, it can be seen that adding water to the non-catalytic run of vacuum dried Wyodak coal increased coal conversion from 14.5 to 22.5 wt% (dmmf). Using only ATTM improved coal conversion to 29.8 wt%. When both water and ATTM are used in combination, however, there is a remarkable increase in coal conversion to 66.5 wt%.

Referring now to Figure 1 for the runs of Pittsburgh #8 coal at 350°C, it can be seen that compared to the non-catalytic run of vacuum-dried coal, adding water increased coal conversion from 21.9 to 33.6 wt% (dmmf). Surprisingly, using ATTM at 350°C had little apparent benefit on conversion for this coal, giving a conversion of only 25.1 wt%. This is in stark contrast to the results for Wyodak subbituminous coal. Adding water to the catalytic run, however, significantly increased conversion of Pittsburgh #8 coal to 48.0 wt%, representing a 91% increase from the catalytic run without water, and a 119% increase from the non-catalytic run without water. Clearly, as previously seen for Wyodak coal, there is an apparent synergistic enhancement in conversion at 350°C for Pittsburgh #8 coal resulting from co-use of water and dispersed Mo sulfide catalyst. These interesting findings reveal that dispersed Mo sulfide catalyst and added water can act in concert to promote coal liquefaction at relatively low temperature. It is noteworthy, however, that the overall improvement in conversion observed for the higher-rank coal Pittsburgh #8 is somewhat less dramatic than that for Wyodak subbituminous coal. Considering product quality, it is apparent from Figure 1 that Pittsburgh #8 high-volatile bituminous coal is converted largely to preasphaltenes (ie. THF-soluble but toluene-insoluble) at 350°C. The enhancement in conversion through co-use of water and catalyst is also manifest primarily as an increase in preasphaltene yields. As one might expect, gas yields from Pittsburgh #8 coal (particularly CO₂) are significantly lower than from Wyodak subbituminous coal. Interestingly, however, we observed that CO₂ yields are doubled or even tripled for all reactions with added water. Similar observations have also been made for the hydrous experiments with Wyodak coal [7]. This suggests that water is interacting with certain coal functionalities, ultimately resulting in the evolution of CO₂ through oxidative processes and/or enhanced decarboxylation.

Comparing the conversion data for Pittsburgh #8 (Figure 1) at 350°C to that for Wyodak coal (Figure 3), it is interesting to note that for the non-catalytic reactions, the high-volatile bituminous coal is apparently more reactive than the lower-rank subbituminous coal, both in the absence and presence of water (ie. 21.9 wt% vs 14.5 wt% for anhydrous experiments) and (33.6 wt% vs 22.5 wt% for hydrous experiments), respectively. In contrast, however, for the catalytic reactions, Wyodak coal always gives higher conversion than Pittsburgh #8 (ie. 29.8 wt% vs 25.1 wt% for anhydrous experiments) and (66.5 wt% vs 48.0 wt% for hydrous experiments). These results clearly demonstrate that in the presence of an effective dispersed catalyst, lower-rank subbituminous coals are more reactive than first thought [10], and may in fact be more amenable feedstocks for direct liquefaction than bituminous coals (similar trends are also apparent for the reactions of these coals at 400°C).

Effect of Temperature on Coal Conversion with H₂O and ATTM. For Wyodak coal runs at 400°C (Figure 4), using ATTM without water always gave the highest conversions. The use of ATTM alone at 400°C afforded a very high conversion for this coal (85.4 wt% (dmmf)), and a high oil yield (45.8 wt%), illustrating that, at this temperature, dispersed Mo sulfide catalyst is highly effective at promoting the hydroliquefaction of Wyodak subbituminous coal. However, addition of water to the catalytic run decreased coal conversion (to 62.1 wt%) and oil yield (to 28.2 wt%). An important implication from Figure 4 is that the presence of water at 400°C apparently decreased the effectiveness (or activity) of the dispersed catalyst. This is in distinct contrast to the strong promotional trends observed in the corresponding runs at 350°C.

Considering now the runs at 400°C for Pittsburgh #8 high-volatile bituminous coal (Figure 2), it can be seen that the addition of water to the non-catalytic run of vacuum-dried coal resulted in an increase in conversion from 36.3 wt% to 43.5 wt%. The use of ATTM alone resulted in only a modest increase in conversion (to 54.0 wt%). Adding water to the catalytic run gave a similar conversion to that from the use of catalyst alone (54.9 wt%), though interestingly, did not result in a reduction in conversion as was seen for the catalytic run of Wyodak coal at this temperature. Indeed, addition of water to the catalytic run of Pittsburgh #8 appeared to have some benefit, in terms of product quality, in that there was a notable shift from largely preasphaltenes to an increased yield of asphaltenes isolated in the added water reaction. As was the case for Wyodak coal, however, it is apparent that the strong synergistic enhancement in conversion achieved through co-use of water and dispersed catalyst at 350°C, is lost at higher temperature (400°C). As at 350°C, it is interesting to note that in the absence of catalyst at 400°C, Pittsburgh #8 is apparently more reactive than Wyodak coal. In the catalytic reactions, however, Wyodak coal always gives the

highest conversion. The dispersed Mo sulfide catalyst generated from ATTM does not appear to be a very effective catalyst for promoting the hydroliquefaction of the higher-rank coal.

Effect of Catalyst Loading on Conversion of Wyodak Coal at 350°C. Figure 5 summarizes conversion data for Wyodak coal at 350°C obtained using a reduced catalyst loading of 0.1 wt% Mo on dmmf coal basis. Compared to the original data obtained at a loading of 1 wt% Mo on dmmf coal basis (Figure 3), it can clearly be seen that this reduction in the catalyst concentration significantly reduces the overall effectiveness of the catalyst for promoting conversion of Wyodak coal, both in the catalytic runs and catalytic runs with added water. For the catalytic runs, conversion fell from 29.8 wt% to 20.5 wt%. In the case of catalytic runs with added water, conversion fell from 66.5 wt% to 40.3 wt%. This latter observation indicates that the magnitude of the promotional effect arising through co-use of water and ATTM is not only sensitive to the water/dmmf coal ratio but is also dependent upon the catalyst concentration employed.

SUMMARY

We have found that there are strong synergistic effects between water and a dispersed molybdenum sulfide catalyst (1 wt% Mo on dmmf coal basis) for promoting the low temperature (350°C) liquefaction of both Wyodak subbituminous and Pittsburgh #8 bituminous coals. Relative to the catalytic runs of the dried coal, the co-use of catalyst and water (at water/dmmf coal = 0.46) can more than double the coal conversion at 350°C for 30 min, from 29.8 wt% to 66.5 wt% for Wyodak coal. In the case of Pittsburgh #8 coal, under the same prevailing conditions, the overall improvement in conversion on addition of water to the catalytic run is less dramatic, i.e. from 25.1 to 48.0 wt%. One of the contributing factors to this observation may be that the dispersed Mo sulfide catalyst generated from ATTM is, in general, less effective for promoting the hydroliquefaction of the higher-rank coal. At higher temperature (400°C) the promotional effects of adding water are lost and, in the case of Wyodak coal, actually inhibits catalyst activity resulting in a reduction in conversion. For Pittsburgh #8 coal, adding water to the catalytic run at 400°C results in a similar conversion to that from the use of catalyst alone. There is, however, some apparent benefit in terms of a slight improvement in product quality for the added water reaction. We plan to perform a more thorough study of the effects of reaction temperature (i.e. 325-425°C) on the water-promoted catalytic liquefaction of Pittsburgh #8 coal in order to construct a temperature vs conversion profile, as we have already done for Wyodak coal [5,9]. In this way, we hope to identify the optimum temperature window in which water-dispersed catalyst synergistic interaction is maximized for conversion of Pittsburgh #8 coal.

In the present study, the water/dmmf coal ratio employed was kept constant at around 0.46. This ratio was selected for this preliminary series of reactions with Pittsburgh #8 as it was previously found to be the optimum ratio for Wyodak coal experiments. Clearly, however, it may not necessarily be the most suitable for Pittsburgh #8, we therefore intend to perform a series of catalytic runs at various H₂O/coal ratios in order to determine the optimum ratio for maximizing conversion of this particular coal.

We observed that dropping the catalyst loading, from 1.0 wt% to 0.1 wt% Mo on dmmf coal basis, had an adverse effect on conversion for Wyodak coal at 350°C both for catalytic runs and catalytic runs with added water. The latter finding demonstrates that the magnitude of the promotional effects arising through co-use of ATTM and water is dependent upon the catalyst concentration. We further plan to investigate the effectiveness of a 0.5 wt% Mo catalyst loading.

ACKNOWLEDGEMENT

We are grateful to Prof. H. H. Schobert for his encouragement and support. Financial support was provided by U.S. DOE and U.S. Air Force. We also thank Mr. W. E. Harrison III of AFWL and Dr. S. Rogers of PETC for their support.

REFERENCES

1. Bockrath, B.C.; Finseth, D.H.; Illig, E.G. *Fuel Process. Technol.* **1986**, 12, 175.
2. Ruether, J.A.; Mima, J.A.; Kornosky, R.M.; Ha, B.C. *Energy & Fuels*. **1987**, 1, 198.
3. Kamiya, Y.; Nobusawa, T.; Futamura, S. *Fuel Process. Technol.* **1988**, 18, 1.
4. Weller, S. *Energy & Fuels*, **1994**, 8, 415.
5. Song, C.; Saini, A.K. *Energy & Fuels*, **1995**, 9, 188.
6. Song, C.; Schobert, H.H.; Saini, A.K. *Am. Chem. Soc. Div. Fuel Chem. Prepr.* **1993**, 38, 1031.
7. Song, C.; Schobert, H.H.; Saini, A.K. *Energy & Fuels*. **1994**, 8, 301.
8. Song, C.; Saini, A.K. *Am. Chem. Soc. Div. Fuel Chem. Prepr.* **1994**, 39, 1103.
9. Song, C.; Saini, A.K.; Mc Connie, J. *Proc. of 8th Int. Conf. Coal Science*, Oviedo, Spain, Sept 10-15, **1995**, in press.
10. DOE COLIRN Panel. "Coal Liquefaction", Final Report, DOE-ER-0400, **1989**, Vol. I and II.

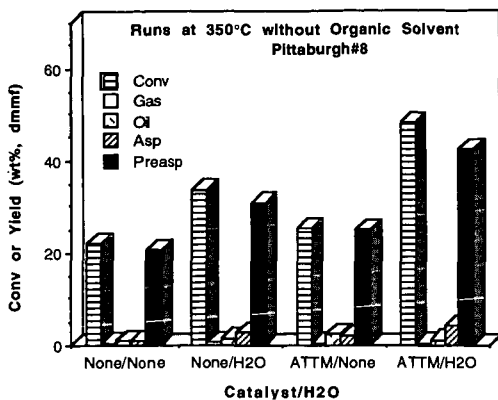


Figure 1 Effect of water on catalytic liquefaction of Pittsburgh #8 coal at 350°C for 30 min.

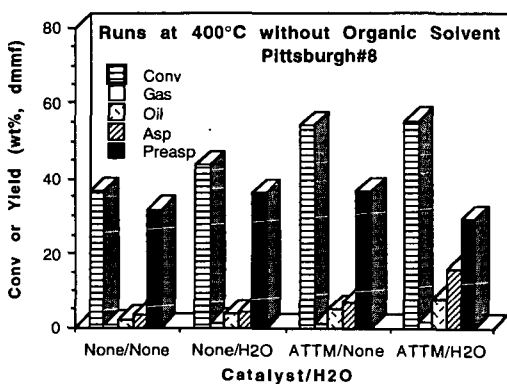


Figure 2. Effect of water on catalytic liquefaction of Pittsburgh #8 coal at 400°C for 30 min.

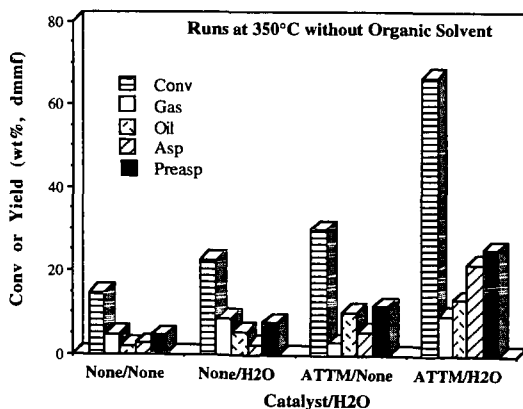


Figure 3. Effect of water on catalytic liquefaction of Wyodak coal at 350°C for 30 min.

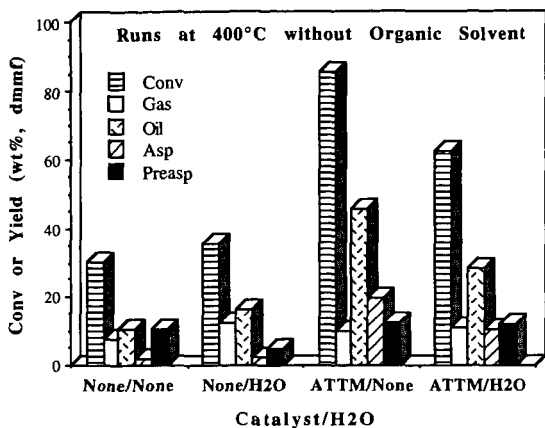


Figure 4 Effect of water on catalytic liquefaction of Wyodak coal at 400°C for 30 min.

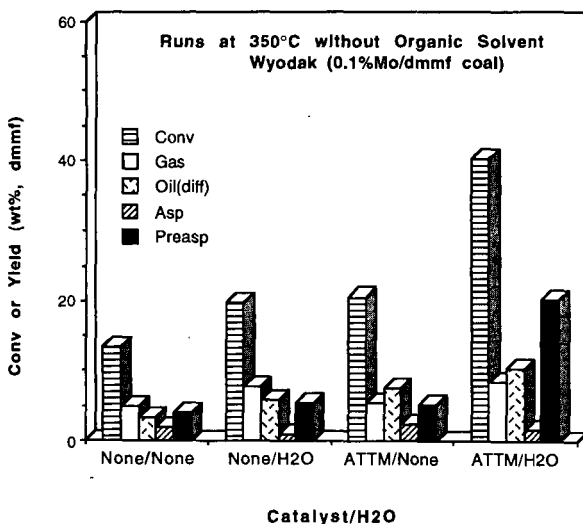


Figure 5 Effect of water on catalytic liquefaction of Wyodak coal using catalyst loading of 0.1 wt% Mo to dmmf coal at 350°C for 30 min.

PROCESS DESIGN OF A NOVEL CONTINUOUS-MODE MINI-PILOT PLANT, FOR DIRECT LIQUEFACTION OF COAL AND UPGRADING OF COAL LIQUIDS

P. Vijay, Chunshan Song*, and Harold H. Schobert

Fuel Science Program
Dept. of Materials Science and Engineering
209 Academic Projects Bldg.
The Pennsylvania State University
University Park, PA 16802-2303

ABSTRACT

On the basis of existing coal liquefaction process units, and our own laboratory research efforts on microautoclave reactor systems, a continuous flow process reactor system for the direct liquefaction of coal and upgrading of coal liquids was designed. In our mini-pilot plant scale process system, two novel technologies have been coupled to improve the economics over existing coal liquefaction processes. The "technologies" incorporated are temperature programmed liquefaction (TPL) of coal and the co-use of water and dispersed metal catalyst in the low-temperature catalytic coal conversion. Details of this continuous-mode process reactor scheme along with its peripheral units will be presented. The progress of this ongoing project will be updated and presented.

Keywords: Direct Liquefaction of Coal, Upgrading of Coal Liquids, and Continuous Flow Process Reactor System.

INTRODUCTION

Extensive research studies on various aspects of the liquefaction of coal including temperature programmed liquefaction (TPL), and effect of water and dispersed molybdenum catalyst for promoting low-severity liquefaction, in the presence of a solvent were conducted earlier [1, 2]. All these batch-mode experiments were successfully conducted in a 25 mL tubing bomb microautoclave reactor. Coal liquefaction experiments in the presence of dispersed catalyst, water, and solvent are currently being performed in a 300 mL batch-mode reactor system.

In order to simulate conditions prevalent in an industrial-type reaction atmosphere, it is necessary to conduct liquefaction of coal and upgrading of coal liquids in a continuous-mode reactor system. Besides, in this system the dispersed catalyst moves with the products rather than staying in the reactor for extended periods, thus enhancing the once-through reactor productivity. The reactor system can be operated in a continuous-mode for a longer time, leading to an increase in the quantity of the products obtained. If the coal liquefaction products stay in the reactor for a prolonged period of time, retrograde reaction occurs that converts desirable small product molecules into less desirable larger macromolecules, by the recombination of small product molecules or by addition of these product molecules back onto the coal [3]. Since the coal liquefaction products that are formed are continuously removed from the flow reactor system, there would be an alleviation in the effect of retrograde reactions thereby increasing the yield and quality of coal liquids, that can be upgraded to produce transportation fuels, particularly jet fuels.

BRIEF OVERVIEW OF EXISTING COAL LIQUEFACTION UNITS

Three of the following well-documented liquefaction processes were studied, before embarking on the process design and assembly of our novel mini-pilot plant reactor system for liquefaction of coal and upgrading of coal liquids.

Advanced Coal Liquefaction Facility at Wilsonville, Alabama. The liquefaction facility at Wilsonville initially operated with two ebullated-bed reactors in series, with supported catalysts in both the reactors [4]. Due to the several well documented advantages of using dispersed catalysts in the 1st reactor [4], a few experiments using dispersed catalysts in the 1st reactor and supported catalysts in the 2nd reactor were conducted. This hybrid catalyst system improved the distillate production by 30-60 %, and increased the coal & resid conversions compared to using dispersed and supported catalysts separately. This Wilsonville Facility was closed down in 1992.

Hydrocarbon Research Institute (HRI) Inc. Unit, New Jersey. The reactor configuration in the HRI unit is similar to that in Wilsonville [5]. Since very few runs were performed in the Wilsonville facility in the hybrid catalyst mode, HRI, Inc. decided to conduct a few more runs with this reactor scheme. An interstage separator was added between the 2 reactors. Experiments were performed using both pure H₂ feed and syngas (H₂ + CO) feed to the 1st reactor, and pure H₂ feed to the 2nd reactor [5]. A higher distillate yield, coal, and residuum conversion were obtained when syngas was used in the 1st stage instead of H₂.

For a few runs an on-line hydrotreater was in service to further remove heteroatoms from the separator and atmospheric still overhead products. The coal conversions were the highest values obtained for this type of coal. The light distillates (IBF-650 °F) contained ten times less nitrogen

* To whom all correspondence should be addressed.

and 17 wt% more hydrogen than that of the 2 ebullated-bed reactors in series configuration. Other studies in the HRI Inc. unit included an addition of a fixed-bed finishing reactor (second or third stage) after the ebullated bed reactors, a three stage CSTR system with an addition of a third ebullated bed reactor in series along with 2 ebullated bed reactors (plug flow simulation), and lowering the solvent/coal ratio to 0.9 in two ebullated bed reactors in series [6].

Pittsburgh Energy Technology Center (PETC) Coal Liquefaction Unit. In PETC, coal liquefaction research studies are being conducted in a computer-controlled bench-scale continuous unit. In this process, coal-catalyst-solvent slurry continuously flows through a 1-liter reactor, where it reacts in the presence of hydrogen to generate coal liquids [7].

PROCESS DESIGN OF A NOVEL CONTINUOUS MODE MINI-PILOT PLANT FOR LIQUEFACTION OF COAL AND UPGRADING OF COAL LIQUIDS

Mini-Pilot Plant for Coal Liquefaction Process

On the basis of existing coal liquefaction units, and our laboratory research efforts in the 25 mL microautoclave reactor system and the 300 mL batch-mode reactor system, a novel continuous flow process scheme for the liquefaction of coal and upgrading of coal liquids was designed. The process flow diagram of this continuous-mode reactor scheme for the liquefaction of coal is presented in Figure 1. The typical operating conditions of the system are shown in Table 1.

The size of the coal particles is small (≤ 60 -200 mesh) in order to reduce mass transfer limitations. The solvent used will either be a process solvent (e.g., Wilsonville middle distillates) or petroleum resids. The advantages of employing dispersed catalysts instead of supported catalysts in the coal liquefaction reactors include, a lesser amount of catalyst, good control of retrogressive reactions at preconversion conditions and hence reducing char formation and catalyst deactivation, reduced reaction severity, faster hydrogen transfer rate, improved economics due to enhanced yields of desired products, and higher coal conversion.

In our process, two novel technologies have been coupled in an attempt to improve the economics over existing coal liquefaction processes. The technologies incorporated are temperature programmed liquefaction (TPL) of coal [1] and the co-use of water and dispersed catalysts in the coal liquefaction process [2]. Studies conducted in the 25 mL microautoclave reactor and in the 300 mL batch-mode reactor scheme, will help to provide some basic information in guiding the selection of the various operating conditions for the continuous unit.

Features of the Continuous Flow Reactor Scheme. The significant features of this novel reactor scheme for the coal liquefaction process are:

- § Use of dispersed catalysts in the coal-solvent slurry.
- § Temperature-programmed liquefaction (TPL) in a multistage (2 stages) reactor scheme.
- § Option of adding water to the coal-catalyst-solvent slurry to the 1st stage reactor.
- § Incorporation of an interstage separator between the two stages of the reactor.
- § A feed gas compression system.
- § Continuous sampling and G.C. analysis of gas and liquid from the slurry lines at several vantage points to periodically monitor the progress of the reaction.

Details of the Multistage Continuous Flow Reactor System for Coal Liquefaction Process.

* **Slurry Feed Mix Tank** - Feed slurry to the reactors consisting of coal, dispersed catalyst, and solvent (or petroleum resids) will be thoroughly mixed in this 3 gallon feed mix tank equipped with an agitator, to maintain this slurry in suspension. The temperature and the pressure of this vessel will be maintained at around 80-100 °C and at 50-80 psi., respectively.

* **Slurry Pump** - The slurry from the feed mix tank will be fed to the reactors through a preheater by the slurry pump. This pump will be capable of handling high concentration of solids loading in slurry (35 wt %) and pressures as high as 4000 psi.

Prior to entering the preheater, the slurry will be contacted by pure feed gas (H_2 or syngas - $H_2 + CO$). CO will be used in an attempt to improve the economics by incorporating the water-gas shift step. Although it is necessary to recycle gas in an industrial-scale process, we have eliminated all recycle gas streams and the compressors in these lines in our design of the laboratory-scale reactor system, due to budget and space limitations.

* **Feed Gas Compression System** - The maximum pressure of the feed gas from the manufacturer's gas cylinders is 2500 psi. Since we will require a steady flow of feed gas at pressures around 2500 psi., it was necessary to design a feed gas compression system. The feed gas (H_2 or syngas - $H_2 + CO$) will flow from the gas cylinders into a pneumatic compressor, where it is compressed to the desired high pressure and stored in the compressed gas storage tanks. The pneumatic compressor will be capable of compressing the inlet feed gas to pressures as high as 5000 psi, depending on the inlet pressure and the desired exit flow rate to the compressed gas storage tanks.

The outlet lines from the compressed gas storage tanks are provided with a vent line, to depressurize the system at the completion of the experimental runs. The outlet from these storage tanks serves as the feed inlet to the reactor system. The feed gas inlet to the slurry line before the preheater, is equipped with a forward pressure regulator and a mass flow controller.

* **Preheater** - The gas and slurry that enters the 300 mL agitated autoclave vessel that serves as a preheater, will be maintained at a temperature of 200-300 °C. The preheated gas and slurry then flows into the 1st stage reactor.

* **1st Stage Coal Liquefaction Reactor** - The 1st stage reactor is a 1-liter vessel equipped with a dispersimax turbine type impeller, that will be maintained at a temperature of 350-400 °C. The gas and slurry entering from the preheater, will undergo primary reactions here.

Provision is made for continuous injection of water from the water feed reservoir (3 gallon), into the 1st stage reactor, with the aid of a water pump. This water reacts with the gas and slurry to form primary products which includes the product vapors and the coal liquids which remains in the slurry. The unreacted gas, product vapors, and slurry (along with the product liquids) then flows into the interstage separator. A sampling loop for G.C. analysis of liquid is provided.

* **Interstage Separator** - This interstage separator is a 1-liter vessel equipped with a turbine type impeller, whose main function is to ensure the complete removal of water remaining in the system. The product vapors exiting this separator flows through a condenser to remove any condensables remaining in the system like H₂O, H₂S, and NH₃, that are collected in the 300 mL liquid collection bomb. The noncondensables (H₂, C₁-C₄) initially flows through a back pressure controller and a flow meter, and then vented to atmosphere. Provision is made for analysis of gas and liquid from this separator.

* **2nd Stage Coal Liquefaction Reactor** - The process stream consisting of gas and slurry from the exit of the interstage separator, and pure gas from the compressed gas storage tank, is the feed to the 2nd stage reactor, which is a 1-liter vessel equipped with a turbine type impeller, and maintained at 400-440 °C. The gas and slurry entering this reactor undergo secondary reactions to form more coal liquids. The reactor effluent flows into a vapor-liquid separator. A sampling line for G.C. analysis of the liquid reacting in the 2nd stage reactor will be installed.

* **Vapor-Liquid Separator** - The gas and slurry products exiting the 2nd stage coal liquefaction reactor flows into the vapor-liquid separator, which is a 1-liter vessel equipped with a turbine type impeller. The gas exiting this separator is first contacted with water from the reservoir and then cooled by a condenser. The condensables fill the liquid collection bomb, which is a 300 mL cylinder. Provision is made for G.C. analysis of the liquid collected in this bomb. The noncondensables initially flows through a back pressure controller and a flow meter, and then vented to atmosphere. Provision is made for G.C. analysis of this gas exiting the V/L separator.

The gas and slurry exiting the vapor-liquid separator initially flows through a condenser, and is then sent through a Bureau of Mines (BOM) valve which will be capable of handling this slurry, at high temperature and high pressure process conditions. The process stream (gas and slurry) then flows into an atmospheric flash tank.

* **Atmospheric Flash Tank** - The effluent from the V/L separator enters the atmospheric flash tank which is a 1-liter agitated vessel. The flow rate of the gas exiting this vessel is measured and then vented to atmosphere. Periodic G.C. analysis of this exiting gas will be performed. The slurry exiting this atmospheric flash tank flows into a coal liquids collector tank.

* **Coal Liquids Collector Tank / Coal Liquids Upgrading Feed Tank** - The slurry exiting the atmospheric flash tank, enters a 3 gallon coal liquids collector tank through a filter bag placed in the process line. This would aid in the separation of solids from the liquid in the slurry stream. The liquids are collected in this tank, which is also the feed tank for the upgrading section of the mini-pilot plant system. The solids containing insolubles, unreacted coal, resids, and catalysts are removed. The coal liquid is then pumped to the upgrading section of the mini-pilot plant.

Mini-Pilot Plant for Coal Liquids Upgrading Process

The schematic of the process flow diagram of the mini-pilot plant for upgrading of coal liquids is presented in Figure 2. The typical operating conditions of the reactor scheme for upgrading coal liquids is shown in Table 1.

Details of Continuous Flow System and Peripheral Units for Coal Liquids Upgrading Process.

* **Coal Liquids Upgrading Feed Tank** - The feed to the reactor consisting of coal liquids from the liquefaction section of the mini-pilot plant will be stored in this 3 gallon feed tank equipped with an agitator. The temperature and the pressure of this vessel will be maintained at around 80-100 °C and at 50-80 psi., respectively.

The coal liquids from this feed tank is pumped through a feed pump, into the Preheater. Please refer to the earlier section regarding details about the pump and the preheater. Prior to entering the preheater, the liquid feed will be contacted by pure feed gas (H₂) from the compressed gas cylinder. The gas and slurry from the preheater flows into the coal liquids upgrading reactor.

* **Coal Liquids Upgrading Reactor** - This reactor is a 1-liter autoclave vessel equipped with a Robinson-Mahoney Spinning Catalyst Basket, and will be maintained at a temperature of 375 - 440 °C. The catalysts in the spinning catalyst basket that will assist in the upgrading reactions, will include conventional supported catalysts, and catalysts prepared in the laboratory, such as mesoporous aluminosilicate molecular sieve based catalysts. Provision is made for periodic analysis of the liquid inside the reactor to monitor the progress of the reaction.

The effluent from this upgrading reactor consisting of unreacted gases, product gases, and upgraded coal liquid products, flows into the vapor-liquid separator. Please refer to the earlier section regarding the detailed functions of this separator.

* **Atmospheric Flash Tank** - The gas and liquid flowing from the V/L separator, flows through a BOM valve and then enters the atmospheric flash tank which is a 1-liter agitated vessel. The flow rate of the gas exiting this vessel is measured and then vented to atmosphere. Periodic G.C. analysis of this product gas and the liquid collected in the vessel will be performed to monitor the progress of the reaction. The upgraded coal liquid stays in the vessel.

STATUS OF THE MINI-PILOT PLANT REACTOR SYSTEM AND FUTURE PLANS

According to the process configuration in the continuous-mode reactor scheme for coal liquefaction and upgrading of coal liquids, a cost estimation for the various individual components and accessories, that includes the reactors, slurry pump, water pump, etc., was performed. According to the cost analysis study and depending on budgetary constraints, the continuous-mode mini-pilot plant scheme will either have only manual controls, or have computer controls for selected equipments, or will be an entirely computerized system.

Several of the major process equipments (reactors, separators, flash tank, feed tanks, water reservoir, slurry pump, water pump, pneumatic compressor, compressed gas cylinders, liquid collection bombs, etc.) were ordered to be delivered from the manufacturers, and a few of them have been received. The other equipments and accessories will be ordered from the manufacturers soon. The assembly of this mini-pilot plant is expected to commence soon.

ACKNOWLEDGMENT

This project was supported by the U.S. Department of Energy, Pittsburgh Energy Technology Center (PETC), and the Air Force Wright Laboratory at the Wright Patterson Air Force Base (WPAFB), Dayton, Ohio. We wish to thank Mr. W.E. Harrison III of WPAFB and Dr. S. Rogers of PETC for their support. We also thank Dr. A. Cugini and Dr. D. Krastman of PETC for the helpful discussions on the liquefaction reactor system.

REFERENCES

1. Song, C., Parfitt, D. S., and Schobert, H. H.; *Energy & Fuels*, Vol. 8, No. 2, 313-319, 1994; Huang, L., Song, C., and Schobert, H.H.; *Am. Chem. Soc. Div. Fuel Chem. Preprints*, 37(2), 223-227, 1992.
2. Song, C. and Saini, A.K.; *Energy & Fuels*, Vol. 9, No. 1, 188-189, 1995; Song, C. and Saini, A. K.; *Am. Chem. Soc. Div. Fuel Chem. Preprints*, 39(4), 1103-1107, 1994; Song, C., Saini, A.K., and Schobert, H.H.; *Am. Chem. Soc. Div. Fuel Chem. Preprints*, 38(3), 1031-1038, 1993.
3. Provine, W. D., Porro, N. D., LaMarca, C., Klein, M. T., Foley, H. C., Bischoff, K. B., Scouten C. G., and Cronauer, D. C.; *Ind. Eng. Chem. Res.*, Vol. 31 (4), 1170-1176, 1992.
4. Lee, J. M., Vimalchand, P., Cantrell, C. E., and Davies, O. L.; *Proceedings of the Liquefaction Contractors' Review Conference*, September 22-24, 1992, Pittsburgh Energy Technology Center, U.S. Department of Energy, pp 35-96.
5. Lee, L. K., Comolli, A. G., Pradhan, V. R., and Stalzer, R. H.; *Proceedings of the Coal Liquefaction and Gas Conversion Contractors Review Conference*, September 27-29, 1993, Pittsburgh Energy Technology Center, U.S. Department of Energy, pp 547-559.
6. Pradhan, V. R., Comolli, A. G., Johanson, E. S., Lee, L. K., Stalzer, R. H., *Proceedings of the Coal Liquefaction and Gas Conversion Contractors Review Conference*, September 27-29, 1993, Pittsburgh Energy Technology Center, U.S. Department of Energy, pp 425-454.
7. Cugini, A. V., Krastman, D., Hickey, R. F., and Lett, R. G.; *Proceedings of the Liquefaction Contractors' Review Conference*, September 22-24, 1992, Pittsburgh Energy Technology Center, U.S. Department of Energy, pp 203-209.

Table 1. Typical Operating Parameters of the Continuous Flow Reactor Scheme

	Coal Liquefaction Reactor	Coal Liquids Upgrading Reactor
Reactor Feed	Subbituminous Coal / Bituminous Coal	Coal Liquids Product from Liquefaction Reactor
Solvent	Wilsonville Middle Distillates	Wilsonville Middle Distillates
Catalyst	MoS ₂ Catalyst from Soluble Precursors (Dispersed State)	Mesoporous Supported Catalysts
Reactor Temperature	1st Stage 350 - 400 °C 2nd Stage 400 - 440 °C	375 - 440 °C
Reactor Pressure	2500 psi of H ₂	2500 psi of H ₂

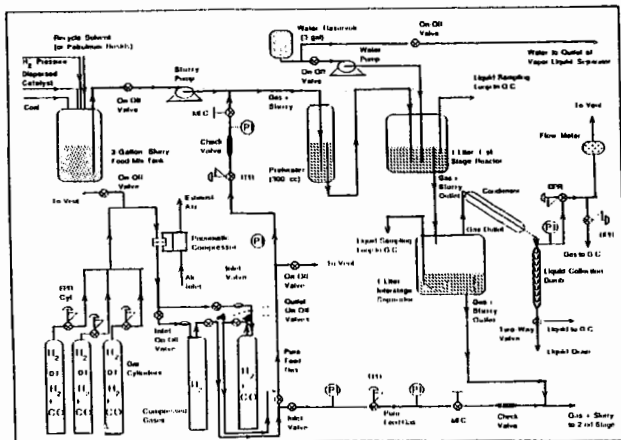


Figure 1. Process Flow Diagram of the Mini-Pilot Plant for Liquefaction of Coal

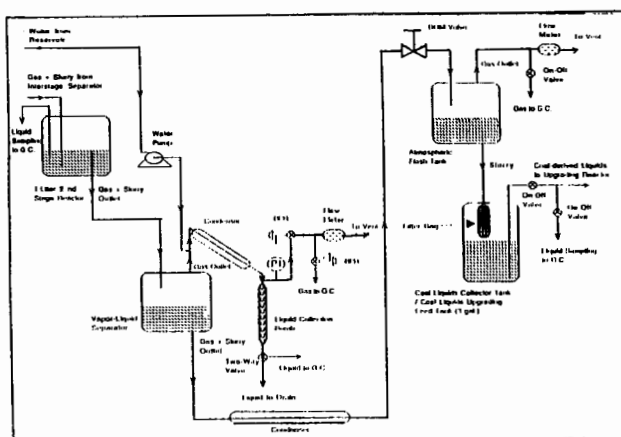


Figure 1 (contd.). Process Flow Diagram of the Mini-Pilot Plant for Liquefaction of Coal

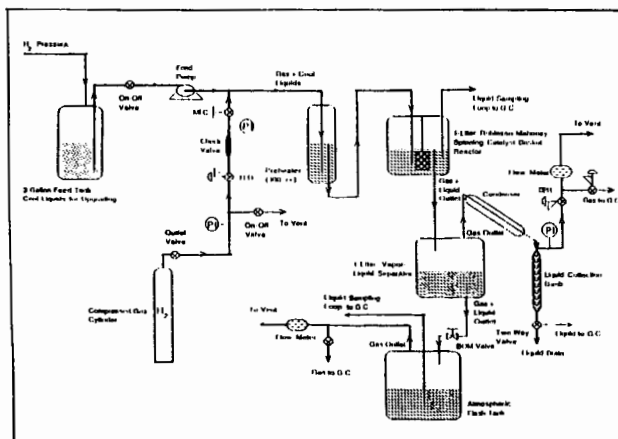


Figure 2. Process Flow Diagram of the Mini-Pilot Plant for Upgrading of Coal Liquids

STRATEGY FOR LARGE SCALE SOLUBILIZATION OF COAL - CHARACTERIZATION OF *NEUROSPORA* PROTEIN AND GENE

Ashish Patel, Y.P. Chen, N.C. Mishra
Department of Biological Sciences
University of South Carolina
Columbia, South Carolina 29208

Key words: coal biosolubilization, involvement of a fungal protein and genetic approach

INTRODUCTION

Coal represents an important source of energy (1,2). Its utilization for generating energy has been offset by environmental problem that it creates by the release of SO_x and NO_x, which are major causes of acid rain and deforestation. Some of these problems can be tackled by the use of industrial scrubbers. However, a biotechnological approach to these problems may prove more efficient and environment friendly. We have employed certain genetically characterized fungi for the biosolubilization of coal in order to yield chemicals that can be converted into utilizable energy and can be rendered free of SO_x and NO_x at the source. Here we describe the purification of a protein which is responsible for the biodegradation of low rank coal both *in vivo* and *in vitro*. We also report the characterization of the biochemical nature of the coal derived products obtained after the biosolubilization of coal by this protein *in vivo* and *in vitro*. Identification and characterization of this fungal protein is expected to help the cloning of the gene encoding this protein which is needed to construct a super strain of *Neurospora* capable of large scale solubilization of coal.

MATERIALS AND METHODS

Neurospora crassa is a very well characterized fungus (3). The wildtype strains of *Neurospora crassa* were used for the *in vivo* solubilization of coal and for the extraction and purification of proteins capable of coal solubilization *in vitro*. The low rank coal used was the North Dakota lignite generously supplied by Dr. Charles Scott of the Oak Ridge National Laboratory. The coal was ground to fine mesh 1-3 mm in size and autoclaved before use. The coal granules were not subjected to any other treatment. The *in vivo* solubilization of coal was determined by the liquefaction of coal granule sprinkled over the fungal mat on a Petri dish obtained after a 5-day growth of *Neurospora crassa*. The *in vitro* solubilization of coal was determined by changes in optical density of coal derived products as measured spectroscopically at 254 nm of UV light in a quartz cuvette after incubation of coal granules with *Neurospora* protein preparation in a microfuge tube containing Bis Tris buffer pH 6.5-7.0.

Protein Purification: *Neurospora* protein capable of coal solubilization was purified by ammonium sulfate precipitation, ion exchange chromatography, and HPLC. The amount of protein was determined by methods of Lowry or Bradford, or spectroscopically via absorption at 280 and 260 nm of light.

Determination of the biochemical nature of the coal derived products: Coal derived products obtained after *in vivo* or *in vitro* solubilization were separated by HPLC or by electrophoresis and then examined by mass spectroscopy to reveal their chemical nature. A large volume of liquid culture was grown with continuous aeration. After five days, the culture was treated with tritone X-100 (conc 0.1-0.5% of total volume). After allowing the reaction to run overnight, the mycelial mass was separated using Whatman 3MM paper. The filtrate (crude extract) was centrifuged to remove any debris; 500 ml of the crude extract was loaded directly on a DE-52 (DEAE cellulose) 3.8x11cm (Whatman Labsales, Hillsboro, OR) column which was pre-equilibrated with 0.1M phosphate buffer (pH 7.0). Proteins were eluted with a linear gradient of NaCl from 0.0 to 1M in 600 phosphate buffer. The protein profiles obtained from the ion exchange column showed several peaks. The enzyme peak eluted at 150 ml was equivalent to approximately 0.25M NaCl. The activity of two fractions was twice that obtained with the crude extract. The enzyme peak was pooled and concentrated by ultrafiltration. This solution was applied to a Bio Rad A 0.5M (BioRad, Richmond, VA) 1.8x68cm column which had been pre-equilibrated with phosphate buffer. Proteins were eluted using the same buffer. The enzymes were analyzed by SDS polyacrylamide gel electrophoresis.

RESULTS

It was found that the coal was biosolubilized both *in vivo* and *in vitro*. The possibility of the solubilization by the ingredients of the media was eliminated by performing the same treatment of coal with the ingredients used to make the media.

In vivo Solubilization: Vogel's and WM media were used to grow *N. crassa* on the plates. After five days of growth, coal particles were scattered on the fungal mat. The coal granules appeared as liquid droplets after three to five days (Fig. 1). Two wildtype strains of *N. crassa* viz. Yeehaw Junction and Everglades were used. It was observed that maximum growth was obtained with Yeehaw Junction and in Vogel's media.

In vitro Solubilization: Liquid cultures were grown with Vogel's minimal media with constant aeration. After five days, the mycelium was separated using Whatman 3MM paper. The filtrate was used for further experiments. 30mg of coal powder was weighed in an Eppendroff tube and 1ml of filtrate was added to it. Absorbance increased with time with maximum increase during the first 4-6 hours. The filtrate was kept in cold room and ammonium sulfate was added slowly to it to a concentration of 90%. Centrifuged at 6000 rpm for 20 minutes. Pellet obtained was collected by mixing with 50mM Bis Tris (pH = 7.0). Supernatant left after centrifugation did not show any activity after being treated with coal. Treatment of coal with the sample (pellet + Bis Tris) showed considerable activity. The sample was passed through Sephadex G-25 and dialyzed against 50mM Bis Tris (pH = 7.0) overnight to remove any salts or low molecular weight substrates, if present. By running a pH gradient, it was observed that low and high pH aggravates the biosolubilization reaction and that pH has minimum effect on the reaction between the range of 6.5-7.0. Elevated temperatures also have similar effects on the solubilization and hence the experiments were carried at room temperature.

Protein Purification: The protein was purified using column-chromatography (as described) and at each stage of purification the samples were subjected to solubilization assay, thus discarding the ones without any activity. Finally, the protein was concentrated by collection in a dialysis bag and then covering it with PEG (4000-8000) from all sides. The concentrated protein was dialyzed overnight against the buffer to remove impurities. Bradford test and the Lowry test performed with this sample gave the concentration to be around 1µg/µl. The protein was analyzed for temperature stability and it was found that it was stable even after treatment to higher temperatures like 80°C for half an hour or more. The amino acid composition analysis shows that it is an unusual protein in which tyrosine was absent but a sugar moiety was present. The SDS gel containing the protein could not be stained with Coomassie blue. But, it was stained with the silver stain.

Product of Coal Solubilization: Nature of the products obtained from biosolubilization of coal was established using HPLC and mass spectroscopy. The products so obtained are described in Table 2. The products obtained by biosolubilization were extracted by Pentane. In the future, extraction will also be performed with acetone, etc., in order to establish the identity of the productions. The products were compared with ones in NBS library for establishment of chemical structures. The products of coal solubilization are mostly hydrocarbons of low molecular weights (see Table 2).

DISCUSSION

A number of fungi have been described to biosolubilize coal (3-7), however, we are the first one to demonstrate the role of a genetically characterized fungus such as *Neurospora* in this process. Here we describe a method for the large scale purification of a protein from a genetically characterized fungus capable of solubilization of coal. The availability of purified proteins in abundant amount will help in determining the N-terminus sequence of the protein (8) required for the generation of the oligonucleotides for the cloning of the gene encoding this protein capable of coal solubilization. Alternatively the large amount of purified proteins will be used to develop antibody against this protein which will be useful for the screening of the *Neurospora* genomic library harboring a clone containing the gene for this protein. Also, here we describe the identification of the coal solubilization product for the first time. Such information will provide an insight into the mechanism of the action of *Neurospora* protein during coal solubilization. These data can be used to develop a bioreactor capable of conversion of coal product into utilizable chemicals (9).

REFERENCES

1. Specks, R. and A. Kughman. 1982. Energy Process 2:2-6.
2. Starr, C., M.F. Searl, and S. Aupert. Science 256:981-986.
3. Mishra, N.C. Advances in Genetics 29:1-62.
4. Scott, C.D., G.W. Strandberg, and S.N. Lewis. 1986. Biotech. Progress 2:131-139.
5. Shepard M. and L. Aterton. 1987. EPRI Journal 12:28-35.
6. Ward, B. 1985. System. Appl. Microbiol. 6:236-238.
7. Fakoussa, R. 1981. Ph.D. Thesis. Friedrich-Wilhelms. University Bonn Germany.
8. Matsudaira, P. 1987. J. Biol. Chem. 262:10035-10038.
9. Faison, B.D. 1991. Critical Rev. Biotech. 11:347-366.

Table 1. *In vivo* biosolubilization

STRAIN	CULTURE MEDIUM	NO. OF COAL GRANULES		% SOLUBILIZATION
		TOTAL	SOLUBILIZED	
Yeehaw	Vogel's Medium	50	47	94
	WM	50	05	10
Everglades	Vogel's	50	13	26
	WM	50	01	02

Table 2. Characteristics of coal derived products

MOLECULAR WT.	POSSIBLE FORMULAS	INFERENCE
84	C_6H_{12}	may be a contaminant sugar molecules present in growth medium
82	C_6H_{10}	hydrocarbons
326	$C_{23}H_{26}$ or $C_{24}H_{38}$ or $C_{26}H_{34}$	hydrocarbons
278	$C_{16}H_{22}O_4$	probably a contaminant from the plastic tube used during the handling of samples

Figure 1. Coal solubilization by *Neurospora crassa*



KINETICS OF COAL LIQUEFACTION AT VERY SHORT REACTION TIMES

He Huang, Keyu Wang, Shaojie Wang, M.T. Klein and W. H. Calkins*
Department of Chemical Engineering
University of Delaware, Newark, Delaware 19716

INTRODUCTION

The direct liquefaction of coal is a complex combination of physical and chemical processes. Initially, extractable material is removed from the coal by the process solvent in an amount that depends upon the coal and the solvent characteristics at the temperature of the process. In the subsequent chemical processes, chemical bonds are cleaved thermally or catalytically to form lower molecular weight products. In competition, bond forming (retrograde) reactions of the coal and coal liquefaction intermediates lead to high molecular weight products. These products can foul catalysts, plug the reactor system, and otherwise obscure the underlying chemical fundamentals. This motivated the investigation of the coal liquefaction process at very low conversions, where secondary and retrograde reactions are minimized and the initial liquefaction products can be isolated and studied. This also permits changes in the still solid but partially reacted coal to be investigated.

The study of coal liquefaction under the typical process conditions of high-temperature and high-pressure requires relatively massive equipment. Such equipment has a high heat capacity and is therefore slow to heat up and cool down. This makes a kinetic study at very low conversion quite difficult. To avoid these problems, a special Short Contact Time Batch Reactor (SCTBR) (1-3) was devised which allows the heat up of the process stream to reaction temperature in less than 1 second. The removal and quenching of the reaction products occurs in a similar time period. This paper presents the results of coal liquefaction kinetic experiments with Illinois #6 coal in this novel equipment.

EXPERIMENTAL

Apparatus and Operation. The reactor system, which has been described previously (1-3), is shown in Figure 1. The reactor itself is constructed of 3/4" stainless steel tubing of approximately 12" in length with a wall thickness of approximately 0.433". The preheater and precooler consist of 21 feet of coiled stainless steel tubing with a wall thickness of 0.035".

In operation, both the empty preheater and the reactor are immersed in a sand bath and brought up to the desired reaction temperature prior to the start of the liquefaction reaction. Using high pressure gas, the reaction mixture is driven into the reactor from a small blow case through the preheater. The temperature of the reactants (ca. 30 ml), initially at ambient temperature, approaches the desired reaction temperature to within 5 - 8 °C in approximately 0.3 sec. It reaches the full reaction temperature within 30 seconds. The temperature in the reactor remains quite constant (within ± 2 °C) throughout the liquefaction experiment. The rapid heat up and stable temperature profile are due to both the small quantity of the reaction mixture relative to the massive reactor and the turbulent flow of the reactants through the preheater.

The liquefaction mixture in the reactor is agitated by gas bubbles introduced from the bottom of the reactor. The degree of agitation is controlled by both regulating the exit gas flow rate from the top of the reactor and the configuration of the gas orifices. A small water cooled condenser is situated above the reactor with a disengaging space above it before the let-down valve to prevent the loss of volatile products from the system and to improve operability.

At a preselected time, the contents of the reactor are driven from the reactor through a precooler into the product receiver with high pressure gas. The total contents of the reactor are not recovered in the receiver (usually only 80 - 90 %) due to the wetting of the walls of the system, and the conversion and other kinetic data are determined by analysis of aliquots.

Product Work-up. The liquefaction products were separated into liquid and partially reacted solids by filtration through a sintered glass filter, and the liquids and solids were analyzed separately. The liquids were bottled and nitrogen blanketed for subsequent analysis. The solids were washed with fresh tetralin (to remove residual coal liquids) and then methylene chloride to remove any tetralin remaining. The washed solids were dried in a vacuum oven at 105°C for 48 hours.

Determination of Percent Conversion. During coal liquefaction, the mineral matter (which is insoluble in tetralin) remains with the partially reacted solid coal and does not go into the liquid (4). When the liquefaction is carried out without catalyst, this provides a means of measuring the conversion of the coal to liquid product by the ash content of the solid residue. The ash content is determined by TGA, and provides the conversion as shown in Eq. 1:

$$\text{Conversion} = \left(1 - \frac{X_0}{X}\right) \times 100 \quad (\text{wt}\%) \quad (1)$$

In Eq. 1, X_0 and X are the ash contents of a control sample and the coal liquefaction residue, respectively. The control sample is the original coal, which is processed exactly as a liquefaction residue except at room temperature. Multiple experiments have shown that the ash content can be determined by TGA with a standard deviation of 0.1%.

When the liquefaction is carried out in the presence of an inorganic catalyst, the conversion calculation must include an ash value corrected for the ash derived from the catalyst.

Catalysts Used. Sulfided molybdenum naphthenate has been the principal liquefaction catalyst used to date. This catalyst has been prepared by dissolving molybdenum naphthenate in tetralin and reacting the solution with methyl disulfide. That this catalyst is only active for liquefaction in the presence of hydrogen is shown in Table 1. Without sulfidation, the molybdenum naphthenate itself is inactive, as is the sulfiding agent.

Table 1 Catalysis of coal liquefaction by molybdenum naphthenate (Illinois #6; 8 of T/C; 390 C; 5 min.)

molybdenum naphthenate g	methyl disulfide g	Mo wt%	Conversion wt%
under 1000 psig nitrogen gas			
0.00	0.00	0.00%	28.1%
0.00	1.03	0.00%	27.5%
0.59	0.00	0.85%	28.0%
0.62	1.07	0.86%	28.4%
under 1000 psig hydrogen gas			
0.00	0.00	0.00%	33.8%
0.00	1.03	0.00%	32.3%
0.61	0.00	0.87%	33.5%
0.61	1.15	0.87%	41.8%

TGA Methods. A typical TG curve and its differential (DTG) for unreacted Illinois #6 bituminous coal at 10°C/min heating rate and 100 ml/min nitrogen gas sweep are shown in Figure 2. The TG curve (solid line) shows a small drop below 200 °C due to loss of moisture. In the neighborhood of 350 - 400 °C, a large loss of weight is observed. When the weight loss has leveled off at 950°C, the temperature is held for 7 minutes. This loss in weight is designated as "Volatile Matter". After oxygen is then introduced, another large drop in weight, designated "Fixed Carbon", follows to a steady weight representing the "Ash Content". The Volatile Matter, Fixed Carbon, and ash

are important parameters to follow during the liquefaction process.

The DTG curve is also of interest since it clearly shows the volatilization processes occurring during the TG analysis. This DTG curve changes very significantly during the liquefaction process as shown in Figure 3.

RESULTS AND DISCUSSION

Figure 4 shows conversion vs time curves for Illinois # 6 coal in nitrogen and in hydrogen in the absence of a catalyst at 390°C. The initial conversion in the first minute is due to the physical extraction of a soluble fraction of the coal into the tetralin, which occurs in both a nitrogen and a hydrogen environment. This is followed by an induction period and then the slow conversion of the coal structure to liquid product. As the liquefaction temperature is increased (Figure 5), the amount of extraction increases and the induction period becomes shorter. In the absence of a catalyst, however, increases in temperature above about 408°C result in little increase in soluble product. The reason for this can be found in the TG analysis of the residue. The rate of removal of Volatile Matter increases steadily as the temperature increases (Figure 6a), regardless of whether the system is in hydrogen or nitrogen. However the Fixed Carbon increases at a very rapid rate above 408 °C (Figure 6b). This is the retrograde process which results in low liquid yields and the formation of tar and coke.

Figure 7 summarizes the conversion vs time for liquefaction of Illinois #6 in

hydrogen at 390°C in the presence of about 1% sulfided molybdenum naphthenate in tetralin. A rapid extraction is again observed in the first minute, followed by the induction period. The subsequent conversion is faster than is observed for the uncatalyzed liquefaction. Figure 8 shows the content of Fixed Carbon in the residue as a function of time. The retrograde process is very significantly reduced. The precursors to the retrograde reactions are apparently being hydrogenated in the presence of hydrogen and the catalyst.

SUMMARY AND CONCLUSIONS

- 1). In the first minute of the liquefaction process, in the presence or absence of a catalyst, and in hydrogen or nitrogen, there is a very rapid conversion to liquid product (approximately 25 - 30 % for Illinois #6 coal) due to the extraction of tetralin-soluble material from the coal into the liquid phase.
- 2). The initial conversion is followed by an induction period and then a slower conversion, presumably of the coal structure itself, which represents the breaking of chemical bonds. This is more rapid in the presence of a sulfided molybdenum naphthenate catalyst.
- 3). At higher temperatures, the degree of extraction is higher and the induction period shorter. However, in the absence of hydrogen and a catalyst, the breakdown of the coal structure into coal liquid is offset by the build up of retrograde products.

ACKNOWLEDGEMENTS

The support of this work by the Department of Energy under DE22-93PC93205 is gratefully acknowledged. The use of Argonne Premium Coal Samples provided by Dr Karl Vorres is also acknowledged.

REFERENCES

1. Huang, H., Calkins, W.H., Klein, M.T., *Prepr. Pap. - Am. Chem. Soc., Div. Fuel Chem.* 1994, 39 (2) 581.
2. Huang, H., Calkins, W.H., and Klein, M.T. *Energy & Fuels* 1994, 8, 1304-1309.
3. Huang, H., Fake, D.M., Calkins, W.H., and Klein, M.T. *Energy & Fuels* 1994, 8, 1310-1315.
4. Calkins, W.H., Huang, H., Klein, M.T. *Proceedings of 1994 Pittsburgh Coal Conference* pp 475-480.
5. Vorres, K.S. 'User's Handbook for the Argonne Premium Coal Sample Program' ANL/PCSP-93/1.

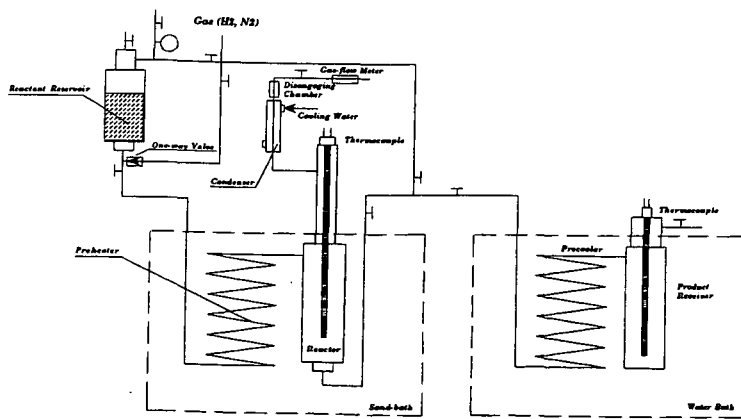


Figure 1 SCTBR system for studying direct coal liquefaction from the initial stages

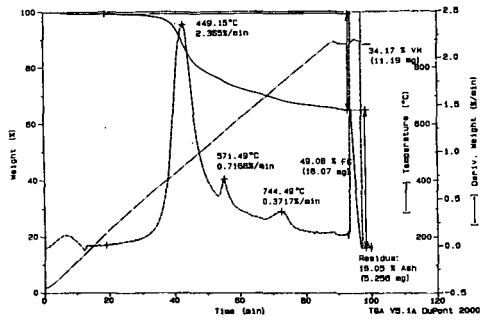


Figure 2 A TG scan on the Illinois #6 coal at 10 °C/min

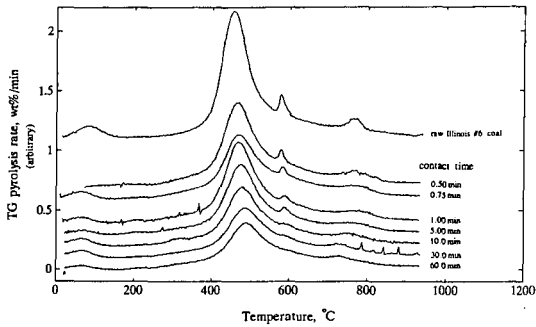


Figure 3 DTG profiles for residues of the Illinois #6 coal after liquefaction in tetralin at the selected contact times (TG scan at 10 °C/min; Liquefaction run at 390 °C under 1000 psig N₂)

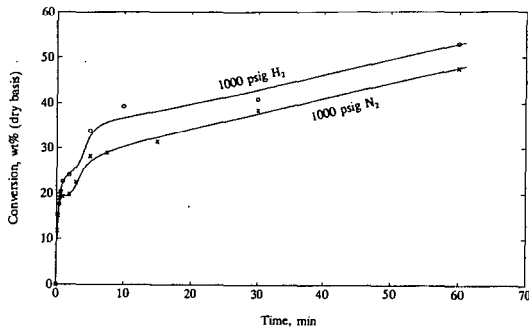


Figure 4 Liquefaction conversion of the Illinois #6 coal at 390 °C

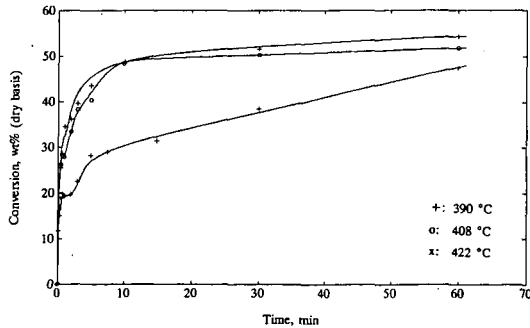


Figure 5 Kinetics of the Illinois #6 coal liquefaction in tetralin under 1000 psig N₂

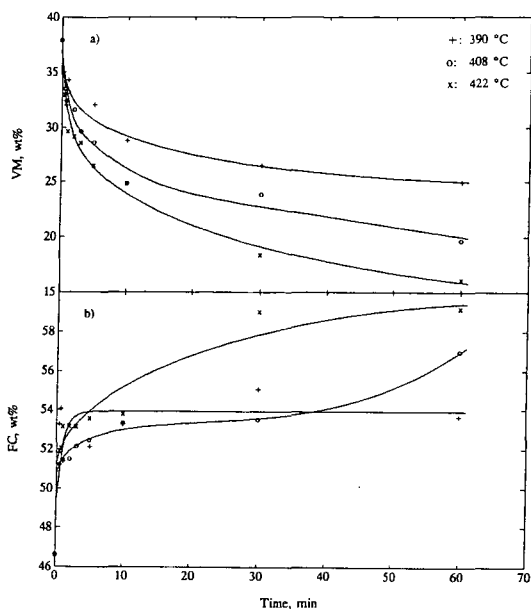


Figure 6 VM (volatile matter) (a) and FC (fixed carbon) (b) in liquefaction residues determined by TGA (Liquefaction: Illinois #6 coal, T:C = 8:1, 1000 psig N₂; TGA: 100 cm³(STP)/min N₂, 100 °C/min)

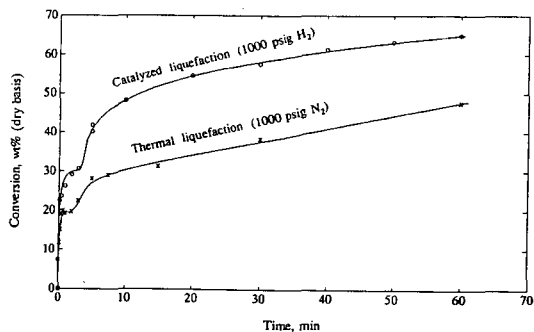


Figure 7 Conversion of the Illinois #6 coal in the thermal and catalyzed liquefaction at 390 °C (Catalyst: ca. 0.9 wt% molybdenum naphthenate; T:C = 8:1)

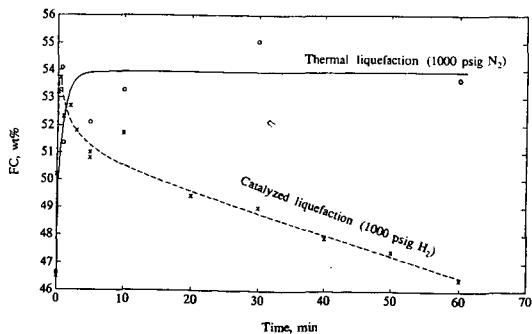


Figure 8 FC (fixed carbon) in liquefaction residues determined by TGA (Liquefaction: Illinois #6 coal, 390 °C, T:C = 8:1; TG scan: 100 cm³(STP)/min N₂, 100 °C/min)

NEW APPROACH TO IMMOBILIZATION OF COAL-MODEL COMPOUNDS ON SILICA USING A CALCIUM CARBOXYLATE LINKAGE

Sreekumar Ramakrishnan
Robert D. Guthrie
Department of Chemistry
University of Kentucky
Lexington, KY 40506

Phillip F. Britt
A. C. Buchanan, III
Oak Ridge National Laboratory
P. O. Box 2008
Oak Ridge, TN, 37381

Burton H. Davis
Kentucky Center for Applied Energy Research
3572 Iron Works Pike, Lexington, KY 40511

Keywords: hydroliquefaction, surface-attached, H/D exchange

INTRODUCTION

In an earlier report,¹ we described our efforts to study the hydrothermolysis of surface-immobilized coal model compounds by attaching 1-(4'-hydroxyphenyl)-2-phenylethane to the surface of fumed silica via a Si-OAr linkage using procedures developed by Buchanan, Poutsma and coworkers² and heating the resultant material (SIO-DPE) under D₂ pressure. These studies were complicated by the fact that phenolic compounds present in equilibrium with ether-linked materials react with thermolytically-produced radicals to form phenoxy radicals which then react with D₂ to give DOAr compounds. These provide D for ring-deuteration via a silica-catalyzed process which is restricted to hydroxyl-substituted aromatic rings. It is believed that the free phenol present in SIO-DPE experiments is due to small amounts of water which is known to be generated continually through the formation of siloxane bonds as silica is heated. In simple thermolysis experiments carried out in vacuum,² any water produced is driven out of the reaction zone. In our experiments, however, the reaction proceeds under D₂ pressure (14 MPa) and reaction products are necessarily available for secondary processes.

Coincident with this process, the benzylic radicals produced under these conditions react with D₂ to form D atoms. The D atoms react both with gas-phase reaction products and surface-attached substrates. We found that much of the behavior of the surface-attached material was similar to that of free diphenylethane, DPE, under these conditions,³ particularly that the differences between thermolysis and hydrothermolysis were preserved. Also, the increased tendency to rearrangement and cyclization for surface-attached radicals was still observed under D₂. Because of the phenol-specific exchange process we could follow the D-atom-induced aromatic substitution only in the non-phenolic rings. We could also demonstrate that the D-atom induced part of H-D exchange is greater for gas-phase than for surface-bound materials.

Despite the successes noted, we sought to find a method for constructing links between silica and organic materials which might better survive hydroliquefaction conditions. Attachment of long-chain aliphatic carboxylic acids to silica through Mg⁺⁺ or Ca⁺⁺ ions is a patented method for silica flotation⁴ which we thought might be adapted to our purposes. This preprint is a preliminary report on the preparation, thermolysis and hydrothermolysis of materials believed to have the general structure, SiO⁻Ca⁺⁺O₂CAr.

EXPERIMENTAL

Preparation of Ca⁺⁺-Linked Arene Carboxylates. Aqueous Ca(OH)₂ (ca. 0.02 M) which had been prepared with deaerated, deionized water was mixed with sufficient fumed silica (Cab-O-Sil M5 Cabot Corporation) to provide a coverage of 0.35 to 0.50 mmoles/g. The aqueous slurry was filtered under an argon blanket and washed with deaerated deionized water. When the filter cake was partially dry, it was remixed with acetonitrile in the filter funnel and the solvent pulled through the filter. This process was repeated and the cake sucked dry under argon. The base-treated silica was then stirred with an acetonitrile

solution of the appropriate carboxylic acid and filtered. The resultant solid was stirred with additional acetonitrile and filtered. The acetonitrile washing was repeated and the coated silica dried in an oven at 110 °C. Evaporation of the combined acetonitrile washings showed that most of the acid was removed by the base-treated silica. In the case of 4-(2'-(4''-methylphenyl)ethyl)benzoic acid, the acid was not completely soluble in acetonitrile and it was necessary to add some methanol. Scanning electron microscopic studies on the DPECO₂-coated material indicated that with the 200 Å resolution of the equipment used, calcium was evenly distributed on the surface.

Synthesis of 4-(2'-Phenylethyl)benzoic Acid. A modified version of a literature procedure⁵ was used. Silver nitrate (2.62 g, 15.4 mmole) in 60 mL water was mixed with sodium hydroxide (1.25 g, 31.2 mmole) in 60 mL water. To this solution was added *trans-p*-stilbene carboxaldehyde, Aldrich Chemical Co. (2.00 g, 9.6 mmole). This was refluxed for 16 h. The reaction mixture was cooled to room temperature and neutralized with concentrated nitric acid. The resultant mixture was extracted with a solvent mixture of equal amounts of CH₂Cl₂ and ethyl acetate. The solvent was removed by rotary evaporation to give 2.11 g of product which was 92 % *trans-p*-stilbene carboxylic acid (86 %). Purification by base extraction and reacidification gave pale yellow crystals, mp 222-223 °C, ¹H NMR (CDCl₃) δ 8.10 (d, 2 H), 7.5 - 7.7 (m, 4 H), 7.1 - 7.4 (m, 5 H). This material (0.475 g, 2.12 mmole) was dissolved in a mixture of 40 mL CH₂Cl₂ and 20 mL methanol. Palladium (5 %) on carbon (200 mg) was added and the mixture shaken under 35 psi H₂ at 25 °C in a Parr apparatus for 24 h. The catalyst was removed by filtration and the solvent removed by rotary evaporation. The product was recrystallized from aqueous ethanol to give a first crop of 280 mg, 58 %, of the desired product, mp 148-150 °C. ¹H NMR (CDCl₃) δ 8.03 (d, 2 H), 7.1 - 7.3 (m, 7 H), 2.92 - 3.04 (m, 4 H). MS, 226, 91. Trimethylsilylation of this material and GC analysis showed it to be >99% pure.

Synthesis of 4-(2'-(4''-Methylphenyl)ethyl)benzoic Acid. This material was synthesized by a Wittig reaction following a literature procedure⁶ using α-bromo-*p*-xylene and 4-carboxybenzaldehyde producing a mixture of *cis*- and *trans*-4-methyl-4'-carboxystilbene which is hydrogenated using the procedure described above for stilbene carboxylic acid. This gives the desired product as white crystals, mp 201-202 °C. ¹H NMR (CDCl₃) δ 7.95 (d, 2 H), 7.1 - 7.16 (m, 4 H), 2.90 - 3.03 (m, 4 H), 2.28 (s, 3 H). Trimethylsilylation of this material and GC analysis showed it to be >99% pure.

General Procedure for Reactions. Hydrogenations of coated solids were carried out in glass tubes with capillary openings in a manner essentially identical to that described earlier¹ for SiO-Ar type materials. Volatile products were pumped out and collected in a liquid N₂ trap and materials remaining on the surface were recovered by hydrolysis of the silica and trimethylsilylation of the carboxylic acids obtained. Deuterium analysis was carried out by gas chromatography/mass spectrometry (GC/MS).

RESULTS AND DISCUSSION

Product distribution for the volatile products of the thermolysis of Ca⁺⁺-immobilized 4-(2'-phenylethyl)benzoate, SiO⁻ Ca⁺⁺ O₂CDPE, is given in Table I. The distribution of products in the residual solid is given in Table II.

Table I. Distribution^a of Volatile Products from Thermolysis of SiO⁻ Ca⁺⁺ O₂CDPE under D₂ and under N₂.

	Time(N ₂ or D ₂)			
	10 min (D ₂)	30 min (D ₂)	50 min (D ₂)	30 min (N ₂)
PhMe	<1%	2.8	5.7	1.1
PhEt	<1%	3.3	4.2	ca. 0.4
DPM	<1%	1.2	1.0	ca. 0.5
1,1-DPE	<1%	1.5	2.2	ca. 1
DPE	78.6	65.7	62.7	94.7
STB	2.6	2.8	2.4	2.3

^a Distribution is given as approximate weight % of total volatiles. The totals are less than

100 % due to the presence of an unidentified product which appears to be an oxidation product of DPE. Some benzene was produced in the reaction but analysis was unreliable in this set of runs. DPM = diphenylmethane, STB = stilbene.

Table II. Distribution^a of Materials Remaining on the Surface after Thermolysis of $\text{SiO}^+ \text{Ca}^{++} \text{O}_2 \text{CDPE}$ under D_2 and under N_2 .

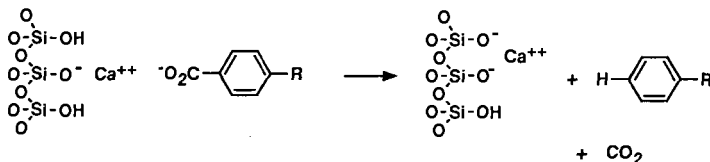
	Time(N_2 or D_2)			
	10 min (D_2)	30 min (D_2)	50 min (D_2)	30 min (N_2)
PhCO_2^-	1.1	1.4	1.3	0.7
MePhCO_2^-	1.4	3.1	4.2	1.7
EtPhCO_2^-	<0.2	0.5	0.7	<0.2
DPMCO_2^-	0.6	1.0	1.1	0.6
1,1-DPECO_2^-	1.8	3.8	5.7	2.7
DPECO_2^-	91.5	86.9	83.9	84.1
STBCO_2^-	3.3	2.5	0.4	3.1

^a Values given are approximate weight %s of materials recovered from hydrolysis of residual solids after trimethylsilylation.

It is clear from these data that the major volatile product of thermolysis, both under N_2 and under D_2 is DPE. This result contrasts with the thermolysis of $\text{SiO}^+ \text{DPE}$ where DPE represents a relatively minor fraction of the volatile products (of the order of 10%). This suggests the possibility that the DPE might be arising by a decarboxylation process.

To determine whether the DPE formed in this reaction is the result of decarboxylation or recombination of benzyl radicals formed from fragmentation, we have also prepared 4-(2-(4'-methylphenyl)ethyl)benzoic acid, HO_2CDPEMe , and attached it to silica in the same manner to give $\text{SiO}^+ \text{Ca}^{++} \text{O}_2 \text{DPEMe}$. Thermolysis of $\text{SiO}^+ \text{Ca}^{++} \text{O}_2 \text{DPEMe}$ both in the presence and absence of D_2 gives 1-phenyl-2-(4'-methylphenyl)ethane, DPEMe , as the major volatile product. A small amount of 1,2-di(4'-methylphenyl)ethane was present, but this was formed in less than 10% of the amount of DPEMe . This clearly demonstrates that decarboxylation is a major reaction path, at least in the initial stages of the reaction. The fact that DPE remains the major product when $\text{SiO}^+ \text{Ca}^{++} \text{O}_2 \text{DPE}$ is subjected to thermolysis under N_2 suggests that protons rather than hydrogen atoms are involved in its production. A reasonable path is that shown in Scheme I wherein the silica surface (directly or indirectly) supplies a proton to the *ipso*-position of the attached substrate, releasing DPE. As this reaction proceeds, the surface should increase in basicity and, possibly, the release of DPE will decrease. The increase in other products relative to DPE supports this hypothesis.

Scheme I



The remainder of the products are analogous to those observed in the thermolysis and hydrothermolysis of $\text{SiO}^+ \text{DPE}$. Toluene, PhMe , results from thermolysis of the central bond in the DPE moiety to give benzyl radicals which react either with D_2 or with residual $-\text{CH}_2\text{CH}_2-$ groups to lead to $\text{PhCH}=\text{CHPh}$, stilbene (STB), or $^-\text{O}_2\text{CC}_6\text{H}_4\text{CH}=\text{CHPh}$, STB-CO_2^- . D atoms produced from the reaction $\text{R} \cdot + \text{D}_2 \rightarrow \text{RD} + \text{D} \cdot$ react to give "hydrocracking" products via $\text{D} \cdot + \text{Ar-R} \rightarrow \text{Ar-D} + \text{R} \cdot$ and also H/D exchange via $\text{D} \cdot + \text{Ar-H} \rightarrow \text{Ar-D} + \text{H} \cdot$. Compared to the $\text{SiO}^+ \text{DPE}$ case, there is more hydrocracking

Table III. Deuterium Distribution in Products from Thermolysis of $\text{Ca}^{++} \cdot \text{O}_2\text{CDPE}$ under D_2 at 420 °C.

Product (time - min)	d_0	d_1	d_2	d_3	d_4	d_5	d_6
PhMe (10)	76.0	23.0					
PhMe (30)	24.9	31.5	23.8	11.4	6.1	2.1	
PhMe (50)	18.6	26.6	29.3	8.1 ^a	10.5 ^a	6.9 ^a	
EtPh (10) → PhCH_2^+	44 58.1	56 33.8	8.1				
EtPh (30) → PhCH_2^+	12.8 29.9	24.1 32.8	21.8 20.8	15.7 10.2	11.7 4.4	8.8 1.6	5.0 0.3
EtPh (50) → PhCH_2^+	8.0 19.5	18.5 30.5	22.5 25.0	19.1 15.0	14.6 7.1	10.7 2.6	6.5 0.3
DPM (30)	18.1	20.5	20.0	15.9	10.6	6.6	3.8
DPM (50)	14.7	18.2	20.7	18.9	13.9	8.9	4.6
1,1-DPE (30)	13.8	14.6	26.5	24.8	16.1	7.9	4.2
1,1-DPE (50)	2.1	7.9	19.3	26.6	22.5	6.3	2.8
DPE (10) → PhCH_2^+	13.5 45.7	45.1 36.8	27.8 13.6	9.6 3.1	2.5 0.6	0.8 0.2	
DPE (30) → PhCH_2^+	5.8 26.4	16.8 31.9	27.9 24.6	24.6 12.1	14.7 3.7	6.5 0.9	2.6 0.2
DPE (50) → PhCH_2^+	3.2 17.9	8.6 25.1	20.1 23.0	26.2 15.4	21.7 6.4	12.4 1.7	5.4 0.3
PhCO₂⁻ (10)	43.1	30.2	19.5	6.2	0.9		
PhCO₂⁻ (30)	16.3	34.2	34.0	12.7	2.2	0.5	
PhCO₂⁻ (50)	9.1	27.1	41.7	18.6	3.6	0.9	
MePhCO₂⁻ (10)	44.6	34.3	14.0	1.8	1.7		
MePhCO₂⁻ (30)	12.9	32.1	32.4	15.5	4.9		
MePhCO₂⁻ (50)	7.2	22.3	34.9	24.1	8.8	2.2	0.5
EtPhCO₂⁻ (10)	41.5	33.8	15.2	6.1	3.4		
EtPhCO₂⁻ (30)	13.1	30.8	31.2	17.1	6.8	0.9	
EtPhCO₂⁻ (50)	4.4	20.4	32.4	26.0	12.5	4.2	
1,1-DPECO₂⁻ (10)	48.3	33.2	12.7	4.2	1.4		
1,1-DPECO₂⁻ (30)	15.7	30.8	31.1	16.3	6.1		
1,1-DPECO₂⁻ (50)	5.2	18.9	32.8	25.2	12.1	4.5	1.4
DPECO₂⁻ (10) → PhCH_2^+	49.5 87.3	35.0 11.3	11.9 1.0	2.7 0.8	0.6		
DPECO₂⁻ (30) → PhCH_2^+	12.8 65.1	30.2 27.9	32.2 5.9	17.0 0.8	5.6 0.2	1.6	0.4
DPECO₂⁻ (50) → PhCH_2^+	3.5 51.2	18.1 35.2	32.0 11.1	27.3 1.9	13.3 0.3	4.4 0.1	1.2

Notes for Table III: ^a Errors accumulate in calculation for toluene at high D content due to large P-1 fragment.

of this substrate and, most strikingly, a marked increase in the amount of rearrangement

of the surface-bound substrate in that 1-phenyl-1(4'carboxyphenyl)ethane, **1,1-DPECO₂H**, has become the major reaction product remaining on the surface. The tendency to increased rearrangement of surface-bound radicals has been discussed earlier.¹

For the runs carried out under D₂, the deuterium distribution of the major products is given in Table III. Many of the features of these data are similar to those noted for hydrothermolysis of **SiO-DPE**. Gas-phase products continue to undergo exchange after separation from the surface so that initially formed **PhMe** (10 min) contains 0.23 atom of D per molecule, more than present in the PhCH₂ part of surface-bound substrate, whereas after 30 min, the D content of **PhMe** averages 1.5 atoms of D per molecule while PhCH₂ in surface-bound substrate averages only 0.43 atoms. It is interesting that the PhCH₂ part of surface-bound **DPECO₂** appears to be protected from exchange relative to gas-phase molecules, showing 0.13, 0.43 and 0.65 atoms of D per molecule in the three runs. These contrast with values of 0.50, 1.32 and 1.69 in the PhCH₂ fragment from **PhEt** and 0.77, 1.38, and 1.53 in this fragment from **DPE**. Thus, PhCH₂ moieties on the surface appear to be less susceptible to D-atom attack by at least a factor of 3 compared with PhCH₂ parts of free molecules. In surface-bound **DPECO₂** exchange in the carboxy-substituted benzyl group exceeds that in the unsubstituted benzyl moiety by a factor of three to four. This could be due either to preference for D-atom attack on the carboxy-substituted ring or to some special mechanism for exchange of carboxy-substituted aromatics. We do not have sufficient evidence to distinguish these alternatives at present.

SUMMARY

A new method for surface attachment has been devised to attach arene carboxylic acids to fumed silica via a SiO⁻ Ca⁺⁺ O₂Ar linkage. This has been used to attach coal-model compounds such as **DPECO₂H** to the surface and the resultant **SiO⁻ Ca⁺⁺ O₂DPE** has been subjected to thermolysis and hydrothermolysis. Part of the material undergoes decarboxylation to give **DPE** and part reacts via the usual homolytic pathways. Radical rearrangement leads to the main surface-retained product and surface-attached molecules are partially protected from D-atom induced exchange. Exchange in carboxy-substituted rings is favored and mechanistic reasons for this are under investigation.

ACKNOWLEDGEMENTS

The authors gratefully acknowledge support from the Department of Energy, Office of Basic Energy Sciences, Division of Chemical Sciences, under Contract No. DE-AC05-84OR21400 with Martin Marietta Energy Systems, Inc. (PFB and ACB) and from the United States Department of Energy, Pittsburgh, for a grant, DE-FG22-91-PC91291 (RDG, SR and BHD).

REFERENCES

1. Guthrie, R. D.; Ramakrishnan, S.; Britt, P. F.; Buchanan, III., A. C.; Davis, B. H. Prepr., Div. Fuel Chem., Am. Chem. Soc. **1994**, 39, 668.
2. Buchanan, A. C., III, Dunstan, T. D. J.; Douglas, E. C.; Poutsma, M. L. J. Am. Chem. Soc. **1986**, 108, 7703-7715.
3. (a) Guthrie, R. D.; Shi, B.; Sharipov, R.; Davis, B. ACS Div. Fuel Chem. Prepr., **1993**, 38, 526-533. (b) Rajagopal, V.; Guthrie, R. D.; Shi, B.; Davis, B. H. ACS Div. Fuel Chem. Prepr., **1993**, 38, 1114. (c) Ramakrishnan, S.; Guthrie, R. D.; Shi, B.; Davis, B. H. ACS Div. Fuel Chem. Prepr., **1993**, 38, 1122. (d) Guthrie, R. D.; Shi, B.; Rajagopal, V.; Ramakrishnan, S.; Davis, B. H., J. Org. Chem. **1994**, 46, 7426-7432.
4. Iler, R. K. "The Chemistry of Silica" Wiley-Interscience, New York, 1979, p. 688.
5. Campaigne, E.; Lesuer, W. M. in *Organic Syntheses*, Coll. Vol IV, N. Rabjohn, Ed., John Wiley and Sons, 1963, p 919.
6. Daniel, H.; LeCorre, M. Tetrahedron Letters **1987**, 28, 1165-1168.

IMPACT OF ORGANIC-MINERAL MATTER INTERACTIONS ON THERMAL REACTION PATHWAYS FOR COAL MODEL COMPOUNDS

A. C. Buchanan, III, Phillip F. Britt, and John A. Struss

Chemical and Analytical Sciences Division
Oak Ridge National Laboratory
P.O. Box 2008
Oak Ridge, Tennessee, 37831-6197

Key Words: Pyrolysis, mineral matter, model compounds

INTRODUCTION

Coal is a complex, heterogeneous solid that includes interdispersed mineral matter. However, knowledge of organic-mineral matter interactions is embryonic, and the impact of these interactions on coal pyrolysis and liquefaction is incomplete.⁽¹⁾ Clay minerals, for example, are known to be effective catalysts for organic reactions.⁽²⁾ Furthermore, clays such as montmorillonite have been proposed to be key catalysts in the thermal alteration of lignin into vitrinite during the coalification process.⁽³⁾ Recent studies by Hatcher and coworkers on the evolution of coalified woods using microscopy and NMR have led them to propose selective, acid-catalyzed, solid state reaction chemistry to account for retained structural integrity in the wood.⁽⁴⁾ However, the chemical feasibility of such reactions in relevant solids is difficult to demonstrate. We have begun a model compound study to gain a better molecular level understanding of the effects *in the solid state* of organic-mineral matter interactions relevant to both coal formation and processing. To satisfy the need for model compounds that remain nonvolatile solids at temperatures ranging to 450°C, model compounds are employed that are chemically bound to the surface of a fumed silica (Si-O-C_{aryl} linkage).⁽⁵⁻⁹⁾ The organic structures currently under investigation are phenethyl phenyl ether (C₆H₅CH₂CH₂OC₆H₅) derivatives, which serve as models for β-alkyl aryl ether units that are present in lignin and lignitic coals. The solid-state chemistry of these materials at 200-450°C in the presence of interdispersed acid catalysts such as small particle size silica-aluminas and montmorillonite clay will be reported. Our initial focus will be on defining the potential impact of these interactions on coal pyrolysis and liquefaction.

EXPERIMENTAL

The synthesis of the precursor phenol, *p*-HOPhCH₂CH₂OPh (HOPPE), has been reported.⁽¹⁰⁾ The *ortho*-methoxy derivative, *p*-HOPhCH₂CH₂OPh-*o*-OCH₃, was synthesized⁽¹¹⁾ by a similar route except the sodium salt of guaiacol, made from guaiacol and NaH in DMF, was used to alkylate the tosylate, *p*-PhCH₂OPhCH₂CH₂OTs,⁽¹⁰⁾ in toluene. The benzyl protecting group was removed by hydrogenolysis with 10% Pd on carbon in CH₃CO₂H with 0.5% H₂SO₄. The phenols were purified to >99.8% (by GC) by elution through a silica column using toluene, followed by multiple recrystallizations from benzene/hexanes.

Detailed procedures for the synthesis of silica-attached diphenylalkanes have been previously described.⁽⁵⁻⁹⁾ Briefly, the precursor phenols were covalently attached to the surface of a dried (200°C), nonporous silica (Cabosil M-5, Cabot Corp., 200 m²g⁻¹, ca. 4.5 OH nm⁻²) by a condensation reaction (225°C, 0.5 h) with the surface hydroxyl groups. For these substrates, unreacted phenol was removed by soxhlet extraction with benzene, rather than high temperature sublimation. The resulting immobilized model compounds are attached to the silica surface by a thermally robust Si-O-C_{aryl} linkage. Surface coverages (ca. 0.25 mmol g⁻¹) were determined by GC analysis using internal standards following a standard base hydrolysis assay.⁽⁵⁻⁹⁾

The silica-immobilized substrates were blended 1:1 with a dried, fumed silica-1% alumina (Aerosil MOX 170, Degussa, 170 m²g⁻¹; 15 nm average particle size), silica-15% alumina (Aerosil COK 84, Degussa, 170 m²g⁻¹), or montmorillonite clay (Montmorillonite K-10, Aldrich, 220-270 m²g⁻¹, <1μ particle size).^(9,11) Similar results were obtained when the solids were either dry mixed or when they were dispersed in benzene followed by solvent evaporation. Thermolyses were performed at 200-450°C (±1.5°C) in sealed tubes under vacuum in a temperature controlled, fluidized sandbath, or in a temperature controlled tube furnace as

previously described.⁽⁵⁻⁹⁾ Volatile products were trapped in liquid nitrogen, and analyzed by GC and GC-MS with the use of internal calibration standards. Surface-attached products were liberated as phenols following digestion of the silica with aqueous base, silylated to the corresponding trimethylsilyl ethers, and analyzed as above.

RESULTS AND DISCUSSION

The two model compounds examined thus far are silica-immobilized phenethyl phenyl ether ($\approx\text{PhCH}_2\text{CH}_2\text{OPh}$, or $\approx\text{PPE}$) and the corresponding methoxy derivative ($\approx\text{PhCH}_2\text{CH}_2\text{OPh-}o\text{-OCH}_3$, or $\approx\text{PPE-}o\text{-OMe}$) as shown in Figure 1. These compounds are models for the β -aryl ether linkages present in lignin and low rank coals. $\approx\text{PPE-}o\text{-OMe}$ contains the guaiacyl unit that is abundant in gymnospermous lignin.⁽¹²⁾

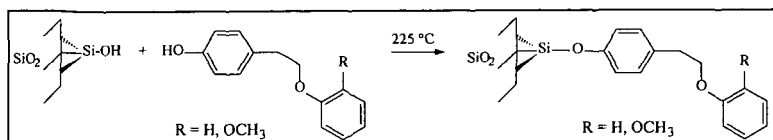


Figure 1. Preparation of silica-attached phenethyl phenyl ether derivatives.

A comparison of the principal products from the thermal and $\text{SiO}_2\text{-1% Al}_2\text{O}_3$ -catalyzed reactions for $\approx\text{PPE}$ at 400°C is shown in Figure 2. In the absence of the silica-alumina, the products are readily explained by a free-radical chain decomposition pathway.⁽¹¹⁾ In the presence of the small particle size silica-alumina, the rate of reaction for $\approx\text{PPE}$ is increased by a factor of three (from 69 to $216\% \text{ h}^{-1}$), and the product distribution is substantially altered. At 400°C where the free-radical and acid-catalyzed reactions can compete, the product distribution is dominated by acid-catalyzed cracking products. A similar product distribution is obtained when the silica-alumina catalyzed reaction is performed at the lower temperature of 300°C , where the free-radical reaction is suppressed.

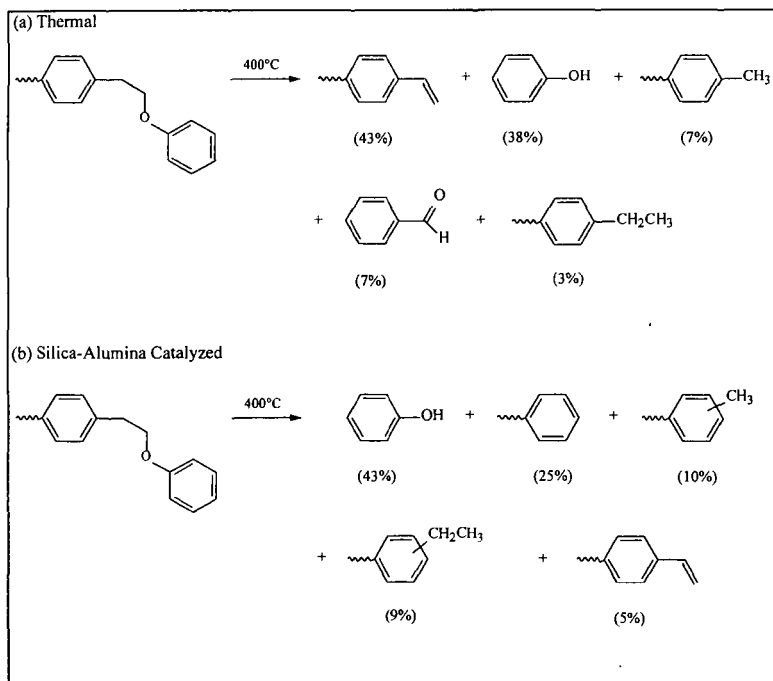


Figure 2. Solid-state reaction for $\approx\text{PPE}$ at 400°C for 15 min in the (a) absence and (b) presence of a silica-alumina catalyst.

The acid-catalyzed products arise from two reaction pathways involving (1) initial protonation of the ether oxygen followed by cracking of the ether linkage to form phenol and silica-attached phenethyl cation ($\approx\text{PhCH}_2\text{CH}_2^+$), or (2) protonation of the surface-attached phenyl ring followed by cleavage to produce $\approx\text{PhH}$ (*ipso*-protonation) or $\approx\text{PhCH}_3$ (*ortho*- or *para*-protonation).⁽¹¹⁾ The silica-attached alkyl benzene products are found to be isomerized to *ortho*-, *meta*-, and *para*-isomers. Furthermore, we observe that alkenes are not stable under these conditions and represent minor products in the presence of the silica-alumina. The mass balances, which are excellent in the non-catalyzed runs (ca. 99%), are substantially diminished in the presence of silica-alumina. The mass balances are 79% at 400°C and 54% at 450°C principally as a consequence of coking reactions on the silica-alumina.

Similar behavior is observed for $\approx\text{PPE-o-OMe}$ whose thermally induced, free-radical reaction (Figure 3) parallels that for $\approx\text{PPE}$, but whose rate is ca. seven times faster as a consequence of the *ortho*-methoxy substituent.⁽¹¹⁾ Again in the presence of the silica-alumina, acid-catalyzed reactions dominate and are analogous to those observed for $\approx\text{PPE}$. Protonation of the β -aryl ether, followed by cleavage produces guaiacol (*o*-methoxyphenol) as the major product at 300°C (46%). However, at 400°C (Figure 3) as a result of the higher reactivity of $\approx\text{PPE-o-OMe}$, conversions in excess of 85% are obtained in only 10 min. The dominant products at 400°C are the alkylated benzenes, $\approx\text{PhH}$, $\approx\text{PhCH}_3$, and $\approx\text{PhCH}_2\text{CH}_3$ with guaiacol accounting for only 13% of the products.⁽¹¹⁾ Isomerized (1) and alkylated (2) starting material are also detected. Coking of the aluminosilicate is again significant and mass balances are low (ca. 40%). Small amounts (2-5%) of catechol (*o*- $\text{Ph}(\text{OH})_2$) are obtained at 275-400°C indicating that demethylation at the methoxy substituent is a minor reaction pathway under these conditions.

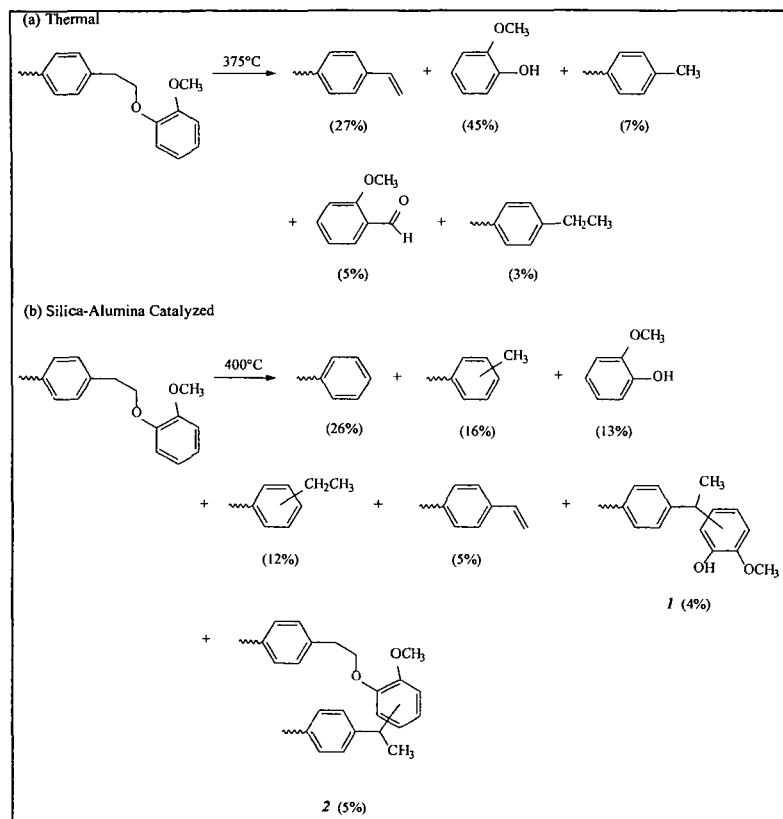


Figure 3. Solid-state reaction for $\approx\text{PPE-o-OMe}$ in the (a) absence and (b) presence of a silica-alumina catalyst.

SUMMARY

The solid-state chemistry of silica-immobilized phenethyl phenyl ethers is being investigated in the presence of interdispersed silica-aluminas at temperatures (300-450°C) relevant to coal processing to gain a better understanding of the impact of related mineral matter on coal pyrolysis and liquefaction mechanisms. The results demonstrate the dramatic effect that silica-aluminas can have in altering the normal thermal reaction pathways for these models of ether linkages in lignin and low rank coals. At temperatures where free-radical reactions and acid-catalyzed reactions can compete, the products are dominated by acid-catalyzed cracking reaction pathways. The yields of alkenes are dramatically reduced, while new products from aromatic dealkylation, rearrangement, and alkylation are observed. Although the presence of silica-alumina assists in the cracking of the ether models, they also lead to the formation of nonvolatile, higher aromatic residues, i.e. coke. An investigation of the chemistry of these model compounds at low temperatures (ca. 150-200°C) in the presence of silica-aluminas, including montmorillonite, is also in progress to delineate the chemical transformations that can occur during lignin maturation.

ACKNOWLEDGEMENTS

This research was sponsored by the Division of Chemical Sciences, Office of Basic Energy Sciences, U.S. Department of Energy, under Contract No. DE-AC05-84OR21400 with Martin Marietta Energy Systems, Inc. The authors also thank Ms. Kimberly Thomas for technical assistance.

REFERENCES

1. Buchanan, III, A. C.; Britt, P. F. *Prepr. Pap.-Am. Chem. Soc., Div. Fuel Chem.* **1994**, 39(1), 22.
2. Laszlo, P. *Science* **1987**, 235, 1473.
3. Hayatsu, R.; McBeth, R. L.; Scott, R. G.; Botto, R. E.; Winans, R. E. *Org. Geochem.* **1984**, 6, 463.
4. Hatcher, P. G.; Faulon, J.-L. *Prepr. Pap.-Am. Chem. Soc., Div. Fuel Chem.* **1994**, 39(1), 7.
5. Buchanan, III, A. C.; Dunstan, T. D. J.; Douglas, E. C.; Poutsma, M. L. *J. Am. Chem. Soc.* **1986**, 108, 7703.
6. Britt, P. F.; Buchanan, III, A. C. *J. Org. Chem.* **1991**, 56, 6132.
7. Buchanan, III, A. C.; Biggs, C. A. *J. Org. Chem.*, **1989**, 54, 517.
8. Buchanan, III, A. C.; Britt, P. F.; Biggs, C. A. *Energy Fuels* **1990**, 4, 415.
9. Buchanan, III, A. C.; Britt, P. F.; Thomas, K. B.; Biggs, C. A. *Energy Fuels* **1993**, 7, 373.
10. Britt, P. F.; Buchanan, III, A. C.; Hitsman, V. H. *Prepr. Pap.-Am. Chem. Soc., Div. Fuel Chem.* **1991**, 36, 529.
11. Britt, P. F.; Buchanan, III, A. C.; Thomas, K. B.; Lee, S.-K. *J. Anal. Appl. Pyrolysis* **1995**, in press.
12. Faulon, J.-P.; Hatcher, P. G. *Energy Fuels* **1994**, 8, 402.

SODIUM METALCARBONYLATES AS POTENTIAL CATALYSTS FOR COAL LIQUEFACTION INVOLVING CO/H₂O OR H₂

C.E. Burgess, C.J.K. Hulston, P.J. Redlich, M. Marshall, and W.R. Jackson
Monash University, Department of Chemistry, Clayton, Victoria, AUSTRALIA

Keywords: sodium metalcarbonylate catalysts, coal liquefaction catalysis

INTRODUCTION

Alkalis such as NaAlO₂ and NaOH catalyze CO/H₂O/coal reactions at 350-400 °C [1-5]. Nickel, molybdenum, and cobalt are effective hydrogenation catalysts above 350 °C [6-13]. Previous work has shown that when using 1,2,3,4-tetrahydroquinoline (THQ) [14-15] and molybdenum sulfide catalyst, individually or together, relatively high conversions can be obtained [16]; by synthesizing a catalyst with THQ and molybdenum sulfide, a synergism was noted with a slight increase in conversion for a subbituminous coal [16]. A combination of transition metals and alkali catalysts, added as separate species to the coal, gives higher conversions than metal or alkali catalysts alone for no-solvent CO/H₂O and CO/H₂/H₂O reactions [17-18], particularly for lower-rank Australian coals. We have synthesized catalyst precursors containing sodium and metal carbonylates to determine in the preliminary stages if the combined precursor would increase coal conversion compared to coal reactions without catalyst and other catalyst systems.

EXPERIMENTAL

Elemental analyses of the two coals used are listed in Table 1. The particle size of both coals are -60 mesh (-250 μm). Loy Yang ROM (run of mine) (LYROM) was obtained from the Loy Yang open cut in Australia, and Surat Basin (SSB) was obtained from the Surat Basin deposit in Australia.

Three methods were used to prepare the sodium metal carbonylates. The first method was used to prepare NaHFe(CO)₄ from Fe(CO)₅ and NaOH [19]. The reaction is such that all the Fe(CO)₅ is consumed and NaOH is in excess. For the preparation, 0.48 g of NaOH dissolved in 50 mL of deoxygenated water was added to an evacuated flask containing 0.75 g of Fe(CO)₅. The reactants were stirred for 24 h under argon. The compound of interest (NaHFe(CO)₅) was not isolated and the resulting aqueous mixture was loaded directly onto 10g of coal, stirred under vacuum for 1h, and the water evaporated under vacuum [17-18].

A similar method was used to prepare NaCo(CO)₄ [20] from Co₂(CO)₈ and NaOH (again in excess). For the preparation, 0.53 g of NaOH dissolved in 50 mL of deoxygenated water was added to an evacuated flask containing 0.60 g of Co₂(CO)₈. The reactants were stirred for 24 h under argon. The compound of interest (NaCo(CO)₄) was not isolated and the resulting aqueous mixture was loaded directly onto 10g of coal, stirred under vacuum for 1h, and the water evaporated under vacuum [17-18]. Since the catalyst of interest was not isolated, we refer to these mixtures as "catalyst mixtures."

A third method was used to prepare NaCo(CO)₄ not contaminated with NaOH [21-22]. (Increased coal conversions were noticed with the catalyst mixtures (Table 2), but it was not certain whether the increases were due to the carbonylate or to the excess NaOH in the catalyst mixture.) In this method, dry NaOH (1.8 g, excess) and Co₂(CO)₈ (1.6 g) were added to a flask in the absence of air. Dry tetrahydrofuran (THF) was added very slowly as the reactants can ebullate violently if THF is added quickly. The mixture was stirred for 2 h until a notable color change from deep orange to a pinkish-lavender occurred. The solid was filtered out, and the THF removed by vacuum distillation from the filtered solution. The NaCo(CO)₄ is not air-stable, so it was prepared under vacuum or argon then solubilized in deoxygenated water in a glove bag before being exposed to the air and loaded onto the coal. The coal/catalyst was stirred under vacuum for 1h, and the water evaporated under vacuum.

Several other catalyst precursors were used as comparisons to the precursors synthesized. The following reagent grade chemicals, all added from aqueous solution [17-18], were used as catalyst precursors: the alkalis sodium aluminate and sodium hydroxide (500 mmol Na/kg dry coal); cobalt (II) acetate and iron (II) acetate (300 mmol metal/kg dry coal); and combined ammonium heptamolybdate (100 mmol Mo/kg dry coal)/nickel (II) or cobalt (II) acetate (40 mmol /kg dry coal). The coal/catalyst was stirred under vacuum for 1h, and the water evaporated under vacuum. When combining the alkalis with the metal catalysts, the alkali was added after the metals unless otherwise noted (it was later found the order of addition caused changes in conversion with mixed catalyst systems).

The reaction took place in a 30 mL horizontal microautoclave as described in other publications [23]. One gram of treated coal was loaded into the reactor. For CO/H₂O reactions, 2.5 g of H₂O was added, and the reactor was pressurized to 3.0 MPa of CO (cold). For hydrogenation reactions, the reactor was pressurized to 6 MPa of hydrogen (cold). The reactors were heated in an ebullating sandbath to the required temperature (2 min to heat the reactor and held at temperature for 30 min).

The work-up procedure was as described previously [17-18, 24-25]. The reactors were vented and scraped out using dichloromethane (DCM). The water was removed from the products by Lundin distillation. The products were ultrasonicated for 10 min and filtered. The residues were dried at 105 °C under nitrogen for 2 h. The DCM was vacuum distilled from the DCM-solubles, and then Shell X4 (40-60 °C b.p. petroleum, mainly hexanes) was added for the extraction of the oil fraction. The product was ultrasonicated for at least 2 min, and the DCM-solubles/X4-insolubles (asphaltenes) were filtered out. Total conversion was calculated by (dry coal with catalyst - dry residue with catalyst)/coal (daf). The oil, gas, and water fraction (OGW) was determined by total conversion minus asphaltene fraction.

RESULTS

Table 2 contains the conversion data for Loy Yang run-of-mine (LYROM) coal for two sets of reaction conditions. The CO/H₂O reactions were all at 365 °C for 30 min. The conversion for this reaction condition of LYROM is 30%, mainly to OGW. Addition of the alkali catalysts gives significantly higher conversions, with sodium aluminate increasing conversion to 51% (45% OGW) and sodium hydroxide increasing conversion to 60% (53% OGW). Metal hydrogenation catalysts give much smaller increases in conversion. Iron increases the conversion to 36% (34% OGW) and cobalt to 42% (41% OGW). For the alkali catalyst and the metal catalyst acting together, the conversion (~50-55%) is similar to the conversion for the reaction when using the alkali alone. The sodium metacarbonylate catalyst precursors were first tested by reacting sodium hydroxide with iron pentacarbonyl or dicobalt octacarbonyl and loading the mixture of the carbonylate and excess NaOH on to the coal. Increases in conversion were noted (to 55-63%), but the conversion was similar to that for sodium hydroxide alone (60%). Finally, sodium cobalt tetracarbonyl was used as catalyst, but the conversion is similar to that with cobalt alone (40%). The low conversion with sodium cobalt tetracarbonyl may be due to the non-alkaline form of the sodium.

Some of these catalyst combinations were also used in coal hydrogenation reactions with LYROM at 400 °C for 30 min. The conversion for this reaction condition of LYROM is 32%, mainly to OGW. With cobalt and alkali catalysts, the conversion is 71-77%, with 62-67% OGW. The metal carbonylate catalysts only give 41 to 48% conversion. On-going work in this laboratory has focused on the use of Ni/Mo metal catalysts with sodium aluminate [18]. The work has shown that the order of addition of the alkali and the metals, and the metal "promoter" of Mo, significantly affect the conversion. When the Ni/Mo is added first, conversion is about 75 %, 60% OGW. When sodium aluminate is added first, the conversion increases to 87% with 69% OGW. Co/Mo gives significantly lower conversions than Ni/Mo. It appears that sodium can greatly influence the reaction, but its effect depends on the form and amount of sodium added and the metal used as the hydrogenation catalyst.

Table 3 contains the conversion data for Surat Basin coal (SSB) for two sets of reaction conditions. The CO/H₂O reactions were at 365 °C for 30 min. The conversion for this reaction condition of SSB is 27%, mainly to OGW. Addition of sodium aluminate catalyst gave slightly higher conversions (to 36%, OGW). Cobalt alone did not increase conversion. However, the sodium aluminate and cobalt give a conversion only slightly lower than with the alkali alone (~33%), but with a decrease in asphaltene yield to 4%. Sodium cobalt tetracarbonyl (300 mmols/kg dry coal for each metal) gives a similar conversion to that for cobalt and sodium aluminate (33%). Although sodium aluminate does increase the conversion for the CO/H₂O reactions, the increase in conversion is much smaller for LYROM.

Some of these catalyst combinations were also used in coal hydrogenation reactions with SSB at 400 °C for 30 min. The conversion for this reaction condition using SSB (CS₂ was also in this reaction) is 25%, mainly to OGW. The sodium cobaltcarbonylate catalyst gives a conversion of 62%. For sodium aluminate and Ni/Mo (Ni/Mo loaded first), conversion is 51%, 37% OGW. When sodium aluminate was loaded first, the conversion decreases to 46% with 35% OGW.

DISCUSSION

For LYROM coal, the alkali catalysts containing sodium do significantly increase conversion for CO/H₂O reactions at 365 °C; adding metals to the alkalis for this reaction condition does not increase the conversion. Sodium cobalt tetracarbonyl does increase conversion compared to no catalyst, but the increase in conversion is about the same as only by the same amount as cobalt alone. For SSB coal, alkali catalysts are effective in increasing conversion, but not to the same extent as for LYROM coal. Cobalt/sodium aluminate and to a lesser extent the sodium cobalt carbonylate improve the oil yield compared to sodium aluminate.

However, for hydrogenation reactions at 400 °C, sodium has had varying effects on conversion depending on the coal used, hydrogenation catalyst metals used, the order of addition of catalyst, and the form of sodium added. On-going work in this laboratory has shown Ni/Mo combined with sodium aluminate also produces increased conversions, particularly when adding the sodium aluminate before the metals (conversion under similar reaction conditions is 87% on a DCM-soluble basis, with 69% yield of OGW) [18]. With LYROM, the sodium metacarbonylates under these reaction conditions only increase conversion from the baseline condition about 10-15%,

whereas cobalt/alkali increase conversion by 40%. It is possible the sodium aluminate alters the coal surface of LYROM coal to increase dispersion of the Ni/Mo catalyst [18], and clearly a mixed sodium-metal compound may not affect the metal surface in the same way. However, the catalysts behave differently with SSB coal for hydrogenation at 400 °C for 30 min. Sodium cobalt tetracarbonyl does significantly increase the conversion under hydrogenation reaction conditions, the conversion being 61% with a OGW yield of 39%. Reactions of SSB coal with Ni/Mo and sodium aluminate give conversions around 50%. The order of addition of the alkali and metal catalysts does not alter the conversion significantly with SSB coal as it does with LYROM; yet a higher conversion is obtained when using the sodium cobalt tetracarbonylate than when using Ni/Mo/NaAlO₂ with SSB coal.

CONCLUSIONS

The use of sodium cobalt tetracarbonyl with LYROM coal does increase coal conversion from baseline conditions for both CO/H₂O reactions and hydrogenation reactions; but adding cobalt acetate and alkali as separate precursors gives much higher conversions. For SSB coal, sodium cobalt tetracarbonyl does increase conversion for hydrogenation reactions at 400 °C to a higher level than NaAlO₂/Ni/Mo. The differing effects of these catalysts when using different coals is not yet understood.

ACKNOWLEDGMENTS

We thank the National Science Foundation for a postdoctoral fellowship (to C.E.B.). This work is part of a collaborative program established by the New Energy and Industrial Technology Development Organization of Japan (NEDO) to promote efficient methods for the production of fluid fuels for power generation from coal, and we thank NEDO for financial support to W.R.J., P.J.R., and M.M.

REFERENCES

1. Del Bianco, A. and Girardi, *Fuel Proc. Tech.*, **23**, 205, (1989).
2. Fischer, F. and Schrader, H., *Brennst. Chem.*, **2**, 257, (1921) (*Chem. Abst.*, **15**, 3900, 1921).
3. Ross, D.S., Blessing, J.T., Nguyen, Q.C. and Hum, G.P., *Fuel*, **63**, 1206, (1984).
4. Lim, S.C., Jackson, W.R., and Marshall, M., submitted for publication in *Fuel*.
5. Hughes, C.P., Sridhar, T., Lim, S.C., Redlich, P.J., Jackson, W.R., and Larkins, F.P., *Fuel*, **72**, 205, (1993).
6. Derbyshire, F.J., *Catalysis in Coal Liquefaction*, IEA Coal Research, London, IEA CR/08, (1988).
7. Weller, S., *Energy & Fuels*, **8**, 415, (1994).
8. Derbyshire, F.J., Davis, A., Lin, R., Stansberry, P.G., and Terrer, M-T., *Fuel Proc. Tech.*, **12** (7), 127, (1986).
9. Anderson, R.R. and Bockrath, B.C., *Fuel*, **63**, 329, (1984).
10. Utz, B.R., Cugini, A.V., and Frommel, E.A., *Amer. Chem. Soc. Div. of Fuel Chem. Preprints*, **34** (4), 1423, (1989).
11. Cugini, A.V., Martello, D.V., Krastman, D., Baltrus, J.P., Ciocco, M.V., Frommel, E.F., and Holder, G.D., *Amer. Chem. Soc. Div. of Fuel Chem. Preprints*, **40** (2), 1423, (1995).
12. Cusumano, J.A., Dalla Betta, R.A. and Levy, R.B., *Catalysis in Coal Conversion*, Academic Press: New York, p. 155, (1978).
13. Song, C., Hanaoka, K. and Nomura, *Energy & Fuels*, **6**, 619, (1992).
14. Bockrath, B.C., in *Coal Science*, Gorbaty, M.L., Larsen, J.W., and Wender, I., Editors. Academic Press: New York. p. 65, (1983).
15. Derbyshire, F.J., Odoefer, G.A. and Whitehurst, D.D., *Fuel*, **60**, 201, (1981).
16. Burgess, C.E. and Schobert, H.H., *Fuel*, **70**, 392, (1991).
17. Hulston, C.K.J., Redlich, P.J., Jackson, W.R., Larkins, F.P., and Marshall, M., "Reactions of Coals of Different Ranks With CO/H₂ Mixtures of Varying Composition With and Without Sodium Aluminate", accepted for publication in *Fuel*, 1995.
18. Hulston, C.K.J., Redlich, P.J., Marshall, M., and Jackson, W.R., "Nickel Molybdate Catalysed Hydrogenation of Brown Coal Without Solvent or Added Sulphur," submitted to *Fuel*, 1995.
19. Sternberg, H.W., Markby, R., and Wender, I., *J. Am. Chem. Soc.*, **79**, 6116 (1957).
20. Wender, I., Sternberg, and Orchin, M. *J. Am. Chem. Soc.*, **74**, 1216 (1952).
21. Edgell, W.F. and Lyford IV, J. *Inorg. Chem.*, **9** (8) 1932 (1970).
22. Schroeder, N.C., Richardson Jr., J.W., Wang, S-L, Jacobson, R.A., and Angelici, R.J. *Organometallics*, **4**, 1226 (1985).
23. Hulston, C.K.J., Redlich, P.J., Jackson, W.R., Larkins, F.P., and Marshall, M., "The Effect of Tubular Reactor Orientation on Conversion of Coal to Liquid Products," submitted to *Fuel*, 1995.
24. Cassidy, P.J., Jackson, W.R., Larkins, F.P., Sakurovs, R.J. and Sutton, J.F., *Fuel*, **65**, 374, (1986).
25. Jackson, W.R., Larkins, F.P., Thewlis, P. and Watkins, I., *Fuel*, **62**, 606, (1983).

Table 1: Elemental and Ash Analyses for Coals

Coal	Rank	Elemental Analysis (wt % daf)					Atomic H/C Ratio ^a	Ash (wt% dry)
		C	H	N	S	O (by diff)		
LYROM ^b	lignite	70.7	4.91	0.7	0.51	23.2	0.86	0.5
SSB ^c	hvb ^d	81.0	6.08	1.8	0.56	10.5	0.9	9.8

^a CO₂-free basis^b Loy Yang run-of-mine coal^c Surat Basin coal^d high volatile bituminous

Table 2: Conversion Data for Loy Yang brown coal (LYROM) Using Various Catalysts and Reaction Conditions

Coal	Metal Catalyst ^a	Alkali Catalyst ^b	Temp (°C)	Gas Atm.	Total Conv. ^c	Asph. ^d	OGW ^e
LYROM	none	none	365	CO/H ₂ O	30	0.6	29
	none	NaAlO ₂	365	CO/H ₂ O	51	5.7	45
	none	NaOH	365	CO/H ₂ O	60	6.9	53
	Fe	none	365	CO/H ₂ O	36	1.9	34
	Co	none	365	CO/H ₂ O	42	1.0	41
	Fe	NaAlO ₂	365	CO/H ₂ O	55	9.8	45
	Co	NaAlO ₂	365	CO/H ₂ O	53	7.8	45
	Co	NaOH	365	CO/H ₂ O	54	6.5	48
	NaHFe(CO) ₄ ^f	--	365	CO/H ₂ O	55	6.7	48
	NaCo(CO) ₄ ^f	--	365	CO/H ₂ O	63	11.6	52
	NaCo(CO) ₄ ^g	--	365	CO/H ₂ O	40	0.1	40
	none ^h	none	400	H ₂	32	2	30
	Co	NaAlO ₂	400	H ₂	71	8.5	62
	Co	NaOH	400	H ₂	77	9.8	67
	NaHFe(CO) ₄ ^f	--	400	H ₂	48	6.6	41
	NaCo(CO) ₄ ^g	--	400	H ₂	41	0.1	41
	Ni/Mo ⁱ	NaAlO ₂	400	H ₂	87	18	69
	Ni/Mo ^j	NaAlO ₂	400	H ₂	75	15	60
	Co/Mo ^j	NaAlO ₂	400	H ₂	48	5	43

^a Metal Catalysts - Loaded as aqueous solutions of salts, i.e. cobalt acetate, nickel acetate, ammonium molybdate. Cobalt and nickel salts loaded 300 mmol metal/kg dry coal unless used as mixed catalyst with molybdenum, then cobalt and nickel loaded 40 mmol and molybdenum 100 mmol metal/kg dry coal.^b Alkali Catalysts - Loaded as salts, 500 mmol/kg dry coal^c Total Conversion - based on DCM-insolubles, [(Coal (dry) - Residue (dry))/Coal (daf)]^d Asphaltenes - DCM-solubles/hexane-insolubles^e OGW - Oil, Gas, (Total Conversion - Asphaltenes)^f Sodium metalcarbonylates - loaded as mixture of NaOH and metal carbonyl^g Sodium Carbonyl - loaded as actual salt, 300 mmol metal/kg dry coal^h Reaction contains CS₂, no baseline data available at this timeⁱ Sodium Aluminate loaded before nickel and molybdenum precursors^j Sodium Aluminate loaded after nickel and molybdenum precursors

Table 3: Conversion Data for Surat Basin coal (SSB) Using Various Catalysts and Reaction Conditions

Coal	Metal Catalyst ^a	Alkali Catalyst ^b	Temp (°C)	Gas Atm.	Total Conv. ^c	Asph. ^d	OGW ^e
SSB	none	none	365	CO/H ₂ O	27	4.3	23
	none	NaAlO ₂	365	CO/H ₂ O	36	12	24
	Co	none	365	CO/H ₂ O	27	3.2	23
	Co	NaAlO ₂	365	CO/H ₂ O	33	3.7	29
	NaCo(CO) ₄ ^f	--	365	CO/H ₂ O	33	7.0	26
	none	none	400g	H ₂	25	2	23
	NaCo(CO) ₄ ^f	--	400	H ₂	61	22.3	39
	Ni/Mo ^h	NaAlO ₂	400	H ₂	46	11	35
	Ni/Mo ⁱ	NaAlO ₂	400	H ₂	51	14	37

^a Metal Catalysts - Loaded as aqueous solutions of salts, i.e. cobalt acetate, nickel acetate, ammonium molybdate. Cobalt and nickel salts loaded 300 mmol metal/kg dry coal unless used as mixed catalyst with molybdenum, then cobalt and nickel loaded 40 mmol and molybdenum 100 mmol metal/kg dry coal.

^b Alkali Catalysts - Loaded as salts, 500 mmol/kg dry coal

^c Total Conversion - based on DCM-insolubles, [(Coal (dry) - Residue (dry))/Coal (daf)

^d Asphaltene - DCM-solubles/hexane-insolubles

^e OGW - Oil, Gas, Water, (Total Conversion - Asphaltene)

^f Sodium Cobalt Carbonyl - loaded as actual salt, 300 mmol loading

^g Reaction time 60 minutes

^h Sodium Aluminate loaded before nickel and molybdenum precursors

ⁱ Sodium Aluminate loaded after nickel and molybdenum precursors

MOLYBDENUM HEXACARBONYL AS A CATALYST PRECURSOR FOR DIRECT COAL LIQUEFACTION

Robert P. Warzinski and Bradley C. Bockrath
U.S. Department of Energy
Pittsburgh Energy Technology Center
Pittsburgh, PA 15236

Keywords: coal liquefaction, dispersed catalyst, molybdenum hexacarbonyl

INTRODUCTION

Various transition metal carbonyls of the formula $M_n(\text{CO})_x$, - where M is Cr, Fe, Co, Ni, Mo, Ru, Rh, W, Re - have been used effectively as catalyst precursors in laboratory-scale investigations of direct coal liquefaction (1-6). Most notable are the use of iron pentacarbonyl (4) and molybdenum hexacarbonyl (5). In particular, $\text{Mo}(\text{CO})_6$ in the presence of sulfur has been shown to be an excellent catalyst precursor for the liquefaction of coal (5,6) and for promoting reactions with coal model compounds (7).

At PETC, $\text{Mo}(\text{CO})_6$ has been used to study the influence of a catalyst on the liquefaction of coal (5,8,9). The inherent volatility of $\text{Mo}(\text{CO})_6$ permits it to form an active liquefaction catalyst in the presence of sulfur with no special preparation, impregnation, or dispersion techniques. The liquefaction of coal is effectively accomplished by the simple direct addition of $\text{Mo}(\text{CO})_6$ to the liquefaction reactor even in the absence of any added solvents or vehicles. The work reported here describes the activation and reactivity of the catalysts formed from $\text{Mo}(\text{CO})_6$.

EXPERIMENTAL

The $\text{Mo}(\text{CO})_6$ was used as received from Strem Chemical Company. Purity was given as 98+ % with moisture being the only major contaminant. Ammonium tetrathiomolybdate (ATM) was purchased from Alfa Products and used as received. Elemental analysis of the ATM showed that it contained some oxygen; however, the S:Mo ratio was 4:1. In all of the experiments with coal, DECS-17 coal from the Penn State Coal Sample Bank was used. The coal was minus-60 mesh and was riffled prior to use. The elemental analysis (on a dry basis) provided with the coal was as follows: 76.3% carbon, 5.8% hydrogen, 1.3% nitrogen, 0.4% sulfur, 6.6% ash, and 9.7% oxygen (by difference).

Microautoclave experiments were performed according to previously described procedures (5,8,9). When $\text{Mo}(\text{CO})_6$ was used with coal, no special impregnation or mixing procedures were used; it was simply added directly to the microautoclave containing the coal sample. Unless otherwise indicated, all of the experiments were conducted for 1 hour using a slow heat-up and rapid cool-down. The products were recovered according to the referenced procedures (5,8,9). Elemental analyses of the products were performed at Huffman Laboratories in Golden, Colorado. ESCA and X-ray diffraction analyses were performed at PETC.

RESULTS AND DISCUSSION

Conversion of $\text{Mo}(\text{CO})_6$ to an Active Catalyst. $\text{Mo}(\text{CO})_6$ is a sublimable solid that decomposes without melting at 150°C (10). In the absence of a liquid phase, the reactions involved in the transformation of $\text{Mo}(\text{CO})_6$ to MoS_2 appear to take place in the gas phase as the carbonyl sublimates and decomposes. We have observed the conversion of $\text{Mo}(\text{CO})_6$ in H_2S to MoS_2 in a high-pressure, windowed view cell. A description of the view-cell system has been published (8). In this experiment, 0.37 mmol of $\text{Mo}(\text{CO})_6$ and 4.4 mmol of H_2S were added to the cell. At 90°C and 7.0 MPa, a brown coating started to cover the $\text{Mo}(\text{CO})_6$ particles and the interior surface of the glass window. At 110°C the coating on the window prevented further visual observation. Inspection of the brown, mirrorlike coating on the window by XPS indicated that it was similar in composition to MoS_2 .

To determine the fate of $\text{Mo}(\text{CO})_6$ in our microautoclave liquefaction system, experiments were performed at several temperatures with $\text{Mo}(\text{CO})_6$ and the results compared to those obtained from similar experiments with ATM, a nonvolatile liquefaction catalyst precursor. In these experiments, 0.9 g of the catalyst precursor and 9.1 MPa of a hydrogen/10% hydrogen sulfide gas mixture were charged to the microautoclave. The products from reactions with $\text{Mo}(\text{CO})_6$ and ATM were recovered as methylene chloride-insoluble and tetrahydrofuran (THF)-insoluble residues, respectively. The S:Mo atomic ratios of the products determined from both elemental analysis and ESCA are contained in Table 1 along with the complete elemental composition.

Table 1. Activation of Mo(CO)₆

Temperature, °C	Precursor	Atomic S/Mo Ratio		Elemental
		Elemental	ESCA	Composition
175	Mo(CO) ₆	2.5	---	---
250	Mo(CO) ₆	2.0	1.3	MoS _{2.3} C _{0.3} H _{1.7} O _{1.1} N _{0.1}
250	ATM	2.3	1.8	MoS _{2.3} C _{0.3} H _{2.4} O _{2.3} N _{0.3}
375	Mo(CO) ₆	2.3	1.8	MoS _{2.3} C _{0.3} H _{0.9} O _{0.3}
375	ATM	2.3	1.9	MoS _{2.3} C _{0.3} H _{2.7} O _{1.8} N _{0.1}

At 175°C, the lowest temperature investigated, approximately 45% of the carbonyl reacted to form a product with a S:Mo ratio of 2.5. Unreacted Mo(CO)₆ was also observed. An experiment with ATM was not performed under these conditions. At 250°C, no unreacted Mo(CO)₆ was observed. At this temperature, 97% of the carbon monoxide in the carbonyl was detected in the product gas. The products formed from Mo(CO)₆ and ATM at 250°C have slightly different S:Mo ratios. However, at 375°C, the products were similar in composition and close to the expected value of 2:1 for MoS₂. ESCA analyses of the samples indicated a lower S:Mo ratio on the surface, which was probably due to surface oxidation of the samples. Direct oxygen analyses of these samples confirmed the presence of oxygen.

X-ray diffraction analysis was also performed at PETC to determine the degree of crystallinity of the products from Mo(CO)₆ and ATM. At 175°C and 250°C, the products were essentially amorphous compounds; however, at 375°C the development of some crystallinity was observed.

Similar work on the transformation of Mo(CO)₆ and ATM under liquefaction conditions was reported by Artok et al. (6). Results with ATM are in agreement with those in Table 1; however, they reported lower S:Mo ratios (1.1 to 1.7) when using Mo(CO)₆. One possible reason may be that in our experiments, the H₂S:Mo ratio in the microautoclave system was initially about 6.3:1; whereas, in the work by Artok et al. it was reported as 2.5:1. Under typical coal liquefaction conditions in our system, at 1000 ppm Mo, the H₂S:Mo ratio was initially about 150:1.

The pressure and temperature data collected during microautoclave experiments were used to follow the change in the total number of moles of gas in the system with time. This provided information concerning the transformation of Mo(CO)₆ to an active catalyst and the temperature of the onset of catalytic activity. Determining the amount of gas in the system, especially during the heat-up period, from the pressure and temperature data was complicated by the fact that a significant portion of the reaction space is outside the heated sandbath. This cooler region consists of the internal volumes of the pressure transducer, connecting tubing, and associated valves. During heat-up and reaction, the gas in the cooler region would be at a higher density than the gas in the microautoclave. Therefore, calculating the moles of gas in the microautoclave system using the ideal gas law would result in an apparent decrease in the moles of gas as temperature increases.

An empirical correction procedure was developed that compensated for both the nonisothermal nature of the microautoclave system and the nonideality of the gas phase. This procedure involved determining a correction factor from pressure and temperature data from experiments with only H₂ or H₂/3% H₂S in the microautoclave system. This correction factor was obtained by fitting a polynomial equation to the apparent change in the moles of gas calculated using the ideal gas law as a function of the microautoclave temperature in these experiments. This correction factor was then applied to the moles of gas calculated using the ideal gas law from experiments with catalyst. This correction procedure is performed for each microautoclave reactor and is checked on a regular basis. Using this method, changes in gas content greater than ± 1 mmol can be reliably observed.

Figure 1 presents changes in the amount of gas present in the microautoclave system and the thermal history as functions of time for an experiment in which 3.7 mmol of Mo(CO)₆ was heated to 425°C under an initial pressure of 7.8 MPa H₂/10% H₂S. In section A of Figure 1, a rapid rise in amount of gas is first observed that starts at about 160°C as Mo(CO)₆ begins to decompose and liberate CO. This is close to the decomposition temperature of 150°C reported for Mo(CO)₆ (10). The amount of gas in the microautoclave continues to increase until, at 280°C, the trend reverses and a gradual decrease is observed. In another similar experiment, the reaction temperature was stabilized at 250°C for one hour after the heat-up period. After reaching 250°C, the gas content continued to increase smoothly to a level of 22 mmol and

remained there for the duration of the experiment. This is equal to the maximum amount of CO that could have been liberated from the $\text{Mo}(\text{CO})_6$ charged. Analysis of the gas composition by gas chromatography indicated that CO accounted for 95% of the carbon-containing gases produced.

To investigate the cause of the abrupt halt in the increase in gas content at 280°C and the onset of a gradual decrease, an experiment was terminated immediately upon reaching 325°C. Analysis of the recovered gases showed that some methanation and water/gas shift conversion had occurred, although carbon monoxide still accounted for 93% of the carbon-containing gases produced. The former reaction accounts for a reduction in the net moles of gas, while the latter gives evidence that water produced in the methanation undergoes catalytic reaction with CO.

In section B of Figure 1, a rapid decrease in the amount of gas occurs at temperatures above 350°C. This may be associated with an increased rate of methanation of the CO released from $\text{Mo}(\text{CO})_6$. A fairly uniform rate of gas consumption (0.39 mmol/mmol Mo/min) occurred in the range of 370°C to 410°C.

At the end of one hour at 425°C the reaction was quenched (section C). Gas analysis indicated that all of the CO was utilized with 90% selectivity towards methane formation. The number of moles of gas present after quenching is lower than at the end of the reaction prior to quenching owing to the condensation of water vapor formed as a result of the methanation reaction. The amount of water indicated in Figure 1 (23 mmol) is in reasonable agreement with that expected based upon the amount of $\text{Mo}(\text{CO})_6$ charged and the methane formed (20 mmol).

In Figure 2, the activation of $\text{Mo}(\text{CO})_6$ in the $\text{H}_2/10\% \text{H}_2\text{S}$ environment is compared to similar experiments conducted in N_2 and H_2 . The use of CS_2 as a source of sulfur in place of H_2S is also shown. In all four cases, the liberation of CO is observed. The largest and most uniform release of CO to the gas phase occurred when both H_2 and H_2S were present. In another experiment (not shown in Figure 2), the rate of release of CO was similar with $\text{N}_2/10\% \text{H}_2\text{S}$ to that observed with $\text{H}_2/10\% \text{H}_2\text{S}$. The data in Figure 2 also show that the most active methanation catalyst was formed in the presence of just H_2 . This is evidenced by the sharp decrease in gas content that occurred at 363°C. The rate of decrease in the temperature range of 380°C to 410°C was 0.55 mmol/mmol Mo/min. When N_2 was used, no significant drop in gas content occurred, either with (Figure 2) or without H_2S (not shown).

X-ray diffraction analyses of samples collected from the above experiments indicated that, in the presence of $\text{H}_2/10\% \text{H}_2\text{S}$, the strongest peak was from MoS_2 . The average crystallite size was 75 Å with a stacking height of 30 Å. The MoS_2 -containing catalyst formed in the presence of $\text{N}_2/10\% \text{H}_2\text{S}$ had similar dimensions. When either N_2 or H_2 alone was used, the strongest peak was from Mo_3C . In these cases, the crystallites were more uniform in size with an average diameter of between 14 Å and 20 Å. Referring to the data in Figure 2, the carbide formed in the presence of H_2 appears to be a more reactive catalyst for methanation than the sulfided species. This agrees with published results obtained at 350°C and 101.3 KPa (11).

Effect of catalyst precursors on coal liquefaction. We have previously shown that $\text{Mo}(\text{CO})_6$ is an effective catalyst precursor for coal liquefaction even in the absence of added liquids and special impregnation procedures (5,9). Compared with uncatalyzed reaction, the conversion of DECS-17 coal to primary (THF-soluble) products was facilitated over a wide temperature range by the catalyst formed from $\text{Mo}(\text{CO})_6$. A different behavior was observed for the conversion of the primary to secondary (cyclohexane-soluble) products. In this case, the onset of catalytic conversion occurred between 375°C and 400°C.

Additional experiments were performed using the DECS-17 coal with various combinations of $\text{Mo}(\text{CO})_6$, hydrogen, hydrogen sulfide, carbon disulfide, and nitrogen. When $\text{Mo}(\text{CO})_6$ was used it was added at a level of 1000 ppm Mo based on daf coal. All of the experiments were performed at 425°C. The conversion results are shown in Figure 3. The error bars represent the range of values obtained about the average. The first set of data illustrates the high conversions obtained using $\text{Mo}(\text{CO})_6$ with $\text{H}_2/3\% \text{H}_2\text{S}$ without added solvents or vehicles. The second and third sets of data show that a drop in both THF and cyclohexane conversions occurs if H_2S is eliminated; however, the conversions are still relatively high. Compared to no added sulfur (third set of data), using CS_2 appears to have no benefit. The fourth and fifth sets of data represent thermal conversions in the absence of catalyst. A small improvement is observed when H_2S is present, even in the absence of catalyst. Finally, the last two sets of data represent experiments performed in N_2 . The presence of $\text{Mo}(\text{CO})_6$ had no effect in the absence of H_2 .

In the work with DECS-17 coal and $\text{Mo}(\text{CO})_6$, it is assumed that $\text{Mo}(\text{CO})_6$ sublimes and disperses onto the coal from the gas phase either prior to being sulfided or as it is converted to the sulfide phase. The previously described experiments in the view cell support this assumption. At the levels of Mo used in the experiments represented in Figure 3 (1000 ppm), the fate of the $\text{Mo}(\text{CO})_6$ could not be determined using X-ray crystallography on the THF-insoluble residues owing to the small amount present and to interferences from the coal mineral matter in the residue. However, the residue from a similar experiment at 425°C in which $\text{Mo}(\text{CO})_6$ was used at a higher level (10,000 ppm) could be examined if the mineral matter was first removed with hydrofluoric acid. In this case, X-ray diffraction analysis identified molybdenum disulfide in the THF insoluble product with a crystallite size of approximately 80 Å and a relatively low degree of stacking.

CONCLUSION

The results presented above confirm that $\text{Mo}(\text{CO})_6$ forms a finely divided active catalyst for coal liquefaction even in the absence of added liquids or special impregnation procedures. Experiments with $\text{Mo}(\text{CO})_6$ in an $\text{H}_2/\text{H}_2\text{S}$ mixture show that the onset of hydrogenation activity related to methanation in the microautoclave system begins near 280°C and increases dramatically at about 350°C. Primary dissolution of coal assisted by the catalyst follows the same pattern; a small catalytic effect is observed at 325°C that increases in magnitude with temperature (5).

The decomposition of $\text{Mo}(\text{CO})_6$ and the liquefaction of coal in the presence of this compound are both facilitated by the presence of H_2S . Substituting CS_2 for H_2S adversely affected $\text{Mo}(\text{CO})_6$ decomposition and liquefaction conversion. In the absence of added sulfur, $\text{Mo}(\text{CO})_6$ forms a carbide phase that is even a more active catalysts for methanation than the sulfide phase; however, this increased activity is not noted in liquefaction experiments with a low-sulfur coal. A different catalyst phase may be formed when coal is present.

The above work also demonstrates that with appropriate correction, the microautoclave pressure and temperature data can be used to follow changes in the amount of gas in the system during an experiment. Using this procedure, information on catalyst activation and reactivity were obtained. The same procedure has also been used to observe the influence of a catalyst on gas uptake during coal liquefaction (5).

ACKNOWLEDGMENTS

The author would like to thank Richard Hlasnik and Jerry Foster for performing the microautoclave work, Sidney Pollack and Elizabeth Frommell for X-ray diffraction analysis and interpretation, and Rodney Diehl for performing the XPS and ESCA analyses.

DISCLAIMER

Reference in this report to any specific product, process, or service is to facilitate understanding and does not imply its endorsement or favoring by the United States Department of Energy.

REFERENCES

1. Sharma, R.K.; Moffett, G. Prepr. Pap. - Amer. Chem. Soc., Div. Fuel Chem. **1982**, 27(2), 11-17.
2. Yamada, O.; Suzuki, T.; Then, J.H.; Ando, T.; Watanabe, Y. Fuel Process. Technol. **1985**, 11, 297-311.
3. Suzuki, T.; Yamada, H.; Yunoki, K.; Yamaguchi, H. Energy Fuels **1992**, 6, 352-356.
4. Suzuki, T. Energy Fuels **1994**, 8, 341-347.
5. Warzinski, R.P. Prepr. Pap. - Amer. Chem. Soc., Div. Fuel Chem. **1993**, 38(2), 503-511.
6. Artok, L.; Davis, A.; Mitchell, G. D.; Schobert, H. H. Energy Fuels **1993**, 7, 67-77.
7. Suzuki, T.; Yamada, H.; Sears, P. L.; Watanabe, Y. Energy Fuels **1989**, 3, 707-713.
8. Warzinski, R. P.; Lee, C.-H.; Holder, G. D. J. Supercrit. Fluids **1992**, 5, 60-71.
9. Warzinski, R.P. Proc. Int. Conf. Coal Sci. **1993**, 2, 337-340.
10. CRC Handbook of Chemistry and Physics; Weast, R. C., Ed.; CRC: Boca Raton, **1988**, B-108.
11. Saito, M.; Anderson, R.B. J. Catal. **1980**, 63, 438-446.

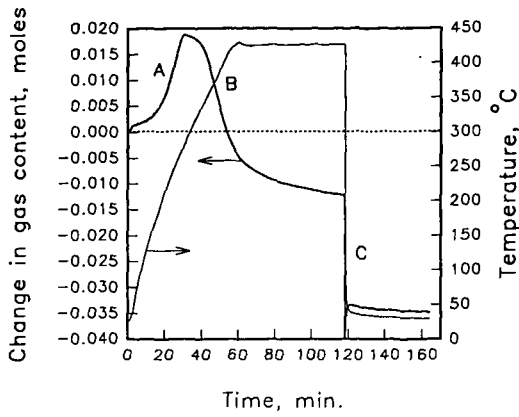


Figure 1. Reactivity of $\text{Mo}(\text{CO})_6$ in $\text{H}_2/10\% \text{H}_2\text{S}$

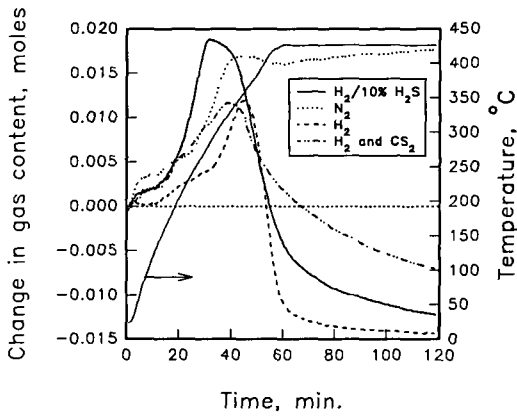


Figure 2. Reaction of $\text{Mo}(\text{CO})_6$ in different systems.

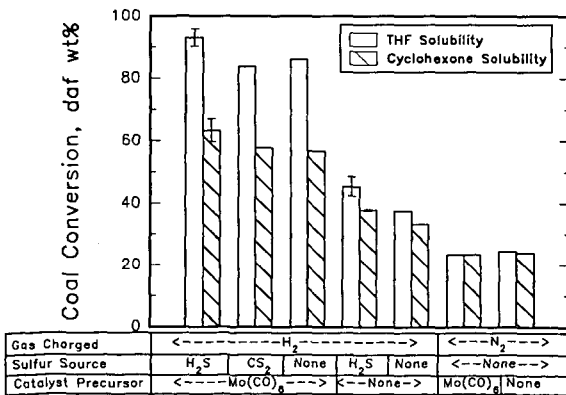


Figure 3. Effect of a catalyst, initial gas composition, and form of sulfur addition on the conversion of DECS-17 coal.

COMPARISON OF THE MEANS OF INTRODUCTION OF MoS₂ LIQUEFACTION CATALYSTS ON PERFORMANCE

Robert P. Warzinski, Anthony V. Cugini, and Bradley C. Bockrath
U.S. Department of Energy
Pittsburgh Energy Technology Center
Pittsburgh, PA 15236

Keywords: coal liquefaction, molybdenum sulfide catalysts, molybdenum hexacarbonyl

INTRODUCTION

The performance of dispersed coal liquefaction catalysts depends on many factors. One long recognized issue is the key importance of intimate contact between the catalyst and the reacting coal. The development of evidence for this critical relationship has been recently reviewed (1). The method of catalyst addition bears directly on this problem. For example, impregnation of coal with a catalyst precursor provides improved liquefaction conversion when compared to adding the precursor as a powder or as a particulate in a liquefaction solvent (2). Exploitation of the advantages obtained by impregnation of a catalyst or its precursors is still pursued.

Unlike most liquefaction catalyst precursors, Mo(CO)₆ has been found to be an effective catalyst precursor even in the absence of such impregnation procedures (3). The purpose of this paper is to compare the activity of the catalyst formed from Mo(CO)₆ with that of preformed MoS₂-containing catalysts known to be active for coal liquefaction. All of the liquefaction experiments were performed without the addition of liquefaction solvents or vehicles to avoid the leveling effect they may exert, especially if they are good hydrogen donors. The elimination of added solvents or vehicles also amplifies the importance of coal/catalyst contacting because mass transport becomes more restricted in reacting phases of higher viscosity.

EXPERIMENTAL

Coal and Chemicals: All experiments were performed with DECS-17 (Blind Canyon) coal (minus 60 mesh) from the Penn State Coal Sample Bank. The elemental analysis (on a dry basis) provided with the coal was as follows: 76.3% carbon, 5.8% hydrogen, 1.3% nitrogen, 0.4% sulfur (0.02% pyritic sulfur), 6.6% ash, and 9.7% oxygen (by difference). The moisture content of the as-received coal was 3.7%. The coal was riffled prior to use. Mo(CO)₆ was obtained from Strem Chemical Company, ammonium heptamolybdate (AHM) was obtained from Fisher Chemical Company, and Panasol (a mixture of alkylated naphthalenes) was obtained from Crowley Chemical Company. All of the chemicals were used as received.

Catalyst Preparation: Three methods of introducing catalyst were used; addition of a catalyst precursor, recycle of the catalyst-containing residue from coal liquefaction experiments with the precursor, and addition of preformed catalyst particles. The catalyst precursor, Mo(CO)₆, was simply added directly to the microautoclave containing the coal sample without a special impregnation or mixing procedure. A MoS₂-containing liquefaction residue was prepared in a microautoclave using 6.6 g DECS-17 coal and Mo(CO)₆ (10,000 ppm Mo based on daf coal) under 7.2 MPa H₂/3% H₂S at 425°C for 1 h. Finely divided MoS₂-containing particles were prepared in a 1-L semi-batch stirred autoclave using 400 g Panasol and 10,000 ppm Mo (based on Panasol) as aqueous AHM (12% by weight) under 17.3 MPa, 30 mL/s H₂/3% H₂S at 400°C for 0.5 h (4). The MoS₂-containing particles and liquefaction residue were both recovered from tetrahydrofuran (THF) by pressure filtration following extraction of the respective reaction products. The dried liquefaction residue and MoS₂-containing particles contained 4.4% and 30% Mo, respectively.

Microautoclave Liquefaction Experiments: Microautoclave experiments were performed according to procedures described previously (3,5). The Mo(CO)₆, the liquefaction residue, or the MoS₂-containing particles were added directly to the microautoclave along with the coal (3.3 g) to give a Mo loading of 1,000 ppm (based on daf coal). No solvents or vehicles were used for catalyst addition or in the liquefaction experiments. All of the experiments were conducted for 1 hour at reaction temperatures from 350°C to 425°C under 7.2 MPa H₂/3% H₂S (cold pressure) using a slow heat-up and rapid cool-down. The products were recovered using sequential extractions with THF and cyclohexane according to the referenced procedures (3,5).

Catalyst Characterization: X-ray diffraction and BET surface area analyses were performed at PETC. A JOEL 200CX TEM located at the University of Pittsburgh was also used to obtain images of the MoS₂-containing particles. Additional details have been published (4).

The catalysts were also characterized by their activity for CH_4 production from CO in the absence of coal in the microautoclave under conditions similar to those used in the liquefaction experiments. In these experiments, either the liquefaction residue or the MoS_2 -containing particles were added to the microautoclave at a level of approximately 0.4 mmol Mo. In the case of $\text{Mo}(\text{CO})_6$, the MoS_2 -containing catalyst phase was first formed in a separate experiment using 1.0 g of $\text{Mo}(\text{CO})_6$ under 7.7 MPa $\text{H}_2/10\% \text{H}_2\text{S}$ and 1 h at 425°C (slow heat-up). A portion of the product sufficient to provide 0.4 mmol Mo was then added to the microautoclave. CO and a $\text{H}_2/3\% \text{H}_2\text{S}$ mixture were then combined in the microautoclave to give a gas mixture of approximately 75% H_2 , 23% CO, and 2% H_2S at 7.7 MPa. Both slow and rapid heat-up experiments were performed at 375°C with a 1-h residence time at reaction temperature. The rates of gas uptake associated with the methanation reaction were obtained from records of the change in pressure with time. These data were used to calculate the change in moles of gas present in the system at reaction temperature.

RESULTS AND DISCUSSION

Microautoclave experiments were performed with Blind Canyon (DECS-17) coal to investigate the effect of the means of introducing catalysts on liquefaction. The catalyst was introduced either in the form of the chemical precursors $\text{Mo}(\text{CO})_6$ and H_2S , or as MoS_2 -containing compounds. Two MoS_2 -containing compounds were used: (1) a liquefaction residue prepared from the precursors and the DECS-17 coal, and (2) high-surface-area MoS_2 -containing particles prepared prior to the liquefaction experiments from AHM and Panasol.

We have previously shown that $\text{Mo}(\text{CO})_6$ is an effective catalyst precursor for coal liquefaction even in the absence of added solvents or vehicles and special impregnation procedures (3). Table 1 contains the liquefaction conversion results from experiments using only the DECS-17 coal with and without 1000 ppm Mo added as $\text{Mo}(\text{CO})_6$ in one-hour reactions at temperatures from 325°C to 425°C. All results are the average of at least two experiments. The influence of native catalyst precursors is negligible, owing to the low levels of pyrite in this coal.

Table 1. Liquefaction of DECS-17 coal using $\text{Mo}(\text{CO})_6$ without added solvents or vehicles

Reaction Temperature, °C	THF Conversion, %		Cyclohexane Conversion, %	
	Thermal	Catalytic	Thermal	Catalytic
325	14	19	7	9
350	29	46	12	15
375	46	83	23	25
400	48	94	31	52
425	45	93	38	65

Compared to the uncatalyzed reaction, the conversion of coal to primary (THF-soluble) products was facilitated by the catalyst formed from $\text{Mo}(\text{CO})_6$ even at the lowest temperature used, 325°C. The difference between catalytic and non-catalytic coal conversion continuously increased with temperature. In the case of secondary (cyclohexane-soluble) products, the onset of a significant catalytic effect occurred between 375°C and 400°C.

The observation of a catalytic effect at the lowest temperature used in the liquefaction experiments implies an active catalyst is formed at even lower temperatures. A detailed investigation of the activation of $\text{Mo}(\text{CO})_6$ in the absence of coal under conditions similar to those used in the microautoclave liquefaction experiments has been reported (6). $\text{Mo}(\text{CO})_6$ is a sublimable solid that decomposes without melting at 150°C (7). In microautoclave experiments, the evolution of CO associated with the decomposition was observed to begin at about this temperature. If H_2S was present, MoS_2 formed readily. When heated in an $\text{H}_2/\text{H}_2\text{S}$ mixture, the development of catalytic activity was indicated by the conversion of the evolved CO to CH_4 . The onset of catalytic methanation was detected near 280°C and increased dramatically at about 350°C. This result and the THF-conversion data shown in Table 1 confirm that an active catalyst is formed before significant thermal conversion of the coal begins.

A series of catalysts were formed in the microautoclave by heating $\text{Mo}(\text{CO})_6$ in $\text{H}_2/10\% \text{H}_2\text{S}$ to various temperatures (6). The products were submitted to analysis by X-ray diffraction to determine the degree of crystallinity. At 175°C or 250°C, the products were essentially amorphous compounds. The development of some crystallinity was observed on raising the reaction temperature to 375°C. At 425°C, a higher degree of crystallinity was observed. The average crystallite size formed at this temperature was 75 Å with an average stacking height of 30 Å (~5 layers).

When the catalyst is formed in conjunction with coal, the $\text{Mo}(\text{CO})_6$ apparently sublimates and disperses onto the coal from the gas phase either prior to being sulfided or as it is converted to the sulfide phase (6). At the levels of Mo used in the liquefaction experiments with $\text{Mo}(\text{CO})_6$ (1000 ppm), it was not possible to determine the fate of the $\text{Mo}(\text{CO})_6$ using X-ray crystallography on the THF-insoluble residues owing to the small amount of catalyst present and to interferences from the coal mineral matter which was concentrated in the residue. It was possible, however, to examine the MoS_2 -containing liquefaction residue prepared from the DECS-17 coal and $\text{Mo}(\text{CO})_6$ (see Experimental) by X-ray diffraction if the mineral matter was first removed by digestion with hydrofluoric acid. In this case, X-ray diffraction analysis identified MoS_2 in the THF insoluble residue with a crystallite size of approximately 80 Å and a relatively low degree of stacking as indicated by a very broad 002 line.

An alternative method for forming MoS_2 -containing particles from AHM in Panasol has been reported (4). Elemental analysis of the MoS_2 -containing particles was consistent with a composition of 50 wt% carbon and 50 wt% MoS_2 (4). X-ray diffraction showed that the MoS_2 was poorly crystalline. The average size in the basal plane was 25 Å. Absence of the 002 line implied the MoS_2 was essentially single layer. The dimensions obtained by X-ray diffraction were confirmed by TEM. The surface area of the particles determined by the BET method with nitrogen was 262 m^2/g .

To compare the three different means of introducing MoS_2 , liquefaction experiments were carried out in the microautoclave using the DECS-17 coal at temperatures from 350°C to 425°C. All of the experiments were performed at least in duplicate. A comparison of the results for the two preformed catalysts with those obtained using $\text{Mo}(\text{CO})_6$ (Table 1) was made by taking the difference between the conversion values for the catalysts. These differences are shown in Figure 1. The large error bars indicated on the zero line represent the range of conversion values obtained using $\text{Mo}(\text{CO})_6$. The small error bars associated with the symbols for the two preformed catalysts represent the range of values obtained for these experiments. Error bars are not shown if they are smaller than the size of the symbol.

With respect to conversion to primary (THF-soluble) products, the data in Figure 1 show that the form of introduction of the catalyst has a significant effect on the primary dissolution and liquefaction of the coal. The catalyst formed in-situ from $\text{Mo}(\text{CO})_6$ consistently yielded the highest conversions, especially at the lower temperatures. The MoS_2 -containing particles were better than the MoS_2 -containing liquefaction residue except at the lowest temperature where the conversions were similar. At 425°C, the MoS_2 -containing particles did yield high levels of conversion similar to when $\text{Mo}(\text{CO})_6$ was used.

A different picture emerges from Figure 1 regarding secondary conversion of the primary products to cyclohexane-soluble material. The form of introduction of the catalyst did not appear to have any significant effect at any temperature in this case.

The changes in the total number of moles of gas in the microautoclave system during experiments with and without the catalysts were determined from the pressure and temperature data collected during the experiments. A correction procedure was used to compensate for the nonisothermal nature of the microautoclave system and for nonideality in the gas phase (6). After subtracting the thermal results from the respective results obtained with the catalysts, plots of moles of gas versus reaction time show decreasing amounts of gas at all temperatures investigated. The onset of rapid hydrogen consumption differed for the different forms of catalyst. For $\text{Mo}(\text{CO})_6$, the liquefaction residue, and the preformed particles, the onset of rapid hydrogen consumption occurred at approximately 370°C, 400°C, and 390°C, respectively. At 350°C, the rate of consumption for all catalysts was nearly constant for the entire reaction time at this temperature. At the higher temperatures, the rates of consumption were initially constant but decreased with time as the reaction proceeded.

The increment in coal conversion due to catalyst is plotted against values for the initial rates of gas uptake caused by catalyst in Figure 2. The increase in THF conversion attributed to catalyst correlates well with the initial rates of gas uptake when the uptake is plotted on a logarithmic scale. No such correlation is evident for conversion to cyclohexane soluble material.

MoS_2 is known to catalyze the hydrogenation of CO to form CH_4 (8). As an independent measure of catalyst activity, the rates of gas uptake associated with the conversion of a CO/H_2 mixture were obtained in the presence of the three forms of the catalyst. The preformed catalysts were simply added to the microautoclave as in the liquefaction experiments. For $\text{Mo}(\text{CO})_6$, the catalyst species was first formed in a separate experiment without coal and a portion of this product was then used in the methanation test. Details are contained in the

Experimental section. Table 2 contains the rates of gas uptake observed using both slow and rapid heat-up to 375°C along with the respective conversions to THF-soluble products observed in the previously described liquefaction experiments at this same temperature (no rapid heat-up liquefaction experiments were performed).

Table 2. Comparison of methanation activity and liquefaction conversion at 375°C for different forms of MoS₂-containing catalysts.

Catalyst	Heat-up	Gas Uptake Rate (mmol gas/mmol Mo/min)	Liquefaction Conversion, daf wt% ¹
Mo-containing THF insols	slow	0.029	63
	rapid	0.041	--
MoS ₂ Particles	slow	0.079	76
	rapid	0.085	--
Derived from Mo(CO) ₆ ²	slow	0.032	83
	rapid	0.044	--

¹THF conversions. The cyclohexane conversions were the same (25% to 26%) in all cases. ²The methanation tests were performed with catalyst prepared in the absence of coal. The catalyst was formed in situ in the liquefaction tests.

The highest rate of gas uptake is that of the preformed MoS₂ particles derived from AHM and Panasol. The rates for the two materials derived from Mo(CO)₆ are lower and nearly the same whether the catalyst was formed with or without coal present. There is no direct correlation between the gas uptake rates observed for methanation and the values for coal conversion. A rationale for the different order of catalytic performance found for the gas-phase methanation and the coal liquefaction reactions may be more easily constructed when more data is in hand. For the present, it is worth noting that the experimental reactions are quite different with regard to rate restrictions that may be imposed by mass transport. Thus, coal/catalyst contacting may be a significant determining factor in the liquefaction experiments. The solvent-free character of these experiments accentuates the importance of mixing and contact with the reacting coal. For example, the most intimately mixed catalyst, that formed in situ from Mo(CO)₆, provides the highest coal conversion. When recovered in the liquefaction residue and recycled, conversion drops significantly. However, the activity determined by the gas-phase reaction for the liquefaction residue is not much less than observed for the catalyst made in the absence of coal. On the other hand, the particulate catalyst formed from AHM and Panasol shows higher activity for the gas-phase reaction, but does not perform as well as the more intimately mixed catalyst in the liquefaction experiment. The solvent-free liquefaction experiment reflects a combination of catalyst activity and coal contacting, while the gas-phase methanation test more nearly reflects a catalytic activity. It should also be borne in mind that the catalytic sites responsible for the two different reactions may not be the same. In view of the importance of establishing what factors limit the performance of dispersed catalysts, for example catalyst activity versus transport limitations, experiments now in progress are aimed at further exploring the relationship between methanation activity and liquefaction results.

CONCLUSION

The results show that the means of introduction of MoS₂-containing catalysts has a significant effect on the initial dissolution and conversion of coal to THF-soluble products, especially at temperatures below 425°C. The self-dispersing Mo(CO)₆ precursor provided the best conversions under the conditions of these experiments. More intimate contact between the catalyst and the reacting coal is thought possible in this case than with the preformed catalysts. Better contact could promote more hydrogen transfer from the gas phase to the reacting coal, preventing retrogressive reactions. The initial softening point of the DECS-17 coal is 385°C, and maximum fluidity is achieved at 420°C (Gieseler plastometer data provided with the coal). This increase in fluidity may be the reason performance of the different catalysts becomes more similar at the higher temperatures. Experiments with coals with different softening characteristics might be used to test this hypothesis.

On the other hand, the conversion of the coal to cyclohexane-soluble products was not affected by the form of introduction of the catalyst. This would imply that the reactions involved in forming these lighter materials occur at a point in the liquefaction process when all of the catalysts would be more uniformly distributed throughout the reaction mass.

Finally, the presence of coal appears to have an influence on the character of the catalyst formed from $\text{Mo}(\text{CO})_6$. The X-ray data presented indicates that a reduced degree of stacking is observed for catalyst samples prepared in the presence of coal.

ACKNOWLEDGMENTS AND DISCLAIMER

The author would like to thank Richard Hlasnik and Jerry Foster for performing the microautoclave work, Sidney Pollack and Elizabeth Frommell for X-ray diffraction analysis and interpretation, and Donald Martello for performing the TEM analysis. Reference in this report to any specific product, process, or service is to facilitate understanding and does not imply its endorsement or favoring by the United States Department of Energy.

REFERENCES

1. Weller, S. W. *Energy & Fuels* 1994, **8**, 415-420.
2. Derbyshire, F. J. *Catalysis in Coal Liquefaction: New Directions for Research*; IEA Coal Research: London, 1988.
3. Warzinski, R.P. *Prepr. Pap. - Amer. Chem. Soc., Div. Fuel Chem.* 1993, **38**(2), 503-511.
4. Cugini, A.V.; Martello, D.V.; Krastman, D.; Baltrus, J.P.; Ciocco, M.V.; Frommell, E.F.; Holder, G.D. *Prepr. Pap. - Amer. Chem. Soc., Div. Fuel Chem.* 1995, **40**(2), 370-376.
5. Warzinski, R. P.; Lee, C.-H.; Holder, G. D. *J. Supercrit. Fluids* 1992, **5**, 60-71.
6. Warzinski, R.P. and Bockrath, B.C. *Prepr. Pap. - Amer. Chem. Soc., Div. Fuel Chem.* 1995, this volume.
7. *CRC Handbook of Chemistry and Physics*; Weast, R. C., Ed.; CRC: Boca Raton, 1979, B-99.
8. Saito, M. and Anderson, R. B. *J. Catal.* 1980, **63**, 438-446.

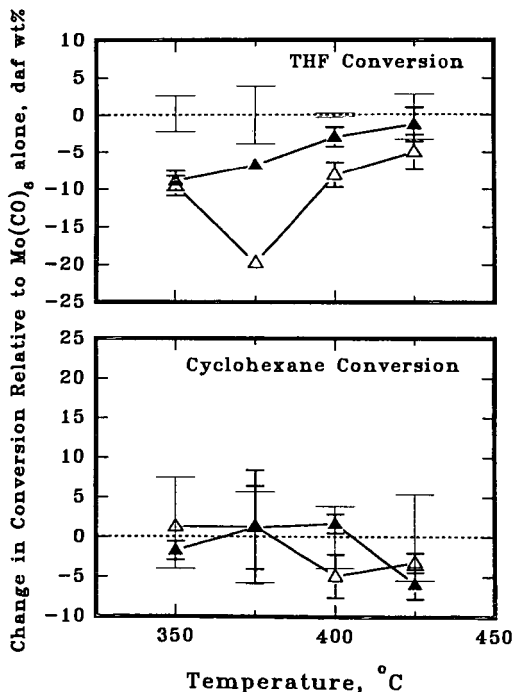
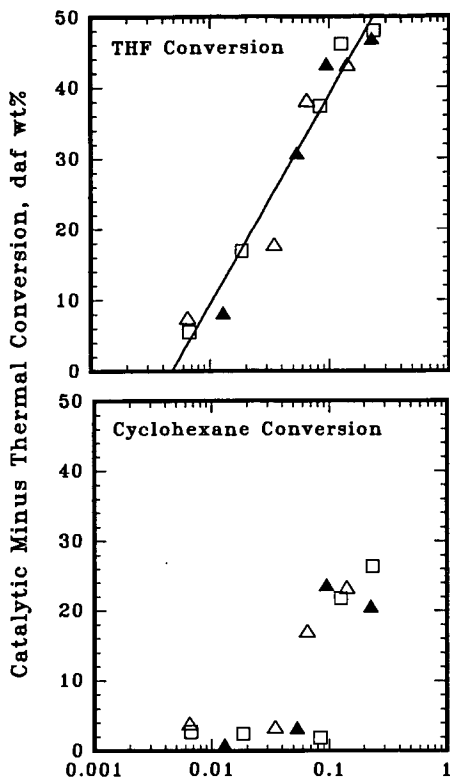


Figure 1. Effect of the means of introduction of catalyst on conversion of DECS-17 coal relative to direct addition of $\text{Mo}(\text{CO})_6$. (Δ MoS_2 -containing liquefaction residue; \blacktriangle preformed MoS_2 -containing particles.)



Initial Rate of Gas Uptake Due to the Presence of the Catalyst, mmol/mmol Mo/min

Figure 2. The dependence of catalyst-assisted conversion on the initial rate of gas uptake caused by the catalyst. (□ Mo(CO)₂; △ MoS₂-containing liquefaction residue; ▲ preformed MoS₂-containing particles.)

INFLUENCE OF SULFUR ADDITION AND S-INDUCED WALL CATALYTIC EFFECTS ON C-C BOND CLEAVAGE AND AROMATICS HYDROGENATION

Eckhardt Schmidt*, Chunshan Song and Harold H. Schobert

Fuel Science Program, Department of Materials Science and Engineering, 209 Academic Projects Building, The Pennsylvania State University, University Park, PA 16802

Catalytic hydrocracking of 4-(1-naphthylmethyl)biphenyl, designated as NMBB, predominantly yielded naphthalene and 4-methylbiphenyl. Sulfur addition to most catalyst precursors lead to substantially higher catalyst activity and subsequently higher conversion. NMBB was also treated with sulfur alone in the absence of catalysts in concentrations of 1.2 to 3.4 wt, corresponding to conditions present in catalytic runs with added sulfur to precursors. It was found that increasing sulfur concentrations lead to higher NMBB conversion. Furthermore, sulfur had a permanent influence on the reactor walls. It reacted with the transition metals in the stainless steel to form a microscopic black iron sulfide layer on the surface, which could not be removed mechanically. The "non-catalytic" runs which were done after experiments with added sulfur yielded higher conversions than normal runs done in new reactors. This "wall catalytic effect" can be reduced by treating sulfided reactors with hydrochloric acid for a short period of time and subsequent immersing into a base bath overnight. These results demonstrate the significant influence of sulfur addition and S-induced residual wall-effect on C-C bond cleavage and hydrogenation of aromatics in batch reactors.

Keywords: Model reactions, hydrocracking, dispersed catalysts, wall-effect.

INTRODUCTION

Since the early 90's, modern coal liquefaction has reached a point where only minor improvements to the process have been made (1). Sophisticated catalysts have been developed to increase efficiency. Much work still needs to be done in order to fully understand the mechanism on a molecular level, which in turn might lead to an optimized liquefaction process. Model compounds, like NMBB serve as excellent examples of a simplified coal model. Recent work (2,3) examined the effect of various catalysts on hydrocracking of this model compound. It turned out that certain precursors, such as Mo-based and bimetallic systems, show very high activity which can generally be increased by sulfur addition. This finding stimulated our interest to study the influence of S in model compound hydrocracking reactions.

We selected for comparison organometallic compounds and inorganic complexes. Good solubility of catalyst precursors in the liquefaction media generally leads to better catalyst dispersion and greater effectiveness for liquefaction reactions (4). One way to achieve better dispersion is by using soluble organometallic precursors. Ligand loss at elevated temperatures results in an in situ preparation of finely dispersed active catalyst particles. Hirschon and Wilson (5) demonstrated that highly dispersed catalysts from organometallic precursors can be effective for hydrogenating the coal with molecular hydrogen without relying upon a donor solvent. Thus the following work describes our efforts to investigate the influence of dispersed catalyst precursors and sulfur on hydrocracking of NMBB.

EXPERIMENTAL SECTION

Catalyst Precursors

A sample of superfine iron oxide was graciously provided by Mach I Inc. in Pennsylvania. NMBB and sulfur was purchased from TCI America. GC-MS confirmed sufficient purity of NMBB (> 99 %) and it was used without further purification.

Model compound reactions

Runs with NMBB were carried out in 33 mL stainless steel reactors (tubing bomb) at 400 °C for 30 min. In a typical run, a reactor was loaded with ca. 0.25 g NMBB, 2.11 wt % catalyst precursor and 0.14 g solvent (tridecane). The reactor was purged three times with H₂ and then pressurized with 6.9 MPa H₂ at room temperature for all experiments. A preheated fluidized sand bath was used as the heating source and the horizontal tubing bomb reactor was vertically agitated to provide mixing (about 240 strokes/min.) After the reaction the hot tubing bomb was quenched in cold water and the gaseous products collected in a gas bag for further analysis. The liquid contents were washed with 15 ml CH₂Cl₂ through a low speed filter paper for qualitative and quantitative GC analysis of the filtrate. All runs were carried out at least twice to confirm reproducibility.

The products were identified by GC-MS using a Hewlett-Packard 5890 II GC coupled with a HP 5971A mass-selective detector operating at electron impact mode (EI, 70 eV). The column used for GC-MS was a J&W DB-17 column; 30-m X 0.25-mm, coated with 50 % phenyl 50 % -methylpolysiloxane with a coating film thickness of 0.25 μm. For quantification, a HP 5890 II GC with flame ionization detector and the same type of column (DB-17) was used. Both GC and GC-MS were temperature programmed from 40 to 280 °C at a heating rate of 4 °C/min and a final holding time of 15 min. The response factors for 10 of the products were determined using pure compounds. More experimental details may be found elsewhere (2).

RESULTS AND DISCUSSION

Hydrocracking of NMBB

Initial tests using superfine iron oxide (SFIO), a commercially available sample with a high surface area (250 m²/g), yielded only moderate conversion (27.1 %), even at elevated temperatures (400 °C). The beneficial effect of sulfur addition could once more be demonstrated. Sulfur added to SFIO led to a considerable increase in conversion (78.2 %). A series of experiments was carried out to determine the impact of sulfur concentration on NMBB conversion. It was found that increasing sulfur concentration (starting at 1.2 wt %) led to increasing model compound conversion. As shown in Tables 1 and 2, several catalysts in combination with S were tested to study the impact of sulfur addition for catalytic hydrocracking of NMBB at 400 °C.

Among the tested catalyst precursors (Figure 1), ferrocene is more effective in hydrocracking reactions of NMBB than the inorganic iron complex FeSO₄ x 7 H₂O, which is the least active. However, in the presence of sulfur, FeSO₄ x 7 H₂O shows remarkable activity. The active form from iron sulfate is considered to be pyrrhotite. High temperature activation of ferrous sulfate transforms the inorganic complex in an H₂S atmosphere into an active pyrrhotite phase (6). Adding sulfur to ferrocene had a negative effect on its. This is possibly due to the formation of iron carbide during the initial stage of the catalyst activation. It is known (7) that sulfur addition to iron oxide, or iron pentacarbonyl initiates the transformation into pyrrhotite (Fe_{1-x}S, where 0 ≤ x ≤ 0.125, because of Fe³⁺ impurities). This activation reaction is difficult to perform and iron carbonyls tend to form less reactive iron carbides and oxides during the activation process. Precursor molecules without CO ligands, but cyclopentadienyl groups, are expected to form much more iron carbide. In most reactions, S-presence attains higher conversion than a reaction for the same precursor in a hydrogen atmosphere. Even though molybdenum-based precursors are generally superior to iron-containing complexes, S-addition transforms the latter compound class into a more active phase, probably by providing a better dispersion of iron (8).

It was also found that sulfur had a permanent effect on the stainless steel reactor walls. Even new reactors turn black inside after reactions with S, depending on the sulfur concentration. We assume that added S reacts with iron on the surface of the reactor walls to form FeS. This black FeS layer can not be removed mechanically, and is not removed by base (KOH/i-Propanol/H₂O) for an extended period of time (1 - 3 days). Further experiments of sulfided reactors with NMBB alone gave dramatically higher conversion than identical thermal runs in new reactors. This so called "wall effect" can be reduced by immersing sulfided tubing bomb reactors in a 6 N HCl bath for 5 min. Subsequent treatment of the same reactor in base bath brings "background activity" down by more than 50 %. However, repeated acid washing leaches out steel components and weakens the steel. Furthermore, the surface characteristics of so treated reactors are changed permanently.

The influence of remaining sulfur in the tubing bomb reactors was also investigated. The question arises whether sulfur itself, of sulfided reactor walls are responsible for NMBB cleavage. To clarify this problem, we washed sulfided reactors subsequently with chloroform and ethanol to remove material trapped in the upper part of the tubing bomb reactors. Experiments after this treatment revealed no difference compared to runs without washing the reactor. Therefore, the "residual" catalytic effect seems to be due mainly to the formation of a sulfided layer on the reactor wall. Treatment of tubing bomb reactors with hydrochloric acid partially removes unwanted FeS particles but does not restore the original low activity of a new reactor. More work still needs to be done to understand the influence of sulfur on coal liquefaction experiments. Coal is going to be studied too, because of varied sulfur concentrations which can activate S-free precursors and change their activity substantially.

PRODUCT DISTRIBUTION

The following compounds can be found as main products: tetralin, naphthalene, bibenzyl and 4-MBB. The identified products can be classified into hydrocracking, hydrogenation and isomerization products. Those coming from hydrocracking reactions form the major pool of reaction products, followed by hydrogenation and isomerization products. Hydrocracking of NMBB yields three product categories from cleavage of the bonds between the aromatic moieties. Figure 1 and 2 show the product distribution from catalytic hydrocracking experiments of NMBB. All iron-containing catalyst precursors give a ratio of main products similar to each other. It is apparent that ferrous catalysts cleave NMBB preferably in position at the C-C bond α to the naphthyl ring. Increasing conversion leads in most experiments to a proportional increase in the yields of major products. When added in larger amounts (3.4 vs. 1.2 wt %), S not only increased NMBB conversion, but also altered product distribution (Table 2).

Several studies, including the present work, have shown that NMBB tends to undergo cleavage of the C-C bond connecting the naphthyl group to the remainder of the molecule when subjected to a variety of catalytic reactions under a variety of conditions. Farcasiu et al. (3) suggested a reaction mechanism in which the first stage consists of the formation of a radical cation. The loss of electron density leads to a weakened α-bond which can then be broken relatively easily. This is in contrast to model studies in which phenyl-containing compounds prefer β-cleavage (9). In the work of Penn and Wang (9) radical cations were generated in the mass spectrometer under a variety of conditions but had little impact on the bond cleavage pathway. Preference for β-cleavage was observed. Which was explained by resonance stabilization of the intermediates. Both intermediates are resonance stabilized. Thermochemical calculations (10) show that reaction pathway β is 30 kcal/mol lower for both neutral and radical cationic species than pathway α. In contrast, neither of the intermediates resulting from bond α cleavage are stabilized. However, in the presence of a catalyst, the major reaction pathway mainly involves the cleavage of bond α.

These studies indicate that a new decomposition pathway mechanism must be developed to explain the results of bond cleavage involving model reactions on NMBB.

ACKNOWLEDGMENTS

This project was supported by the U.S. Department of Energy, Pittsburgh Energy Technology Center under contract DE-AC22-92PC92122. We are grateful to Dr. U. Rao of PETC for his support. We also thank Mr. R. Copenhaver for the fabrication of reactors, and Mach I Inc. for providing the SFIO sample.

REFERENCES

1. Mochida, I. and Sakanishi, K. *Advances in Catalysis*, **40**, 1994, 39-85.
2. a) Schmidt, E. and Song, C. *Prepr. Pap. - Am. Chem. Soc., Div. Fuel Chem.*, **35**, 1994 733-737.
b) Song, C.; Schmidt, E. and Schobert, H. H. *DOE Coal Liquefaction and Gas Conversion, Contractors' Review Meeting, Pittsburgh*, (September 7-8, 1994), 593-604.
3. a) Farcasiu, M.; Smith, C. *Prepr. Pap. - Am. Chem. Soc., Div. Fuel Chem.*, **1990**, **35**, 404-13.
b) Farcasiu, M.; Smith, C. *Fuel Processing Technology*, **1991**, **29**, 199-208.
c) Farcasiu, M.; Smith, C. and Ladner, E. P. *Prepr. Pap. - Am. Chem. Soc., Div. Fuel Chem.*, **1991**, **36**, 1869-77.
4. Artok, L.; Davis, A.; Mitchell, G. D.; Schobert, H. H. and Schobert, H. H. *Energy Fuels*, **1993**, **7**, 67-77.
5. a) Hirschon, A. S.; Wilson Jr, R. B. *Coal Science II, ACS Sym. Ser.*, **1991**, 273-83.
b) Hirschon, A. S.; Wilson Jr, R. B. *Fuel*, **1992**, **71**, 1025-31.
6. Artok, L.; Schobert, H. H.; Davis, A. *Fuel Process Technol.*, in press.
7. a) Herrick, D.; Tierney, J.; Wender, I.; Huffmann, G.P. and Huggins, F.E. *Energy and Fuels*, **4**, 1990, 231.
b) Weller, S. *Energy Fuels*, **1994**, **8**, 415-420.
8. Song C.; Schmidt, E. and Schobert, H. H. *8th ICCS, Oviedo Spain*, September 10-15, 1995, submitted.
9. Penn, J. H.; Wang, J.-H. *Energy Fuels*, **1994**, **8**, 421-425.
10. Ades, H. F.; Companion, A. L.; Subbaswamy, K. R. *Prepr. Pap. - Am. Chem. Soc., Div. Fuel Chem.*, **1991**, **36**, 420-4.

Table 1: Effect of Catalyst Precursors on Hydrocracking Reactions of NMBB at 400 °C.

Catalyst Precursors ^a	Cp ₂ Fe	Cp ₂ Fe + S	FeSO ₄ x 7 H ₂ O	FeSO ₄ x 7 H ₂ O + S	Superfine Fe ₂ O ₃	Superfine Fe ₂ O ₃ + S
Products [mol %]						
Toluene	1.6	1.1		1.3	1.3	1.9
Tetralin	0.4	0.3		0.6	3.0	4.0
Naphthalene	13.8	10.3	4.5	24.0	16.4	64.1
2-Methylnaphthalene						1.4
1-Methylnaphthalene	5.6	0.5		1.5		5.8
Bibenzyl	2.6	0.6	0.6	2.5	1.0	8.9
4-Methylbibenzyl	9.4	7.4	2.6	19.1	17.4	59.6
Conversion [wt %]	15.8	9.6	3.7	23.9	27.1	78.2

^aWhen sulfur was added, the atomic ratio of S:Fe was 1:1.

Table 2: Effect of Sulfur Addition on Hydrocracking Reactions of NMBB at 400 °C.

Catalyst Precursors	None Catalytic	Sulfur [1.2 wt %] ^a	Sulfur [3.4 wt %] ^a	None [sulfided reactor]	None [reactor HCl treated]
Products [mol %]					
Toluene	0.3	1.4	4.9	1.0	1.0
p-Xylene					
Tetralin	0.2	0.8	2.9	0.8	0.4
Naphthalene	0.6	24.8	74.4	19.1	10.8
2-MTHN ^b			0.4		
2-Methylnaphthalene			7.8		
1-Methylnaphthalene		1.7	9.5	0.8	0.7
Benzyl naphthalene	0.9				
Bibenzyl		2.4	42.5	1.0	1.2
4-Methylbibenzyl	1.3	22.1	32.3	18.3	9.7
Conversion [wt %]	3.9	26.1	82.5	23.0	11.6

^aBased on NMBB, ^bmethyltetrahydronaphthalene.

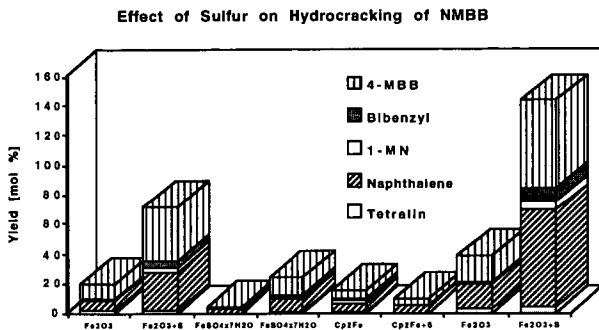


Figure 1: Effect of catalytic hydrocracking of NMBB at 400 ° for 30 min.

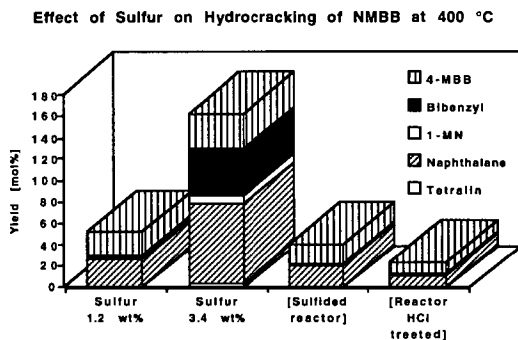


Figure 2: Effect of sulfur on NMBB hydrocracking product distribution at 400 °C for 30 min.

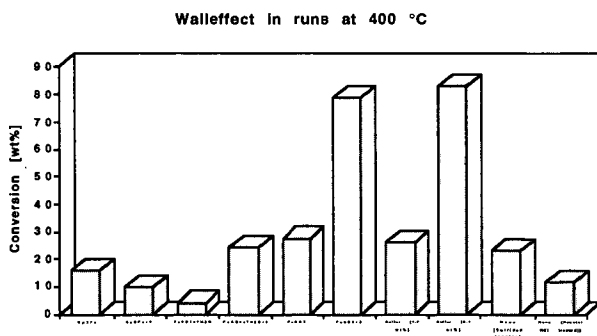


Figure 3: Effect of sulfur on NMBB conversion at 400 °C for 30 min.

A STUDY OF CHEMICAL DEHYDRATION OF COALS AND ITS EFFECT ON COAL LIQUEFACTION YIELDS

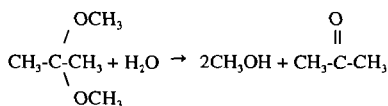
D.A. Netzel, F.P. Miknis, J.C. Wallace, Jr., C.H. Butcher, J.M. Mitzel, T.F. Turner
Western Research Institute, 365 N. 9th Street, Laramie, WY 82070-3380,
and R.J. Hurtubise, Dept. of Chemistry, University of Wyoming, Laramie, WY 82071

Keywords: Coal Drying, Chemical Dehydration, Coal Liquefaction

INTRODUCTION

Although great strides have been made in developing the technology of coal liquefaction processes in recent years, many unsolved problems still remain before a viable and economical process can be achieved. The technological problems that still exist can be solved through a more fundamental understanding of the chemistry associated with each stage of the coal liquefaction process, starting with any pretreatment steps that may be carried out on the coal itself. One pretreatment process which can improve the economics of coal liquefaction is coal drying, particularly for the lower rank coals. However, there is also considerable evidence to show that drying has a detrimental effect on the liquefaction behavior of coals.^{1,3} The problem that needs to be solved is that of economically drying coal without adversely affecting its liquefaction reactivity. Only recently have there been any systematic studies of the methods of coal drying on coal structure and the role water plays in enhancing or lessening coal reactivity toward liquefaction.^{4,5} Thermal methods of drying can alter the physical structure of coal as well as promote undesirable chemical reactions. Low-temperature drying of coal, on the other hand, should preserve the structural integrity, reduce retrograde reactions, reduce thermal degradation, and provide information on nonbonded, chemisorbed, and physisorbed water. Chemical drying of coals is a relatively unexplored technique for removing water at low temperature.

A common chemical dehydrating agent is 2,2-dimethoxypropane. This agent has been used in inorganic chemistry to remove water of hydration in inorganic compounds⁶ and in biological sciences for drying tissues for microscopic examination.^{7,8} The reaction of 2,2-dimethoxypropane (DMP) with water is shown in scheme I.⁹



Scheme I

This reaction is rapid and endothermic. The reaction products, methanol and acetone, are removed by vacuum at ambient temperature. Removing water by chemical means rather than by physically forcing exchange by mass action preserves the ultrastructural integrity of the coal cellular components. The use of the dehydration agent, 2,2-dimethoxypropane, in this study to dry coals is a novel and innovative approach to the understanding of the role of water in coal chemistry.¹⁰

EXPERIMENTAL

Of the six coals used in this study four were obtained from the Pennsylvania State University, Coal Research Section, and two were obtained from the Powder River Basin in Wyoming. The coals selected for study consisted of a lignite, three subbituminous, and two bituminous coals. Bulk samples of these coals were premoisturized in a constant humidity chamber at 30°C for 24 hours. The moisture content determined thermally was used as the reference moisture content for the coals.

Coal samples were dried with DMP before coal liquefaction. Depending upon the amount of moisture in the coal, between 22 and 72 grams of DMP, and between 6 and 25 mL of 0.2 N methanesulfonic acid in methanol were added to a 20 g sample of coal. The acid-methanol solution was added to the sample, followed by DMP. The contents of the flask were shaken to ensure good mixing and contact. The mixture was allowed to stand for 24 hrs. The liquid was then decanted and a vacuum was applied to remove the remaining liquid (excess DMP and methanol).

A modified "Borgialli" microreactor¹ was used for the liquefaction of the coals. The key features of this reactor system are: rapid heating through submergence in a fluidized sandbath,

pneumatic control of the extent of autoclave submergence, and continuous stirring using a magnetically-coupled stirrer. The gases produced during the coal liquefaction process were collected in a gas bomb and analyzed using an HP 5890 Series II GC fitted with both FID and TCD detectors. A 6 ft, Porapak N, packed column was used to separate the gases. Upon completion of the coal liquefaction experiment, the reactor was opened, and the soluble coal products and residue were rinsed using CH_2Cl_2 into a Soxhlet thimble. Soxhlet extraction was carried out for 30 hr at the refluxing temperature of CH_2Cl_2 . The solid residue in the Soxhlet thimble and the thimble were placed into a furnace set at $\sim 100^\circ\text{C}$ for 20 hrs to remove solvent. The coal residues were characterized using solid-state carbon-13 NMR. Solvent swelling of the coal samples was conducted using the procedure described by Green et al.¹²

Solid-state ^{13}C NMR measurements were made using a Chemagnetics 100/200 solids NMR spectrometer. Carbon aromaticity measurements were made at 25 MHz using the technique of cross polarization (CP) with magic-angle spinning (MAS) and high-power decoupling. These measurements were made using either a large-volume sample spinner (2.1 mL) at a spinning rate of ~ 3.8 kHz or a 7.5 mm (OD) sample spinner at a spinning rate of 4.5 kHz. Between 3,600 and 7,200 transients were recorded. Other instrument parameters were a pulse delay of 1 s, a contact time of 1 ms, a 6.2 μs (large volume spinner) and 5 μs (7.5 mm spinner) pulse widths, a sweep width of 16 kHz, and 1 K data acquisition points. A 25 or 50 Hz exponential multiplier was applied to the free induction decay of each ^{13}C spectrum before integration.

A TA instruments 2910 Differential Scanning Calorimeter (DSC) with a liquid nitrogen cooling accessory (LNCA) was used in this study to determine the amount of solvents retained by the coals after chemical dehydration.

RESULTS AND DISCUSSION

A. Effects of Chemical Drying Process on the Structure of Coals

1. Chemical Drying Kinetics. A typical plot of the weight percent of moisture removed from the coal samples as a function of time in which the coals are in contact with DMP is shown in Figure 1. In all cases a significant amount of moisture is removed in the first minute of the reaction. The initial reaction is DMP with physisorbed surface water and free water in the pores near the surface of the coal. Removal of the remaining moisture requires longer times and is due to diffusion control of DMP into the smaller pores within the coals.

The chemical drying data after the fast initial reaction were fit to 1st- and nth-order kinetic equations. The kinetic parameters are listed in Table I. The initial concentration, C_i , shown in the table is defined as the percent of physisorbed and free surface moisture removed from the coal during the initial reaction of water and DMP. This reaction occurs almost instantaneously. The value of C_i for both the first order and nth order reactions increases with decreasing coal rank. That is, the higher rank coals are generally less porous and have less adsorbed water than the lower rank coals. For Wyoming Black Thunder coal, the C_i value is higher than expected and may be due to the smaller mesh size of the coal sample compared to the other coals.

The percent of moisture in coal at $t = \infty$, but not including the water removed during the initial reaction, is M_∞ . The sum of C_i and M_∞ gives the total amount of water in each coal sample. These values exceed their respective thermal moisture values especially for the low rank coals.

Table I also lists the percent of readily accessible water (sorbed surface water) for each coal. As shown in the table, the percent of loosely bound surface water increases with decreasing rank of the coal. Based on a first-order kinetics analysis of the data, the Utah Blind Canyon coals have the lowest amount of surface water (12.2%) whereas the Texas Bottom coal and North Dakota Beulah lignite have almost two-thirds of the total water near or on the surface and readily accessible to react with DMP (62.0 and 64.4%, respectively). Figure 2 is a plot of the percent of surface water as a function of the rank of coal based upon the fixed carbon content. Wroblewski and Verkade¹² also measured the different types of moisture in coals using several extraction solvents and measuring the moisture content in the extracts over an eight hour period. These authors found that of the total moisture content, the higher rank coals have less surface water than the lower rank coals in qualitative agreement with the results shown in Figure 2.

2. ^{13}C NMR. The ^{13}C CP/MAS NMR spectra of the premoisturized and chemically dried Wyoming Eagle Butte coal is shown in Figures 3a and 3b. There appears to be enhanced resolution in the aromatic (100-210 ppm) and aliphatic (0-80 ppm) carbon regions of the spectra. Decarboxylation in the aromatic region is not apparent. The enhanced resolution in the aliphatic carbon region may be due to (1) the tightly bound residual solvents and/or reaction products such as methanol that had replaced the water and (2) increased mobility of some coal

components because of less secondary interactions resulting from the loss of the strongly hydrogen bonded water. Only slight changes (within experimental error) are noted for the carbon aromaticity values for chemical dried coals relative to the premoisturized coals. Thus, chemical drying had little or no effect on the organic composition of the coals. However, the extent of physical association of the coal molecule had been altered due to the loss of water which may have affected the overall coal structure.¹³

3. Differential Scanning Calorimetry of Coals. The solid-state ¹³C NMR spectra of chemically dried coals showed additional carbon resonances and/or increased resolution in the aliphatic carbon region. The changes in the spectra were assumed to be due to sorbed solvents and/or reaction products occupying surface and pore sites previously held by water. DSC was used to identify and quantify the sorbed species for the chemically dehydrated coals. For the chemically dried coal samples, losses could conceivably be from vaporization of methanol, acetone, water, or a combination of the three. Fortunately, the heats of vaporization of the three materials are significantly different, and a tentative identification of the material is possible if it is assumed that only one material is lost. For all chemically-dried coals, except Utah Blind Canyon, the material lost appears to be methanol with an average heat of vaporization of 1136 J/g and a standard deviation of 100 J/g. The literature value is 1224.5 J/g. The measured heat of vaporization for the Utah coal is close to the literature value for acetone, however, the weight loss for this material and the transition energy are small decreasing the accuracy of both measurements and placing the identification of the material in some doubt.

4. Swelling Index. The swelling index profile parameter¹⁴ of the chemically dehydrated coals is given in Table II. This parameter for Illinois # 6 and Texas Bottom coals shows a small decrease relative to the swelling index parameter of the premoisturized coals, whereas, Utah Blind Canyon, Wyoming Eagle Butte, Wyoming Black Thunder, and North Dakota Beulah coals show a significant increase. The data show that only a small increase or no change in the cross-linking internal structure for the Illinois # 6 and Texas Bottom coals had occurred as a result of chemical dehydration. However, a significant decrease in the cross-linking structure ($1 - X > 1$) is observed for the other four coals. The incorporation of CH₃OH at the sites previously occupied by water molecules would decrease the extent of relatively strong secondary interactions involving ionized groups, charge-transfer complexes and π - π interactions as well as hydrogen bonding and weak van der Waal's forces.¹⁵ A decrease in these interactions, in effect, would reduce the cross-linking due to physical association relative to the premoisturized coal.

B. Effects of Chemical Drying Process on the Reactivity of Coals

Table III gives the results of the coal liquefaction of the six coals that were chemically dried. The table contains data on the percentage of gas, liquid, and residue produced, and the percent conversion. Relative to the premoisturized coals (0% water removed), drying the coals by chemical dehydration, in general, increased the conversion yield. Utah Blind Canyon and North Dakota Beulah coals showed little or no change in the conversion yield.

Except for the chemically dried coals, the conversions are generally less for coals dried by thermal methods.^{14,16} The reason for the differences in liquefaction behavior of the chemically dried and the thermally dried coals appears to be due to the retention of the reaction products and solvents by the chemically dried coals. DSC has shown that some of the methanol was incorporated into the coal pore structure in place of the water, thus possibly preventing collapse of the pore structure during the dehydration reaction. This would allow for greater diffusion of tetralin during liquefaction and hence greater conversion. Relative to the premoisturized coal, all chemically dried coals show an increase in the coal liquid yield. This increase may also be the result of replacement of water by CH₃OH in the internal structure of coal thereby reducing the strong hydrogen bonding effect caused by water. In general, there is increase in total percent of gas produced with decreasing rank of the premoisturized coals (Utah to North Dakota). Both the Utah and North Dakota coals show a significant decrease in gas produced when completely dried. The total amount of gases produced from the other four dried coals is essentially the same as their corresponding premoisturized coals. The amount of coal residue produced during liquefaction of the premoisturized coals (Table III) decreases with the increase in the moisture content of the coal (decrease in coal rank).

The ¹³C CP/MAS NMR spectra of the coal liquefaction CH₂Cl₂ extracted residues from the premoisturized and chemically dried Texas Bottom coals are shown in Figures 4a and 4b. When compared to the starting coal spectrum, the NMR spectra of the residues show a significant reduction in the aliphatic component relative to the aromatic component. There is also a shift in the resonance position from ~ 30 ppm to ~ 20 ppm for the aliphatic carbons. The residual

aliphatic component at ~ 20 ppm could be due to methyl groups attached to aromatic rings that would not be cleaved during liquefaction at 425°C.

The significant difference in the residue NMR spectra of the Texas Bottom coal as well as for the other five coals is the enhanced resolution of the aliphatic carbons for the coals dried via chemical dehydration. This enhanced resolution of the aliphatic carbons in the ^{13}C NMR spectra was also noted in the NMR spectra of the chemically dried coals before liquefaction. However, it is unlikely that the carbon resonances observed are due to solvent and reaction products of the chemical drying technique unless the methanol is strongly adsorbed even at the liquefaction temperature of 425°C. It may be that the methanol solvent removed some of the soluble aliphatic carbon substituents (decreasing the chemical shift dispersion) and, thus, in effect giving higher resolution of the remaining carbons types.

REFERENCES

1. Silver, H.F., and W.S. Frazee, EPRI Report AP-4193, 1985.
2. Silver, H.F., P.J. Hallinan, and W.S. Frazee, *ACS Div. of Petrol. Chem. Preprints*, 1986, 31(3): 755-760.
3. Serio, M.A., P.R. Solomon, E. Kroo, R. Basilakis, R. Malhotra, and D. McMillen, *ACS Div. of Fuel Chem. Preprints*, 1990, 35(1): 61-69.
4. Song, C., A.K. Saini, and H.H. Schobert, *Energy and Fuels*, 1994, 8: 301.
5. Okuma, O., M. Masuda, K. Murakoshi, S. Yanai, and T. Matsumura, *Nenryo Kyokaiishi*, 1990, 69: 259.
6. Donoghue, J.T., and R.S. Drago, *Inorg. Chem.*, 1962, 1: 866-872.
7. Adams, R.F., *J. of Chrom.*, 1974, 95: 189-212.
8. Muller, L.L., and T.J. Jacks, *J. of Histochemistry and Cytochemistry*, 1975, 23: 107-110.
9. Critchfield, F.E., and E.T. Bishop, *Anal. Chem.*, 1961, 33: 1034-1033.
10. Netzel, D.A., F.P. Miknis, J.C. Wallace, Jr., C.H. Butcher, J.M. Mittel, T.F. Turner, and R.J. Hurtubise, DOE Final Report, Western Research Institute, WRI Report No. WRI-95-R023.
11. Green, T.K., J. Kovac, and J.W. Larsen, *Fuel*, 1984, 63: 935-938.
12. Wroblewski, A.E., and J.G. Verkade, *Energy and Fuels*, 1992, 6: 331.
13. Nishioka, M., *Fuel*, 1994, 73: 57.
14. Solomon, P.R., M.A. Serio, G.V. Deshpande, and E. Kroo, *Energy and Fuels*, 1990, 4: 42.
15. Nishioka, M., 1992, *Fuel*, 1992, 71: 941.
16. Saini, A.K., C. Song, and H. Shobert, *ACS Div. Fuel Chem. Preprints*, 1993, 38 (2): 593.

Table I. Kinetic Parameters for the Chemical Dehydration of Coals

Coal		Kinetic Parameters					
		Order n	Rate Constant k, hr ⁻¹	Initial Concentration of water, C _i (%)	Final Concentration of water, M _∞ (%)	Total Concentration of Water (%) C _i + M _∞	Percent of Surface Water C _i /(C _i +M _∞)
Utah Blind Canyon	1 st order	1	3.59 x 10 ⁻³	0.89	6.41	7.3	12.2
	n th order	0.893	4.15 x 10 ⁻³	0.94	6.31	7.3	13.0
Illinois # 6	1 st order	1	1.93 x 10 ⁻²	4.6	6.5	11.1	41.4
	n th order	1.07	2.49 x 10 ⁻²	4.5	6.6	11.1	40.5
Wyoming Eagle Butte	1 st order	1	2.17 x 10 ⁻³	12.5	11.5	24.0	52.1
	n th order	3.62	0.157	11.2	18.8	30.0	37.3
Wyoming Black Thunder	1 st order	1	1.85 x 10 ⁻³	19.9	2.2	22.1	90.1
	n th order	0.943	1.62 x 10 ⁻²	15.3	7.1	22.4	68.3
Texas Bottom	1 st order	1	8.39 x 10 ⁻³	18.4	11.3	29.7	62.0
	n th order	5.61	12.8	13.0	23.6	36.6	35.5
North Dakota Beulah	1 st order	1	1.11 x 10 ⁻³	24.6	13.6	38.2	64.4
	n th order	1.32	4.29 x 10 ⁻⁴	24.6	15.4	40.0	63.1

Table II. Solvent Swelling Profile Parameter^a of Premoisturized Coals and Chemically Dried Coals

Coal	Swelling Parameter (1-X) using 1,4-Dioxane	
	Premoisturized Coal	Chemically Dried
Utah Blind Canyon	1.0	1.61
Illinois # 6	1.0	0.95
Wyoming Eagle Butte	1.0	1.50
Wyoming Black Thunder	1.0	1.51
Texas Bottom	1.0	0.84
North Dakota Beulah	1.0	1.10

^a $X = (Q_{\text{coal}} - Q_{v,\text{dry}}) / (Q_{\text{coal}} - 1)$ where X = swelling index; Q_{coal} = swelling ratio of the premoisturized coal; and $Q_{v,\text{dry}}$ = swelling ratio of the dried coal.

Table III. Percentages of Gas, Liquid, Residue, and Conversion from the Liquefaction of Coals Dried using the Chemical Dehydration Method

Coal	Percent Water Removed	Percent Gas	Percent Liquid	Percent Residue	Percent Conversion
Utah Blind Canyon	0	9.1	61.0	30.0	70
	100	4.0	63.7	32.3	67.7
Illinois # 6	0	3.4	64.3	32.4	67.6
	100	5.3	74.4	20.2	79.8
Wyoming Eagle Butte	0	10.9	62.3	26.8	73.2
	100	10.0	75.1	14.9	85.1
Wyoming Black Thunder	0	11.4	67.6	21.0	79.0
	100	9.7	72.4	17.9	82.1
Texas Bottom	0	12.4	70.0	17.6	82.4
	100	10.2	77.2	12.6	87.4
North Dakota Beulah	0	35.6	38.8	25.6	74.4
	100	12.1	62.1	25.8	74.2

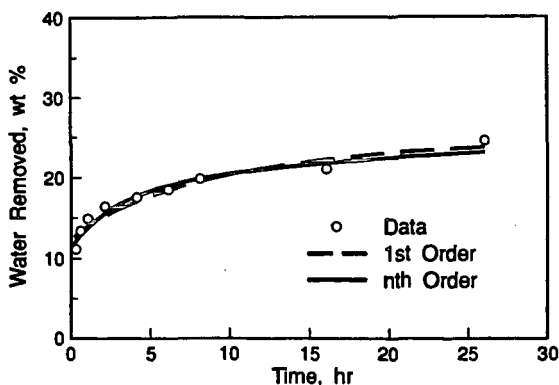


Figure 1. Weight Percent of Water Removed by DMP in Wyoming Eagle Butte Coal as a Function of Time

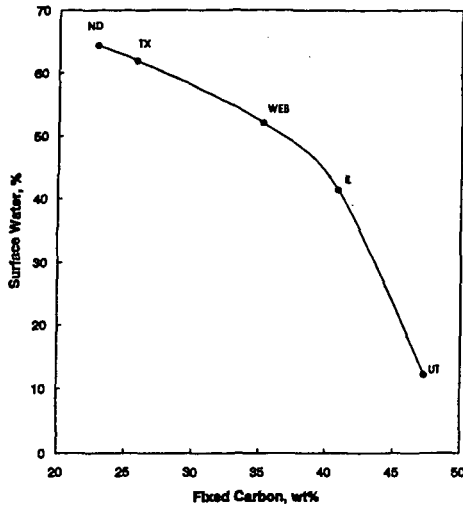


Figure 2. A Plot of the Percent Surface Water for Coals as a Function of the Coal Rank (wt % of fix carbon)

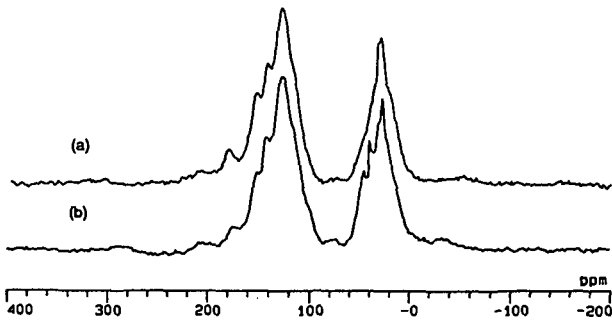


Figure 3. Carbon-13 NMR Spectra of Wyoming Eagle Butte Coal: (a) Premoisturized Coal and (b) Chemically Dried Coal

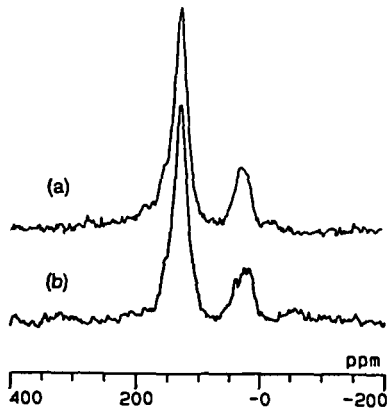


Figure 4. Carbon-13 NMR Spectra of Texas Bottom Coal Residues from Coal Liquefaction of (a) Premoisturized Coal and (b) Chemically Dried Coal

INFLUENCE OF BINARY SWELLING SOLVENTS: MECHANISM OF ACTION

R. Ding, D. Tucker and Lowell D. Kispert
Department of Chemistry, Box 870336
The University of Alabama
Tuscaloosa, AL 35487-0336

KEYWORDS: Binary, Swelling Solvents, Hydrogen Bonding, Spin Probes

ABSTRACT

This study addresses the dramatic up-take of a poor swelling solvent in Argonne Premium Coal Samples (APCS), Illinois #6, Beulah-Zap and Lewiston-Stockton when such a solvent is spiked with various amounts of the strong swelling solvent, pyridine. The unexpected up-take can be explained in terms of four different processes: (1) disruption of weak hydrogen bonds which isolate the interconnected micropore system; (2) disruption of weak hydrogen bonds which protect individual micropores; (3) competition of pyridine for the active sites involved in the hydrogen bonds or the "poisoning" of active sites; and (4) disruption of stronger hydrogen bonds within the macromolecules which causes an opening of the structure. When more than 5% pyridine is used, no additional disruption of the hydrogen-bonded network occurs. The structural changes were monitored by spin probe incorporation which was measured by EPR spectroscopy.

INTRODUCTION

In swelling coals with chlorobenzene, it has been observed by Green and Larsen that when small amounts (0.35 mmol/g coal) of pyridine are added to chlorobenzene, the up-take of chlorobenzene by the coal is dramatically increased.¹ Since the EPR spin probe method has been shown to be very sensitive to changes in the physical and chemical structure of coal during this swelling process,² it was thought that some insight into the effect of pyridine on the coal structure could be gained by applying this method to a binary swelling solvent. Toluene was used as the swelling solvent because it does not significantly swell the coal or disturb any cross-linking, so that the interactions between the coal structure and pyridine can be studied.

Previously, Painter has asserted that hydrogen bonds in coal are short lived and do not make major contributions to the cross-linked structure.³ A recent model assumes that coal is made up of interconnected chains which are solubilized during this swelling process.⁴ These connected chains have segments referred to as dangling ends, whose mobility is limited by the surrounding solubilized chain segments suggesting a dynamic structure for coal during the swelling process. The same conclusion can be reached from the results of short term oxidation studies,⁵ where removal of water during exposure to dry gas causes changes in as little as 30 seconds. It is possible that hydrogen bonding can establish cross-linking within a macromolecule causing a blockage of the micropore areas, making them inaccessible to guest molecules until they are disrupted by a swelling solvent as supported by observations of Larsen and Wernett.⁶ It was observed that the surface area measured for Beulah Zap lignite by N₂ or hydrocarbon surface analysis was 30 times less than by CO₂ surface analysis. This was attributed to the greater solubility of CO₂ in coal and it was concluded that an interconnected micropore network does not exist.

Two assumptions are necessary to explain the observations made in the current study: one, that coal has a dynamic structure and two, that hydrogen bond interactions form cross-links which inhibit accessibility of guest molecules to the coal micropores. The two spin probes used in this study were TEMPAMINE (VII) and TEMPO (VIII) (Figure 1). These compounds have similar molecular volumes, but VII contains an amino group which can interact with hydrogen bonding sites in the coal structure.

EXPERIMENTAL

Swelling solvent/spin probe solutions were prepared in 1 millimolar concentrations of VII or VIII in toluene. Each spin probe solution was split into 16 aliquots of 10 mL and spiked with 0% to 9% pyridine.

APCS coal samples (Beulah-Zap, Illinois #6 and Lewiston-Stockton) were opened under argon and 30 mg portions were immediately placed into vials and covered with 2 mL of a toluene spin probe solution spiked with pyridine. Each sample was then swelled for 18 hours and worked up as previously described.⁷ The concentration of the incorporated spin probes was determined by EPR spectroscopy.

RESULTS AND DISCUSSION

Illinois #6 Subbituminous Coal

The retention of spin probe VII (amine substituent) in Illinois #6 is shown in Figure 2. It can be seen that oscillations occur in the concentration of spin probe retained as the amount of pyridine that is added to the swelling solvent is increased. These oscillations decrease in intensity as the concentration of pyridine in the solvent solution is increased up to 2% pyridine in toluene. From a 2% up to 5% pyridine concentration (not shown) there is no significant change in the retention of spin probe VII. The largest changes in spin probe retention are observed for concentrations of pyridine less than 0.5%. A three fold increase in spin probe retention is observed upon the addition of 500 ppm pyridine (0.05%) to the toluene swelling solvent.

Figure 3 illustrates the effect of pyridine concentration in toluene on the retention of spin probe VIII in Illinois #6, where the size of the probe is the controlling factor. The effects are similar to those observed for the retention of spin probe VII, although the extent of retention is decreased by 90%. Significant oscillations in spin probe retention are observed for concentrations of pyridine less than 2%. As above, increases in pyridine concentration beyond 2% have very little effect on the retention of spin probe VIII.

Since retention of spin probe VII was much greater than that observed for spin probe VIII, it seems that structural changes, brought about by small amounts of pyridine, provide for significantly increased accessibility of the spin probe to active sites in Illinois #6 APCS coal. The enhanced retention of VII indicates that the active sites are capable of strong interactions with the amino group.

The fact that the addition of 0.1% pyridine causes a large decrease in retention for both spin probes shows that a structural change is primarily responsible since spin probe VIII has no functional interactions. The decrease in retention of spin probe VIII indicates either that the structure of the coal collapsed, blocking access to the coal micropores, or that the structure opened up to such a large extent that the spin probes could not be trapped. It seems likely at this point that the structure is opened to an extent such that the spin probes are removed during the cyclohexane wash since the concentration of spin probe VII is still greater than the retention observed in the absence of pyridine. Evidently very small amounts of pyridine open the structure of the coal enough so that "pockets" of active sites are made accessible to the spin probes.

It is possible that opening the structure only slightly allows for diffusion of the spin probes into the structure, while somewhat greater opening of the structure allows for pockets to be formed which trap the spin probes more effectively. In this way, the coal pockets could trap polar spin probes of the requisite size with hydrogen bond interactions exactly like an inclusion compound (as opposed to a simple intercalation process). As the structure is opened further, the larger pockets can no longer trap the guest molecules, and so the retention of the spin probes in the structure decreases.

At 0.2% pyridine, the concentration of the retained spin probe VIII drops even further; however, the retention of spin probe VII increases again. This shows that the structure has opened even further (decrease in spin probe VIII), allowing greater accessibility to hydrogen-bonding sites (increase in spin probe VII), but not creating any additional pockets which might trap the non-hydrogen bonding probes (spin probe VIII).

As the amount of pyridine is increased to 0.4%, a decrease in retention is observed for spin probe VII while an increase in retention is observed for spin probe VIII. This indicates that pyridine causes a poisoning of the active sites available for interaction with the polar spin probe, while at the same time opening the structure to create more areas that are able to trap small spin probes. It should be noted that the amount of amino substituted spin probes retained at this pyridine concentration is still much greater than that of the non-substituted spin probes, indicating that there is still a significant number of active sites available for trapping polar spin probes.

At 0.6% pyridine, an increase in retention is observed for spin probe VII while a decrease is observed for spin probe VIII. At this point and beyond, further oscillations in the retention of each spin probe appear to be due to competing processes of opening micropores, opening larger structural areas, and poisoning of active sites with pyridine.

With higher concentrations of pyridine both the period and the amplitude of the oscillations decreased. After the concentration of pyridine reached 10%, the spin retention observed is similar to that observed for pure pyridine. The data suggest that complete structural opening occurs so that if this is desired, it may be possible to achieve this goal without wasting large amounts of an expensive, toxic, strong swelling solvent.

Beulah-Zap Lignite

Spin probe VII retention in Beulah-Zap lignite swelled in toluene spiked with up to 1.2% of pyridine is expressed as a function of pyridine concentration in Figure 4. Again an oscillatory behavior is observed for spin probe retention as the concentration of pyridine in the swelling solvent solution is increased. Similar to the behavior of Illinois #6, the oscillations observed for the retention of spin probe VII in Beulah-Zap have decreasing periods as the concentration of pyridine is increased. Increasing the pyridine concentration above 4% has little effect on the amount of spin probe retention. It is likely that the structure of the lignite has then been completely opened by disrupting all hydrogen bonded networks, as was observed when pure pyridine was used as the swelling solvent.

The retention of spin probe VIII (size dependence) in Beulah-Zap lignite as a function of pyridine concentration in the toluene swelling solvent is shown in Figure 5. Oscillatory behavior similar to that of Illinois #6 is observed. However, after 0.6%, additional pyridine has a negligible effect on the incorporation of the spin probe. Addition of 100 ppm pyridine (0.01%) to the swelling solvent for Beulah-Zap has almost no effect on the retention of spin probe VIII. When the concentration of pyridine is increased to 200 ppm (0.02%), a large increase in the retention of spin probe VIII is observed, while a small, yet significant decrease in the retention of spin probe VII is observed. The large increase in spin probe VIII retention indicates that hydrogen bonds which block access to the interconnected micropore network have been disrupted without significantly affecting the macromolecular structure. Although a greater number of micropores was made available, a decrease in the retention of spin probe VII was observed. This would seem to indicate that in Beulah-Zap the pyridine necessary to provide initial access to the micropore structure competes significantly for the active hydrogen bonding sites available to the amino spin probes.

As the concentration of the pyridine in the swelling solvent is increased from 200 ppm to 500 ppm (0.05%), a large decrease in the retention of spin probe VIII occurs, but a corresponding increase in the retention of spin probe VII is observed. The large decrease in retention of spin probe VIII indicates that the macromolecular structure was opened to a significant extent. This disruption of hydrogen bonds in the macromolecular structure caused a dramatic increase in the available active sites for hydrogen-bonded interactions, as evidenced by the large increase in retention of spin probe VII.

A further increase in the concentration of pyridine to 700 ppm (0.07%) results in an increase in retention of spin probe VIII and a huge decrease in retention of spin

probe VII. Again, additional micropore structure is made available to guest molecules (indicated by an increase in spin probe VIII retention), but as the concentration of pyridine approaches the concentration of the spin probes, a large percentage of the active sites in the micropore system is poisoned (indicated by the large decrease in spin probe VII retention).

When the concentration of pyridine is 0.1%, a decrease in retention of both spin probes is observed. At this point, the macromolecular structure is opened to such an extent that the spin probes can no longer be trapped in the available micropores.

Further increases in pyridine concentration do not significantly affect the retention of spin probe VIII. The retention of spin probe VII continues to oscillate as the concentration of pyridine increases. At this point the structure of the coal is opened extensively. Variations in the retention of spin probe VII are primarily due to increases in available micropore structure and decreases in active sites due to pyridine site competition.

The observed data can be explained in terms of the following four processes: one, disruption of weak hydrogen bonds which protect or isolate the interconnected micropore system; two, disruption of weak hydrogen bonds which protect individual micropores; three, competition of pyridine for the active sites capable of establishing hydrogen bonds or the "poisoning" of active sites; four, disruption of stronger hydrogen bonds within the macromolecular structure which causes more extensive opening of the structure. The contributions of each of these factors to the spin probe retention with increasing concentrations of pyridine vary to a significant extent up to 1% pyridine. At concentrations above 1% pyridine, the first factor becomes less significant, and variations in the others require greater change in pyridine concentration.

The spin probe retention does not vary to such a degree with percent added pyridine in a higher rank coal such as Lewiston-Stockton where a larger amount of covalent cross-linking and a smaller degree of hydrogen bonding occur. Furthermore, it was found that the spin probe VIII retention as a function of % added pyridine decreased nearly exponentially. The reduced hydrogen bonding in the higher rank coals is reflected by the reduced number of available micropore structures and decreases in active sites due to pyridine site competition.

CONCLUSION

Inclusion of guest molecules into the macromolecular structure of coal can be achieved by spiking a "poor" swelling solvent with as little as 100 ppm of a strong swelling solvent. The optimum amount varies with rank. Dramatic oscillations in spin probe retention are most severe below 0.5% for IL and below 0.1% pyridine for BZ and LS. Above this amount any additional break-up of the hydrogen-bonded structure is not detectable by use of spin probes.

ACKNOWLEDGMENT

This work was supported by the U. S. Department of Energy, University of Coal Grant Program, Grant No. DE-FG22-93PC93202.

REFERENCES

1. Green, T. K.; Larsen, J. W. *Fuel* **1984**, *63*, 1538.
2. Sady, W.; Tucker, D.; Kispert, L. D.; Spears, D. R. *Prepr. Pap. Am. Chem. Soc., Div. Fuel Chem.* **1993**, *38*, 1323.
3. Painter, P. *Am. Chem. Soc. Div. Fuel Chem. Symp. Macrom. Str. Coal.* August 22-26, **1993**, Chicago, IL.
4. Painter, P. *Prepr. Pap. Am. Chem. Soc., Div. Fuel Chem.* **1993**, *38*, 1304.
5. Tucker, D.; Kispert, L. D. *Prepr. Pap. Am. Chem. Soc., Div. Fuel Chem.* **1993**, *38*, 1335.
6. Larsen, J. W.; Wernett, P. C. *Prepr. Pap. Am. Chem. Soc., Div. Fuel Chem.* **1992**, *37(2)*, 849.
7. Kispert, L. D.; Tucker, D.; Sady, W. *Prepr. Pap. Am. Chem. Soc., Div. Fuel Chem.* **1994**, *39*, 54.

Figure 1
Spin probes VII and VIII.

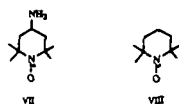


Figure 2
The retention of spin probe VII in Illinois #6 APCS coal after swelling with toluene spiked with pyridine.

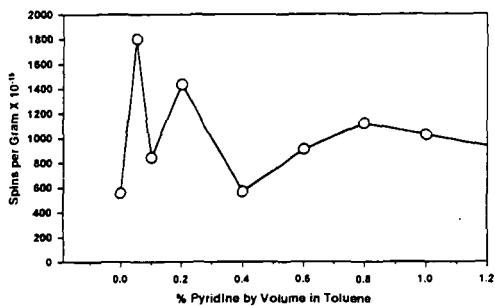


Figure 3
The retention of spin probe VIII in similarly swelled Illinois #6 APCS coal.

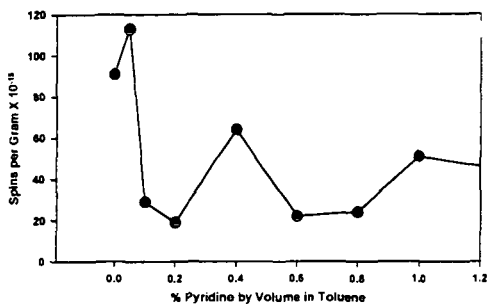


Figure 4
The retention of spin probe VII in similarly swelled Beulah-Zap APCS coal.

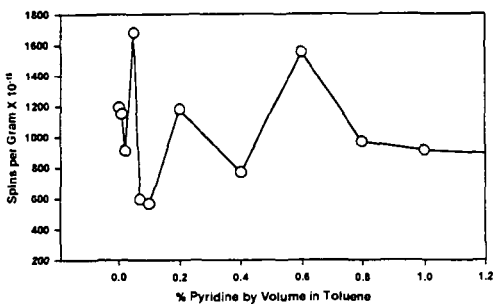
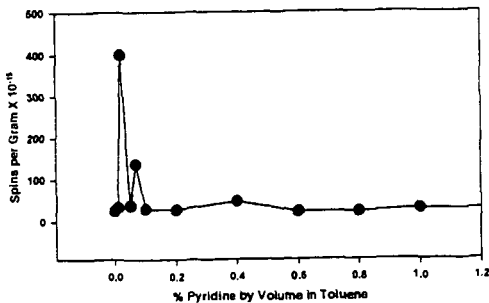


Figure 5
The retention of spin probe VIII in similarly swelled Beulah-Zap APCS coal.



NAPHTHENE UPGRADING WITH PILLARED SYNTHETIC CLAY CATALYSTS

Ramesh K. Sharma and Edwin S. Olson
University of North Dakota
Energy & Environmental Research Center
PO Box 9018
Grand Forks, ND 58202

Keywords: Naphthene, Hydrocracking, Hydroisomerization

ABSTRACT

Catalytic hydrotreatment of methylcyclohexane was investigated to model upgrading of coal-derived naphthenes. Nickel-substituted synthetic mica montmorillonite (NiSMM), alumina-pillared NiSMM, and zirconia-pillared NiSMM were prepared and tested for hydrocracking and hydroisomerization of methylcyclohexane. Infrared and thermal desorption studies of the pyridine-adsorbed catalysts indicated the presence of Lewis as well as Brønsted acid sites. Total acidity and surface area increased with pillaring of NiSMM with polyoxy aluminum and polyoxy zirconium cations. Most of the products were branched alkanes (isoparaffins). These compositions are highly desirable for environmentally acceptable transportation fuels. Furthermore, dehydrogenation was not a major pathway, as indicated by the minimal formation of aromatic hydrocarbons, coke, or other oligomeric materials. This paper describes the effect of various operating conditions, which included reaction temperature, contact time, hydrogen pressure, and catalyst on the product distribution.

INTRODUCTION

A growing need exists for new and improved catalysts to improve the overall economics of coal liquefaction. Coal-derived liquids are heavy, viscous, aromatic, hetero-compound-rich, and are very difficult and expensive to refine into transportation fuels. Natural clays were used as catalysts in petroleum cracking until replaced by more active and selective zeolites (1). Synthetic clays (SMM) containing a hydrogenation component were more active for hydrocracking and hydroisomerization (2-4). Synthetic clays such as nickel-substituted synthetic mica montmorillonite (NiSMM) were effective for cleaving carbon-carbon bonds and isomerizing the alkyl chains to give branched alkanes without extensive formation of aromatic hydrocarbons (5-8). These catalysts have also been found to be effective in hydrocracking and reforming of biomass materials to the isoparaffinic composition desired for transportation fuels (9-10). In the pillared clays, intercalation of hydroxylated or complexed metal cations maintains the clay layer structure after loss of water and generates large pore sizes. These structures are stable to 450° and 500°C. Pillared clays containing a hydrogenation component could be used for hydrogenation and hydrocracking processes.

The goal of this study was to develop an understanding of the hydrocracking and hydroisomerization of coal-derived cycloalkanes (naphthenes). Catalytic hydrotreating reactions of methylcyclohexane (MeCH) were conducted to evaluate the potential of synthetic and pillared synthetic clay catalysts for the upgrading of coal-derived liquids to an isoparaffinic product. The reactions of MeCH were carried out under several conditions to determine the effects of temperature, reaction time, and hydrogen pressure on the hydrocracking and hydroisomerization activity of NiSMM, alumina-pillared NiSMM, and zirconia-pillared NiSMM.

EXPERIMENTAL

Catalyst Preparation and Characterization

NiSMM was prepared by the procedure of Heinerman (11). Pillaring of NiSMM was carried out according to the procedure described earlier (12). The acidity of the solid acid catalysts was determined by pyridine adsorption and desorption studies. A small amount of sample (100 mg) was placed in a glass chamber attached to a vacuum pump, a gas inlet, and a gas outlet. The chamber was evacuated, and argon saturated with pyridine was introduced into the chamber until the weight increase ceased. At this stage, the chamber was evacuated until the physisorbed pyridine was removed, as indicated by the constant weight of the base absorbed sample. The amount of pyridine chemisorbed was used to determine total acidity of the catalyst. Surface area measurements were performed with Micromeritics AccuSorb 2100E static unit for nitrogen physisorption at 77K (BET method).

Catalytic Reactions

In a typical experiment, 0.5 g of MeCH and 0.25 g of the catalyst were placed in a tubing bomb (15-mL microreactor). The microreactor was evacuated, pressurized with desired amount of hydrogen, and placed in a rocking autoclave preheated to the desired temperature. At the end of the reaction period, the microreactor was cooled in a dry ice-acetone slurry, degassed, and opened. The

desired amount of the internal standard was added to the product slurry; the product slurry was transferred into a centrifugation tube by washing with methylene chloride; and the solid catalyst removed by centrifugation. Quantitative gas chromatography-flame ionization detection (GC-FID) analyses of the liquid samples were performed with a Hewlett-Packard 5890a gas chromatograph equipped with a Petrocol capillary column. The solid was dried in vacuum at 110°C for 3 hours. Since it was not found in the reaction products, octadecane was added as the internal standard. Alkane components were determined from the area percent ratio with respect to octadecane, assuming the same response factor.

RESULTS AND DISCUSSION

Total acidity of the NiSMM as measured by the amount of chemisorbed pyridine was found to be 0.84 mmol/g of catalyst, indicating the presence of acidic sites in the catalyst. These sites may be Lewis as well as Brønsted acids. Pillaring the clay with polyoxyaluminum cations increased the total acidity to 1.02 mmol/g of catalyst. The increase in acidity is due to the additional acidic sites created by the dehydroxylation of the hydroxylated aluminum cations.

The surface area of the NiSMM was found to be 240 m²/g. Pillaring the clay with polyoxy zirconium cations resulted in an increase in the surface area (274 m²/g). The increase in surface area may be due to the micropores created by the dehydroxylation of the intercalated hydroxylated metal cations (pillars).

The results from the catalytic hydrocracking/hydroisomerization reactions of MeCH are given in Tables 1 and 2. In all these tests, conversion to liquid and gas products was 100%, and no coke or insoluble materials were detected on the recovered catalyst.

Temperature effects

A reaction of MeCH was carried out with alumina-pillared NiSMM at 350°C for 30 min in the presence of 1000 psi of initial hydrogen pressure. This reaction gave only 29% conversion of MeCH to products. The yields of liquid and gas products were 23% and 6% respectively. A reaction at 400°C gave considerably higher conversion (93%) of MeCH to liquid (72%) and gas (21%) products. There is therefore a large temperature effect and this experiment established that 400°C is a more appropriate temperature. Subsequent reactions were performed at 400°C.

The reaction products were a complex mixture of hundreds of components formed as result of the extensive rearrangements or isomerization of the primary cracked products. The major products from higher-temperature reactions were the desired isoparaffins (mono-, di-, and trimethylalkanes) with lower amounts of *n*-alkanes. The amount of aromatic hydrocarbons was insignificant.

Pressure effects

Reactions of MeCH were conducted under different initial hydrogen pressures to determine the effect on product yields and distribution. The reaction of MeCH with NiSMM at 400°C for 90 min in the presence of 1000 psi of initial hydrogen pressure gave almost complete conversion of the substrate to liquid (41%) and gas (58%) products. The reaction at 500 psi resulted in significant improvement in the yield of liquid products (72%), and gas yield was significantly lower (25%), owing to lower hydrocracking of MeCH and rearrangement products at the lower pressure. Pillared clay catalysts exhibited the same effect. The reaction of MeCH with alumina-pillared NiSMM (AlPNiSMM) at 400°C for 90 min in the presence of 200 psi of hydrogen (initial) gas only 36% conversion of the substrate to liquid (25%) and gas (11%) products. Increasing the hydrogen pressure to 500 psi resulted in substantial increase in the conversion of MeCH (90%) to give 68% yield of liquid products and 22% of gas products. The reaction with 1000 psi initial hydrogen pressure gave significantly high conversion of MeCH (99%), but the yield of liquid products was significantly lower (42%) with the remaining gas. The reaction of zirconia-pillared NiSMM (ZrPNiSMM) with MeCH at 400°C for 90 min in 500 psi (initial) hydrogen pressure gave 98% conversion to liquid product (68%) and gas product (30%). However, similar reaction with 1000 psi hydrogen pressure gave significantly lower amounts of liquid products and high gas yield (Table 1). Thus there is a large pressure effect on conversion of MeCH and also a large pressure effect on gas yield.

Reaction Time

The effect of reaction time on the product yields and product distribution was investigated with AlPNiSMM. The 30-min reaction gave 93% conversion of MeCH to products; the yields of liquid and gas products were 72% and 21% respectively. The reaction for 90 min resulted in almost complete conversion of MeCH to give a liquid product yield of 42%. The remaining substrate was converted into gaseous products. After 180 min, MeCH was completely converted into liquid (21%) and gaseous (79%) products. The effect of time was also studied by comparing the reactions of MeCH with AlPNiSMM for 30 and 90 minutes at 400°C in the presence of 200 psi of initial

hydrogen pressure. These reactions gave similar conversions of MeCH to volatile products (Table 1). The liquid product yield was somewhat higher for the 30-min reaction than for the 90-min reaction. Thus, over a longer period of time, primary cracked products are further cracked to form undesirable gaseous components, and a shorter reaction time favors liquid isoparaffinic products.

Selectivity

A comparison of the conversions obtained with the three catalysts at 500 and 1000 psi at 400°C indicate that there is no difference in activity. There is also no difference in the selectivity for total liquid product at 500 psi. At 1000 psi, the ZrPNiSMM appeared to give a somewhat better liquid yield (54%) than the NiSMM and AlPNiSMM.

Further information on the selectivity for hydrocracking and hydroisomerization reaction of the MeCH can be gained from comparison of the cyclic and isoparaffinic components in the products (Table 2). The reaction of MeCH with AlPNiSMM in 200 psi hydrogen gave larger amounts of dimethylcyclopentane (DMCP), indicating that hydrocracking is incomplete at lower hydrogen concentrations. The formation of four DMCP isomers (1,1-DMCP, *trans*-1,2-DMCP, *cis*-1,3-DMCP, and *trans*-1,3-DMCP) indicates that carbonium ions form initially on all carbons of the MeCH ring and rapidly rearrange via protonated cyclopropane (actually bicyclohexane) intermediates to the isomeric DMCPs.

The products at 500 psi with the three catalysts are mainly the isoparaffins. Thus, at higher pressures, cracking of the DMCP rearrangement products as well as the MeCH via carbonium ion intermediates increases, giving branched C₇ isomers and subsequently other isoparaffins. The ZrPNiSMM appears to be the most efficient catalyst for the ring hydrocracking reaction. This result is consistent with the higher acidity of this pillared catalyst. Previous work demonstrated that there is no difference in the three catalysts with respect to shape selectivity (9); hence, the effects seen here are likely the result of the acidity effects. The amounts of aromatic hydrocarbons were found to be minimal with all the catalysts, so dehydrogenation is not a major reaction of the MeCH.

The AlPNiSMM gives a quite different distribution of products from those of the other two catalysts. Since the *n*-heptane yield is high, the initial carbonium ion reaction may favor the rearrangement of 2-methylcyclohexylcarbonium ion to 2-ethylcyclopentylcarbonium ion, which cracks to *n*-heptane rather than branched heptanes. Ethylcyclopentane is one of the larger components in the products from this reaction. The lowered content of branched alkanes increased the DMCP:BA ratio. Thus the acidic AlPNiSMM is also efficient at hydrocracking but different initial rearrangements lead to different products.

ACKNOWLEDGMENT

This work was performed under the auspices of the U.S. Department of Energy, Contract No. DOE-FC21-86MC10637.

REFERENCES

1. Gates, B.C.; Katzer, J.R.; Schuit, G.C.A. *Chemistry of Catalytic Processes*; McGraw-Hill: New York, 1979; p 1.
2. Jaffe, J.; Kittrell, J.R. U.S. Patent 3 535 229, 1970.
3. Mulaskey, B.F. U.S. Patent 3 682 811, 1972.
4. Csicsery, S.M.; Mulaskey, B.F. U.S. Patent 3 655 798, 1972.
5. Swift, H.E.; Black, E.R. *Ind. Eng. Chem. Prod. Res. Dev.* **1974**, *13*, 106.
6. Black, E.R.; Montagna, A.A.; Swift, H.E. U.S. Patent 4 022 684, 1977.
7. Black, E.R.; Montagna, A.A.; Swift, H.E. U.S. Patent 3 966 642, 1976.
8. Olson, E.S.; Sharma, R.K., *Prepr. Pap.—Am. Chem. Soc., Div. Fuel Chem.* **1994**, *39*, 706.
9. Olson, E.S.; Sharma, R.K. *Energy from Biomass and Wastes XVI*; Klass, D.L. Ed.; Institute of Gas Technology: Chicago, IL, 1993; p 739.
10. Sharma, R.K.; Olson, E.S. *Prepr. Pap.—Am. Chem. Soc., Div. Fuel Chem.* **1994**, *39*, 1040.
11. Heinerman, J.J.L.; Freriks, I.L.C.; Gaaf, J.; Pott, G.T.; Coqlegem, J.G.F. *J. Catal.* **1983**, *80*, 145.
12. Gaaf, J.; van Santen, R.; Knoester, A.; van Wingerden, B. *J. Chem. Soc. Chem. Commun.* **1983**, 655.

Table 1. Catalytic Reactions of Methylcyclohexane^a

Catalyst	Time, min	Temp, °C	Hydrogen, psig	Conversion, %	Products, %	
					Liquid	Gas
NiSMM ^b	90	400	500	97	72	25
NiSMM	90	400	1000	99	41	58
AIPNiSMM ^c	30	350	1000	29	23	6
AIPNiSMM	30	400	1000	93	72	21
AIPNiSMM	30	400	200	37	28	9
AIPNiSMM	90	400	500	90	68	22
AIPNiSMM	90	400	200	36	25	11
AIPNiSMM	90	400	1000	99	42	57
AIPNiSMM	180	400	1000	100	21	79
ZrPNiSMM ^d	90	400	500	98	68	30
ZrPNiSMM	90	400	1000	99	54	45

^a Substrate = methylcyclohexane; catalyst:substrate ratio = 0.5.

^b Nickel-substituted synthetic mica montmorillonite.

^c Alumina-pillared NiSMM.

^d Zirconia-pillared NiSMM.

Table 2. Products from Reactions of Methylcyclohexane^a

Catalyst	Hydrogen, psig	BA ^b	DMCP	OCA ^c	i-C ₄	i-C ₅	i-C ₆	i-C ₇
		nA ^d	BA	BA	n-C ₄	n-C ₅	n-C ₆	n-C ₇
NiSMM	500	3.2	0.2	0.2	2.2	5.1	5.7	3.1
ZrPNiSMM	500	2.7	0.1	0.1	2.1	4.3	5.2	4.2
AIPNiSMM	500	1.9	0.6	0.2	2.6	6.6	7.5	0.7
AIPNiSMM	200	4.9	6.7	2.3	2.3	7.9	10.6	12.4
AIPNiSMM	1000	3.3	0.6	0.3	2.5	6.6	8.4	2.6

^a Reaction temperature = 400°C; reaction time = 90 min; catalyst:substrate ratio = 0.5.

^b Branched alkanes.

^c Cycloalkanes other than DMCP.

^d Normal alkanes.

HYDRODESULFURIZATION OF DIBENZOTHIOPHENE OVER Mo-BASED DISPERSED CATALYSTS

William S. Cooke, Eckhardt Schmidt*, Chunshan Song and Harold H. Schobert

*Fuel Science Program, Department of Materials Science and Engineering, 209 Academic
Projects Building, The Pennsylvania State University, University Park, PA 16802*

The hydrodesulfurization (HDS), hydrocracking (HC) activity and selectivity of several Mo, Co and Fe-based catalyst precursors have been examined in model compound reactions of dibenzothiophene (DBT). Reactions were carried out at 400 °C with 6.9 MPa of H₂ for 30 min. A metal loading of 0.5 mol % (based on DBT) in tridecane as solvent resulted in a low conversion rate and only hydrogenation products. Even the addition of sulfur to the catalyst in a 4:1 molar ratio only led to a minor increase in conversion and HDS. However, a change in the molar ratio of solvent to model compound from 1:1 to 19:1 and a metal loading of 36.16 mol % lead to a dramatic increase in conversion, HDS, and HC. Furthermore, the use of higher boiling point solvents such as hexadecane and octadecane had a beneficial effect on both HDS and HC. The addition of sulfur in a 6:1 ratio of S:metal to the higher-metal-loaded runs had varying effects that were dependent upon the catalyst used.

Keywords: Model reactions, hydrocracking, dispersed catalysts.

INTRODUCTION

The objective of this work is to examine the hydrodesulfurization activity of dispersed catalysts under coal liquefaction conditions. Most coal hydroliquefaction reactions (1) are performed at temperatures in excess of 400 °C and 6.9 MPa H₂ for at least 30 min. These severe conditions are required to break the heteroatom and alkyl bridges that connect the aromatic species. Different metal catalysts, in particular molybdenum (2), have been known to be effective in coal liquefaction reactions. The complex nature of coal renders the study of reactions of a specific coal molecule impossible and thus obscures the effectiveness of a particular catalyst. Some catalysts are particularly effective for HC, others better for desulfurization and denitrogenation. Coals with a high heteroatom (sulfur) content, are of concern in combustion processes and pose an environmental risk. Multistage liquefaction is expected to improve selectivity for specific reactions, such as desulfurization, to meet current refining regulations. The model compound chosen for the examination of the hydrodesulfurization was dibenzothiophene (DBT). The catalysts chosen for this study were, ammonium tetrathiomolybdate (ATTM), molybdenum hexacarbonyl, MoCl₃, Co₂(CO)₈, Fe(CO)₅ with and without added sulfur, and the thiocubane type bimetallic catalyst precursor Cp₂Co₂Mo₂(CO)₂S₄ [MoCo-TC2].

EXPERIMENTAL

Materials

The model compound dibenzothiophene (98% purity) and the solvents tridecane, heptadecane, and octadecane (all 99% purity) were obtained from Aldrich; Mo(CO)₆ obtained from Johnson Matthey, ATTM and MoCl₃ from Aldrich, Fe(CO)₅ and Co₂(CO)₈ from Strem. The thiocubane type complex Cp₂Co₂Mo₂(CO)₂S₄ [MoCo-TC2] was prepared according to the method of Brunner and Wachter (3). Elemental sulfur was obtained from J. T. Baker Chemical Co. All chemicals and precursors were used as received.

Conditions and Procedures

Experimental runs with the model compound DBT were carried out in 33 mL reactors using ca. 1 g of DBT and various solvent to model compound ratios at 400 °C for 30 min, in the presence of catalyst precursors (0.5-36.16 mol % metal based on DBT). When sulfur was added to a S-free precursor, the S:metal atomic ratio was 4:1, unless otherwise mentioned. For those experiments involving water, the above procedure was used with the addition of water in a H₂O:DBT molar ratio of 10:1. The remainder of experiments involved a metal loading of 36.16 mol % (with respect to DBT). In another set of experiments, catalysts were added to a reaction solution consisting of 1% DBT and 99% solvent. Sulfur was added to S-free precursors in a S:metal ratio of 6:1. The reaction temperature primarily employed was 400 °C, except for those experiments involving water in which case 350 °C was used. The reactor was purged three times with H₂ and then pressurized with 6.9 MPa H₂ at room temperature for all experiments. A preheated fluidized sand bath was used as the heating source and the horizontal tubing bomb reactor was vertically agitated to provide mixing (about 240 strokes/min). After the reaction the hot tubing bomb was quenched in cold water. The liquid contents were washed with 15 ml CH₂Cl₂ through a low speed filter paper for qualitative and quantitative GC analysis of the filtrate. Most runs were carried out twice to confirm reproducibility.

Analysis

The products were identified by GC-MS using a Hewlett-Packard 5890 II GC coupled with a HP 5971A mass-selective detector operating at electron impact mode (EI, 70 eV). The column used for GC-MS was a J&W DB-17 column; 30-m X 0.25-mm, coated with 50 % phenyl-50 % methylpolysiloxane with a coating film thickness of 0.25 µm. For quantification, a HP 5890 II GC with flame ionization detector and the same type of column (DB-17) was used. Both GC and GC-MS were temperature programmed from 40 to 260 °C at a heating rate of 4 °C/min. The response

factors for 5 of the products were determined using pure compounds. Conversion was determined by the amount of unreacted DBT recovered after the reaction. Yields of products were calculated as molar percentage based on DBT reactant. More experimental details may be found elsewhere (4).

RESULTS AND DISCUSSION

Initially, DBT hydrodesulfurization tests were performed at 400 °C over ATTM and $\text{Mo}(\text{CO})_6$ using a metal loading of 0.5 mol % with and without added sulfur in a S:metal ratio of 4:1. Table 1 and Figure 1 show the results of these runs. At such a low loading level, both precursors displayed only moderate catalytic activity. However, when S was added to the S-free precursor, conversion increased significantly. The HDS activity of $\text{Mo}(\text{CO})_6$ was improved when a higher metal loading of 5 mol % Mo (with respect to DBT) was used. This suggests that a much higher metal concentration would be needed to completely convert and hydrodesulfurize DBT under the conditions used.

To study the impact of different metal concentrations on DBT conversion, a much higher metal loading, 36 mol % with respect to DBT, was also used in examining the performance of various catalyst precursors. Table 2 and Figure 2 give the results with $\text{Mo}(\text{CO})_6$ and ATTM. The reactions with $\text{Mo}(\text{CO})_6$ and ATTM were performed using tridecane and octadecane as solvents. The liquid products identified from these reactions were biphenyl (BP), tetrahydrodibenzothiophene (TH-DBT), cyclohexylbenzene (CHB), bicyclohexyl (BCH), and benzene (BNZ). It should be noted that there are un-identified products, which are not included in Table 2. One of them has MW of 166. It could be cyclopentylmethylcyclohexane, but this needs to be confirmed. For the runs with $\text{Mo}(\text{CO})_6$, increase in Mo loading from 0.5, to 5 and to 36 mol % with respect to DBT increased the DBT conversion with tridecane solvent from 5.5 to 26.2 to 53.4 mol %. Adding sulfur further increased the catalytic activity for DBT conversion. A comparison of the results for ATTM with different metal loadings (Tables 1 and 2) showed a substantial increase of DBT conversion and HDS degree (as expressed by the sum of HDS products). Reactions with ATTM at 0.5 mol % metal loading gave DBT conversions up to 21.2 %, with only HDS and partial hydrogenation products (Table 1). A great impact on conversion, HDS, and product distribution could be found in model reactions with ATTM at 36 mol % metal loading (Table 2). The products include not only HDS products such as BP and CHB, but also hydrocracking products such as benzene. Highest conversions were achieved using octadecane as a (high boiling) solvent in combination with added S.

As shown in Table 3 and Figure 3, the precursors used in the high metal-loading runs also included were MoCl_3 , $\text{Co}_2(\text{CO})_8$, $\text{Fe}(\text{CO})_5$ with and without sulfur, and the bimetallic catalyst MoCo-TC2 , in addition to ATTM and $\text{Mo}(\text{CO})_6$. Again, most of these catalysts were run with tridecane and octadecane as solvents, and in some cases heptadecane was also used. The ratio of S:metal ratio employed was 6:1. As seen in Tables 2 and 3 the use of high metal concentrations dramatically increased conversion and HDS.

From the DBT conversion data in Tables 2 and 3, $\text{Mo}(\text{CO})_6$ appears to be the most active precursor and showed highest selectivity. The reactions of $\text{Mo}(\text{CO})_6$ lead to 50.8 % HDS and a conversion of 53.4 % using tridecane as a solvent. These percentages increase when tridecane was replaced with octadecane. The use of octadecane increased HDS (50.8 % to 80.0 %) and increased conversion (53.4 % to 75.8 %). When sulfur was added in a 6:1 S:metal ratio the results for tridecane were 41.2 % HDS and 100 % conversion, and for octadecane 43.2 % for HDS. The influence of S was studied in a set of experiments using a 2:1 and a 6:1 S:metal ratio. Both runs were conducted with heptadecane as a solvent. Sulfur addition resulted in high HDS yield and complete conversion but different product distribution. In the latter reaction cyclohexylbenzene (CHB), bicyclo-hexyl (BCH), and benzene (BNZ) accounted for most of the products. This effect is also present when using a higher boiling point solvent. CHB, BCH, and BNZ accounted for 100 % of the products of the run with $\text{Mo}(\text{CO})_6$, added sulfur and octadecane, as compared to runs, using heptadecane and tridecane under the same conditions. These results indicate that oil-soluble $\text{Mo}(\text{CO})_6$ may be used for HDS reactions. Curtis (5) demonstrated that catalytic desulfurization can be achieved in high yields by using molybdenum naphthenate, which is another oil-soluble precursor.

The 36 mol % metal loaded samples of ATTM easily outperformed the 0.5 mol % samples. The total yields of HDS products with ATTM, however, are lower than those with $\text{Mo}(\text{CO})_6$ without sulfur and much lower than those with $\text{Mo}(\text{CO})_6$ with sulfur. This is surprising, considering that ATTM has a S:metal ratio of 4:1 compared to no precursor sulfur for $\text{Mo}(\text{CO})_6$, and ATTM was shown to be more effective than $\text{Mo}(\text{CO})_6$ in our coal liquefaction experiments. The performance of ATTM, like $\text{Mo}(\text{CO})_6$, was also affected by the solvent used. The use of octadecane increased HDS from 24.8 % to 36.0 % and conversion from 40.4 % to 74.6 %. The product distribution also changed. An increase in HDS and hydrogenation products, such as BP, TH-DBT, and CHB could also be observed.

MoCl_3 gave about the same results as ATTM, in terms of HDS and conversion in both solvents (Table 3). However, the addition of sulfur to MoCl_3 resulted in a considerable decrease in both HDS and conversion. The use of $\text{Co}_2(\text{CO})_8$ in octadecane gave relatively low conversion, which indicates that the material from $\text{Co}_2(\text{CO})_8$ itself is less active for DBT conversion under the conditions employed. Although sulfur was not used, it could possibly increase the activity of $\text{Co}_2(\text{CO})_8$ as it did for $\text{Mo}(\text{CO})_6$. The use of the bimetallic catalyst MoCo-TC2 did not give an improvement over the individual Co or Mo catalysts. In fact, the results were almost identical to runs using $\text{Co}_2(\text{CO})_8$. It should be mentioned that the above results apply only to the HDS using in situ generated catalyst from MoCo-TC2 . The last precursor used was $\text{Fe}(\text{CO})_5$, with and without

added sulfur. They were the least active precursors, among all those tested with octadecane solvent. This is probably due to the low hydrogenation activity and HDS activity of the Fe catalysts. An additional reason for the lack of activity of $\text{Fe}(\text{CO})_5$ is the preferred formation of less reactive iron carbides (6) and iron oxides over iron sulfides.

$\text{Mo}(\text{CO})_6$ and ATTM were also used at 0.5 mol % metal loading in reactions at 350 °C involving water. Previous work by Song (7) demonstrated the promoting effect of water addition in coal liquefaction experiments under low severity reaction conditions. Water was added in a $\text{H}_2\text{O}:\text{DBT}$ molar ratio of 10:1. The results obtained so far were not conclusive. The product recovery was poor with CH_2Cl_2 as the solvent for recovering products from the reactions with H_2O . It is considered that replacing CH_2Cl_2 with acetone as the wash solvent may improve the product recovery.

CONCLUSIONS

Dibenzothiophene appeared to be relatively stable under thermal conditions and reacts only with very active catalysts and high metal loadings to form hydrodesulfurized products. $\text{Mo}(\text{CO})_6$ (36 mol % metal loading) with added sulfur in a S:metal ratio of 6:1 and octadecane as solvent was found to be the most active catalyst yielding 100% HDS and conversion at 400 °C. ATTM and MoCl_3 appear to be less active for DBT HDS under similar conditions. The other catalyst precursors, $\text{Co}_2(\text{CO})_8$, MoCo-TC_2 , and $\text{Fe}(\text{CO})_5$, showed only moderate activity. The use of high boiling solvent seems to be beneficial to HDS, conversion, and the formation of hydrogenation products.

In model reactions using ATTM and $\text{Mo}(\text{CO})_6$ (0.5 mol % metal loading) with and without added sulfur only low catalytic activity could be observed. The product distribution in runs using a metal loading of 0.5 mol % revealed only hydrogenation products.

REFERENCES

1. Kamiya, Y.; Nobusawa, T. and Futamura, S. *Fuel Process. Technol.*, **18**, 1988, 1.
2. a) Artok, L.; Davis, A.; Mitchell, G. D. and Schobert, H. H. *Energy & Fuels*, **1993**, *7*, 67-77.
b) Garg, D. and Givens, E. N. *Fuel Process. Technol.*, **8**, 1984, 123-34.
3. Brunner, H. and Wachter, J. J. *J. Organomet. Chem.*, **C41-44**, 1982, 240.
4. a) Schmidt, E. and Song, C. *Prepr. Pap. - Am. Chem. Soc., Div. Fuel Chem.*, **35**, 1994 733-737.
b) Song, C.; Schmidt, E. and Schobert, H. H. *DOE Coal Liquefaction and Gas Conversion, Contractors' Review Meeting in Pittsburgh*, (September 7-8, 1994), 593-604.
5. Kim, H. and Curtis, C. W. *Energy & Fuels*, **Vol. 4**, No. 2, 1990, 206.
6. Herrick, D.; Tierney, J.; Wender, I.; Huffman, G. P. and Huggins, F. E. *Energy & Fuels*, **Vol. 4**, 1990, 231.
7. Song, C. and Saini, A. K. *Energy & Fuels*, **9**, 1995, 188-9.

Table 1. Catalytic Hydrodesulfurization of Dibenzothiophene with Mo-Based Precursors [0.5 - 5 mol % metal loading].

Experiment #	BLDA3/4	BLDA5	BLDM5/6	BLDM12	BLDM10/11	BLDMS1/2	BLDMS5
Catalyst Precursor	ATTM ^a	ATTM ^{b, #}	Mo(CO) ₆ ^a	Mo(CO) ₆ ^b	Mo(CO) ₆ [5 mol % ^a]	Mo(CO) ₆ + S ^a	Mo(CO) ₆ + S ^b
Products [mol %] ^c							
TH-DBT	5.4	4.6	0.4	0.8	2.5	7.7	8.0
BP	2.5	2.0	1.9	3.0	5.6	3.9	4.3
CHB	1.2	0.9	0	0.1	0.4	1.8	2.1
BCH	0		0	0	0	0	0
BNZ	0		0	0	0	0	0
HDS products	3.7	2.9	1.9	3.1	6.0	5.7	6.3
Conversion [wt%]	21.2	7.4	5.5	17.1	26.2	38.2	17.8

Solvent: ^atridecane, ^boctadecane. ^c biphenyl (BP), tetrahydro-dibenzothiophene (TH-DBT), cyclohexylbenzene (CHB), bicyclohexyl (BCH), and benzene (BNZ).
Needs to be re-run to check the reproducibility.

Table 2. Catalytic Hydrodesulfurization of Dibenzothiophene with Mo-Based Precursors [36 mol % metal loading].

Experiment #	BCDA5	BCDA4	BCDM1/2	BCDM6/5	BCDMS1/2	BCDMS5/6	BCDMS7	BCDMS8
Catalyst Precursor	ATTM ^a	ATTM ^b	Mo(CO) ₆ ^a	Mo(CO) ₆ ^b	Mo(CO) ₆ +S ^a	Mo(CO) ₆ + S [2:1] ^c	Mo(CO) ₆ + S [6:1] ^c	Mo(CO) ₆ + S [6:1] ^b
Products [mol %]								
TH-DBT	3.3	4.7	2.1	2.1	5.5	0	0	0
BP	6.4	11.4	39.1	48.3	26.6	9.9	2.6	0
CHB	11.7	17.7	8.5	14.1	41.7	20.7	23.0	19.1
BCH	3.2	3.2	0	14.6	0	2.5	4.7	11.0
BNZ	3.5	3.7	3.2	3.0	25.7	15.8	10.9	13.8
HDS	24.8	36	50.8	80.0	94.0	48.9	41.2	43.9
Conversion [wt%]	40.4	74.6	53.4	75.8	70.5	99.1	100.0	100.0

Solvent: ^atridecane, ^boctadecane, ^cheptadecane.

Table 3. Catalytic Hydrodesulfurization of Dibenzothiophene with Mo-Based Precursors [36 mol % metal loading].

Experiment #	BCDT3	BCDT2	BCDTS3	BCDTS2	BCDC1	BCDC2	BCDMC1	BCDF1	BCDFS1
Catalyst Precursor	MoCl ₃ ^a	MoCl ₃ ^b	MoCl ₃ +S ^a	MoCl ₃ +S ^b	Co ₂ (CO) ₈ a, #	Co ₂ (CO) ₈ b	MoCo- TC ₂ ^b	Fe(CO) ₅ ^b	Fe(CO) ₅ +S ^b
Products [mol %]									
TH-DBT	0	6.9	4.1	4.5	0	0	2.5	0	0
BP	33.3	42.5	11.3	12.0	0	5.6	7.0	4.4	4.5
CHB	0	2.3	2.8	11.5	0	13.1	11.5	10.0	15.1
BCH	0	0	0	3.8	0	13.1	0	0	0
BNZ	7.0	13.2	7.4	5.0	0	0	0	0	0
HDS	40.3	58.0	21.5	32.3	0	31.8	18.5	14.4	19.6
Conversion [wt%]	52.6	67.3	45.2	48.4	0	19.6	16.3	5.0	8.5

Solvent: ^atridecane, ^boctadecane. # Needs to be re-run to check the reproducibility.

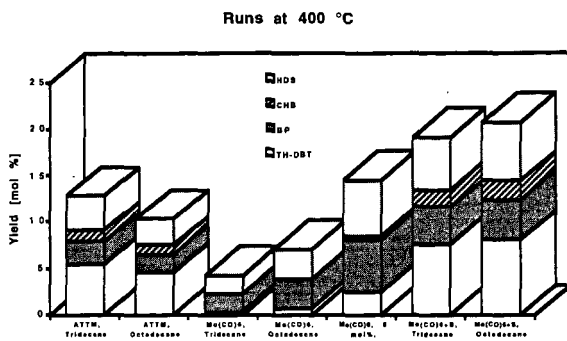


Figure 1. Catalytic Hydrosulfurization of Dibenzothiophene with Mo-Based Precursors [0.5 - 5 mol % metal loading].

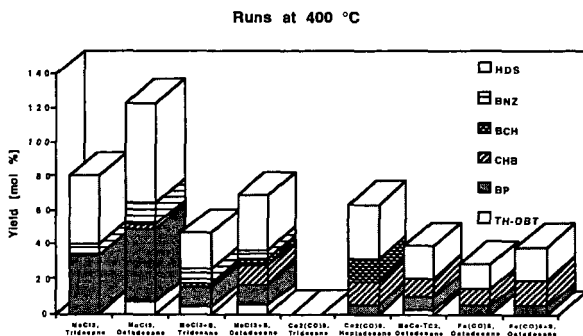


Figure 2. Catalytic Hydrosulfurization of Dibenzothiophene with Mo-Based Precursors [36.16 mol % metal loading].

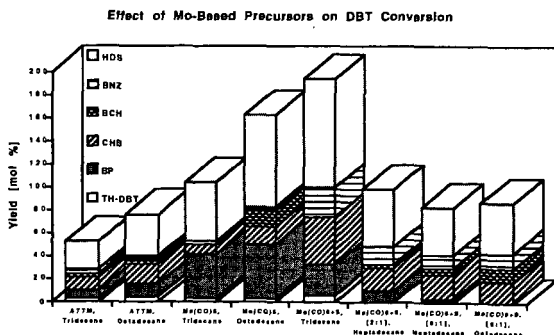


Figure 3. Catalytic Hydrosulfurization of Dibenzothiophene with Mo-Based Precursors [36 mol % metal loading].

CATALYTIC HYDRODESULFURIZATION OF BITUMEN

Ramesh K. Sharma and Edwin S. Olson
University of North Dakota
Energy & Environmental Research Center
PO Box 9018
Grand Forks, ND 58202
(701) 777-5000

Keywords: Catalytic hydrodesulfurization, Bitumen

ABSTRACT

Investigations of the catalytic hydrodesulfurization of Venezuela bitumen and its water emulsion (Orimulsion) were carried out. This material contained a large amount of sulfur and organometallics, such as vanadium and nickel compounds. A variety of nickel and molybdenum catalysts were prepared. These, as well as two commercial catalysts, were tested with Orimulsion and vacuum-dried, pentane-insoluble and -soluble bitumen. Catalytic hydrotreatment removed up to 75% of sulfur from the bitumen. Hydrodesulfurization was found to be affected by reaction temperature, reaction time, catalyst, and feed material. Moisture-free bitumen and a pentane-soluble bitumen fraction were desulfurized more effectively than Orimulsion. Zeolite-based catalysts gave higher desulfurization than synthetic clay catalysts.

INTRODUCTION

The sulfur content of many coals, crude oils, and bitumens results in serious problems in the utilization and processing of these resources, both as fuel and nonfuel materials. Emission regulations demand that cleaner fuels be utilized. The production of low-sulfur, low-metal petroleum coke (petcoke) is also being sought for the manufacture of needle cokes, carbon electrodes, metallurgical reductions, and fuels. Unfortunately, the feedstocks available for production of fuels and carbon products tend to have higher sulfur contents, e.g., the very large reserves of crude oil and bitumens that are available in South America with sulfur contents of greater than 3 wt%. Lower-value sour crudes are also an increasing problem for oil production in parts of the United States.

Previous work at the Energy & Environmental Research Center (EERC) was concerned with the development of catalysts for production and upgrading of coal liquids, including hydrodesulfurization. The types of catalysts investigated included zinc chloride-silica complexes (1), metal-impregnated natural and synthetic clays (2-5), and zeolites (5). Molybdenum sulfide impregnated in a nickel-substituted synthetic mica montmorillonite (NiSMM) and in a hydrotalcite clay were demonstrated to be highly effective catalysts for hydrodesulfurization of coal-derived products.

Further demonstrations of the activities and stability of these catalysts for desulfurization of petroleum resids and bitumens are needed. Currently used resid desulfurization catalysts experience severe deactivation as a result of plugging of the catalyst pores or sintering of the metal sulfides. Several catalysts that previously exhibited activity for hydrodesulfurization of coal-derived materials were tested for desulfurization of a Venezuela bitumen. This material is marketed as a water emulsion product called Orimulsion.

EXPERIMENTAL

The hydrodesulfurization tests were conducted in a small batch reactor with hydrogen pressures of about 1000 psi at a temperature of 390°C. The emulsion form (a 70% bitumen-30% water emulsion) is convenient for weighing and transferring the bitumen, and therefore the emulsion as well as the moisture-free bitumen (71 wt%) obtained by drying the water emulsion were used in tests. The moisture-free bitumen was further fractionated into pentane-soluble (83%) and pentane-insoluble (17%) fractions.

Catalysts

Catalysts used in this study included the following: 1) chromia-pillared clay + molybdenum (6), NiSMM + molybdenum (7, 8), 2) Y-Zeolite + nickel-molybdenum (9), 3) Y-Zeolite + nickel-tungsten (9), 4) Y-Zeolite-aluminosilicate (10) + nickel-molybdenum, 5) Hydrotalcite + molybdenum (4), 6) uranium oxide-nickel oxide (11), 7) uranium oxide-nickel oxide + molybdenum prepared by impregnation of above catalyst, 8) AMOCAT and HDN-30.

Catalytic Reactions

The catalysts were presulfided by heating with elemental sulfur plus hydrogen (200 psig) at 400°C for 2 hr. In a typical experiment, 1.50 g of Orimulsion or 1.0 g of dry bitumen or 1.0 g of pentane-soluble fraction and 0.5 g of the catalyst were placed in a tubing bomb (15-mL microreactor). The microreactor was evacuated, pressurized with 1000 psig of hydrogen, and placed in a rocking autoclave heated to the desired temperature. Heating was continued for 1 or 3 hours. At the end of the reaction period, the microreactor was cooled to room temperature, degassed, and opened. The product slurry was extracted

with tetrahydrofuran, and the solid catalyst removed by centrifugation. The supernatant liquid was evaporated to remove solvent, and the dried product was analyzed for sulfur. Total sulfur determinations were done with a LECO Model 532 sulfur analyzer using the American Society for Testing and Materials (ASTM) D1551 method.

RESULTS AND DISCUSSION

Synthetic and Pillared Clay-Supported Molybdenum

In a 1-hr test with the as-received emulsion (Orimulsion), the synthetic clay-supported molybdenum catalyst (NiSMM + 5% molybdenum, presulfided) gave a product with 3.0% sulfur (dry basis), which is a 23% reduction in the sulfur content of the bitumen (Table 1). Minimal hydrocracking and gas formation occurred under these conditions, although it is likely that some asphaltene hydrogenation occurred. The viscosity was not significantly changed.

A chromia-pillared clay containing impregnated molybdenum (molybdenum-high-chromium-pillared clay [Mo-HCPC]) was presulfided, and the catalyst was tested for hydrodesulfurization activity with the Orimulsion (Table 1). This catalyst exhibited a similar poor desulfurization activity (10% sulfur reduction).

The reaction of Orimulsion with the molybdenum sulfide-impregnated hydrotalcite (MoHT) catalyst gave a product with 3.6% sulfur (8% reduction) (Table 1). This catalyst gave respectable desulfurization with coal-derived liquids as well as model compounds (4), but apparently it is hindered by the aliphatic content of the bitumen, which may inhibit diffusion into the small pores of the catalyst.

Commercial Catalysts

The presulfided commercial molybdenum catalysts, AMOCAT and HDN-30, both removed 39% of the sulfur of the Orimulsion (dry weight basis) in the 1-hr batch hydrodesulfurization test (Table 1). On this basis, we concluded that the EERC catalysts that previously showed desulfurization activities with coal liquids were far inferior to the commercial catalysts for desulfurization of the highly aliphatic bitumen. The form of sulfur present in the bitumen is likely to be partly heterocyclic as it is in the coal, but the matrix is entirely different in the bitumen.

Y-Zeolite-Supported Catalysts

Further catalyst screening was carried out with zeolite catalysts modified by metal impregnation and also by coating the zeolite with aluminosilicate (cogel) as is done with fluid catalytic cracking (FCC) refining catalysts. The zeolite-supported nickel-molybdenum catalyst gave a 32% reduction of sulfur, and a similar zeolite-supported nickel-tungsten catalyst gave only a 22% sulfur reduction in 1-hr tests (Table 1).

More encouraging results were obtained with the catalyst prepared by impregnating nickel and molybdenum into a zeolite-aluminosilicate cogel (Table 2). The cogel-supported nickel-molybdenum catalyst gave 43% removal of sulfur in a 1-hr test. This catalyst is similar to that recently reported by a Canadian group (12). Further testing with Orimulsion for 3 hours gave 58% removal. When a dry fraction of the bitumen was hydrotreated with this catalyst for 3 hours, 37% of the sulfur was removed. Similar reaction with a pentane-soluble fraction of the bitumen resulted in 74% sulfur removal to give a product with 1.0% (dry weight basis) sulfur content. However, when the same reaction was carried out using 10 wt % of the catalyst, only 25% sulfur was removed.

Mixed Oxide Catalysts

Good results were also obtained with a nickel catalyst supported on uranium oxide, which gave 38% removal of sulfur from the as-received Orimulsion in the 1-hr period (Table 3). The function of the uranium oxide is to prevent sintering of the nickel during regeneration of the catalyst. A hydrodesulfurization reaction of the moisture-free bitumen with this catalyst for 3 hours gave the same reduction in sulfur as that obtained with the Orimulsion. Thus with this catalyst, the water present in the emulsion does not appear to interfere with the reaction. Impregnation of molybdenum (5%) into this nickel catalyst resulted in a slight increase in catalytic activity (41% sulfur reduction). Better desulfurization was expected for this catalyst, but since far superior results were obtained with the zeolite catalyst, further work with the molybdenum-nickel-uranium oxide catalyst was suspended.

CONCLUSIONS

Two catalysts that had previously exhibited activity for hydrocracking coal tar constituents were active for hydrodesulfurization of the high-sulfur Venezuelan bitumen. The most active catalyst for hydrodesulfurization was a nickel- and molybdenum-impregnated Y-zeolite-aluminosilicate cogel. This catalyst removed 75% of the sulfur from the moisture-free bitumen and 58% of the sulfur from the Orimulsion. A nickel-molybdenum catalyst supported on uranium oxide gave slightly better results than

desulfurization with the commercial catalysts. Other catalysts that had exhibited activity for desulfurization of coal-derived liquids were less active for desulfurization of the bitumen than the commercial hydrotreating catalysts.

ACKNOWLEDGMENTS

The support of the U. S. Department of Energy is gratefully acknowledged.

REFERENCES

1. Sharma, R.K.; Diehl, J.W.; Olson, E.S. "Hydrodesulfurization with a New Solid Acid Catalyst," In *Processing and Utilization of High-Sulfur Coals III*; Markuszewski, R.; Wheelock, T.D., Eds.; Elsevier: Amsterdam, 1990; pp 735-743.
2. Olson, E.S.; Buchwitz, C.M.; Yagelowich, M.; Sharma, R.K. *Prepr. Pap.—Am. Chem. Soc., Div. of Fuel Chem.* **1993**, *38*, 156-162.
3. Olson, E.S.; Yagelowich, M.C.; Sharma, R.K. *Prepr. Pap.—Am. Chem. Soc., Div. Fuel Chem.* **1992**, *37*, 262-267.
4. Sharma, R.K.; Olson, E.S. "Catalytic Hydrodesulfurization with Hydrotalcites," In *Processing and Utilization of High-Sulfur Coals IV*; Dugan, P.R.; Quigley, D.R.; Attia, Y.A., Eds.; Elsevier: Amsterdam, 1991; pp 377-384.
5. Olson, E.S.; Sharma, R.K. "New Catalysts for Production of Synthetic Fuels," In Proceedings of the Australian/U.S.A. Workshop on Low-Rank Coals, Billings, MT, May 23-24, 1991; EERC publication.
6. Sharma, R.K.; Olson, E.S. *Prepr. Pap.—Am. Chem. Soc., Div. Fuel Chem.* **1994**, *39* (3), 702.
7. Heinerman, J.J.L.; Freriks, I.L.C.; Graaf, J.; Pott, G.T.; Coglegem, J.G.F. *J. of Catal.* **1983**, *80*, 145.
8. Olson, E.S.; Sharma, R.K. *Prepr. Pap.—Am. Chem. Soc., Div. Fuel Chem.* **1994**, *39* (3), 706.
9. Haynes, H. W., Jr. *Ind. Eng. Chem. Process. Des. Dev.* **1983**, *22*, 401.
10. Pecorara, T.A. U.S. Patent 5 001 097, 1991.
11. Berry, F.J.; Murray, A.; Parkyns, N.D. *Appl. Catal. A* **1993**, *100*, 131.
12. Diaz-Real, R.A.; Mann, R.S.; Sambhi, I.S. *Ind. Eng. Chem. Res.* **1993**, *32*, 1354.

Table 1. Hydrodesulfurization Reactions of Bitumen

Catalyst	Substrate	Subst.: Cat. Ratio ^a	Time, hr	Sulfur in Substrate, ^b %	Sulfur in Product, %	Sulfur Removed, %
Mo-NiSMM	Orimulsion	2	1	3.9	3.0	23
Mo-HCPC	Orimulsion	2	1	3.9	3.5	10
NiMo- Y-Zeolite	Orimulsion	2	1	3.9	2.7	32
NiW- Y-Zeolite	Orimulsion	2	1	3.9	3.0	22
MoHT	Orimulsion	2	1	3.9	3.6	8
AMOCAT	Orimulsion	2	1	3.9	2.3	39
HDN-30	Orimulsion	2	1	3.9	2.4	39

^a Ratio is based on the dry weight of bitumen contained in the Orimulsion.

^b Percent sulfur is based on the dry weight of bitumen contained in the Orimulsion.

Table 2. Hydrodesulfurization Reactions of Bitumen with NiMo-Y-Zeolite-Aluminosilicate Cogel

Substrate	Substrate: Cat. Ratio	Time, hr	Sulfur in Substrate, ^a %	Sulfur in Product, %	Sulfur Removed, %
Orimulsion	2 ^b		3.9	2.3	43
Orimulsion	2 ^b	3	3.9	1.8	58
Dry Bitumen	2	3	3.7	2.5	37
Pentane-Soluble	2	3	3.6	1.0	74
Pentane-Soluble	10	3	3.6	2.8	25

^a Ratio is based on the dry weight of bitumen contained in the Orimulsion.

^b Percent sulfur based on the dry weight of the bitumen contained in the Orimulsion.

Table 3. Hydrodesulfurization Reactions of Bitumen with Ni-U Oxide Catalysts.

Catalyst	Substrate	Subst.: Cat. Ratio	Time, hr	Sulfur in Substrate, ^a %	Sulfur in Product, %	Sulfur Removed, %
Ni-U Oxide	Orimulsion	2 ^b	1	3.9	2.5	38
Ni-U Oxide	Dry bitumen	2	3	3.7	2.4	39
Ni-U Oxide + 5% Mo	Dry bitumen	2	3	3.7	2.4	41

^a Ratio is based on the dry weight of bitumen contained in the Orimulsion.

^b Percent sulfur is based on the dry weight of the bitumen contained in the Orimulsion.

CAUSTIC WASHING FOR REFINING OF DIRECT COAL LIQUEFACTION PRODUCTS

Richard A. Winschel, Peizheng Zhou*, Francis P. Burke,
Gary A. Robbins, Susan D. Brandes
CONSOL Inc., Research & Development, 4000 Brownsville Road, Library, PA 15129
*Burns and Roe Services Corp., P.O. Box 18288, Pittsburgh, PA 15236

KEYWORDS: Liquefaction, Refining, Phenols

INTRODUCTION

Extensive research and development sponsored by the U.S. DOE/PETC over the past two decades has resulted in dramatic improvements in the quality of direct coal liquefaction products. High-quality coal-derived distillates are obtainable from catalytic two-stage liquefaction (TSL) processes, such as those developed at the Wilsonville, AL pilot plant and the Hydrocarbon Technologies Inc. (HTI) pilot plant and bench units. The products of the Wilsonville and HTI TSL operations are suitable as high quality feedstocks for producing transportation fuels in a refinery. These products have important quality advantages over crude petroleum: they are distillates boiling below about 700°F and are thus virtually free of resid and metals, and they have very low sulfur contents and low nitrogen contents.¹⁻³ The coal liquids have carbon and hydrogen contents and Watson characterization factors within the range of crude petroleum.¹⁻³ However, relative to crude petroleum, the crude coal products have elevated oxygen contents.¹¹⁻¹³ Although these oxygenated species are found at elevated concentrations throughout the boiling range of the coal liquids, they are most frequently concentrated in the heavy naphtha and light kerosene fractions. For example, when the oxygen content of coal liquids is plotted as a function of boiling point, there is often a maximum in the curve between 355 °F and 465 °F (Figure 1 and References 1, 2, and 4).

Phenolic compounds are the predominant oxygen-containing components in the coal liquids;⁴ the curve maximum represents phenols with zero to three alkyl carbon substituents. Phenolic compounds must be reduced to low concentrations to produce finished transportation fuels. In a typical modern petroleum refining scheme, this would be accomplished by hydrotreating. However, because coal liquids have high concentrations of phenolics, it may be advantageous to reduce their concentration prior to hydrotreating by some other route, for example, by caustic extraction. Although caustic washing could not replace hydrotreating to produce finished fuels from the oils described here, this route for pre-removal of phenols could have several advantages over hydrotreating the phenolic containing oils: it would reduce the overall hydrogen demand, it could produce a valuable by-product (cresylic acid), and it would simultaneously strip from the oil mercaptans and hydrogen sulfide in addition to the phenolics. Indeed, caustic washing was once a common unit operation in petroleum refineries because of its ability to sweeten light distillates.⁵ The cresylic acid could be sold as a by-product or perhaps methylated to produce methyl aryl ethers,⁶ which could be used as a high octane oxygenate gasoline extender. Presented here are results of experiments conducted to recover a cresylic acid by-product from crude coal liquids, while simultaneously improving the quality of the liquid. The quality improvement in the coal liquid and the characterization of the by-product cresylics are discussed.

EXPERIMENTAL

The net products of three liquefaction runs that represent variations of state-of-the-art technology were characterized in detail. The three samples were generated at the Wilsonville 6 ton/day pilot plant (Run 260D) and the HTI 2 lb/hr bench unit (Runs CC-15 and CMSL-2), as described in Table 1. The characterization scheme included fractional distillation and analysis and inspection of the fractions. Some of the distillation fractions were caustic washed to remove phenolics and the recovered raffinate and caustic extract fractions were also characterized. The exact caustic washing procedure used varied among the samples; however, the general scheme was to contact the oil in a separatory funnel multiple times with NaOH (either 20 wt % or 6 wt % solutions) then with water, to acidify the extract with concentrated aqueous HCl, then to extract the phenols with methylene chloride and to remove the methylene chloride by rotary evaporation. Raffinate and caustic extract yields are determined gravimetrically. Some losses resulted from evaporation and handling during the extraction scheme. The complete backgrounds of the samples, details of all experimental methods and characterization data appear in the original reports of this work.⁷⁻⁹ Phenolic -OH concentrations were determined by Fourier-transform infrared spectroscopy.¹⁰ The caustic extracts also were characterized by gas chromatography/mass spectrometry (GC/MS) with a HP 5970 system equipped with a 30 m x 0.25 mm DB-5 column (0.25 μm film thickness) as follows: 20 psig He carrier gas; splitless injection as 1% solutions in THF; injection port at 300 °C; column temperature program - 5 min at 35 °C, to 100 °C at 35 °C/min, to 320 °C at 4 °C/min; scan from 45 to 300 amu; spectra searched against the Wiley/NBS mass spectral library; identifications based on search results and supplemented by

retention times; normalized quantitation is based on peak area divided by total peak area of all phenolics found.

DISCUSSION

The oxygen contents, determined by difference, of the distillation fractions of the three crude coal liquids are plotted in Figure 1 as a function of the mid boiling point of the fraction. Two of the three curves show maxima between 355 and 465 °F. Material in this boiling range tends to have relatively high concentrations of phenolic compounds. For example, Table 2 shows that the 380-510 °F fraction has the highest phenolic -OH concentration of the four distillation fractions of the Wilsonville Run 260D sample.

The fractions of the Wilsonville Run 260D sample that were caustic washed include the naphtha (IBP-380 °F), Jet or kerosene (380-510 °F), diesel fuel (510-650 °F), and residuum (650 °F) fractions. Table 2 shows the yields of raffinate and extract from each extraction and the phenolic -OH concentration in each fraction. The phenolic -OH concentrations (Table 2) of the raffinates show that caustic washing was quite effective at removing phenolics from the fractions boiling below 510 °F. In fact, for these raffinates, phenolic -OH was near or below detection limits. Caustic washing was not very effective for the higher boiling fractions. Not only was caustic washing less effective for the higher boiling fractions, it was also less selective; GC/MS analyses showed that the caustic extracts of the higher boiling fractions were contaminated with hydrocarbons. For this reason, and because the highest concentration of phenolics tend to exist in fractions that boil between 355 and 465 °F (Figure 1 and References 1, 2, and 4), only the naphtha (IBP-380 °F) and kerosene (380-510 °F) fractions of the HTI Run CC-15 sample and the "swing cut" (350-400 °F) fraction of the HTI Run CMSL-2 sample were caustic washed. The raffinates of the fractions from HTI Runs CC-15 and CMSL-2 were characterized by the same set of inspection tests as the original, unextracted fractions. The caustic extracts of the fractions from all three runs were characterized by GC/MS analysis and phenolic -OH determination.

The caustic extract yields range from 1.1 to 4.6% and losses (100% - yield of raffinate - yield of extract) range from 0.1 to 4.7%. The variations result from the different properties of the fractions, and perhaps from the use of different caustic washing procedures.

Table 3 compares the inspection data of the raffinates with the corresponding data of original, unextracted fractions. For the IBP-380 °F fraction of Run CC-15, the lower Reid vapor pressure of the raffinate appears to result from the loss of light material during the caustic wash. Properties of that fraction that showed improvement from caustic washing include acidity, copper strip corrosion, existent gum, bromine number, basic nitrogen, oxidation stability, heat of combustion, and mercaptan sulfur. The quality of the fraction in terms of its suitability as gasoline are somewhat improved relative to the unextracted fraction. The major improvements in the 380-510 °F fraction of Run CC-15 from caustic washing include acidity and mercaptan sulfur. Other improvements include oxygen (by diff.), viscosity and bromine number.

For the 350-400 °F fraction of HTI Run CMSL-2, the property which showed the greatest improvement from caustic washing is the mercaptan sulfur content. Many other properties (e.g., bromine number, acidity, oxygen by diff.) show some changes that indicate the raffinate is a better stock for production of transportation fuels. The oxidation stability decreased; this may result from the removal of hindered phenols, which are known to act as antioxidants. However, the opposite effect was seen with the IBP-380 °F fraction of HTI Run CC-15, as discussed above.

The major components of the caustic extracts, as determined by GC/MS analysis, are provided in Table 4. Although the extracts of the higher boiling fractions contained some hydrocarbons, each caustic extract consisted primarily of phenolics. The high measured phenolic -OH concentrations of the caustic extracts (Table 2) confirm this. Depending on the boiling point of the fraction extracted, the caustic extracts consist of phenols with zero to four alkyl substituents.

SUMMARY

Caustic washing was found to be highly efficient and highly selective for the extraction of phenolics from the light distillate fractions (b.pt. <510 °F) of the products of modern two-stage direct coal liquefaction products. The extracts were composed almost entirely of phenolics and the lower boiling raffinates were almost devoid of phenolics. The properties of the raffinates as feedstocks or blendstocks for transportation fuels were moderately improved relative to the unextracted materials. Notable improvements included reduced acidity, mercaptan sulfur, oxygen (by diff.) and copper corrosion; other minor improvements also were seen. The composition of the caustic extracts (cresylic acids) depends on the boiling point of the material extracted, but primarily consists of phenols with zero to four alkyl substituents.

ACKNOWLEDGEMENT

This work was supported by the U.S. Department of Energy under contracts DE-AC22-89PC89883, DE-AC22-89PC88400, and DE-AC22-94PC93054. The inspection data and caustic washing of the HTI samples were performed by G. Sturm, J. Kim and J. Shay of the National Institute for Petroleum and Energy Research.

REFERENCES

1. Zhou, P.-Z.; Winschel, R. A.; Klunder, E. B., *Am. Chem. Soc. Div. Fuel Chem. Prepr.* 1994, 39(4), 1205-1209.
2. Zhou, P.-Z.; Rao, S. N. "Assessment of Coal Liquids as Refinery Feedstocks", DOE Contract No. DE-AC22-89PC88400, February 1992.
3. Zhou, P.-Z. "Characterization of Direct Liquefaction Distillate Products", DOE Contract No. DE-AC22-89PC88400, 1994.
4. Zhou, P.-Z. "Recovery of Phenols From Coal Liquids", DOE Contract No. DE-AC22-89PC88400, March 1993.
5. Nelson, W. L., *Petroleum Refinery Engineering*, Fourth Ed.; McGraw-Hill: New York, 1958; Chapter 10.
6. Singerman, G. M. "Methyl Aryl Ethers from Coal Liquids as Gasoline Extenders and Octane Improvers", Report DOE/CE/50022-1, November 1980.
7. Kramer, R. L. in Report DOE/PC89883-34, November 1991.
8. Sturm, Jr., G. P.; Kim, J.; and Shay, J. in Report DOE/PC89883-92, January 1994.
9. Robbins, G. A.; Brandes, S. D.; Winschel, R. A.; Burke, F. P., Reports DOE/PC89883-43, March 1992, DOE/PC89883-86, March 1994, and DOE/PC 93054-4, October 1994.
10. Burke, F. P.; Winschel, R. A.; Robbins, G. A., Report DOE/PC30027-61, March 1985.

TABLE 1. SOURCE DATA OF COAL LIQUID SAMPLES

Plant/Run	Feed Coal Seam	Process Description		
		Operating Mode	Catalyst	Reactor Temp., °F
Wilsonville 260D HTI CC-15 HTI CMSL-2	Wyodak and Anderson Wyodak and Anderson Illinois No. 6	Catalytic/Thermal Thermal/Catalytic Catalytic/Catalytic	Shell 324/Fe ₂ O ₃ Fe ₂ O ₃ /Shell 317 Shell 317/Shell 317	790/774 800/775 752-777/795-811

TABLE 2. YIELDS AND PHENOLIC -OH CONCENTRATIONS OF FRACTIONS

Fraction	Yield, wt % of Feed Fraction		Phenolic -OH Concentration, meq/g Sample		
	Raffinate	Caustic Extract	Feed Oil	Raffinate	Caustic Extract
<u>Wilsonville Run 260D</u>					
IBP-380 °F	92.7	3.7	0.40	0.02(a)	-
380-510 °F	94.7	3.6	0.92	0.07(a)	-
510-650 °F	94.4	4.6	0.52	0.27	-
650 °F* - Trial 1	95.4	1.9	0.41	0.28	-
650 °F* - Trial 2	97.9	2.0	0.41	0.31	-
<u>HTI Run CC-15</u>					
IBP-380 °F	92.9	2.4	0.13(b)	(c)	8.90
380-510 °F	92.1	4.0	0.24(b)	(c)	7.49
<u>HTI Run CMSL-2</u>					
350-400 °F	95.4	1.1	(c)	(c)	5.02

- (a) Quantitation is uncertain at these extremely low concentrations
- (b) Amine signal probably contributing to reported phenolic -OH concentrations
- (c) Amine observed, no phenolic -OH detected

TABLE 3. INSPECTIONS OF ORIGINAL AND RAFFIANTE FRACTIONS

Property	HTI Run CC-15				HTI Run CMSL-2	
	<380 °F		380-510 °F		350-400 °F	
	Original	Raffinate	Original	Raffinate	Original	Raffinate
Spec. Gravity @ 60 °F (D4502)	0.7798	0.7775	0.8899	0.8882	0.8492	0.8484
API Gravity (calculated)	50.0	50.5	27.5	27.8	35.1	35.3
Elemental Analysis, wt %						
Carbon (D5291)	85.93	86.12	87.12	87.75	86.78	86.86
Hydrogen (D5291)	13.96	13.77	11.77	11.68	12.72	13.06
Sulfur (D3120)	0.03	0.03	0.03	<0.01	0.01	0.01
Nitrogen (D4629)	0.09	0.07	0.33	0.33	0.03	0.02
Oxygen (by diff)	0.00	0.01	0.75	0.23	0.46	0.03
Basic Nitrogen (JOP269)	0.082	0.058	0.274	0.264	0.023	0.023
Mercaptan Sulfur (D3227), ppm	51.5	9.7	45.2	<0.1	19.0	6.0
Viscosity (D445), cSt						
@ 210 °F	-	-	-	-	0.6653	0.8741
@ -20 °C	-	-	10.80	9.665	4.683	4.359
Refractive Index (D1218), @ 20 °C	1.42882	1.42836	1.49196	1.49072	-	-
Freezing Point (D2386), °F	-	-	-12	-13	-99	-95
Cloud Point (D2500), °F	-	-	-	-	<-60	<-60
Pour Point (D97), °F	-	-	-	-	<-60	<-60
Reid Vapor Pressure (D5191), psi	2.54	2.09	<0.01	<0.01	0.02	<0.01
Flash Point (D56, D93), °C	-	-	83	82	50	57
Group Analy. (ASTM D5134 & HC22)						
Paraffins, vol %	38.0	34.7	9.6	9.1	7.5	8.0
Naphthenes, vol %	45.7	48.8	43.1	46.0	61.3	61.5
Aromatics, vol %	8.7	9.2	41.4	41.9	28.4	27.6
Olefins, vol %	4.6	4.2	5.8	3.0	2.6	2.5
Benzene (PIANO, mod D5134)	0.089	0.078	-	-	-	-
Naphthalenes (D1840), vol %	-	-	4.23	3.74	0.48	0.32
Bromine Number (D1159)	3.62	2.37	5.08	2.69	3.00	2.71
Aniline Point (D611), °F	103.8	108.0	71.5	75.2	-	-
Smoke Point (D1322), mm	-	-	10.9	11.6	15.8	15.4
Acidity (D3242), mg KOH/g	0.05	<0.01	0.04	0.01	0.01	<0.01
Copper Corrosion (D130)	3b(dark)	2d(mod)	1a(slight)	1a(slight)	1a(slight)	1a(slight)
Existent Gum (D381), mg/100 mL	11.2	9.0	-	-	6.4	6.2
Oxidation Stability (D525), min	105	1440	-	-	1440	720
Thermal Stability (JFTOT) (D3341)	-	-	Fail	Fail	-	-
Octane No., Motor Method (D2700)	60.7	58.1	-	-	-	-
Octane No., Rarch Method (D2699)	61.6	60.2	-	-	-	-
Heat of Combustion (D2382, D240), Net Btu/lb	16,509	18,651	17,918	18,043	16,401	18,411
Luminometer Number (D1740)	-	-	-	-	27.3	27.0

TABLE 4. COMPOSITIONS OF CAUSTIC EXTRACTS

Component	GC/MS Intensity, as % of Total Phenolic Intensity (No. of Resolved Peaks in Parentheses)				
	Wilsonville Run 260D		HTI Run CC-15		HTI Run CMSL-2
	IBP- 380 °F	380- 510 °F	IBP- 380 °F	380- 510 °F	350-400 °F
phenol	24(1)	0.4(1)	13(1)	-	-
o-cresol	15(1)	1(1)	21(1)	-	1.5(1)
m/p-cresol	31(2)	4(1)	24(1)	0.4(1)	1.5(1)
dimethyl phenol	13(6)	14(6)	21(5)	13(6)	32(5)
ethyl phenols	16(2)	13(3)	17(2)	8(2)	10(2)
C ₃ -phenols	1(5)	31(12)	4(6)	51(12)	37(11)
C ₄ -phenols	-	16(10)	-	24(12)	17(9)
indanol	-	18(1)	-	4(1)	0.3(1)
dihydroxytoluene	-	1(1)	-	-	-
tetralinol	-	2(1)	-	-	-

Only traces of hydrocarbon contaminants found in IBP-380 °F extracts.
Some hydrocarbon contaminants found in others.

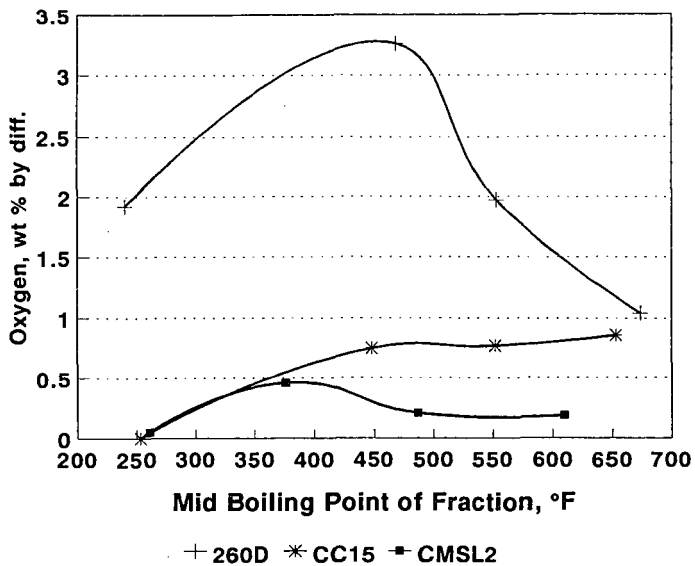


Figure 1. Oxygen Content (by diff.) versus Mid Boiling Point of Coal Liquid Fractions.

HYDRODENITROGENATION WITH NiMo SUPPORTED ON Al_2O_3 - $AlPO_4$

R. Menon, H.S. Joo, J.A. Guin, Department of Chemical Engineering
Auburn University, Auburn, Alabama, 36849

P. J. Reucroft and J.Y. Kim, Department of Chemical and Materials Engineering
University of Kentucky, Lexington, Kentucky, 40506

Aluminum phosphate - metal oxides can be used as nonconventional supports for NiMo hydrotreating catalysts. Several Al_2O_3 - $AlPO_4$ (AAP) supports were prepared by coprecipitation. Effect of variations in Al/P atomic ratios, precipitation method, final pH, and washing agent on various support properties were examined. Catalysts containing 3 wt% Ni and 13 wt% Mo were prepared by incipient wetness and characterized by several methods. Hydrodenitrogenation (HDN) activities of the catalysts were examined in model compound and coal liquid reactions.

Keywords : catalyst support, aluminum phosphate, solid acid catalyst, HDN

INTRODUCTION

New and more stringent environmental regulations are expected to have a major impact on the refining industry. To achieve future government specifications for fuels, significant changes will likely be required in refinery operations to produce products with good combustion characteristics and reduced emissions. Emphasis in this research is on the development of new and improved catalysts for upgrading coal-liquids and coal/waste liquefaction liquids (CWL) to clean transportation fuels. Because coal liquids contain significant quantities of heteroatoms, (S, O, and N) and have higher aromaticity than their petroleum based counterparts, hydroprocessing operations will form the nucleus of technology for their upgrading.

One of the latest studies in catalysis (Catalytica, 1994) suggests solid acids (metal oxides, heteropoly acids, metal sulphates, *metal phosphates* etc) as important industrial catalysts. The incentive for developing new solid acid and base catalysts to replace hazardous or corrosive liquid ones is again environmental considerations (Tanabe., 1994; Catalytica, 1994). The use of phosphorous as a promoter element for Co-Mo and Ni-Mo/ Al_2O_3 catalysts has received significant attention in coal-liquids upgrading (Tischer et al., 1987), with varying degrees of success; however, actual metal phosphate supports have received little attention as upgrading catalyst supports. There is considerable evidence of their utility as a possible catalyst support material in light of their high stable surface area, pore geometry, surface acidity properties and surface chemistry (Marcelin et al., 1983; Moffat, J.B., 1978; Rebenstorf et al., 1991). Chen et al (1990) studied hydrodesulfurization reactions of residual oils over CoMo/Alumina-Aluminum phosphate catalysts. They reported that larger surface area, smaller acid amount and weaker interaction of AAP supports made the metal more highly dispersed, produced more active sites and resulted in high initial HDS activity. In this study we explored the performance of metal phosphates of aluminum, zirconium and titanium as potential new supports for HDN upgrading catalysts. Preparation of cogels of $AlPO_4$ and Al_2O_3 by coprecipitation of an aluminum salt and H_3PO_4 has been discussed in the literature (Kearby, K., 1961; Mitchell et al., 1987; Vogel et al., 1982; Campelo et al., 1986).

EXPERIMENTAL SECTION

PREPARATION OF ALUMINA-ALUMINUM PHOSPHATES (AAP)

The experimental procedures used here in were based on earlier works (Chen et al., 1990; Cheung et al., 1986; Marcelin et al., 1983). Various factors taken into consideration were an appropriate aluminum compound, precipitating agent, gelation conditions, washing agent, drying and calcination temperatures. Three methods were examined.

METHOD A: Supports were prepared by a coprecipitation method. Phosphoric acid solution (H_3PO_4 , 85 wt%) was added to an aqueous solution of aluminum nitrate nona hydrate $Al(NO_3)_3 \cdot 9H_2O$, slowly in an amount to give the desired Al/P ratio. After the addition, the acidic solution was well stirred for at least 10 minutes. A basic solution was prepared by mixing ammonium hydroxide (NH_4OH , 28-30%) and distilled water with a volume ratio 1:1. Both the acidic and basic solutions were added slowly to a third well stirred vessel containing 1L of distilled water. The pH value in the third vessel was maintained at 8.0 throughout the precipitation process by adding small amounts of the acidic and basic solutions. This process was continued until the acidic solution was consumed. The resulting precipitates were centrifuged, washed three times with distilled water, dried overnight at 393K in a vacuum oven, and calcined in a muffle furnace for 12h at 773K. Varying the Al/P ratio allowed various AAP composites to be obtained. Each support is designated based on the Al/P mole ratio.

METHOD B: Certain modifications were made in Method A. [1] Coprecipitation was done at 273K; not at room temperature, [2] A ripening period of 12h was allowed at room temperature, [3] The washing agent was chosen as isopropanol and [4] pH =5.0 instead of 8.0 during precipitation.

H₃PO₄ (85wt%) was added to a solution of Al(NO₃)₃·9H₂O. The acidic solution was well-stirred and cooled to 0°C. A basic solution was prepared by mixing ammonium hydroxide and distilled water with a volume ratio 1:1. Both the acidic and basic solutions were added slowly to a third vessel of distilled water at 0°C. After standing overnight, the gel was thoroughly extracted with isopropanol three times, allowed to stand at room temperature overnight to evaporate residual isopropanol, dried at 106-110°C for 12h in a vacuum oven, and calcined at 500°C for 12h in a muffle furnace. Two sets of experiments were done to study the effects of pH on the textural properties of AAPs. The first set of experiments was done with varying Al/P ratio and keeping the pH constant at 5.0 during precipitation. In a second set of experiments, Al/P ratio was kept constant at 1.0 and constant values of pH 5.0, 6.0, 7.0, 8.8 and 9.2 were used during precipitation. Heat treatment was same as above.

METHOD C: The precipitation methods were modified. Solutions of Al(NO₃)₃·9H₂O and H₃PO₄ were stirred together to form an acidic solution to which ammonium hydroxide solution (13%) was added rapidly. Precipitation occurred rapidly at 0°C. During precipitation pH was not held constant. As ammonia was added to the acidic solution, the pH rose from less than 1.0 to neutrality, and precipitation occurred during a 1-2 min interval. A ripening period of 12h was allowed. The gel was centrifuged and washed with isopropanol three times, followed by drying in the vacuum oven for 12h at 108°C and calcination in the muffle furnace at 649°C for 3h. The samples prepared were AAP1, AAP2, AAP3.5, AAP4, AAP5, AAP6 and AAP8. An Al₂O₃ support also was prepared for comparison purposes.

PREPARATION OF NiMo/AAP CATALYSTS

Supports AAP1, AAP2, AAP4, AAP5, AAP8, and Al₂O₃ prepared in the lab using Method C were chosen for final catalyst preparation. All were made by Method C. Three commercial materials were also used: Shell 424 NiMo/Al₂O₃ as catalyst and AlPO₄-G (Grace Davison), and Al₂O₃-H (Harshaw) as supports. The metal compounds chosen were ammonium molybdate tetrahydrate (NH₄)₂MoO₄·4H₂O and nickel nitrate hexahydrate, Ni(NO₃)₂·6H₂O. The compounds were dissolved in an exact amount of water to fill the pore volume of the support. The supports were impregnated with ammonium molybdate first, dried for 16h at 120°C in a vacuum oven, and calcined at 500°C for 5h in a muffle furnace. Then, they were impregnated with nickel nitrate solution, dried for 16h at 120°C and calcined again for 5h at 500°C.

CHARACTERIZATION OF CATALYSTS

Surface area and pore volume measurements: Surface area was determined by nitrogen adsorption (BET Method) using a Quantasorb adsorption unit manufactured by Quantachrome Corp. The samples were degassed for 4.5h at 350°C prior to the measurements. The pore volumes were measured by using water as a pore filling medium.

XPS Studies: X-Ray photoelectron spectroscopy was used for the surface (in the top 2-5 nm of the solid) elemental analysis of the catalysts.

X-ray Diffraction studies: Catalysts were characterized by X-ray diffraction to investigate their crystallographic properties. A powder diffractometer was used, at 40 kV and 40 mA with Cu K α radiation.

ICAP: Bulk metal analysis was done by a Jarrell Ash ICAP (Inductively Coupled Argon Plasma) 9000. The values are given in Table 1.

MEASUREMENT OF HDN ACTIVITY: All reactions were performed in 20cc 316 ss tubing bomb microreactors (TBMR) which were agitated in a fluidized sand bath and replicated at least twice. A reactant solution (5g) containing 2 wt% pyridine in hexadecane was used for model compound studies and coal liquid (3g) for upgrading. Experiments were charged with 1000 psig cold hydrogen pressure and performed at 350°C for 20 min using 0.1 g catalyst for model compound reactions and at 375°C for 1 hr using 0.4 g catalyst for upgrading coal liquid. Catalyst was sulfided *in situ* with dimethyl disulfide.

RESULTS AND DISCUSSION

Elemental Analysis: Bulk metal concentrations calculated, based on the amount of reagents used and the amount of the support formed (experimental) and actual analysis by ICAP is shown in Table 1. A comparison between the experimental and theoretical (based on weight of support expected) weights of the supports (Method C) are given in Table 3.

XPS Studies: The Al/P ratios were similar for both bulk and surface with a slight depletion of Al or enrichment of P on the surface compared to the bulk (Table 1). AAP4, AAP8 and Al₂O₃-H

showed lower Mo/Ni values on the surface compared to the bulk.

Surface areas and pore volumes: In METHOD A, the surface area of AAPs increased as the A/P ratio varied from 1.0 to 8.0 (Fig. 1a). The area of AAP1 was only 41 m²/g. The modifications done to Method A, in Method B, provided an AAP1 with much higher surface area (141 m²/g). However, the AAPs showed a different trend and the highest area did not exceed 200 m²/g. In Method C, the AAPs exhibited higher surface areas, the maximum being at 267 m²/g (AAP5). With increasing pH surface areas of AAPs declined (METHOD B), but above pH= 8 it showed a tendency to increase (Fig 1b). The pore volume and pore diameter (Method C) increased with increasing P/Al ratio (Fig 1c & Fig 1d). After impregnation with Mo and Ni, the catalyst surface areas (Fig 2) were reduced considerably (Table 2), possibly due to the plugging of small pores. By studying the effect of gelation condition, precipitating agent, washing agent etc, on the textural properties of AAPs, a systematic method of preparation for these catalysts can be recommended. Rapid precipitation at 273K, a ripening period before centrifuging the gel, choice of isopropanol as washing agent and an optimum calcination temperature can provide catalysts with desired pore size for hydrotreating reactions.

X-Ray Diffraction Patterns: For NiMo/AAP1 the position of the main peaks (at $2\theta = 27.3$ and 26.6) suggested the presence of MoO₃ and Al(PO₃)₃ phases. This also agrees partially with those of aluminophosphates with P/Al = 1.0 (Cheung et al., 1986) and with CoMo/AAP1 (Chen et al., 1990). For NiMo/AAP2, the peaks at $2\theta = 23$ and 26.4 were in partial agreement as those of MoO₃ and AlPO₄. No characteristic peaks of Al₂O₃ was observed. This may be due to the formation of a mixture of crystalline bulk oxide and surface compounds and can be attributed to the metal oxide-support interaction. Reducing the phosphorous content (NiMo/AAP4 and NiMo/AAP8) demonstrated an amorphous (X-Ray indifferent) pattern, giving no hint of alumina, NiO or MoO₃. The broad XRD pattern of NiMo/Al₂O₃ (Method C) indicated a low order of crystallinity. Al₂O₃-H showed a more crystalline pattern than the above, but after impregnation with Ni and Mo, the catalyst gave an amorphous pattern. The AlPO₄-G sample gave a broad peak around $2\theta = 28$ which is characteristic of the tetrahedral structure in amorphous AlPO₄. The main peaks ($2\theta = 23, 27.0$) for NiMo impregnated AlPO₄-G indicated the presence of an MoO₃ phase.

HDN Activity: Pyridine HDN occurs through a sequential pathway as shown in Fig. 3 in which pyridine is saturated to form piperidine followed by the formation of pentylamine through piperidine hydrogenolysis. Subsequent nitrogen removal from pentylamine results in pentane and ammonia as final products. Pentylpiperidine is formed in a side reaction from the alkyl-transfer reaction of piperidine and pentylamine. Di-n-pentylamine was also found to a minor extent in our experiments. In this experiment, a loss of N can be caused by the adsorption of N-containing compounds (pyridine, piperidine, pentylamine, and pentylpiperidine) on catalyst and the wall of reactor and evaporation (Joo et al., 1995). Because of these losses, in this paper, all values of pyridine HDN are considered as semi quantitative. Pyridine and coal liquid HDN activities of a series of catalysts which have different A/P atomic ratio and the same Ni/Mo content are in Fig. 4a. HDN activity generally increased with the increase of A/P ratio (or surface area of catalyst). As shown in Fig. 4b, generally HDN activity is linearly correlated with surface area of catalyst. The surface area is directly related to pore size. When the size of reactants are small enough in comparison with pore size, *hindered* internal diffusion is not the rate determining step. In this type of reactions, higher surface area of catalyst can give higher catalytic activity due to higher metal dispersion (Ni and Mo). However, *hindered* diffusion may take place with very heavy feeds. It has been reported that an optimum pore diameter for hydrodemetalization (HDM) of heavy oil exists around 20 nm (Smith et al., 1994). AAP catalyst having an optimum pore size obtained by manipulating A/P ratio and other preparation conditions can be effective in this type of reaction.

REFERENCES

1. *Appl. Catal. A: General*, Volume 113, No.1-9, June 1994.
2. Tanabe, K., *Appl. Catal. A: General* 113, p147-152 (1994).
3. Tischer, R.E., *Ind. Eng. Chem. Res.* 1987, 26, 422-426.
4. Marcelin, G., *J. Catal.* 83, 42-49 (1983)
5. Moffat, J.B., *Catal. Rev.-Sci. Eng.*, 18(2), 199-258 (1978).
6. Rebenstorff, B., *J. Catal.* 128, 293-302 (1991).
7. Kearby, K., Proc. of the Second International Congress on Catalysis (1961), p2567, Paris.
8. Chen et al., *Ind. Eng. Chem. Res.* 29, 1830 (1990).
9. Cheung et al., *J. Catal.* 102, 10-20 (1986).
10. Mitchell, S.F., *J. Catal.* 105, 521-524 (1987).
11. Vogel, R.F., *J. Catal.* 80, 492-493 (1983).
12. Campelo et al., *J. Catal.* 101, 484-495 (1986).
13. H.S. Joo, X. Zhan, J.A. Guin, No.41d., AICHE Spring Meeting Houston, 1995.
14. K.J. Smith and L. Lewkowicz, *Canadian J. of Chem. Eng.*, 72, August, 637-643, 1994.

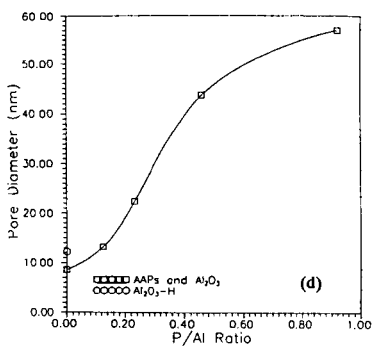
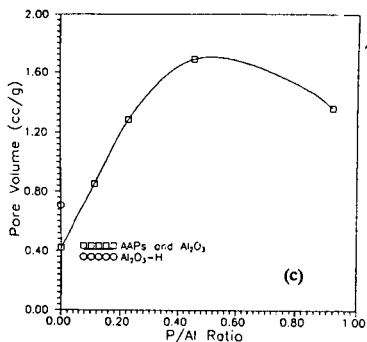
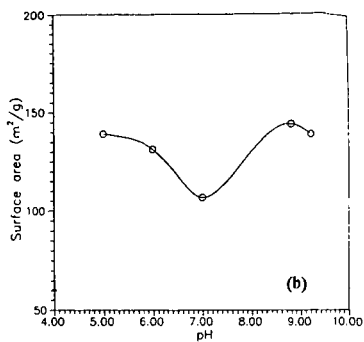
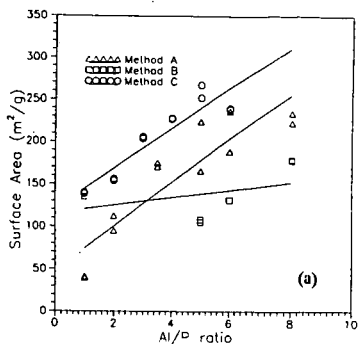


Fig 1. Effect of variables on support properties

(a) Surface area (m²/g) Vs Al/P ratio (b) Surface area (m²/g) Vs pH
(c) Pore volume (cc/g) Vs P/Al ratio (d) Pore diameter (nm) Vs P/Al ratio

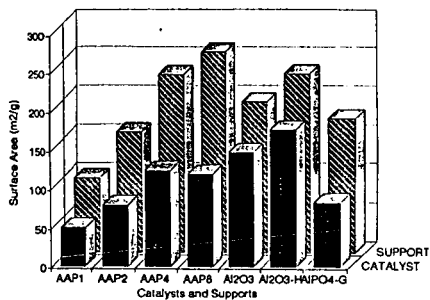


Fig 2. Surface Area of Catalysts

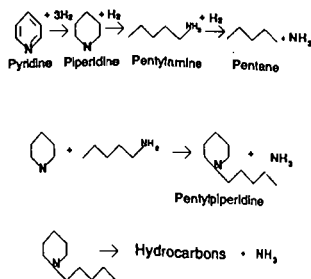


Fig 3. Reaction Pathways for Pyridine HDN

Support	Al		Mo		Ni		P		Al/P mole ratio- calc	Al/P mole ratio XPS	Mo/Ni mole ratio XPS
	ICP	calc	ICP	calc	ICP	calc	ICP	calc			
AAP1	19.0	18.2	na	13.3	3.06	3.23	19.1	19.1	1.09	1.2	21
AAP2	20.7	22.8	12.7	13.5	2.79	3.25	14.9	12.0	2.18	1.55	high
AAP4	na	41.8	12.8	13.3	2.84	3.21	na	11.1	4.3	4.25	2.07
AAP8	24.1	36.2	12.6	13.2	2.87	3.1	5.67	4.8	8.6	6.5	2.23
Al ₂ O ₃	na	43.9	15.5	13.3	na	3.22	0.006	0			na
Al ₂ O ₃ -H	na	41.5	12.7	13.3	na	3.22	0.002	0			1.77
AlPO ₄ -G	14.9	17.1	11.8	13.3	na	3.21	22.1	20.2	0.97	0.93	9.33

na: not available

Table 1. Calculated and Measured Catalyst Composition (wt%)

Support	Support Pore Volume (cc/g)	Surface Area(m ² /g)	
		Support	Catalyst
AAP1	1.37	96	50
AAP2	1.69	154	79
AAP4	1.29	229	123
AAP8	0.85	259	118
Al ₂ O ₃	0.42	194	146
Al ₂ O ₃ -H	0.71	230	176
AlPO ₄ -G	1.02	172	82

Table 2. Physical Characteristics of Supports (Method C) and Catalysts

Support	Support Weight (g)	
	Expt	Calc
AAP1	29.18	28.99
AAP2	46.78	41.82
AAP4	25.2	33.71
AAP5	62.0	79.9
AAP8	57.0	59.19
Al ₂ O ₃	12.03	12.73

Table 3. Comparison of Support Weights (g)

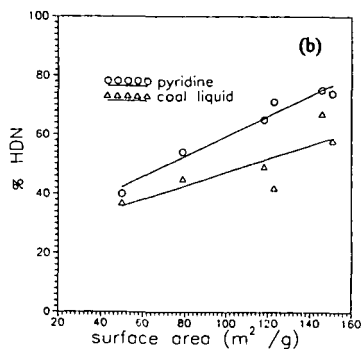
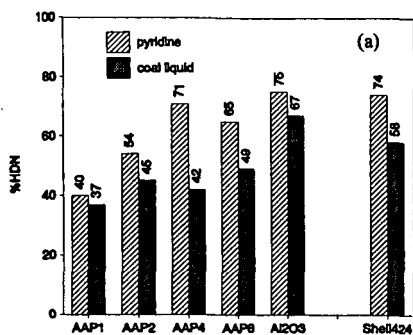


Fig 4. HDN with AAP Catalysts
(a) HDN Activity
(b) %HDN vs. Surface Area

HYDROTREATING OF COAL-DERIVED LIQUIDS*

Frances V. Stohl, Stephen E. Lott, Kathleen V. Diegert,
David C. Goodnow, John B. Oelfke

Sandia National Laboratories
Process Research Department 6212
Sandia National Laboratories
P.O. Box 5800
Albuquerque, NM 87185-0709

KEYWORDS: Refining, Coal Liquids, Hydrotreating

ABSTRACT

The objective of Sandia's refining of coal-derived liquids project is to determine the relationship between hydrotreating conditions and product characteristics. The coal-derived liquids used in this work were produced in HTI's first proof-of-concept run using Illinois #6 coal. Samples of the whole coal liquid product, distillate fractions of this liquid, and Criterion HDN-60 catalyst were obtained from Southwest Research Inc. Hydrotreating experiments were performed using a continuous operation, unattended, microflow reactor system. A factorial experimental design with three variables (temperature, (310°C to 388°C), liquid hourly space velocity (1 to 3 g/h/cm³(cat)), pressure (500 to 1000 psig H₂)) is being used in this project. Sulfur and nitrogen contents of the hydrotreated products were monitored during the hydrotreating experiments to ensure that activity was lined out at each set of reaction conditions. Results of hydrotreating the whole coal liquid showed that nitrogen values in the products ranged from 549 ppm at 320°C, 3 g/h/cm³(cat), 500 psig H₂ to <15 ppm at 400°C, 1 g/h/cm³(cat), 1000 psig H₂.

INTRODUCTION

DOE/PETC's refining of coal liquids program is aimed at determining the most cost effective combination of existing refinery processes and blending options necessary to upgrade direct and indirect coal liquids into transportation fuels that meet year 2000 specifications. A main reason for this program is that coal liquefaction processing has improved significantly since the last refining evaluation was done by Sullivan and Frumkin (1) at Chevron in the early 1980s. In addition, a recent publication by Zhou, Marano and Winschel (2) indicates that blending coal liquids with petroleum may allow refiners to produce specification products with less refining than if each fraction was processed separately. Sandia's role in this program is to develop a database relating hydrotreating parameters to feed and product quality by experimentally evaluating options for hydrotreating whole coal liquids, distillate cuts of coal liquids, petroleum, and blends of coal liquids with petroleum. Sandia's project is unique because our small-scale, continuous operation flow reactor system enables us to evaluate many hydrotreating options in a cost effective manner while keeping waste production to a minimum. Sandia's project is integrated with other program participants including participants in the Refining and End-Use of Coal Liquids Study project (Bechtel, Southwest Research Inc. (SwRI), Amoco, M. W. Kellogg), Hydrocarbon Technology Inc. (HTI, formerly HRI) the MITRE Corporation, and PETC. Sandia's data will be used by other program participants in refinery linear programming models to identify the most cost effective options for introducing and processing coal liquids in a refinery. This paper will cover results obtained from hydrotreating whole coal liquid product from HTI's first proof of concept run with Illinois #6 coal.

EXPERIMENTAL PROCEDURES

Sandia's experimental procedures included using a factorial experimental design, hydrotreating the whole coal-derived liquid, characterizing the feeds and hydrotreated products, and reporting results to other program participants.

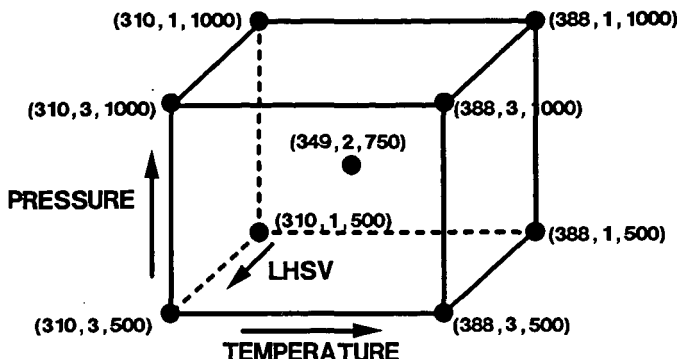
Continuous Operation Reactor System: Sandia's hydrotreating studies are being performed using a continuous operation, trickle-bed, microflow reactor system. The system has all required safety features to enable it to be operated unattended. The capabilities of this reactor system include catalyst loadings up to 25 cm³, liquid flow rates from 0.05 to 4 cm³/min, gas flows for hydrogen and nitrogen up to 2 l/min, gas flows for H₂S/H₂ up to 0.5 l/min, maximum temperature of 620°C, and a maximum pressure of 1800 psig. The reactor volume is 59 cm³. Four samples can be collected automatically during unattended operation. For liquid hourly space velocities (LHSV) of 1 and 3 g/h/cm³(cat), samples would weigh about 7 and 22 g respectively.

Factorial Experimental Design: Based on experience, three parameters were chosen for the factorial experimental design (Figure 1): temperature, pressure, and LHSV. The ranges of hydrotreating conditions used with the design were temperatures of 310 to 388°C, pressures of 500 to 1000 psig H₂, and LHSVs from 1 to 3 g/h/cm³(cat). Evaluation of the first set of hydrotreating conditions (388°C, 500 psig H₂, 1 g/h/cm³(cat)) was repeated once during the run and once at the end of the run so that effects of catalyst deactivation could be determined. Prior to the use of the testing using the factorial experimental design, two additional sets of reaction conditions were evaluated to see the effects of high pressure and temperature: 388°C, 1500 psig H₂, 1 g/h/cm³(cat) and 362°C, 1500 psig H₂, 1 g/h/cm³(cat).

Reactor Feeds and Catalyst: Sandia received (from SwRI) a sample of fresh Criterion HDN-60 catalyst and about 3.5 gallons of whole coal liquid product that was produced in HTI's first proof-of-concept run using Illinois #6 coal. The whole coal liquid product was collected when HTI's third stage reactor was not on line and while catalyst replacement was being used. Sandia's reactor was loaded with 10g of fresh catalyst that was sulfided in situ using temperature staging. The presulfiding procedure consisted of heating the catalyst to 177°C under He, starting the flow of a 10 mol% H₂S/H₂ mixture and maintaining

177°C for 1 hour. The catalyst was then heated to 288°C under flowing H₂S/H₂ and maintained at 288°C for 1 hour. Next the catalyst was heated to 404°C under flowing H₂S, the temperature was maintained at 404°C for 1 hour. H₂S flow was stopped and H₂ flow started.

Figure 1: Factorial experimental design (temperature = °C, LHSV = g/h/cm³(cat), pressure = psig)



Analytical Procedures: Small samples were collected either manually or automatically throughout the run. Nitrogen and sulfur analyses were used to determine when line out was achieved at each reaction condition. These analyses were performed using an Atek 7000 Sulfur & Nitrogen Analyzer with an automatic sampler. Standards were prepared using phenanthridine for nitrogen, thianthrene for sulfur, toluene for the solvent, and four to five dilutions. Standards were measured at least twice and a polynomial fit of the intensity versus concentration data was used for analysis of unknowns.

RESULTS AND DISCUSSION

Analyses of the whole coal liquid by HTI, SwRI, and Sandia are shown in Table 1. SwRI used their measured specific gravity. Sandia used 0.9 g/ml for the first and second samples. Data for the second sample was also calculated using SwRI's specific gravity to show the effect of different values. Results show some variability but indicate the whole coal liquid has about 600 ppm nitrogen and 400 ppm sulfur.

Table 1. Sulfur and nitrogen analyses of whole coal liquid. Specific gravities used: HTI unknown; SwRI = 0.8628 g/ml; Sandia = 0.9 g/ml (except as noted).

HTI		SwRI		Sandia	
N	S	N	S	N	S
581	345	529	405	616	428
				621	399
				649*	417*

* Same data as second analysis but calculated with specific gravity = 0.8628.

The first condition used in the run was 388°C, 1500 psig H₂, and LHSV = 1 g/h/cm³(cat). This condition was chosen to line out the freshly sulfided catalyst and to evaluate high severity conditions as a check on parameters for the factorial experimental design. Product analyses showed no detectable nitrogen or sulfur. Therefore, temperature was decreased to 362°C with pressure and LHSV remaining the same. At this condition, nitrogen and sulfur contents of the hydrotreated products were still very low (less than 5 ppm). Since hydrogen pressure is the most restrictive variable in a refinery and because low pressure gives more versatility for processing, the maximum pressure used in the factorial experimental design was decreased to 1000 psig H₂. In addition, the lower limit for temperature was also decreased. The goal was to have as broad a range of parameters as possible without decreasing sensitivity to the parameters. The order in which the various conditions were evaluated is shown in Figure 2.

Figure 2 shows the nitrogen contents that were obtained at the various processing conditions. Results were considered lined out when the temperature, pressure and LHSV were relatively constant and the nitrogen and sulfur results were relatively constant. The brackets above each grouping of nitrogen values show which results met these criteria. These results were used to determine the average nitrogen content at that condition. The average nitrogen contents and standard deviations are shown along the X-axis. In addition, the order in which conditions were evaluated is also shown. No data is shown for conditions 6 or 15 because the reactor went down before there were enough data points for analysis. Sample 17 was a large batch (about 890 ml) of hydrotreated product collected at the same condition used for sample 16 (368°C, 1000 psig H₂, 3 g/h/cm³(cat)). Sample 19 was a large batch (865 ml) collected at the same condition as sample 16 (368°C, 1000 psig H₂, and 1 g/h/cm³(cat)). These large batches were collected so that there would be enough hydrotreated product for additional analyses. Samples 17 had 151 ppm nitrogen, which is a little lower than sample 16, which had 178 ppm nitrogen. Samples 19 and 18 had similar nitrogen contents, 42 and 44 ppm respectively. Both samples 17 and 19 had <7 ppm sulfur.

Figure 2. Nitrogen (ppm) vs reaction conditions. Temperature ($^{\circ}\text{C}$), Pressure (psig), LHSV g/h/cm^3 (catalyst). Dashed line = Reactor Shutdown.

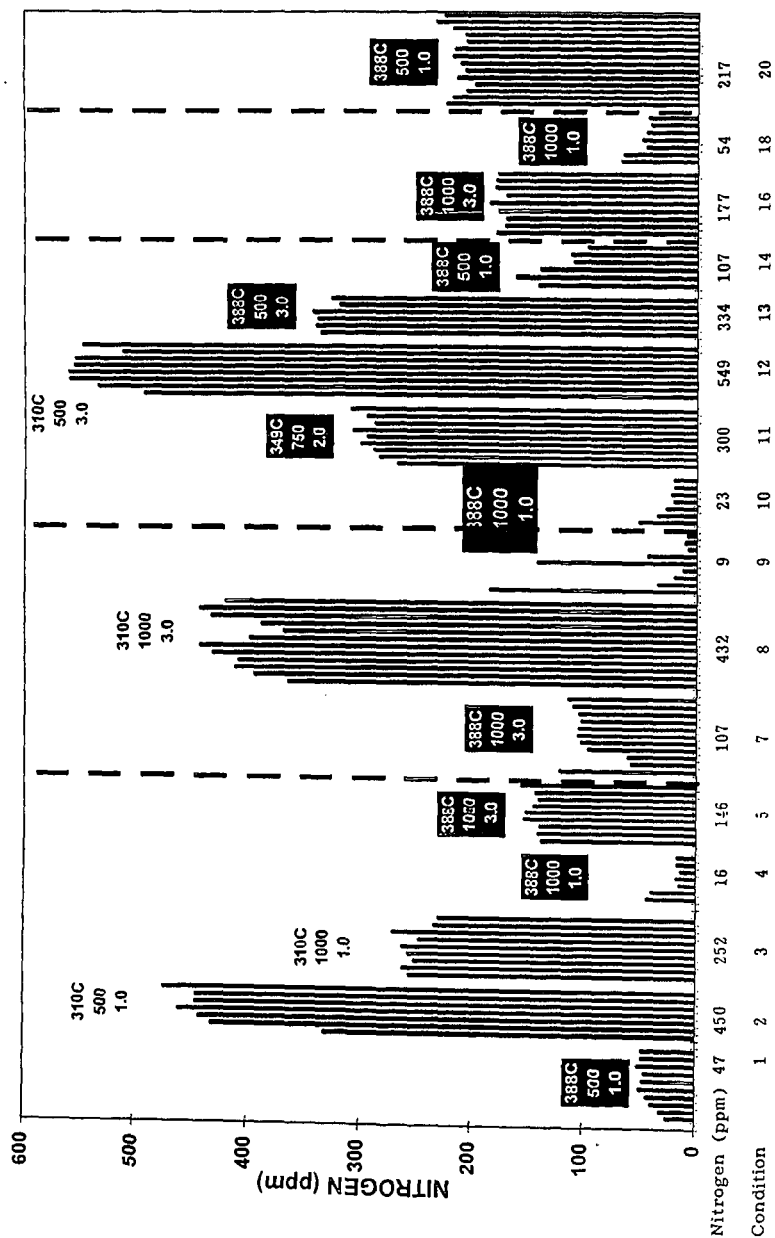


Figure 3 shows nitrogen contents as related to the conditions for the experimental design. Multiple values at a given condition show effects of catalyst deactivation. The total amount of reaction time (excluding down time) for this run was just over 32 days. Comparison of results for conditions 1 and 20 shows the effects of catalyst deactivation. Figure 4 shows the sulfur contents for the conditions of the factorial experimental design.

Figure 3: Average nitrogen values (ppm) with standard deviations.

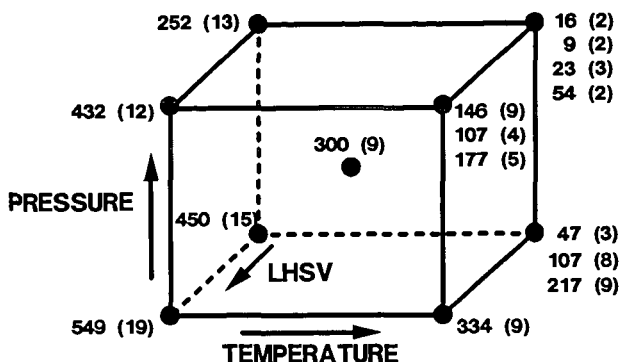
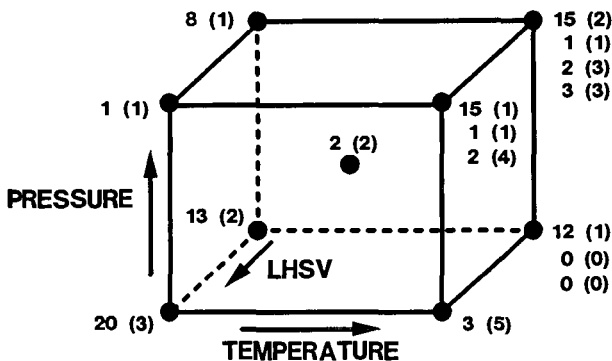


Figure 4: Average sulfur values (ppm) with standard deviations.



CONCLUSIONS AND FUTURE WORK

Results of this work show that good denitrogenation and good desulfurization can be obtained under relatively mild conditions with coal liquids from current processes. At the lowest severity condition, there is only about 10% nitrogen removal, whereas at the highest severity condition, there is about 97% nitrogen removal. Sulfur removal is good over the whole range of conditions and is greater than 95%. Ongoing and future work will involve additional characterization of reaction products by techniques such as distillation, PONA or PIONA analyses, density determinations, and proton NMR for hydrogen distributions. Results will be corrected for catalyst deactivation and analyzed statistically to determine the effects of process conditions on product quality. Future hydrotreating experiments will be performed with distillate fractions of this coal liquid and with coal-derived liquids from subbituminous coal.

* **Acknowledgment:** This work was supported by the U. S. Department of Energy at Sandia National Laboratories under contract DE-AC04-94-AL85000.

References:

- 1) Sullivan, R. F., Frumkin, H. A., ACS Div. of Fuel Chem. Preprints **31**(2), 325, 1986.
- 2) Zhou, P.-Z., Marano, J. J., Winschel, R. A., ACS Div. of Fuel Chem. Preprints **37**(4), 1847, 1992.

INVESTIGATION OF HYDROGEN TRANSFER IN COPROCESSING USING MODEL SYSTEMS

Jing Shen and Christine W. Curtis
Chemical Engineering Department
Auburn University, AL 36849

Introduction

The objective of this research was to evaluate the role of the resid in the coprocessing of coal and petroleum resid. The question being asked was whether the resid is an active solvent in coprocessing reactions and whether resid donates any hydrogen to coal during coprocessing. An effective means of determining whether resid participates in the reactions at coprocessing conditions is to use model systems and trace their reaction pathways. The research performed in this study evaluated the hydrogen donability of a naphthenic compound perhydropyrene, a compound type prevalent in resids that are hydrogen-rich. Model species were also used as acceptors that represented the aromatic aspect of coal. The model acceptors that were used were anthracene and phenanthrene.

Perhydropyrene has been used previously as a model donor representing resids by Owens and Curtis (1994) and Wang and Curtis (1994). In a N_2 atmosphere, perhydropyrene donated hydrogen to anthracene, increased the conversion of coal to THF soluble material, and reduced retrogressive reactions of petroleum resid (Owens and Curtis, 1994). Reactions of a number of hydrogen donor compounds such as cyclic olefins, hydroaromatic compounds, and naphthenes like perhydropyrene under equivalent reaction conditions showed that perhydropyrene had the least propensity for hydrogen donation among those compounds in both N_2 and H_2 atmospheres (Wang and Curtis, 1994). In the current study, the model perhydropyrene was used to represent petroleum and was reacted individually and with model acceptors primarily in a H_2 atmosphere to simulate coprocessing although some reactions were performed in N_2 to provide a reference point.

The model acceptors that were used included anthracene and phenanthrene, both of which are aromatic and represent molecules typically found in coal. Anthracene and phenanthrene have been used as coal model compounds and evaluated according to their ability to accept hydrogen from either a model donor or molecular hydrogen. Hydrogenation reactions of anthracene and phenanthrene were performed at temperatures of 325 °C (Salim and Bell, 1984) and 400 °C (Nakatsuji et al., 1978; Song et al., 1989 and 1991; Fixari and Perchec, 1989; Miyak et al., 1982) for 60 min with a hydrogen pressure of 5 to 9.8 MPa at ambient temperature. Different catalysts were used by the researchers including NiMo/Al₂O₃, NiCl₂, and sulfided NiMo/Al₂O₃ at loadings of 10 to 15 % on a reactant charge basis. The catalyst used in this study was a slurry phase catalyst molybdenum naphthenate which was added directly to the reactor contents along with excess sulfur. Mo naphthenate has been used extensively in coal and resid coprocessing reactions (Cassell and Curtis, 1988; Pellegrino and Curtis, 1989; Kim and Curtis 1990, 1990a, 1990b, 1991; Ting et al. 1992; Brannan et al. 1995).

Experimental

Materials. The chemicals used in these experiments included anthracene (ANT, 99%), phenanthrene (PHEN, 98+ %), biphenyl, dihydroanthracene (DHA), pyrene (PYR), hexahydropyrene (HHP), and perhydropyrene (PHP). These chemicals were obtained from Aldrich Chemical Company and were used as received. The slurry phase catalyst, Mo naphthenate (MoNaph, Mo 6 wt %), was obtained from Shephard Chemical Company and was used as received. Sulfur added to the MoNaph reactions was introduced as elemental sulfur and was obtained from Aldrich. The solvent used to recover the reaction products was HPLC grade THF from Fisher Scientific Company.

Reaction Procedures. The reactions were conducted for 30 min in stainless steel tubular microreactors with a volume of ~20 mL. Each reaction was duplicated. The reactors were charged with the model reactants and with H_2 at 3.4 or 8.7 MPa at ambient temperature. When reacted individually, the model donor or model acceptors were added at ~ 0.1 g each of the donor or acceptor. When the donor and acceptor were charged simultaneously at a 1:1 ratio, each reactant was charged at 0.05 g, but when the ratio charged was 5:1, then 0.1 g of donor and ~ 0.02 g of acceptor were added. The reactions were performed at two different temperatures: 400 and 440 °C. The reactors were situated horizontally in a heated sand bath and were agitated at 400 rpm during the reaction. After 30 min of reaction the reactors were quickly quenched in

room temperature water. The liquid and solid products were removed from the reactor after being washed with 5 mL of THF and recovery obtained is given in the data tables.

Catalytic reactions were performed with MoNaph being charged to the reactors at a loading level of 1000 ppm of Mo on a total reactant charge basis. Elemental sulfur was added to MoNaph reaction in a 3:1 S to Mo ratio since MoS₂ was shown to be produced under these reaction conditions (Kim et al. 1989). The catalyst generated in situ at reaction temperature formed finely divided catalyst particles.

Analysis. The products that were recovered with THF from the reaction were analyzed on a Varian Model 3300 gas chromatograph equipped with an SGE HT-5 column and flame ionization detector. The HT-5 column had a 0.1 μm coating thickness, 0.33 mm in diameter and 25 m in length. The temperature program started at 60 °C with a final temperature of 320 °C and with a program rate of 2.5 °C/min. The temperatures of the injector and detector were 320 and 325 °C, respectively. Biphenyl was used as the internal standard.

Results and Discussion

The reactions were conducted at liquefaction conditions and in the absence of a solvent. The reaction systems were composed of the model donor and model acceptors reacted individually and combinatorially under thermal and catalytic conditions. The model donor used in all of this work was perhydrophyrene and two model acceptors were anthracene and phenanthrene.

Reactions of the Model Acceptors. The two model acceptors used in this study had different propensities for accepting H₂ from the naphthenic donor and from molecular H₂. Reactions of anthracene and phenanthrene were performed individually in N₂ and H₂ at 400 and 440 °C and are described in Tables 1 and 2. Reactions of anthracene in N₂ resulted in less than 2% conversion of anthracene to DHA. The source of the hydrogen most likely came from anthracene itself when anthracene dimerized and the released H₂ which hydrogenated anthracene to form DHA.

Coprocessing of coal and petroleum resid is typically performed at temperatures ranging from 400 to 440 °C and under a H₂ pressure of 18 to 20 MPa at reaction temperature. H₂ pressure was used in these model reactions to simulate actual reaction conditions. Therefore, reactions of the two model acceptors were performed in H₂ at temperatures of 400 and 440 °C and at H₂ pressures of 18 to 20 MPa at reaction temperature. (The corresponding pressure at ambient temperature is 8.7 MPa.) The reaction products obtained from anthracene were DHA and THA; the products from phenanthrene were dihydrophenanthrene (DHPN) and tetrahydrophenanthrene (THPN). The amount of H₂ that was accepted in each reaction is given in the tables by the column headed by the "H₂ accepted" which is the moles of H₂ accepted per 100 moles of acceptor. Comparison of these quantities gives a measure of the amount of H₂ that had been accepted by the given acceptor under specific reaction conditions.

Anthracene was reactive in a thermal reaction with molecular H₂ present, yielding nearly 86% conversion to partially saturated products at both 400 and 440 °C (Table 1). The primary product formed was DHA at 440 °C which accounted for nearly 81% of the product; the minor product was THA which only accounted for about 5% of the product. At 400 °C, the same products were formed although the quantities were somewhat different; a lesser amount of DHA, 67.5%, and greater amount of THA, 18.4%, were formed.

Phenanthrene, in contrast to anthracene, had a lesser propensity for accepting molecular H₂ at 400 and 440 °C as evidenced by the conversion of phenanthrene being 4.7% and 9.1%, respectively (Table 2). The products from phenanthrene were DHPN and THPN which were produced in equivalent amounts in the 400 °C reaction and in an almost 2:1 ratio of DHPN to THPN in the 440 °C reaction. This lower proclivity for accepting molecular H₂ made phenanthrene the reactant of choice in the reactions with the naphthene perhydrophyrene. The donation of H₂ and acceptance of H₂ from perhydrophyrene would be more apparent when hydrogenation from molecular H₂ was minimized.

These model acceptors were also reacted with the slurry phase catalyst, MoNaph+S, at the same temperatures and pressures as the thermal reactions; the result of these reactions are shown in Table 1 for anthracene and Table 2 for phenanthrene. Fairly small increases in the conversion were obtained in the reactions with anthracene and phenanthrene. For example, the conversion for phenanthrene increased from 4.7 to 9.0% at 400 °C and from 9.1 to 18.7% at 440 °C with the addition of MoNaph+S. Similarly, the conversion of ANT increased at both reaction

temperatures; the increase at 400 °C was from 85.9 to 88.6% conversion, while at 440 °C the increase was from 85.8 to 96.9% conversion.

Reaction of the Model Donor. The model donor used in this study was the naphthene, perhydropyrene. Perhydropyrene was used in the current study as a test naphthene molecule to examine if hydrogen transfer occurred between the model naphthene and aromatic species in H₂ and N₂ atmospheres. Perhydropyrene was reacted alone in H₂ and N₂ atmospheres thermally and catalytically at 400 and 440 °C. Perhydropyrene was stable showing almost no reactivity at these conditions. At 400 °C in N₂, no conversion of perhydropyrene occurred thermally while with MoNaph+S 1% conversion to pyrene occurred. At 440 °C in N₂, slightly higher conversion of perhydropyrene occurred. In H₂ at both 400 and 440 °C, perhydropyrene was stable yielding at most 3% conversion. The MoNaph+S catalyst promoted conversion.

Reactions of Model Donor and Acceptors. Reactions were performed that combined the model donor perhydropyrene with the model acceptors anthracene and phenanthrene. The reactions of perhydropyrene with anthracene at 1:1 and 5:1 ratio under thermal and catalytic conditions are given in Table 1. The moles of H₂ accepted per 100 moles of anthracene or phenanthrene as well as the conversion of anthracene or phenanthrene served as a measure of the activity of the system.

The thermal reaction of perhydropyrene with anthracene at 400 °C and a 1:1 ratio gave a H₂ accepted of 103.9 while the addition of MoNaph+S increased the amount of H₂ accepted to 120.9. Increasing the ratio of perhydropyrene to ANT to 5:1 did not change the amount of H₂ accepted; the H₂ accepted in the thermal reaction was 104.0 while the addition of MoNaph+S increased H₂ accepted to 121.2. The primary product in all of these reactions was DHA but the addition of MoNaph+S increased the amount of THA produced. These conversion and H₂ accepted values were nearly equivalent to those obtained without perhydropyrene at 400 °C.

Phenanthrene accepted much less donor and molecular H₂ than anthracene at equivalent reaction conditions. For example, when perhydropyrene and phenanthrene were reacted together thermally at a 1:1 and 5:1 ratio at 400 °C, the amount of conversion was 2.9 and 4.6% and the H₂ accepted was 1.2 and 1.8 moles, respectively, as shown in Table 2. The respective values for anthracene ranged from 80 to 95% conversion and 104 to 120 moles of H₂ accepted. The primary product from phenanthrene was usually DHPN with THPN being the secondary product.

Although the reactivity of phenanthrene was much lower than that of anthracene, reactions of phenanthrene with perhydropyrene responded to the presence of perhydropyrene, to change in reaction temperature, and to the type of catalyst used. The reactivity of the perhydropyrene and phenanthrene systems is given on Table 2. Comparison of the conversion and H₂ acceptance values at two different temperatures but at otherwise equivalent conditions showed that reactions at 440 °C promoted a higher level of conversion and H₂ accepted than those at 400 °C.

Despite this lower reactivity at 400 °C, notable differences in the reactivity were observed in the thermal reactions of phenanthrene and perhydropyrene compared to catalytic reactions containing MoNaph+S. Reactions at 5:1 ratio of donor to acceptor in N₂ at 400 °C showed that a small amount of perhydropyrene donated to phenanthrene yielding THPN as product. By comparison, the reaction of phenanthrene in N₂ at 400 °C did not convert any phenanthrene and, hence, did not yield any hydrogenated product. Thermal reactions at 400 °C in H₂ with a 1:1 ratio of perhydropyrene to phenanthrene converted 2.9% phenanthrene while the 5:1 ratio converted 4.6%. The amount of H₂ accepted gave a corresponding amount of 4.4 and 7.4 moles of H₂ accepted per 100 moles of phenanthrene. The increased amount of naphthene present in the reaction at 400 °C increased the amount H₂ accepted by phenanthrene.

In the catalytic reactions using MoNaph+S, an excess amount of perhydropyrene at 400 °C also increased the amount of phenanthrene conversion and the amount of H₂ accepted by phenanthrene. MoNaph+S promoted hydrogenation of phenanthrene to DHPN and THPN. Comparing the combined donor and acceptor reactions to the acceptor reaction alone showed that perhydropyrene being present in the thermal reaction did not increase either phenanthrene conversion or the amount H₂ accepted. However, the addition of MoNaph+S with perhydropyrene present increased both conversion and H₂ accepted at 400 °C when compared to the catalytic reaction with phenanthrene alone.

Reactions of perhydropyrene and phenanthrene at 440 °C (Table 2) showed an overall higher reactivity than at 400 °C at corresponding reaction conditions. In N₂ with MoNaph+S, the amount of phenanthrene conversion to DHPN and THPN was 2.2%. The source of H₂ in the reaction was H₂ donated from perhydropyrene. In the reaction perhydropyrene produced pyrene

and several partially saturated pyrene compounds, thereby donating 8.9 moles of H₂ per 100 moles of perhydropyrene. In H₂ at 440 °C, the ratio of perhydropyrene to phenanthrene affected the amount of phenanthrene conversion as well as the amount of H₂ accepted. Both the thermal and catalytic reactions at the higher ratio gave larger amounts of these quantities than at the lower 1:1 ratio. The thermal reaction at 400 °C resulted in 9.3 moles of H₂ accepted per 100 moles of phenanthrene while at 440 °C 16.8 moles of H₂ were accepted. The MoNaph+S catalyst promoted hydrogenation of phenanthrene at both ratios yielding at the 1:1 ratio 15.8 moles of H₂ accepted by phenanthrene while at the 5:1 ratio 26.2 moles of H₂ were accepted.

Perhydropyrene reacted in these reactions with phenanthrene to form decahydropyrene (DCP), hexahydropyrene (HHA), tetrahydropyrene (THP), dihydropyrene (DHP), and pyrene (PYR). More different products were made from perhydropyrene when phenanthrene was present than when perhydropyrene was reacted alone, where only pyrene was produced. A calculation of the amount of H₂ donated from these products is given in the tables and is designated as the moles of H₂ donated per 100 moles of donor or H₂ donated. In the H₂ atmosphere at 400 °C, the amount of H₂ donated from perhydropyrene remained nearly the same except for reactions containing MoNaph+S which increased H₂ donated to 6.3 from 1 to 2 in the thermal reactions. At 440 °C, higher amounts of H₂ were donated from perhydropyrene to the acceptors.

Summary

Determining whether hydrogen donation occurred from perhydropyrene as a representative of a resid naphthene at typical coprocessing conditions was a goal of this investigation. The reactions of the model naphthene perhydropyrene and the model acceptors, anthracene and phenanthrene, clearly showed that different chemical species present in the coal have different propensities for accepting H₂ regardless of its source, molecular or donor. The model naphthene under some circumstances, like in the anthracene reaction, was a positive influence on the reaction, causing the overall amount of H₂ accepted to increase. Catalytic reactions with MoNaph+S also promoted the apparent transfer of H₂ from perhydropyrene to anthracene. Phenanthrene was not as active an acceptor as anthracene. Thermal hydrogenation of anthracene and phenanthrene with molecular hydrogen at 400 °C yielded 85% and 4.7% conversion, respectively. Excess donor model was required to observe a positive effect of the naphthene on the H₂ accepted by the model acceptor.

References

- Cassel, F.N.; Curtis, C.W. *Energy Fuels*, 2, 1, 1988.
Faxari, B. and Perchec, P.L., *Fuel*, 1989, Vol. 68, February, 218-221.
Kamiya, Y., Futamura, S., Mizuki, T., Kajioka, M. and Koshi, K. *Fuel Processing Technology*, 14, 79-90, 1986.
Kim, H.; Curtis, C.W. *Energy Fuels*, 4, 214, 1990a.
Kim, H.; Curtis, C.W. *Energy Fuels*, 4, 206, 1990b.
Kim, H.; Curtis, C.W. *Fuel Sci. Tech Intl.* 9, 229, 1991.
Kim, H.; Curtis, C.W.; Cronauer, D.C.; Sajkowski, D.J. *ACS Fuel Dive Prep.* 34, 4, 1446, 1989.
Miyak, M., Sakashita, H., Norura, M. and Kikkawa, S. *Fuel*, 1982, Vol 61, February, 124-128.
Nakatsuji, Y., Kubo, T., Nomura, M., and Kikkawa, S., *Bulletin of the Chemical Society of Japan*, Vol. 51 (2), 618-624, 1978.
Owens, R.; Curtis, C.W. *Energy Fuels*, 8, 823, 1994.
Pellegrino, J.L.; Curtis, C.W. *Energy Fuels*, 3, 160, 1989.
Salim, S.S. and Bell, A.T. *Fuel*, 1984, Vol 63, April, 469-476.
Song, C.; Nomura, M. and Ono, T. *Preprint - Am. Chem. Soc. Div. Fuel Chem.*, 36, 2, 586-596, 1991.
Song, C.; Ono, T.; and Nomura, M. *Bulletin Chemical Society Japan* 62, 630-632, 1989.
Ting, P.S.; Curtis, C.W.; Cronauer, D.C. *Energy Fuels*, 6, 511, 1992.
Wang S.L.; Curtis, C.W. *Energy Fuels*, 8, 446, 1994.

Acknowledgements

The support of the United States Department of Energy under contract No. DE-AC22-91PC91055 for this work is greatly appreciated.

Table 1. Anthracene at Reactions 400 °C and 440 °C:
Reacted Alone and With Perhydrophyrene

Reaction Condition	Reactants	Atmosphere	T (°C)	Product Distribution (mol%)			Recovery (%)	ANT Conversion, %	H ₂ Accepted H ₂ Donated
				ANT	DHA	THA			
Thermal	ANT	N ₂	400	98.3±0.17	1.70±0.17	0±0	92.5	1.7	
Thermal	ANT	H ₂	400	14.1±0.8	67.5±0.4	18.4±1.2	90.1	104.3	
MoNaph + S	ANT	H ₂	400	11.4±0.6	70.0±9.3	26.6±8.6	94.4	123.2	
Thermal	ANT	H ₂	440	14.2±0.40	80.9±0.42	4.9±0.82	84.4	90.75	
MoNaph + S ^b	ANT	H ₂	440	3.8±0.06	55.8±0.62	40.4±2.1	80.1	136.58	
Thermal	PHP: ANT 1:1	N ₂	400	94.0±1.8	6.0±1.8	0.0±0.0	82.5	6.5±0.7	
MoNaph + S	PHP: ANT 1:1	N ₂	400	95.4±1.1	3.2±1.2	1.4±0.1	85.2	6.0±0.9	
Thermal	PHP: ANT 1:1	N ₂	440	94.4±0.4	4.6±0.1	1.0±0.3	83.8	6.5±0.7	
MoNaph + S	PHP: ANT 1:1	N ₂	440	96.3±0.1	3.7±0.1	0.0±0.0	87.1	4.3±0.3	
Thermal	PHP: ANT 1:1	H ₂	400	5.9±0.5	84.3±4.5	9.8±4.0	98.2	103.9	
MoNaph + S	PHP: ANT 1:1	H ₂	400	3.4±0.8	72.5±5.2	24.1±6.0	96.8	120.9	
Thermal	PHP: ANT 5:1	H ₂	400	6.3±2.1	83.4±0.6	10.3±2.7	92.2	104.0	
MoNaph + S	PHP: ANT 5:1	H ₂	400	5.3±2.0	68.2±6.5	26.6±4.5	82.9	121.2	

^a Reaction time = 30 min; 8.7 MPa H₂ or N₂ at room temperature.

^b MoNaph + S = Mo naphthalene with added elemental S.

^c ANT = anthracene; DHA = dihydroanthracene; THA = tetrahydroanthracene; H₂ = (1 x DHA mol% + 2 x THA mol%) x 100

^d Reactant loading: Approximately 0.05 g of each ANT and PHP in PHP:ANT = 1:1 thermal and catalytic reactions; Approximately 0.02 g of ANT and 0.1 g of PHP in PHP:ANT = 5:1 thermal and catalytic reactions. Mo naphthalene loading is approximately 0.0017 g = total reactant charge (0.1 g)/60, computed according to 1000 ppm MoS₂ and 6 wt% Mo in Mo naphthalene.

Table 2. Phenanthrene Reactions at 400 and 440 °C: Reacted Alone and With Perhydropryrene

Reaction Condition	Reactant	Atmosphere	T(°C)	Product Distribution (mol %)			Recovery (%)	PHEN Conversion (%)	H ₂ Accepted ^b	H ₂ Donated ^c
				PHEN ^a	DHPN	THPN				
Thermal	PHEN	N ₂	400	100±0.0	0.0	0.0	86.6	0.0	NA ^a	
MoNaph	PHEN	N ₂	400	100±0.0	0.0	0.0	85.5	0.0	NA	
Thermal	PHEN	H ₂	400	95.3±0.7	2.6±0.5	2.1±0.2	83.5	6.8±0.9	NA	
MoNaph+S ^b	PHEN	H ₂	400	91.0±0.0	6.0±0.0	3.0±0.1	87.3	12.0±0.1	NA	
Thermal	PHEN	N ₂	440	100±0.0	0.0	0.0	87.6	0.0	NA	
MoNaph+S	PHEN	N ₂	440	100±0.0	0.0	0.0	85.3	0.0	NA	
Thermal	PHEN	H ₂	440	90.9±1.2	5.9±0.7	3.2±0.5	91.8	12.3±1.7	NA	
MoNaph+S	PHEN	H ₂	440	81.3±3.8	12.8±2.4	5.9±1.4	82.0	24.6±5.2	NA	
Thermal	PHP: PHEN 1:1	H ₂	400	97.1±0.2	1.5±0.0	1.4±0.2	88.5	4.4±0.3	1.2±0.1	
MoNaph+S	PHP: PHEN 1:1	H ₂	400	86.9±2.0	9.0±1.5	4.1±0.5	90.0	17.2±2.5	6.2±0.0	
Thermal	PHP: PHEN 5:1	N ₂	400	98.4±0.2	0.0±0.0	1.6±0.2	92.3	3.2±0.4	3.8±0.0	
MoNaph+S	PHP: PHEN 5:1	N ₂	400	99.0±0.0	0.0±0.0	1.0±0.0	86.6	2.0±0.0	3.9±0.0	
Thermal	PHP: PHEN 5:1	H ₂	400	95.4±0.2	1.8±0.4	2.8±0.8	86.9	7.4±2.1	1.8±0.0	
MoNaph+S ^b	PHP: PHEN 5:1	H ₂	400	82.8±0.1	10.7±0.6	6.5±0.1	92.9	23.7±0.1	6.3±0.0	
Thermal	PHP: PHEN 1:1	H ₂	440	93.2±1.4	4.4±0.8	2.4±0.6	92.5	9.3±2.1	0.9±0.1	
MoNaph+S	PHP: PHEN 1:1	H ₂	440	87.2±1.3	9.9±0.7	2.9±0.6	94.8	15.8±1.9	7.5±0.1	
Thermal	PHP: PHEN 5:1	H ₂	440	87.1±1.1	9.0±0.0	3.9±1.2	86.0	16.8±2.3	8.6±0.1	
MoNaph+S ^b	PHP: PHEN 5:1	H ₂	440	79.5±3.6	14.9±2.1	5.6±1.5	80.0	26.2±5.1	10.7±0.6	
MoNaph+S	PHP: PHEN 5:1	N ₂	440	97.8±0.2	0.5±0.1	1.7±0.7	86.4	3.9±1.0	8.9±0.1	

^a Reaction Conditions: 30 min; 8.7 MPa H₂ or N₂ at ambient temperature; catalyst loading = 1000 ppm on total reactant charge basis; the total amount of reactant charged is approximately 0.1 g.

^b Moles of H₂ Accepted per 100 moles of PHEN; H₂ accepted = (2 x THPN mol% + 1 x DHPN mol%) x 100.

^c Moles of H₂ Donated per 100 moles of PHP; H₂ Donated = (3 x DCP mol% + 5 x HHP mol% + 6 x THP mol% + 7 x DHP mol% + 8 x PYR mol%) x 100.

EFFECT OF TETRALIN ON THE DEGRADATION OF POLYMER IN SOLUTION

Girdhar Madras, J.M. Smith, and Benjamin J. McCoy
Department of Chemical Engineering and Materials Science
University of California at Davis
Davis, CA 95616

Keywords : polymer, hydrogen donor, thermal degradation, continuous kinetics, solvent effect

ABSTRACT

The effect of a hydrogen-donor solvent tetralin on thermal degradation of poly(styrene-allyl alcohol) in liquid solution was investigated in a steady-state tubular flow reactor at 1000 psig at various tetralin concentrations, polymer concentrations, and temperatures. The experimental data were interpreted with continuous-mixture kinetics, and rate coefficients determined for the specific and random degradation processes.

Introduction

Thermolytic degradation of polymers is similar in some respects to other important thermal decomposition processes like petroleum cracking and coal thermolysis. All these processes involve complex mixtures, both as reactants and as products. Polymer degradation usually occurs in a polydisperse mixture, and observing the temporal change of the molecular weight distribution (MWD) caused by degradation affords a means to test kinetic models. Due to the advance of technology in analytical instrumentation, dynamic MWD data can be obtained by gel permeation chromatography (GPC). A continuous-mixture approach is applicable for these cases, since it is based on mass balance equations that govern the temporal change of a distribution function (Aris and Gavalas, 1966; Cheng and Redner, 1990). This approach has been used for a theoretical discussion of polymer degradation (Ziff and McGrady, 1985, 1986), for the kinetics of reactions in reversible oligomerization (McCoy, 1993), as a model for coal liquefaction (Prasad et al., 1986), and for coal thermolysis (Wang et al., 1994). Recently, Wang et al. (1995) measured the rates of specific and random scission for the degradation of poly(styrene-allyl alcohol) in t-butanol using the continuous-mixture approach.

There is little information of the effect of hydrogen-donor solvents on the degradation of polymer in solution. Sato et al. (1990) investigated the solvent effect on the thermal degradation of polystyrene at 300-450 C and 2 MPa. They observed that solvents with higher hydrogen donating capability produced less conversion of polystyrene. These experiments indicated that the degradation behavior, and the conversion of the polymer are affected by the solvents. Murakata et al. (1993) investigated the effect of hydrogen-donor solvents on the degradation of poly- α -methylstyrene and observed that there was no effect of the solvent on the degradation mechanism and the conversion of the polymer. The effect of hydrogen-donor solvents has been extensively investigated for coal liquefaction. The literature on this subject, including generally accepted pathways for hydrogen transfer from a donor solvent, was summarized by Chawla et al. (1989).

The objective of this study was to investigate the effect of the hydrogen-donor solvent, temperature, and residence time on the degradation of the poly(styrene-allyl alcohol). The experimental data was obtained by passing the polymer solution through a steady-state flow reactor, and analyzing the products using HPLC-GPC. Continuous kinetics ideas were employed to interpret the experimental data and fundamental data.

Experiments

The polymer used in this study was poly(styrene-allyl alcohol) (Polysciences, Inc.) of number-average molecular weight 1100. The polymer was pretreated to remove components in the lower molecular weight range, which would interfere with the analysis of the product peaks. A detailed explanation of the pre-treatment is given by Wang et al. (1995). The polymer was pretreated by dissolving 50 grams of the polymer in 500 ml of t-butanol. The polymer solution was continuously stirred using a magnetic stirrer and heated to 40 C on a heating plate. A volume of 1350 ml of distilled water was added drop by drop to this polymer solution. The high molecular-weight polymer precipitated and settled at the bottom. The dried precipitate was blanketed under nitrogen in a closed bottle to avoid oxidation. The MW of the treated polymer was 1640.

The experiments were carried out at high pressure, 1000 psig (6.8 MPa), to prevent the vaporization of the solvent, 1-butanol, at high temperatures and to ensure that the reaction of the polymer occurs in the liquid phase. The polymer solution was prepared by dissolving the polymer in 1-butanol at a known concentration in the range of 1-4 g/L. The polymer solution flows through the reactor, a water cooled heat exchanger, two pressure reduction valves placed in series, and finally exits through a rotameter. The flow rate (and hence the residence time of the

fluid in the reactor) is controlled by the rotameter. Degradation experiments were carried out at three different polymer concentrations, four different temperatures, and four different tetralin concentrations to study the effects of these parameters on the rate of polymer degradation. At each condition, the experiment was conducted at four different residence times (i.e., four different flow rates). Since the flow rates were measured at ambient conditions, the residence times for each temperature were corrected with the density calculated from Lee-Kesler equation (Lee and Kesler, 1975). After reaching steady state, two 20 ml samples were collected at each residence time for the HPLC-GPC analysis. Experiments of 1-butanol and 10 to 50% tetralin, in the absence of polymer, were conducted at 150 to 200 C to investigate interactions between the solvents. The GPC analysis of samples from these experiments indicated no products.

The significant difference of these experiments compared to pyrolysis experiments in gas or vacuum is that all the reactions take place in the liquid phase, and thus the residence time for both the reactants and products is the same. Further, the mild temperatures limit the amount of random chain scission and eliminate repolymerization.

Before analyzing the effluent sample by GPC, one needs to concentrate the sample and dissolve the reactant and products in tetrahydrofuran. Hence, 20 ml of the effluent sample is concentrated to 4 ml by evaporating the 1-butanol under vacuum at 353 C. The molecular weight distribution of the effluent samples was determined by gel permeation chromatography using PLgel columns (Polymer Labs) in a high performance liquid chromatograph (Hewlett Packard 1050). For this purpose, two columns packed with crosslinked poly(styrene-divinyl benzene) of 100 and 500 Å pore size, respectively, were used in series after a guard column. Tetrahydrofuran (THF, HPLC grade, Fisher Chemicals) was continuously pumped through the columns at a constant flow rate of 1 ml/min. A sample of 100 microliters was injected at the start of each run and the ultraviolet detector was used to measure the absorbance of the compounds in the effluent samples. The wavelength of 254 nm was chosen since this wavelength provided the maximum absorbance of the reactant and products. The molecular weight corresponding to the retention time in the columns was calibrated with polystyrene samples obtained from Polymer Lab. The calibration procedure is described in detail by Wang et al. (1995).

Mechanism

The mechanism of degradation of polymer is similar to that of Wang et al. (1995). The thermal degradation of the polymer is of two kinds: random scission at any position along the polymer chain, and specific scission leading to specific products. Both types of scissions occur in the degradation of poly(styrene-allyl alcohol), as seen from Figure 1, which is the MWD plotted as concentration distribution (g/L MW) versus Log_{10} MW. The figure shows three distinct peaks in the molecular weight range 100-500 indicating specific scission products. The higher MW range peak shifts to a lower MW range relative to the feed polymer indicating random scission.

Though only three distinct peaks are observed in the figure, we expect the formation of styrene, since it was observed by Wang et al. (1995). The styrene peak should appear at a MW of 104. However, since tetralin and styrene have comparable MW of 132 and 104, respectively, the peaks of these two compounds are superimposed. Lacking a method to distinguish styrene from tetralin, we therefore removed this peak from the chromatogram and its subsequent analysis. The remaining peaks in the effluent chromatograms were approximately of MW 162, 222, and 486, respectively, and are proposed to be the oligomer of an allyl alcohol and a styrene molecule (SA), and an oligomer of two allyl alcohols and one styrene molecule (ASA), and a trimer of SA ((SA)₃). Any allyl alcohol (A) produced during the degradation would evaporate during the sample preparation.

Theoretical Model

The theoretical model is similar to the one proposed by Wang et al. (1995). The MWD of the feed polymer is described by a gamma distribution. The parameters of the gamma distribution are obtained by calculating the zeroth, first, and the second moments of the experimental peak. This gamma distribution is used as the initial MWD in the kinetics model.

A continuous mixture can be defined as a mixture of a very large number of different-size polymer molecules, whose distribution can be expressed by a continuous index such as the molecular weight. We consider that all the degradation products are dissolved in solution, that no repolymerization reactions occur, and that the flow reactor can be treated as a steady-state plug-flow reactor. Model equations based on continuous kinetics for polymer degradation were developed by Wang et al. (1995).

Results and Discussion

For the degradation of poly(styrene-allyl alcohol) in a solvent of pure t-butanol, both random and specific scission of the polymer occurred at 130-200 C and 1000 psig (Wang et al., 1995). However, in the present case of 1-butanol solvent, no degradation of the polymer was observed at these conditions in the absence of tetralin. This suggests that t-butanol was involved in the reaction, possibly as a hydrogen donor. Sato et al. (1990), on the other hand, reported decreased degradation of several polymers in presence of hydrogen donors. These results indicate the significance of the solvent effect in thermolytic degradation reactions, and the importance of continued investigation along these lines.

An experimental MWD and model simulation are presented in Figure 2. As explained earlier, a peak of styrene has been removed since the peak of tetralin is superimposed on it. The three distinguishable peaks, SA, ASA, (SA)₃, are the products of specific chain scission. The same products (S, SA, ASA, (SA)₃) are produced with either t-butanol or 1-butanol plus tetralin.

The parameters in the model are the parameters of the gamma MWD describing the feed polymer and the rate coefficients for specific and random degradation. The rate coefficients for specific degradation are determined from the equation (Wang et al., 1995):

$$q = k_j p t \quad (1)$$

where p is the feed concentration (mol/L), t is the residence time, and q is the concentration of the specific product (mol/L). These concentrations are the zeroth moments of their MWDs divided by MW. Since the zeroth moment is the area under the curve, the area of each specific product peak was determined by numerical integration using the trapezoidal rule. The slope of the line gives the rate coefficient for specific degradation, k_j. The rate coefficients for random degradation are obtained by fitting the experimental MWD data of random degradation with gamma distribution parameters, using the relationship derived by Wang et al. (1995).

The dependence of the specific and random degradation rate coefficients on the temperature, concentration of the polymer, and concentration of the hydrogen-donor solvent (tetralin) are shown in the Tables 1-3. The rate constants are independent of polymer concentration, confirming that the reactions for both specific and random degradation are first-order. This is consistent with the assumption of Wang et al. (1995).

The activation energies for random and specific degradation are extracted from the temperature dependence of the rate coefficients (Figure 3) and are given in Table 4. The dependence of the rate constants on the concentration of tetralin were modeled by the following equation:

$$k = k_1 C_t / (1 + \kappa C_t) \quad (2)$$

where k is the rate constant and C_t is the vol% of tetralin. Parameters k₁ and κ are obtained by plotting the inverse of the rate versus the inverse of tetralin concentration and are given in Table 5. Tetralin is essential for the degradation of the polymer at this temperature and pressure. A tetralin concentration of 25% produces rate coefficients nearly an order of magnitude higher than the rate coefficients obtained by Wang et al. (1995), who degraded the same polymer using t-butanol without tetralin. However, the activation energies for the specific and random degradation of the polymer by 1-butanol and 25% tetralin are comparable to the activation energies for the specific and random degradation of the polymer by t-butanol.

Acknowledgement

The financial support of Pittsburgh Energy Technology Center Grant No. DOE DE-FG22-94PC94204, and of the University of California UERG is gratefully acknowledged.

References

- Aris, R.; Gavalas, G.R. *Phil. Trans. R. Soc., London* 1966, A260, 351.
- Cheng, Z.; Redner, S. I. *Phys. A: Math. Gen.* 1990, 23, 1233.
- Chawla, B.; Keogh, R.; Davis, B.H. *Energy and Fuels* 1989, 3, 236-242.
- Lee, B.F.; Kesler, M.G. *AIChE J.* 1975, 21, 510-527.
- McCoy, B. J. *AIChE J.* 1993, 39, 1827.
- Sato, S.; Murakata, T.; Baba, S.; Saito, Y.; Watanabe, S. *J. Appl. Poly. Sci.* 1990, 40, 2065.
- Murakata, T.; Saito, Y.; Yosikawa, T.; Suzuki, T.; Sato, S. *Polymer* 1993, 34, 1436.
- Wang, M.; Zhang, C.J.; Smith, J.M.; McCoy, B.J. *AIChE J.* 1994, 40, 131.
- Wang, M.; Smith, J.M.; McCoy, B.J. *AIChE J.* 1995, 41 (6), In press.
- Ziff, R. M.; McGrady, E.D. *J. Phys. A: Math. Gen.* 1985, 18, 3027.
- Ziff, R. M.; McGrady, E.D. *Macromolecules* 1986, 19, 2513.

Table 1. Rate coefficients (1/sec) for specific and random degradation of the polymer at various temperatures and at a constant polymer concentration of 2 g/L and a tetralin concentration of 25%.

Temperature	k for SA ($\times 10^3$)	k for ASA ($\times 10^3$)	k for (SA) ₃ ($\times 10^3$)	k _r ($\times 10^4$)
130	1.68	2.52	3.36	0.22
150	1.89	3.09	4.05	2.1
170	3.9	4.68	5.85	18
200	5.95	6.43	7.14	130

Table 2. Rate coefficients (1/sec) for specific and random degradation of the polymer at various polymer concentrations and at a constant temperature of 150 C and a tetralin concentration of 25%.

Polymer Conc. (g/L)	k for SA ($\times 10^3$)	k for ASA ($\times 10^3$)	k for (SA) ₃ ($\times 10^3$)	k _r ($\times 10^4$)
1	1.73	3	4.2	2.3
2	1.89	3.09	4.05	2.1
4	1.75	2.89	3.9	2.3

Table 3. Rate coefficients (1/sec) for specific and random degradation of the polymer at various tetralin concentrations and at a constant temperature of 150 C and a constant polymer concentration of 2 g/L.

Tetralin Conc.	k for SA ($\times 10^3$)	k for ASA ($\times 10^3$)	k for (SA) ₃ ($\times 10^3$)	k _r ($\times 10^4$)
5 %	0.58	1.6	1.78	0.4
10 %	0.8	2.3	2.5	1.0
25 %	1.89	3.09	4.05	2.1
50 %	2.09	3.57	4.9	2.5

Table 4. Activation energies for specific and random degradation

Specific Product	Activation energies (kcal/mol)
SA	7.5
ASA	5.2
(SA) ₃	4.4
Random degradation	33.1

Table 5. Parameters for the dependence of rate coefficients of polymer degradation on tetralin concentration.

Specific Product	k _t ($\times 10^4$) (1/sec/vol%)	κ (1/vol%)
SA	1.33	0.043
ASA	5.59	0.138
(SA) ₃	4.96	0.085
Random degradation	1.07	0.012

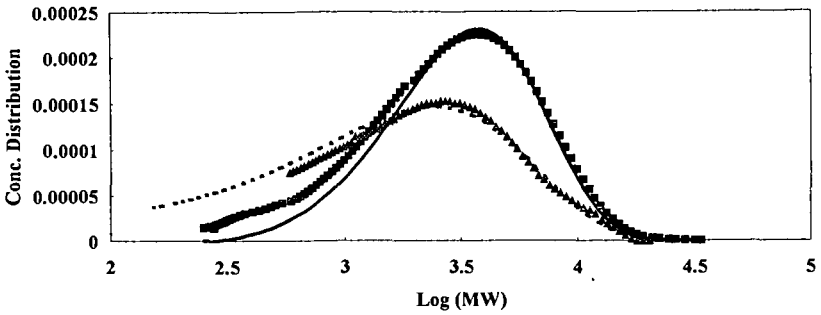


Figure 1. The MWD before and after thermal degradation (■ : chromatograph before degradation, — : Gamma Distribution fit ; ▲ : chromatograph after degradation at 150 C, 25% tetralin, and residence time of 42.51 min. ; : Gamma Distribution fit).

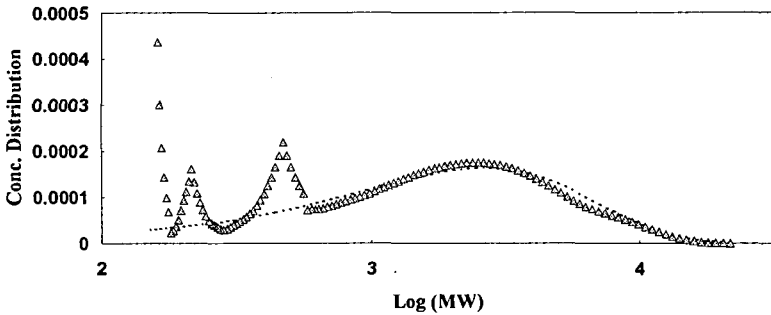


Figure 2. Comparison of experimental results of MWD with model simulation at 150 C, 25% tetralin and at a residence time of 42.51 minutes (Δ : experimental data; : Gamma Distribution fit) .

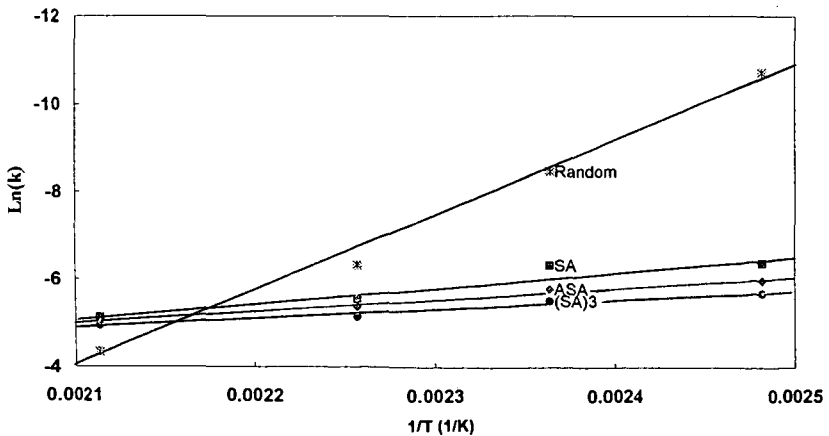


Figure 3. Arrhenius plot of the degradation coefficients versus temperature to determine the activation energies of the specific scission and random degradation.

WASTE OILS UTILIZED AS COAL LIQUEFACTION SOLVENTS ON DIFFERENT RANKS OF COAL

Edward C. Orr, Yanlong Shi, Jing Liang, Weibing Ding,
Larry L. Anderson, and Edward M. Eyring

Department of Chemistry and Department of Chemical and Fuels Engineering, University of Utah, Salt Lake City, UT 84112

Keywords: tires, plastic, coal, liquefaction

Introduction

Solvent plays an important role in direct coal liquefaction. The solvent acts as a medium to transport hydrogen, as a heat transfer medium, as an additional reactant along with the coal, as a coal dissolution medium, and as the medium to transport coal liquefaction products away from the coal matrix. Recent investigations of coprocessing coal with solid waste materials (plastics, rubbers, cellulose) to raise the hydrogen content of the coal products with a concomitant decreased need for the addition of hydrogen gas have involved reacting solid waste plastics and solid waste rubbers directly with coal with little preparation other than grinding or shredding the waste material.¹⁻⁴ (An indirect benefit to coprocessing waste with coal is that less waste must be disposed of in landfills or by incineration.) Dry mixing of coal and waste materials may be the most cost effective method for coprocessing waste with coal because there is less preparation of the waste material. However, the metals, anti oxidants, carbon black, and plasticizers present in the waste materials make some preparation of the reactants necessary. A possible pretreatment of the waste materials would be a vacuum pyrolysis of the waste materials that would produce cleaner oils. To examine this issue, we have recently carried out coal liquefaction experiments in which coals of different ranks were reacted with oils obtained by the vacuum pyrolysis of waste materials, specifically plastics and rubber tires. We have also used waste automotive oils to determine whether the automotive oil is effective, and whether trace heavy metals found in the waste automotive oil can be scavenged by the coal.

Experimental

Coal samples were obtained from the Penn State Coal Sample Bank. Six different coals were used as received: Pocahontas DECS-19 (low volatile bituminous coal), Blind Canyon DECS-2 (high volatile A bituminous coal), Illinois-6 DECS-2 (high volatile B bituminous coal), Wyodak-Anderson DECS-26 (subbituminous B coal), Smith-Roland DECS-8 (subbituminous C coal), and Buelah DECS-11 (lignite A). Waste automotive crankcase oil was obtained from Book Cliff Energy, Green River, Utah. Oils from the vacuum pyrolysis of waste rubber tires and from waste plastics were obtained from Conrad Industries, Chehalis, Washington. All oils were stored under ambient conditions. All coals were ground to a -60 mesh. Samples were mixed in a 1 part coal to 1 part solvent ratio determined by weight. Each sample was placed in a 27 cm³ stainless steel tubing reactor with no catalyst. Solvents were stirred prior to being placed in the tubing reactor. Tubing reactors were purged with N₂ and pressurized with H₂ to 1000 psig (cold). Tubing reactors were placed in a sandbath heated to 430 °C and shaken vertically for one hour. The tubing reactor was then removed from the sandbath and allowed to cool for 5 minutes. The tubing reactor was then quenched using cold water. The tubing reactors were left sealed over night. Products were then removed and placed in soxhlet extractor thimbles and extracted with THF. Soxhlet extraction was continued until the extraction solvent appeared clear. The THF was then removed with a rotary evaporator leaving behind the soluble product. The THF soluble product was then dried under vacuum for two hours and weighed. The sum of the THF soluble mass and THF insoluble mass was subtracted from the original coal (daf) weight to account for gas mass. The dried THF soluble portion was then extracted with cyclohexane. The remaining insoluble portion is referred to as asphaltenes and the soluble portion as oil. An effort was made to keep samples under a nitrogen atmosphere in order to minimize air oxidation. GC-MS analyses were completed on a Hewlett Packard 5890 series II Gas Chromatograph coupled to a Hewlett Packard 5971 Mass Spectrometer. A J & W 100 meter long DB-1 column was used for the GC-MS analyses. Trace metals were analyzed by ICP (Data Chem. Laboratories, Salt Lake City, UT).

Results

The waste automotive crankcase oil from Book Cliff Energy is a mixture of many automotive oils received onsite at their refinery. The vacuum pyrolyzed plastic oil and the vacuum pyrolyzed tire oil from Conrad Industries were prepared from large samples of various plastics and tires. Thus the oils used in this study are representative of those that would be supplied to a coal liquefaction refinery instead of working with oils vacuum pyrolyzed from only one plastic sample or rubber sample.

ICP analysis of the waste automotive oil in Table 1 indicates the presence of many heavy metals. Of specific interest are the high zinc and phosphorous concentrations. This suggests the presence of a lubricant additive identified by Tarrer and coworkers.³

ICP analysis of the pyrolyzed plastic oil (Table 1) shows the presence of calcium, iron, and zinc. The calcium arises from the addition of calcium oxide during the pyrolysis of plastic to react with any hydrochloric acid formed from the breakdown of polyvinyl chloride polymers. GC-MS analysis indicates the presence of alkanes as large as C₃₆, as well as the presence of cyclic rings, and aromatic species such as benzene and naphthalene.

The ICP results for pyrolyzed tire oil (Table 1) show that zinc is the only heavy metal present. The vacuum pyrolyzed tire oil is low in zinc relative to a standard rubber tire. Past analysis indicates that a rubber tire contains on average 1.5 % by weight zinc oxide. Vacuum pyrolysis of the waste rubber tire circumvents the problems associated with removal of carbon black from the products.⁶ Vacuum pyrolysis of waste rubber tires also permits formation of polyaromatics.⁷ These polyaromatics are known to be useful in coal reactions because of their hydrogen shuttling and hydrogen donating characteristics.^{8,9} Analysis by GC-MS indicated the presence of benzene, methylated forms of benzene, naphthalene, methylated forms of naphthalene, anthracene, methylated forms of anthracene, phenanthrene, methylated forms of phenanthrene, pyrene, methylated forms of pyrene, and naphthacene.

Table 2 contains the product distributions for conversion results obtained from reacting coals of differing ranks with waste oils at 430 °C for 1 hour. It is important to note that the total conversions reported are for the combination of both the coal and the solvent. This appears to be a better way of comparing all three solvent systems because the solvents react differently.

The coals are listed according to rank with Pocahontas being the highest ranking coal used and Buelah being the coal of lowest rank. The Pocahontas coal was not effectively converted using any of the three solvents. This is not surprising since higher rank coals are harder to depolymerize than are lower rank coals. The waste automotive oil solvent and the plastic solvent show similar overall coal rank trends with respect to total conversion. The asphaltene yield was slightly higher for runs using automotive oil solvent than runs using plastic solvent. This is surprising because the plastic oil with its abundance of large alkanes would be expected to increase asphaltene percentages even if larger alkanes did not react with other coal fragments. This indicates some cracking of the plastic solvent during coprocessing. Examination of the reactors indicated some char formation for the plastic solvent whereas no charring was observed for the automotive oil solvent. The lack of charring for the waste automotive oil solvent is what one might predict for an automotive lubricant but increased asphaltenes were not foreseen. It is interesting that trace metals identified in the automotive solvent have no detectable effect in promoting conversion of the coal.

The total conversion yields for the tire solvent indicated no rank correlation in contrast to the automotive oil solvent and the plastic oil solvent. The tire solvent did produce more measurable asphaltenes than did the other two solvents. Visual examination of the tubing reactors revealed enhanced charring with the tire oil present. This is not surprising with char precursors pyrene and anthracene in the initial reaction mixture. These molecules are also known to be beneficial to coal reactions because of their capacity to act as hydrogen donors and shuttlers.⁹ The tire oil did not seem to be beneficial for the lower rank coals. The lower rank coals may be too reactive and combine with the solvent to form asphaltenes. The greatest total conversion for all three solvents came from tire oil solvent coprocessed with Illinois #6 coal. The Illinois #6 has a greater proportion of sulfur and iron oxide. These are known to form a sulfided iron which then can act as a catalyst in coal liquefaction. Previous experiments have shown that the pyrolyzed tire oil is beneficial

only in the presence of hydrogenation catalysts. It may be that the hydrogenation catalyst partially hydrogenated the pyrolyzed tire oil which could then act as a hydrogen donor.¹⁰

The ICP analyses for metals in the product oils for the three solvents coprocessed with the six different coals are shown in Table 3. The ICP analysis shown in Table 1 for the automotive oil solvent before it was coprocessed with any coal is also presented at the far right hand column of the Table in order to compare the amount of metal present in products derived from three coal/solvent distributions. Table 3 shows a decrease in almost every metal detected in the original solvent. A substantial decrease is observed for zinc, phosphorous, magnesium, iron, copper, barium, and aluminum. Tarrer and coworkers have indicated that the high content of zinc and phosphorous is due to the presence of zinc dialkyldithiophosphate.⁵ It appears that the oils produced from the Illinois #6 coal and the Wyodak-Smith coal are the cleanest overall with respect to trace heavy metals.

The results from oils and asphaltenes indicate that no one coal is significantly more efficient than the others at capturing heavy metals. Therefore, it is difficult to say if there is any rank effect correlation for capturing heavy metals. The data appear to indicate that all coals have to some degree an ability to capture heavy metals. It is possible that the heavy metals in the automotive oil solvent were not plentiful enough to saturate the scavenging abilities of the coals in order to determine which coal would be the best scavenger. This scavenging or capture may involve the chemistry of the coal or a physical effect of incorporating the heavy metals into the carbon matrix of the coal. In past studies¹¹ using Electron Probe Microanalysis (EPMA), heavy metals were observed to reside in coal particles after coprocessing coal with waste rubber tires. In the EPMA micrographs the area of high heavy metal localization also coincided with areas of high sulfur concentration indicating that metals were present as sulfides. Therefore, sulfur in the coal may be beneficial for scavenging. This was also reported by Tarrer and associates for work completed on scavenging of zinc dialkyldithiophosphate. They found the scavenged zinc from the automotive oil residing in coal in the form of zinc sulfide. The ultimate analysis shows that the Illinois #6 has an abundant amount of sulfur. Illinois #6, along with the Wyodak-Anderson appeared to localize trace metals only slightly better than the other metals according to Table 3.

Conclusion

The Pocahontas coal is not a good coal to be coprocessed with any waste oil solvent to produce liquid transportation fuels. The other coals showed similar conversions with waste oil solvents except the Illinois #6. Results for different coal ranks liquefied in different solvents indicate that the Illinois #6 gives the best total conversion when reacted with oil derived from the vacuum pyrolysis of waste rubber tires. As for the heavy metals in waste automotive oils, coprocessing the automotive oils with the coal diminishes the amount of metal found in the products. Scavenging of metal did not appear to be coal rank dependent under the experimental conditions used in this study.

Acknowledgments

We gratefully acknowledge Lester J. Thompson and Eugene Dalton with Book Cliff Energy, Green River, UT for their generous donation of waste automotive crankcase oil. We gratefully acknowledge Phillip Bridges of Conrad Industries, Chehalis, WA for his generous donations of pyrolyzed plastic oil, pyrolyzed tire oil, and for insights regarding our results. Financial support by the U.S. Department of Energy, Fossil Energy Division, through the Consortium for Fossil Fuel Liquefaction Sciences, Contract No. UKRF-4-21033-86-24, is gratefully acknowledged.

References

1. Farcasiu, M.; Smith, C, 1992, Prepr. Pap. Am. Chem. Soc., Div. Fuel Chem., 37 (1), 472.
2. Anderson, L. L.; Tuntawiroon, W., 1993, Prepr. Pap. Am. Chem. Soc., Div. Fuel Chem., 38 (4), 810.
3. Huffman, G. P.; Feng, Z.; Mahajan, V.; Sivakumar, P.; Jung, H.; Tierney, J. W.; Irving, W., 1995, Prepr. Pap. Am. Chem. Soc., Div. Fuel Chem., 40 (1), 34.
4. Parker, R. J.; Carson, D. W., 1995, Prepr. Pap. Am. Chem. Soc., Div. Fuel Chem., 40 (1), 51.

5. Tarrer, A., Technical Report on DOE Contract No. DE-FC22-93PC93053, Period: May1, 1994-October 31, 1994.
6. Orr, E. C.; Ding, W. B.; Bolat, E.; Rumpel, S.; Eyring, E. M.; Anderson, L. L., 1995, Prepr. Pap. Am. Chem. Soc., Div. Fuel Chem., 40 (1), 44.
7. Williams, P. T.; Taylor, D. T., 1993, Fuel, 72, 1475.
8. Grint, A.; Jackson, W. R.; Larkins, F. P.; Louey, M. B.; Marshall, M.; Trehwella, M. J.; Watkins, I. K., 1994, Fuel, 73 (3), 381.
9. McMillen, D. F.; Malhotra, R.; Tse, D. S.; Nigenda, S. E., 1988, Prepr. Pap. Am. Chem. Soc., Div. Fuel Chem., 33 (1), 58.
10. Badger, M. W.; Harrison, G.; Ross, A. B., 1994, Prepr. Pap. Am. Chem. Soc., Div. of Petroleum Chem., 39 (3), 438.
11. Orr, E. C.; Tuntawiroon, W.; Anderson, L. L.; Eyring, E. M., 1994, Prepr. Pap. Am. Chem. Soc., Div. Fuel Chem., 39 (4), 106

Table 1 ICP Analysis of Automotive Solvent, Pyrolyzed Plastic Solvent, and Pyrolyzed Tire Solvent

Metal	Automobile Oil Solvent µg/g	Pyrolyzed Plastic Oil Solvent µg/g	Pyrolyzed Tire Oil Solvent µg/g
Aluminum	81		
Antimony			
Arsenic			
Barium	9.3		
Beryllium			
Cadmium	1.4		
Calcium	920	520	
Chromium	1.7		
Cobalt			
Copper	54		
Iron	310	50	
Lead	27		
Lithium			
Magnesium	240		
Manganese	7		
Molybdenum			
Nickel	13		
Phosphorous	870		
Potassium	510		
Selenium	1.3		
Sodium	34		
Silver			
Strontium	2.7		
Thallium			
Vanadium			
Zinc	850	20	40

Blank areas indicate that none of the element was detected

Table 2 Comparison of Total Conversions (Percent by Weight) for Coals of Different Coal Rank Coprocessed With Waste Oils at 430 °C for 1 Hour

	Automotive Oil Solvent	Pyrolyzed Plastic Oil Solvent	Pyrolyzed Tire Oil Solvent
Pocahontas			
Gas + Oil	54.5	54.3	47.0
Asphaltenes	2.4	0.5	9.0
Total Conversion	56.9	54.8	56.0
Blind Canyon			
Gas + Oil	65.4	66.5	60.4
Asphaltenes	3.7	3.6	10.3
Total Conversion	69.1	70.1	70.7
Illinois #6			
Gas + Oil	66.1	64.4	65.8
Asphaltenes	10.4	7.2	17.8
Total Conversion	76.5	71.6	83.6
Wyodak			
Gas + Oil	70.2	71.5	63.1
Asphaltenes	3.7	1.4	5.1
Total Conversion	74.0	72.9	68.3
Smith - Roland			
Gas + Oil	74.8	73.4	67.9
Asphaltenes	3.2	1.4	4.8
Total Conversion	77.9	74.7	72.7
Beulah			
Gas + Oil	74.2	77.2	66.1
Asphaltenes	2.0	0.4	3.8
Total Conversion	76.2	77.6	69.9

Table 3 Comparison of ICP Analyses of Oils Produced From Coal and Waste Automotive Oil Solvent Coprocessed at 430 °C for 1 Hour

Oil	Pocah.	Blind Canyon	Illinois #6	Wyod.-And.	Smith-Roland	Beulah	Auto Oil
Aluminum							81
Antimony							
Arsenic					31		
Barium							9.3
Beryllium							
Cadmium		1.2		0.9			1.4
Calcium	260	56	42	51	64	200	920
Chromium	1.1	1.4			3.4	2.5	1.7
Cobalt						10	
Copper		2.2			7.4		54
Iron	23	62	19	77	42	45	310
Lead							27
Lithium					3.4		
magnesium							240
Manganese							7
Molybdenum							
Nickel	11	10		6.2	16		13
Phosphorous							870
Potassium	690	400	470		770	340	510
Selenium	31						1.3
Silver					1.3	1.3	34
Sodium		400					
Strontium							2.7
Thallium							
Vanadium							
Zinc	15	14	8	11	15	11	850

PLASTICS PYROLYSIS AND COAL COPROCESSING WITH WASTE PLASTICS

M. S. Mulgaonkar, C. H. Kuo, A. R. Tarrer
Chemical Engg Dept
Auburn University
Auburn, AI-36849

Keywords: pyrolysis, plastics, coal liquefaction

ABSTRACT

Pyrolysis of waste plastics is one of the routes to waste minimization that has been gaining in interest in recent times. A compact unit is designed that can pyrolyze a mixture of waste plastics and used oil. The product of the process is a liquid oil that has considerably reduced viscosity and which can be either used as fuel directly or as a feedstock for refineries. Pyrolysis was carried out for the waste oil alone and for its mixture with plastics of one type (HDPE). Different temperatures of reaction and the product viscosities related to the temperatures of operation. Residence times were as low as 2-8s. The reactor was divided into two parts, the first part at the inlet was deliberately kept at a lower temperature to first bring up the Reynolds numbers (>15,000) to high values before introduction to the high temperature second section.

The liquid product of pyrolysis can be used for the co-liquefaction of coal. Several coal liquefaction studies were carried out to determine the effect of the use of the waste plastic-used oil product of pyrolysis as solvent. The results indicate considerable enhancements of the conversions and selectivities of coal for such prepyrolyzed liquid.

Introduction

Plastics form a major portion of all municipal wastes. It was reported (1) that some 30 billion pounds of plastic waste are generated in the US per year. Also the demand for plastics would reach 76 billion pounds by the turn of the century. Currently, only about 1% of the plastics waste is recycled. The recycling of the plastic can be costly and difficult because of the constraints on water contamination and inadequate separation prior to recycling.

Therefore several new processes are currently under development for the treatment of waste plastics. Two processes have shown promise, pyrolysis and hydrolysis, in recovering the basic chemicals and fuels from the waste plastics. In pyrolysis, the plastics are heated in the absence of oxygen in a closed environment, with the resulting products of pyrolysis available for use as a chemical feedstock, or fuel. Hydrolysis decomposes plastic wastes through a series of chemical reactions. These new processes will reduce the cost of monomers and the consumption of petroleum. In one instance, scientists have demonstrated a new process for sequential pyrolysis for waste carpet recycling. In this case caprolactum, the starting material for nylon production, was separated with yields of around 85% without separating the nylon from the backing material of the carpet. It is reported that a commercial plant could produce high grade caprolactum at a cost of \$0.15-0.50/lb compared to the commercial cost of \$1.00/lb. Thus costs could be reduced by as much as 50%. Thus pyrolysis appears to be an attractive alternative to plastics landfilling or incineration.

Many companies are already showing considerable interest in pyrolysis of waste plastics. The Japanese company, Fuji has started a commercial scale plastics to gasoline plant at Aioi, that is capable of processing 11 million lb/yr of waste plastic. In this process the plastic is first preheated to 250°C. The preheated plastic is then fed by an extruder to a furnace, and then to a cracking unit that uses aluminosilicate catalyst. The process yields 40% gasoline, 20% kerosene, 20% gas-oil mixture, 15% gas and 5% residuals. Retrieved energy is used to power the plant. Annually the plant would produce one million gallons of gasoline (2)

Chuo Kagaku Co., the largest PS food tray manufacturer in Japan has a 2-million-lb/yr plant for reclaiming PS waste that is based on the Fuji design. The plant is anticipated to yield on startup, a fuel mixture of 90% aromatics, 6% paraffins and 4% olefins. When blended with gasoline, it produces a high octane fuel.

Amoco Chemical, Chicago, is also concentrating on the development of a pyrolysis unit. Scientists at Amoco have concluded that use of a small scale pyrolysis unit to crack mixed plastics into liquid chemical prior to feeding them to a refinery unit appears to be the optimal route. Liquids being easily transportable, this would avoid the costly step of shipping bulk plastic scrap to far-flung U.S. oil refineries (2). Also in the U.S., the American Plastics Council, Washington, DC, is sponsoring two pyrolysis projects by recycler Conrad Industries, Chehalis,

WA. One of the plants is already on stream. A drum of the pyrolyzed plastic oil (PPO) of this company was obtained and was used in the coal coprocessing experiments as indicated in Table 2. Typical composition of household wastes is shown in Table 1.

System Design

The new compact pyrolysis unit has been designed to pyrolyze a mixture of waste molten plastic and waste oil. This unit operates at very low residence times (2-8 seconds) and can operate continuously. The reactor consists of a 125 ft long 2.5 mm diameter S.S. tube that is divided between two different heating or reaction sections. The temperatures of operation can be finely controlled so as to give liquid products of various viscosities. The temperatures of operation range from 350-600°C, the pressures are low (ambient) to medium (100-300 psi). The reaction is carried out in two stages. In the first reactor tube section the temperatures are kept low (300-400°C) to allow the viscosity to reduce sufficiently to give high Reynolds numbers in the subsequent high temperature (450-600°C) section. As a result, Reynolds numbers higher than 15,000 are obtained in this section. A detailed schematic of the process is included. Two sand baths are used for the liquefaction process and the temperatures of the two are set independently to give the required temperature steps in the operation.

The feed liquid which consists of waste oil and waste plastics (which is kept molten) at 250-300°C are subjected to nitrogen pressure to push the liquid through the cracking sections. The tube outlet pressure can be controlled by means of a back pressure regulator that can be adjusted to any required set point. Thus complete variation in operational pressure is possible. The reaction can be carried out at different pressures and the effect of operation pressure can be investigated almost independently of the residence times.

Several runs of pyrolysis with waste oil were carried out in the laboratory. Two typical temperature profiles are included and the corresponding viscosities of the product are also included in the figures.

Decomposition temperature ranges of the plastics are usually obtained from thermogravimetric methods (4). These methods have been used by other investigators for obtaining the reaction rate parameters, i.e., the pre-exponential factors and the activation energies. These constants are used in the present experiments to decide on the residence time variations that would be necessary to treat plastics of different compositions and also to predict the properties of the products where possible, using model based simulation.

Several pyrolysis runs were carried out with plastics dispersed in the oil and the pyrolysis products obtained. The temperature profile for one run with 2.5% HDPE pellets are included.

Results and Discussion

Once the pyrolysis products of the plastics are obtained, they can be used to carry out the liquefaction of the coal in a batch or continuous manner. Here, the results of tubing bomb experiments based on batch coal coprocessing show that the reaction of liquefaction occurs to increased levels of conversion with the addition of (waste) plastics, such as polystyrene or HDPE. Increases in conversions of around 20% are obtained with the unpyrolyzed waste plastics, and selectivities are enhanced by 15-25% on an average. The conversions further increase if the plastics and the waste oil solvents are in addition prepyrolyzed (two stage liquefaction). This is the basis for the design of the pyrolysis section followed by the coal coprocessing.

The main design parameters are the residence time, feed temperature, the two stage temperatures, and the flow inducing pressure difference. These parameters have to be very carefully chosen in order to get the right conversions and yields of liquids. The effects of temperature and residence times are relatively well understood for the pyrolysis reactions. Too high a residence time results in excessive gas formation and when the temperatures are high to high coke formation. The temperatures that are attainable in any pyrolysis unit thus determines the yields of gas, liquids and coke. Usually the threshold temperatures for pyrolysis depends on the type of material to be processed. In general the lower limit of temperature for most pyrolysis is 350-400°C. The actual temperatures chosen are usually much above this. Since thermal cracking reactions proceed with significant activation energies, temperature has an important effect on rate. Activation energies are in the range of 55-65 kcal/mol (6).

Temperature is also known to have a very important effect on the selectivities of paraffin pyrolysis. In the present case the aim is to maximize the formation of liquids and therefore the temperatures are lower, of the order of about 500-700°C. The exact temperature chosen would then depend on the nature of the material to be processed. If the feed material is simply waste lubricating oil, then the temperatures of 450-500°C are found to be sufficient for the maximization of liquids. If in addition we are adding waste plastics then the temperature of cracking must usually be raised in order to bring about sufficient chain scission and obtain products in the liquid form suitable for use as liquid fuels or as feed to a refinery unit.

Conclusions

Exploratory batch reaction studies have shown two-stage coal coprocessing with waste plastics and oils to yield high conversions of coal (>80%) with a high selectivity for oil (>60%). The waste oils and plastics were first thermally cracked in a first stage to yield a liquid solvent for the second-stage coal coprocessing. A pilot scale unit was constructed for performing the first stage cracking studies. Waste oil mixed with HDPE were successfully cracked using this unit, there being no significant amounts of coke or solids produced.

The use of low residence time cracking would offer a number of advantages. Two of these are (1) transportation costs could be significantly reduced by removing contaminants close to the generation site and by reducing the bulk density of the plastics; and (2) handling of waste plastics/oils during coal coprocessing would be simplified due to the low viscosities and fluidic properties of the cracked products.

References

- 1) J. E. Lynx, American Dyestuff Reporter, Dec. 1993, pp. 9
- 2) R. D. Leaversuch, Modern Plastics, June 1992, pp. 49-50
- 3) C.-H. Wu et al., Waste Management, Vol. 13, pp 221-235
- 4) P. Mapleston, Modern Plastics, Nov. 1993, pp 58-61
- 5) Textbook Of Polymer Science, F. W. Billmeyer, Third Edition, Wiley-Interscience
- 6) Pyrolysis: Theory and Industrial Practice, L. F. Albright et al., Academic Press, 1983

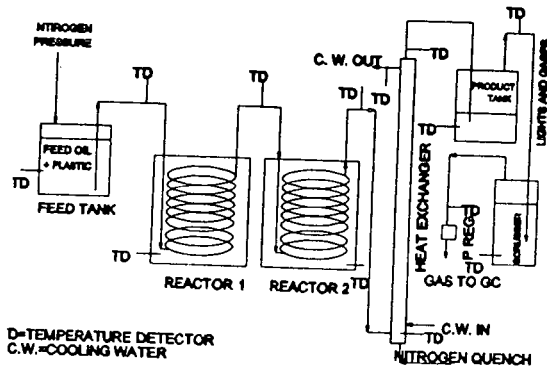


Figure 1: Pyrolysis Unit

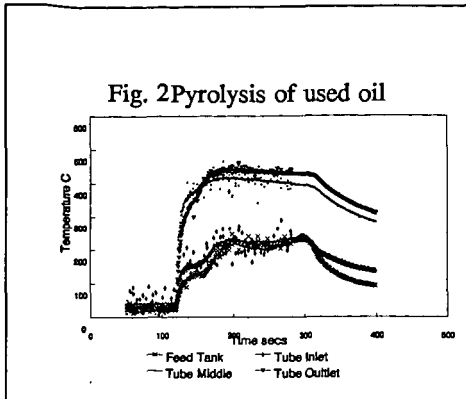


Figure 2. Pyrolysis of waste oil of viscosity 275 cSt to give product of viscosity 50 cSt

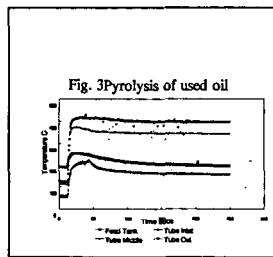


Figure 4. Pyrolysis of waste oil of viscosity 275 cSt to give product of viscosity 130 cSt

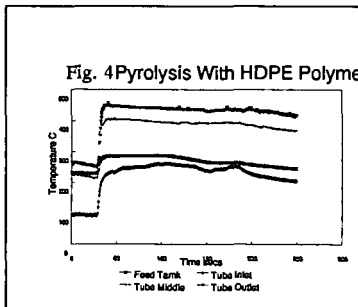


Figure 3. Temperature Profile for Pyrolysis of HDPE (2.5%) Dispersed in Used Oil, Product Viscosity was 80cSt @30°C

Table 1. Composition Of Mixed Plastics Wastes:

Composition (% wt)	
Polyethylene	60
Polypropylene	05
Polyvinylchloride	10
Polystyrene	15
Polyethyleneterephthalate	05
Polyamide	05

Table 2. Response of coal conversion /selectivity to addition of pyrolyzed plastic , PS & waste oil

Solvent	Hexane Convrsn(%)	Total Convrsn(%)	Selectivity(%)
Waste Oil	43	73	59
Waste Oil/polystyrene(PS) 1:1	39	60	65
Prehydrocracked waste oil	60	86	70
Waste oil/PS prehydrocracked 1: 1	63	97	65
Pyrolyzed plastic oil(PPO)	64	91	70
Prehydrocracked PS/waste oil 1:1	73	100	73
PPO/waste oil 1:1	56	81	69

Reaction conditions: 2.5g DECS-6 coal, 10g solvent, 0.25g Fe₂O₃, 425°C, 1250 psig H₂, 1 hour

COPROCESSING OF WASTE PLASTICS WITH COAL AND PETROLEUM RESID

Hyun Ku Joo and Christine W. Curtis
Chemical Engineering Department
Auburn University, AL 36849

Introduction

Waste plastics have become an increasing problem in the United States since land filling is no longer considered a feasible disposal method. Since plastics are petroleum-derived materials, coprocessing them with coal to produce transportation fuels is a feasible alternative. In this study, catalytic coprocessing reactions were performed using Blind Canyon bituminous coal, Manji and Maya petroleum resids, and plastics. Model polymers including polystyrene, low density polyethylene and poly(ethylene terephthalate) were selected because they represent a substantial portion of the waste plastics generated in the United States. The objective of this research is to determine the effect of using resid as a solvent in the coprocessing of coal and waste polymers on the conversion and product distribution obtained. This study was conducted by first evaluating the reactivity and conversion of the individual systems at coprocessing reaction conditions. Then systems containing binary combinations of either coal, resid, or waste plastic were performed. The last set of reactions performed were ternary systems of coal, resid and waste plastic. All reactions that contained combinations of reactants were reacted catalytically using presulfided NiMo/Al₂O₃. The effect of each component on the coprocessing reaction was evaluated.

Experimental

Materials. The model plastic compounds, low density polyethylene (LDPE), polystyrene (PS), and poly(ethylene terephthalate) (PET), used in this study were obtained from Aldrich Chemical Co. and were used as received. The coal used was Blind Canyon bituminous coal (DECS-17) obtained from the Penn State Coal Sample Bank. The proximate analysis of the coal is 45% fixed carbon, 45% volatile matter, 6.3% ash and 3.7% moisture. The ultimate analysis of the coal is 82.1% C, 6.2% H, 0.4% S, 1.4% N, and 0.12% Cl. The resids used were Manji and Maya obtained from Amoco. The analyses of the resids were 85.1% C, 10.8% H, 0.7% N, 2.6% S, 231 ppm V, 220 ppm Ni and 23 ppm Fe for Manji and 84.1% C, 9.9% H, 0.7% N, 5.1% S, 550 ppm V, 100 ppm Ni and 17 ppm Fe for Maya. The solvents used for extraction analyses were HPLC grade hexane, toluene, and tetrahydrofuran (THF) from Fisher Scientific.

Reactions and Procedures. Reactions were performed using a single component, two components, and three components to evaluate the reactivity and mutual effects among the reactants. All reactions were performed in 20 cm³ stainless steel tubular microreactors at 430 °C for 60 min with 8.3 MPa of H₂ introduced at ambient temperature. The microreactors were agitated horizontally at 450 rpm in a fluidized sand bath and were immediately quenched in water after reaction. The reactants were charged at 1.0 g for coal and polymer and 1.5 g for resid, giving resid to polymer and resid to coal ratios of 3:2 in binary system and coal to resid to polymer ratios of 2:3:2 in ternary systems. The coal was stored in a vacuum desiccator before being used. Reactions were performed thermally and catalytically using 1 wt % of powdered, presulfided NiMo/Al₂O₃ on a total charge basis. Reactions with LDPE and coal or resid were performed at higher catalysts loadings of 3 and 10 wt %. The NiMo/Al₂O₃ catalyst was composed of 2.72 wt % Ni and 13.16 wt % Mo. The procedure for presulfiding NiMo/Al₂O₃ began with predrying NiMo/Al₂O₃ with N₂ for one hr at 300 °C. Then, 10 vol % H₂S/H₂ gas mixture was flowed over the catalyst at 225 °C for one hr, at 315 °C for one hr, and 370 °C for two hr. The final step was flowing N₂ at 370 °C over NiMo/Al₂O₃ for one hr.

The reaction products were determined by using solvent fractionation and by weighing the gaseous products. The liquid products were fractionated using a series of solvents into hexane soluble materials (HX); toluene soluble, hexane insoluble material (TOL); and THF soluble, toluene insoluble material (THF), and THF insoluble material or IOM which is defined as insoluble organic matter that is ash-free. Solvent fractionation was also performed on the unreacted materials to determine their solubility. Low recoveries for PS and PET resulted from volatile material being produced during reaction and being lost during the rotary evaporation of hexane. When rotary evaporation was performed at 25 °C with minimal vacuum, the PS reactions products were so volatile that 75% loss occurred while PET lost 67%. The definition for conversion used in this study is the conversion of the reactant to THF soluble material. For coal, the definition for conversion is

$$\% \text{ conversion} = \left[1 - \frac{\text{g IOM}}{\text{g maf coal}} \right] \times 100$$

Plastics and resids have the same definition; however, the plastics are solids at room temperature and have varying but limited solubility in THF, while resids are a semi-solid at room temperature and are totally soluble in THF.

Results and Discussion

The product distributions for the unreacted plastics were determined at ambient temperature to establish a baseline for comparison with their reactivity at coprocessing conditions (Table 1). Previous research performed by Luo and Curtis (1995) has shown that under typical thermal coprocessing conditions only limited conversion of the waste plastics occur. Therefore, the plastics used in this study were reacted under catalytic conditions only using presulfided NiMo/Al₂O₃. This catalyst was chosen because it has been used almost as a standard in coal liquefaction reactions and because it was used as the catalyst in the waste plastics and waste tire coprocessing pilot scale run performed by HRI and sponsored by the Department of Energy (Pradhan et al., 1994).

Table 1. Product Distributions from Unreacted and Thermally Reacted Material

Reactants ^a	Product Distribution (%)					Conversion (%)	Recovery (%)
	Gas ^b	HX	TOL	THF	IOM		
Unreacted							
PS	0.0	0.0	21.0	14.1	64.9	35.1	112
LDPE	0.0	0.0	1.4	3.1	95.5	4.5	104
PET	0.0	0.0	0.7	0.7	98.6	1.4	104
Manji	0.0	87.1±0.4	12.9±0.4	0.0	0.0	100	103
Maya	0.0	63.0±0.8	37.0±0.8	0.0	0.0	100	101
Thermal Reactions							
Coal	19.1±0.6	15.9±1.1	3.5±0.5	6.2±4.2	55.5±5.4	44.6±5.4	98
Manji	11.6±1.1	71.0±2.1	9.9±0.6	4.9±1.5	2.7±0.1	97.4±0.2	85
Coal/Manji	9.8±0.2	56.9±0.8	8.6±0.4	11.8±1.8	13.1±3.3	87.0±3.3	84

^a Coal = Blind Canyon DECS-17, Manji and Maya resid. PS = Polystyrene; LDPE = low density polyethylene; PET = poly(ethylene terephthalate). ^b Gas = gaseous product; HX = hexane solubles; TOL = toluene solubles; THF = THF solubles; IOM = insoluble organic matter.

Single Component Reactions. The conversions and product distributions for all of the coprocessing reactions are given in Table 2. The conversions for the single component reactions showed that coal and LDPE yielded lower conversions than the others; their respective conversions were 64.7 and 69.8%. The other plastics, PET and PS, and both resids yielded high conversions, ranging from a low of 94.7% for PET to 100% for PS. A positive influence of the catalyst was observed in the system since coal conversion increased from 44.6% in the thermal reaction to 64.7% in the catalytic reaction. Likewise, when the catalytic conversion of the three plastics are compared to the conversions of the unreacted materials and to the thermal conversions at 440 °C given by Luo and Curtis (1995) the effects of temperature, compared to the unreacted materials, and of catalyst, compared to the thermally reacted and unreacted materials, were positive.

The product distributions of the three plastics reacted at 430 °C with presulfided NiMo/Al₂O₃ were quite different. Although PS and PET both yielded high conversions, the gas produced from PET was substantially higher yielding 36.8% compared to 8.0% for PS. The yield of hexane solubles from PS was the highest obtained at 91%; however, these hexane soluble materials were very volatile as shown by the low recovery that was discussed in the experimental section. The products produced from the conversion of the plastics were primarily the lighter fractions of gas or hexane solubles. Very small amounts of THF and toluene soluble materials were produced.

The catalytic reaction of the resids produced a small amount of heavier material, IOM and THF soluble material, that was not present in the original resid. The majority of the products were hexane soluble, although the amounts produced were slightly less than in the original resids. At 430 °C and with NiMo/Al₂O₃, 10 to 15% gas was produced from the resids so that the total amount of hexane solubles and gas produced was equal to the unreacted Manji hexane solubles and higher than the Maya unreacted hexane solubles indicating that Maya was upgraded at these reaction conditions.

Binary Systems. Reactions containing different combinations of the coal, resid, and plastics used in this study were performed, and the conversion and product distributions were obtained. High conversions of 90 to 100% were obtained for the binary combinations of coal plus resid and resid plus polymer, although conversion of resids with LDPE at 77.4 to 80.9% were lower than resid with the

other two plastics. The binary combination of coal and plastics yielded much lower conversions of 47.7 to 66.9% than the other systems, indicating that plastics and coal did not provide a mutually beneficial solvating medium.

Table 2. Reactor Results from Coprocessing Polymers with Coal and Resid*

Reactants	Product Distribution (%)					Conversion (%)	Recovery (%)
	Gas	HX	TOL	THF	IOM		
Single Component							
PS	8.0±2.5	91.0±2.7	0.5±0.6	0.5±0.7	0.0	100	42
LDPE	20.0±1.3	41.8±2.8	4.4±1.8	3.6±0.3	30.3±0.6	69.8±0.6	91
PET	36.8±1.6	54.7±1.6	2.0±1.2	1.3±0.1	5.4±1.2	94.7±1.2	56
Coal	18.3±0.1	22.6±1.8	4.2±0.1	19.6±2.5	35.4±3.9	64.7±3.9	94
Manji	10.4±0.4	78.3±0.3	8.5±0.2	1.9±0.8	0.7±0.8	99.3±0.8	85
Maya	14.5±0.4	65.8±0.9	15.1±1.4	1.5±0.4	3.3±0.4	96.8±0.4	93
Two Components							
Coal/Manji	10.8±0.3	64.1±1.6	12.2±0.0	9.7±0.8	3.2±0.6	96.8±0.6	88
Coal/Maya	10.6±0.4	59.4±0.1	20.4±0.1	1.9±0.2	8.0±0.8	92.1±0.8	85
Maya/PS	8.3±0.3	80.4±1.8	8.3±0.6	1.5±0.2	1.7±0.6	98.4±0.6	57
Maya/LDPE	9.5±0.2	58.0±2.0	7.5±0.8	2.5±0.8	22.7±2.2	77.4±2.2	90
Maya/PET	19.0±0.8	65.8±0.1	7.6±0.4	2.4±0.1	5.4±0.4	94.7±0.4	67
Manji/PS	4.7±0.1	86.5±0.9	5.9±0.4	1.4±0.1	1.6±0.6	98.4±0.6	58
Manji/LDPE	9.0±0.3	63.5±0.9	5.7±0.8	2.8±0.1	19.1±0.0	80.9±0.0	89
Manji/PET	18.2±0.4	70.7±0.1	5.5±0.1	1.9±0.1	3.7±0.6	96.3±0.6	63
Coal/PS	7.6±0.1	54.0±2.9	0.8±0.4	2.0±0.5	35.7±2.2	64.4±2.2	56
Coal/LDPE	11.6±1.0	30.1±2.8	4.6±0.1	1.6±0.1	52.3±1.8	47.7±1.8	95
Coal/PET	21.6±0.6	41.6±3.2	1.4±0.6	2.5±1.2	33.1±5.5	66.9±5.5	67
Three Components							
Coal/Maya/PS	7.7±0.4	69.2±0.8	9.4±0.5	5.9±0.1	8.0±0.9	92.1±0.9	66
Coal/Maya/LDPE	9.0±1.8	52.9±2.1	9.1±0.0	5.7±0.1	23.4±0.4	76.7±0.4	90
Coal/Maya/PET	16.9±1.5	55.9±2.5	7.5±0.0	6.8±0.1	13.0±0.9	87.1±0.9	74
Coal/Manji/PS	5.4±0.4	75.5±1.7	7.5±0.4	6.6±0.2	5.2±1.6	94.8±1.6	62
Coal/Manji/LDPE	9.4±1.9	57.2±1.1	9.1±0.6	5.0±0.0	19.4±0.3	80.6±0.3	88
Coal/Manji/PET	14.9±0.1	61.6±0.6	7.1±0.4	7.0±0.0	10.1±1.1	89.9±1.1	71
Two Components at Higher Catalyst Loading							
Coal/LDPE	10.7±0.4	36.1±1.8	3.5±0.2	3.8±1.3	46.0±2.6	54.1±2.6	90
Maya/LDPE	9.2±0.1	57.4±0.5	6.9±0.9	3.2±0.6	23.5±0.4	76.6±0.4	90
Manji/LDPE	8.3±0.1	61.0±1.5	4.1±0.1	2.2±1.3	24.5±0.1	75.5±0.1	93
Three Components at Higher Catalyst Loading							
Coal/Manji/LDPE	6.9±0.1	60.7±1.1	8.4±0.3	4.7±0.6	19.4±0.6	80.7±0.6	88

* Reaction Conditions 430 °C, 8.3 MPa H₂, and one hour; 1 wt% NiMo/Al₂O₃ of total feedstock for catalytic reactions.

A parameter, termed coprocessing effect factor (f_i), was defined that evaluated the effect of combining two materials rather than reacting them individually. The three coprocessing effect factors that were evaluated were the conversion, hexane soluble, and gas coprocessing effect. The equation that defines this parameter is

$$f_i = \frac{(\% CP_i - \% HM_i)}{\% CP_i} \times 100$$

where i is either gas, hexane solubles, or conversion, HM is the hypothetical mean, and CP is the coprocessing result.

The reactions of coal and resid showed positive coprocessing effect factors for hexane solubles and conversion which means that more hexane soluble material was produced and more conversion of material occurred when coal and resid were reacted together than when they were reacted individually. The coprocessing effect factor for gas products was negative for both coal and resid combinations, meaning that less gas was produced during coprocessing than in the individual reactions. Similarly, the reaction of Maya resid with each of the plastics resulted in each binary

combination having a positive hexane soluble coprocessing effect factor and negative gas coprocessing effect factor. The conversion coprocessing effect factor for Maya and the three plastics varied according to the type of plastic: Maya and PS gave a slightly positive factor while the other two combinations gave negative values. Manji resid reacted with each of the three plastics resulted in a less positive hexane coprocessing effect factor than Maya/polymer and large negative values for the gas coprocessing effect factor. The combination of coal and PS or LDPE was detrimental to the production of hexane soluble material from the coprocessed materials, while the combination of coal with PET was favorable for the production of hexane soluble material. The amount of gas produced during coprocessing was less with the coal and polymers as it was with combined reaction of all the other systems. The coprocessing effect factor for conversion of the coal and polymer systems yielded negative values that were quite large ranging from -19.1 for coal and PET to -41.0 for coal and LDPE. The combination of coal and polymer was detrimental to the conversion compared to that obtained in individual reactions.

Ternary Systems. The coprocessing effect factors for the ternary systems were calculated two ways. The first method of calculation shown on Table 3 used the hypothetical mean of the individual reactions where the ratio of the components in the ternary system was used to weight the various terms. The second method of calculating the hypothetical mean was to use the results of reactions of a single component and a binary system to calculate hypothetical mean in which of the reactants involved were weighted according to the relative amount of each material in the ternary systems.

The results with the calculational method using the individual reactions are given in Table 3. All of the ternary reaction systems showed a positive coprocessing effect factor for the hexane soluble material when compared to the hypothetical mean calculated from the individual reaction systems. The gas coprocessing effect factor for each ternary reaction system resulted in large negative values. Particularly, the ternary systems containing PS and LDPE gave large negative values; PET also gave negative values but the decrease compared to the individual systems was not nearly as large. Reacting the three components yielded a much reduced gas make compared to the individual reactions. Coprocessing the three materials together resulted in positive effects on the conversion of ternary systems containing PS and PET for both coal and resid combinations; however, the systems containing LDPE gave negative values. Reaction with Manji resid was more beneficial to each of the polymers than was Maya.

The coprocessing effect factor calculation with the hypothetical mean from the single component plus binary systems gave negative gas coprocessing effect factors. The hexane soluble coprocessing effect was positive for the coal plus resid/polymer systems and for the resid plus coal/polymer systems; however, only half the polymer plus coal/resid systems gave positive values. LDPE gave negative values for both resids indicating that the binary system did not increase the hexane solubles compared to the hypothetical mean. The conversion coprocessing effect factor was positive for the hypothetical means using coal plus resid/polymer and resid plus coal/polymer. However, all of the conversion coprocessing effect factors for polymer plus coal/resid were negative, indicating that addition of the polymer to the coal/resid system was detrimental to overall conversion.

Effect for Catalyst Loading. The binary and ternary systems containing LDPE gave lower conversions and hexane solubles than the other polymers. The effect of increasing catalyst loading to 3 and 10 wt % based on the total charge on coal conversion and hexane soluble yield in binary and ternary systems containing LDPE was determined. The 3 wt % addition increased the conversion in the coal/LDPE from 47 to 54 % (Table 2); the effect on conversion from the other binary and ternary systems were minimal and with the resids even decreased the conversion slightly. Increasing the catalyst loading to 10 wt % had a similar effect as the 3% loading.

Summary and Conclusions

The coprocessing of coal, plastics and resid yielded favorable results. The amount of gas produced decreased as the number of components in the reaction increased. For binary and ternary systems containing resid, increases in the amount of hexane solubles and in conversion were apparent. The binary reaction of coal and plastics did not show this effect; the combination appeared to be detrimental to both materials. However, when resid was added to the system in the ternary systems, the positive hexane soluble and conversion coprocessing effect factors were obtained. Increasing catalyst loading improved the conversion of and the hexane soluble yield in the coal/LDPE system. Increased catalyst loading had little effect on the binary and ternary systems containing resids.

Table 3. Coprocessing Effect Factors for Binary and Ternary Systems

Reaction Combinations	Coprocessing Effect Factor (<i>f</i>)		
	Gas	HX	Conversion
Two Components			
Coal/Manji	-25.6	12.6	11.7
Coal/Maya	-51.1	18.3	8.8
Maya/PS	-43.4	5.6	0.3
Maya/LDPE	-75.8	3.1	-11.1
Maya/PET	-15.2	6.8	-1.3
Manji/PS	-100.9	3.6	-1.2
Manji/LDPE	-58.2	-0.3	-8.2
Manji/PET	-15.2	2.6	-1.2
Coal/PS	-73.0	-5.2	-27.9
Coal/LDPE	-65.1	-7.0	-41.0
Coal/PET	-27.5	7.1	-19.1
Ternary Systems with Hypothetical Mean of Individual Components^b			
Coal/Maya/PS	-78.3	12.4	3.9
Coal/Maya/LDPE	-90.6	11.9	-4.2
Coal/Maya/PET	-29.9	10.1	0.1
Coal/Manji/PS	-121.7	12.6	5.5
Coal/Manji/LDPE	-63.8	9.2	-0.5
Coal/Manji/PET	-35.6	9.7	2.0
Ternary Systems with Hypothetical Mean of Single and Binary Systems^b			
Coal + Maya/PS	-44.9	7.7	3.6
Coal + Maya/LDPE	-33.5	9.5	3.8
Coal + Maya/PET	-11.2	4.4	1.1
Coal + Manji/PS	-59.0	9.6	6.4
Coal + Manji/LDPE	-24.0	9.4	5.4
Coal + Manji/PET	-22.3	7.5	2.9
Maya + Coal/PS	-37.1	14.7	15.0
Maya + Coal/LDPE	-42.7	14.2	10.4
Maya + Coal/PET	-9.8	7.0	8.5
Manji + Coal/PS	-63.0	14.7	16.3
Manji + Coal/LDPE	-18.0	11.3	13.4
Manji + Coal/PET	-12.8	6.9	10.1
PS + Coal/Maya	-28.0	1.1	-2.5
PS + Coal/Manji	-85.2	4.9	-3.1
LDPE + Coal/Maya	-47.6	-2.8	-11.8
LDPE + Coal/Manji	-42.9	-0.9	-10.5
PET + Coal/Maya	-7.0	-3.9	-6.6
PET + Coal/Manji	-22.3	0.3	-7.0

^a HM = Hypothetical Mean of reactants which is defined as

$$HM_i = \frac{(\% \text{ coal }_i + 1.5 \times \% \text{ resid }_i + \% \text{ polymer }_i)}{\text{total charged (g)}}$$

^b Calculations using different hypothetical mean which is defined as

$$HM_i = \frac{(x) \times \% \text{ one component } + (y) \times \% \text{ two components}}{3.5}$$

where x is 1.0 for coal and polymer and is 1.5 for resid, y is 2.0 for coal and polymer and 2.5 for resid.

Acknowledgements

The support of the United States Department of Energy through Contract No. DE-FC22-93PC93053 for the work is sincerely appreciated.

References

- Luo, M.; Curtis, C.W. Consortium for Fossil Fuel Liquefaction Science, Final Report, June, 1995.
 Pradhan, V.R.; Comoli, A.G.; Lee L.K.; Stalzer, R. H. *ACS Fuel Chem Div. Preprints*, 40(1) 82-86, 1995.

VACUUM PYROLYZED TIRE OIL AS A COAL SOLVENT

Edward C. Orr, Yanlong Shi, Qin Ji, Larry L. Anderson, and Edward M. Eyring
Department of Chemistry and Department of Chemical and Fuels Engineering,
University of Utah, Salt Lake City, UT 84112

Keywords: tires, coal, coprocessing, EPMA

Introduction

Recent interest in coprocessing coal with hydrogen rich waste materials in order to produce liquid transportation fuels has given rise to interesting twists on standard coal liquefaction.¹⁻⁵ In general, coprocessing coal with a waste material has been approached with the idea that the waste material would be mixed with the coal under liquefaction conditions with little or no preliminary processing of the waste material other than shredding into smaller size particles. Mixing the waste material with the coal would occur in the primary stage of liquefaction. The primary stage would accomplish the dissolution of the coal and breakdown of the waste material. The products would then be introduced into the secondary stage where upgrading of product would occur.

Recent work with waste rubber tires directly coprocessed with coal has shown that this is a feasible scheme, but that additional pretreatment of the tires is beneficial to the coprocessing. This additional step is the vacuum pyrolysis of the waste rubber tire to yield an oil that is highly aromatic. The vacuum pyrolysis of the waste rubber tires is also beneficial in separating out the carbon black and ash from the volatile constituents. It has been shown that the breakdown of waste rubber tires during vacuum pyrolysis produces polyaromatic hydrocarbons.⁶ Polyaromatics are known to be beneficial in coal liquefaction.⁷⁻⁹ The present paper explores the usefulness of oil derived from pyrolysis of waste rubber tires as a reactant in a coal coprocessing scheme or as a coal liquefaction solvent.

Experimental

Blind Canyon (Utah) coal (DECS-6, -60 mesh) (BC6) was obtained from the Penn State Coal Sample Bank and stored under nitrogen at 0 °C. Oil obtained from vacuum pyrolysis of waste rubber tires (PTO=pyrolyzed tire oil) was produced by Conrad Industries, Chehalis, WA. The PTO was stored under ambient conditions. GC-MS analysis of the PTO was completed on a Hewlett Packard 5890 series II gas chromatograph coupled to a Hewlett Packard 5971 Mass spectrometer. A J & W 100 meter long DB-1 column was used for the GC-MS analyses. Elemental analyses were completed by Atlantic Microlabs, Norcross, Georgia. The precursor catalyst (ammonium tetrathiomolybdate, Aldrich) was used as received to impregnate the BC6 from aqueous solution by the incipient wetness technique to obtain a 1 % by weight loading of the catalyst. The catalyst was added to the PTO in solid, dry form to achieve a 1 % by weight presence of the catalyst. The BC6/catalyst mixture was vacuum dried for two hours at 100 °C to remove all moisture. The PTO/BC6 samples were placed directly in 27 cm³ tubing reactors, purged with N₂, and pressurized to the pressure of interest. Pressures reported are for H₂ or N₂ and are initial pressures at room temperature before immersion in the sandbath. Reactors were heated by a fluidized sandbath held at various reaction temperatures. The tubing reactors were shaken vertically at 160 rpm for the duration of the experiment, removed and allowed to cool at room temperature for 5 minutes, and then quenched in cold water. Reaction products and solids were removed and extracted with tetrahydrofuran (THF). The THF was removed with a rotary evaporator, and the THF soluble portion was dried under vacuum for two hours and weighed. The THF insoluble residue remaining in the soxhlet extractor thimble was also dried for two hours under vacuum. The sum of the THF solubles and the THF insoluble residue, corrected for ash, was subtracted from the initial coal mass (daf) and solvent mass to calculate the total gas produced. Total conversion was defined as the sum of the gas and THF solubles. The dried THF solubles were then extracted with cyclohexane. The cyclohexane was removed from the oil sample using a rotary evaporator. The cyclohexane insoluble residue is referred to as asphaltenes. The cyclohexane soluble portion is referred to as oil. EPMA samples were prepared by grinding the THF insoluble portions and mixing with Petropoxy 154 (Pullman, Washington). The plug was polished with

a syntron diamond paste polisher for eight hours. Micrographs were obtained using a CAMECA Model SX-50 electron microprobe (Courbevoie, France). Two different micrographs are presented: secondary electron micrographs (SEM) and the characteristic X-ray micrograph for specific elements of interest. (All micrographs shown are for a 50 μm x 50 μm field of view).

Results

In Table 1 the analysis of the **BC6** is reported. Table 2 contains elemental analysis results for the **PTO**. The NMR results indicate the **PTO** is highly aromatic. The GC-MS analysis of the **PTO** indicated the presence of benzene, methylated forms of benzene, naphthalene, methylated forms of naphthalene, anthracene, methylated forms of anthracene, phenanthrene, methylated forms of phenanthrene, pyrene, methylated forms of pyrene, and naphthacene. These results are similar to what Williams and Taylor found for oil derived from the vacuum pyrolysis of waste rubber tires.⁶

Figure 1 contains the product yields based on the original coal (daf) and **PTO** masses. The data show good overall total conversion for the **PTO/BC6** mixtures. The results indicate that a 30 to 40 minute heating period is optimum for maximizing the conversion of **BC6/PTO** with molybdenum catalyst present under a hydrogen atmosphere at 430 °C. Initial conversion is surprisingly high at 10 and 20 minutes. This may indicate that the **PTO** is very effective in solubilizing the coal. In all samples, charring was observed, but charring was more significant in the 50 and 60 minute samples. The significant charring is probably due to the **PTO**. The polyaromatic molecules are char precursors, thus it is not surprising that charring increased with reaction time.

Figure 2 shows the yields based only on coal. These values were calculated on the assumption that **PTO** is only present in the products as gas and oil. Therefore we can subtract out 50 % of the gas and oil and double the remaining conversion value to obtain the coal total conversion. From the new total conversion we subtract twice the amount of asphaltenes in order to obtain the new gas and oil values. This assumes no **PTO** forms char, which is very unlikely, but this permits an approximate calculation of the amount of coal that was actually converted. Thus, it could be predicted that at 30 minutes 92 % of the coal would be converted into gas, oil, and asphaltenes.

Table 3 contains the carbon and hydrogen percentages for the oils, asphaltenes, and char/ash produced from the above reactions. The carbon and hydrogen values were converted to molar values to obtain carbon/hydrogen ratios. The oil quality remained constant throughout the six time periods.

In past work, it was found that Electron Probe Microanalysis (EPMA) was useful in spotting the location of catalysts and metals in coal.¹⁰⁻¹² EPMA is a qualitative tool for determining the degree of dispersion of metal catalysts in coal particles.

The EPMA data in Fig. 3 show a coal particle taken from a sample which contained **BC6** coprocessed with **PTO** at 430 °C for only 20 min. For the coal particle, a secondary electron micrograph (SEM), a sulfur X-ray image, and a molybdenum X-ray image are shown. The SEM image and sulfur X-ray image are presented to show the location of the coal particle. The **BC6** contains approximately 0.4 % by weight sulfur which the EPMA detects. Fresh coal contains no molybdenum, therefore detection of molybdenum by the EPMA indicates the presence of catalyst. The detection limit of the EPMA for molybdenum is approximately 200 ppm. Thus catalyst may be present in samples even though it may not be detected by EPMA.

The molybdenum micrograph in Figure 3 indicates the presence of the molybdenum catalyst in the coal particle. It is somewhat surprising to find catalyst inside the coal particle at such an early time in the liquefaction period. In previous unpublished work we found that when **BC6** was reacted at 350 °C without any solvent and the molybdenum was not incorporated into the coal matrix until 50 to 60 minutes of coprocessing had occurred. The high total conversion

observed after 20 minutes for the PTO/BC6 system indicates that dissolution and thermal cracking of the coal occurred rapidly. PTO probably induces swelling thus allowing for greater dispersion of the catalyst throughout the coal particles. This suggests that increased dispersion of the molybdenum catalyst observed in the coal particles by EPMA may be partially responsible for the high conversion values.

Conclusion

Tire oil obtained by vacuum pyrolysis of waste rubber tires is better than shredded tires for coprocessing with coal. The PTO appears to be a good dissolution solvent for the coal and an effective hydrogen donor. EPMA data indicate that the solvent readily enters the coal matrix thus aiding catalyst dispersion.

Acknowledgements

We gratefully acknowledge Lester J. Thompson and Eugene Dalton with Book Cliff Energy, Green River, UT for providing us with pyrolyzed tire oil. We also acknowledge Phillip Bridges with Conrad Industries, Chehalis, WA for his generous donation of pyrolyzed tire oil and discussions of this work. Financial support by the U.S. Department of Energy, Fossil Energy Division, through the Consortium for Fossil Fuel Liquefaction Sciences, Contract No. UKRF-4-21033-86-24, is gratefully acknowledged.

References

1. Farcasiu, M.; Smith, C., 1992, Prepr. Pap. Am. Chem. Soc., Div. Fuel Chem., 37 (1), 472.
2. Orr, E. C.; Tuntawiroon, W.; Ding, W. B.; Rumpel, S.; Eyring, E. M.; Anderson, L. L., 1995, Prepr. Pap. Am. Chem. Soc., Div. Fuel Chem., 40 (1), 44.
3. Stiller, A. H.; Dadyburjor, D. B.; Wann, J.; Tian, D.; Zondlo, J. W., 1995, Prepr. Pap. Am. Chem. Soc., Div. Fuel Chem., 40 (1), 77.
4. Robbins, G. A.; Winschel, R. A.; Burke, F. P., 1995, Prepr. Pap. Am. Chem. Soc., Div. Fuel Chem., 40 (1), 92.
5. Huffman, G. P.; Feng, Z.; Mahajan, V.; Sivakumar, P.; Jung, H.; Tierney, J. W.; Wender, I., 1995, Prepr. Pap. Am. Chem. Soc., Div. Fuel Chem., 40 (1), 34.
6. Williams, P. T.; Taylor, D. T., 1993, Fuel, 72, 1475.
7. Orr, E. C.; Tuntawiroon, W.; Anderson, L. L.; Eyring, E. M., Fuel Processing Technology, in press.
8. Grint, A.; Jackson, W. R.; Larkins, F. P.; Louey, M. B.; Marshall, M.; Trewbella, M. J.; Watkins, I. K., 1994, Fuel, 73 (3), 381.
9. McMillen, D. F.; Malhotra, R.; Tse, D. S.; Nigenda, S. E., 1988, Prepr. Pap. Am. Chem. Soc., Div. Fuel Chem., 33 (1), 58.
10. Sommerfeld, D. A.; Jaturapitomsakul, J.; Anderson, L. L.; Eyring, E. M., 1992, Prepr. Pap. Am. Chem. Soc., Div. Fuel Chem., 37 (2), 749.
11. Sommerfeld, D. A.; Tuntawiroon, W.; Anderson, L. L.; Eyring, E. M., 1993, Prepr. Pap. Am. Chem. Soc., Div. Fuel Chem., 38 (1), 211.
12. Orr, E. C.; Tuntawiroon, W.; Anderson, L. L.; Eyring, E. M., 1994, Prepr. Pap. Am. Chem. Soc., Div. Fuel Chem., 39 (4), 1065.

Table 1 Analysis of Blind Canyon DECS-6 Coal*

Proximate	Percentage
% Ash	5.84
% Volatile	44.50
% Fixed Carbon	49.66
Ultimate	Percentage
% Carbon	81.28
% Hydrogen	6.24
% Nitrogen	1.55
% Sulfur	0.42
% Oxygen	10.5

* Penn State Coal Sample Bank

Table 2 Elemental Analysis of Oil Derived From The Vacuum Pyrolysis of Waste Rubber Tires

Element	Percentage
Carbon	87.7
Hydrogen	11.0
Nitrogen	0.3
Sulfur	0.6

Figure 1 Conversion results for Blind Canyon DECS-6 and oil obtained from the pyrolysis of waste rubber tires. Coprocessing was carried out in tubing reactors at 430 °C under hydrogen gas with a molybdenum catalyst present. The ratio of coal to oil was 1:1 by weight.

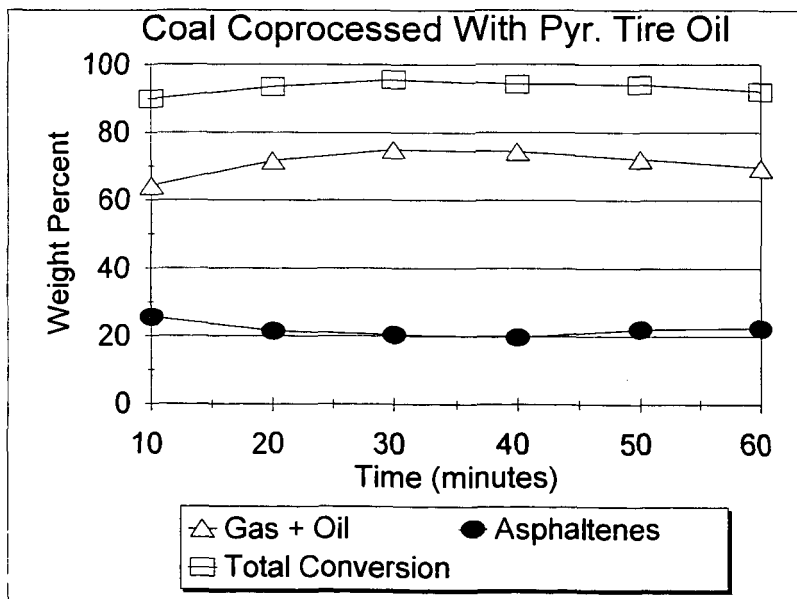


Figure 2 Conversion results for Blind Canyon DECS-6. Coprocessing was carried out in tubing reactors at 430 °C under hydrogen gas with a molybdenum catalyst present. The ratio of coal to oil was 1:1 by weight.

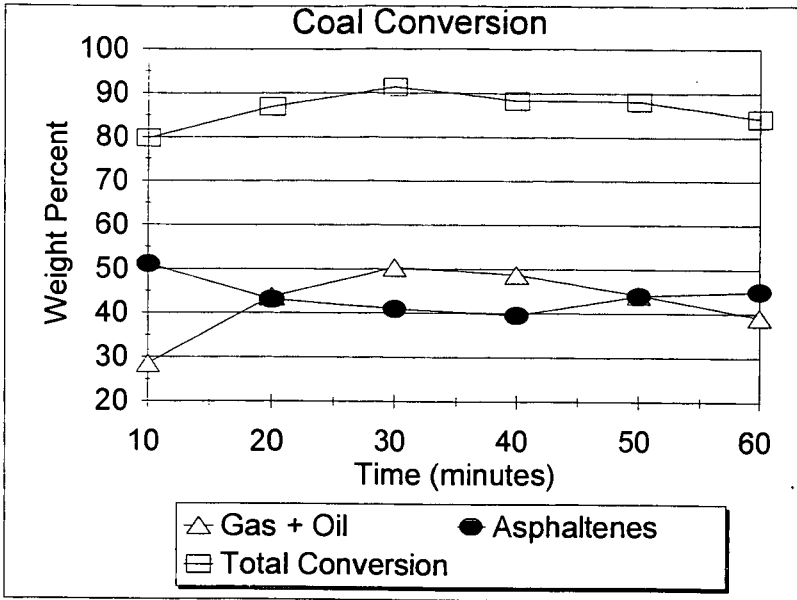


Table 3 Carbon and Hydrogen Analysis of Oil, Asphaltenes, and Char/Ash

	Oil	Asphaltenes	Char/Ash
10 Minutes			
Carbon	86.8	84.3	57.6
Hydrogen	8.6	5.8	3.2
Molar Ratio	.8	1.2	1.5
20 Minutes			
Carbon	86.0	85.6	53.4
Hydrogen	8.4	5.5	2.8
Molar Ratio	.9	1.3	1.6
30 Minutes			
Carbon	84.3	87.1	43.0
Hydrogen	8.3	5.6	2.2
Molar Ratio	.9	1.3	1.6
40 Minutes			
Carbon	86.4	86.9	38.9
Hydrogen	8.5	5.5	2.0
Molar Ratio	.9	1.3	1.6
50 Minutes			
Carbon	84.9	87.6	56.0
Hydrogen	8.3	5.4	2.9
Molar Ratio	.9	1.4	1.6
60 Minutes			
Carbon	85.1	87.7	59.9
Hydrogen	8.1	6.0	2.8
Molar Ratio	.9	1.2	1.8

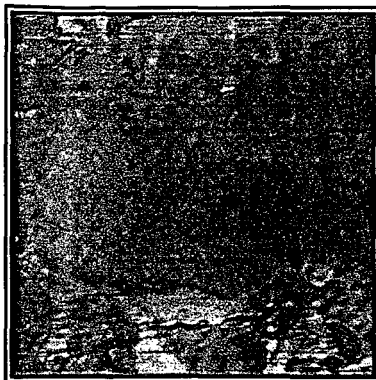
Figure 3

Blind Canyon DECS-6 coal in pyrolyzed tire oil

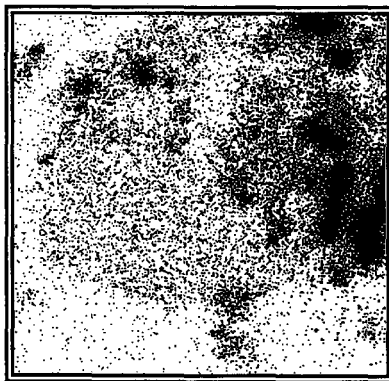
1 % ammonium tetrathiomolybdate

Hydrotreated for 20 minutes, 430° C, 1000 psig (cold) H₂

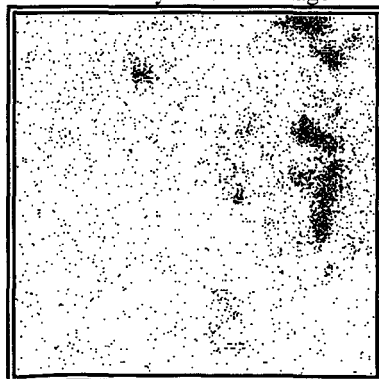
EPMA micrograph dimensions (50 μm x 50 μm)



Secondary Electron Image



Sulfur K_α



Molybdenum L_α